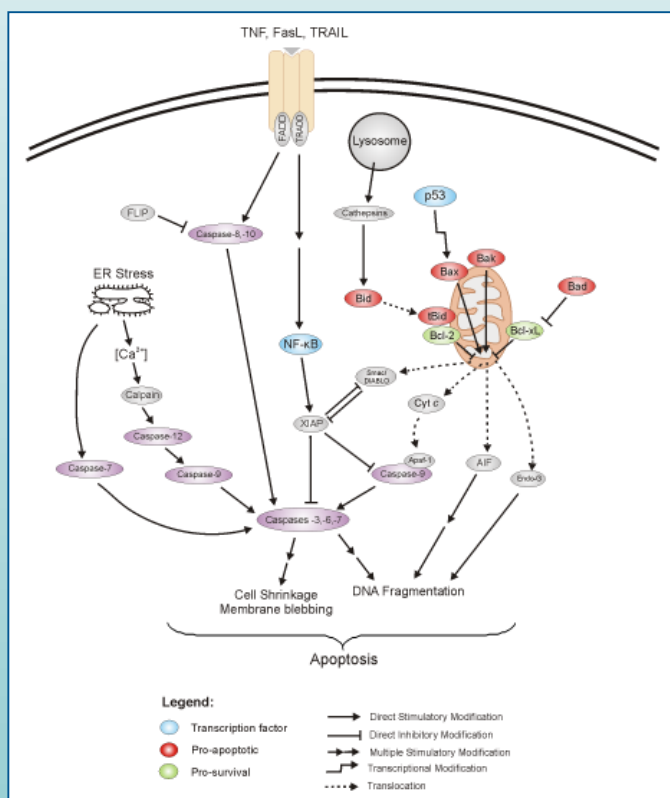


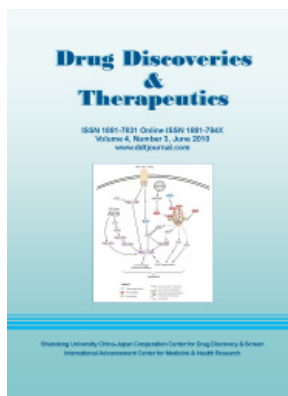
Drug Discoveries & Therapeutics

ISSN 1881-7831 Online ISSN 1881-784X
Volume 4, Number 3, June 2010
www.ddtjournal.com



Shandong University China-Japan Cooperation Center for Drug Discovery & Screen
International Advancement Center for Medicine & Health Research

Drug Discoveries & Therapeutics



Editor-in-Chief:

Kazuhisa SEKIMIZU
(The University of Tokyo, Tokyo, Japan)

Associate Editor:

Norihiro KOKUDO
(The University of Tokyo, Tokyo, Japan)

Drug Discoveries & Therapeutics is a peer-reviewed international journal published bimonthly by *Shandong University China-Japan Cooperation Center for Drug Discovery & Screen (SDU-DDSC)* and *International Advancement Center for Medicine & Health Research Co., Ltd. (IACMHR Co., Ltd.)*.

Drug Discoveries & Therapeutics mainly publishes articles related to basic and clinical pharmaceutical research such as pharmaceutical and therapeutical chemistry, pharmacology, pharmacy, pharmacokinetics, industrial pharmacy, pharmaceutical manufacturing, pharmaceutical technology, drug delivery, toxicology, and traditional herb medicine. Studies on drug-related fields such as biology, biochemistry, physiology, microbiology, and immunology are also within the scope of this journal.

Subject Coverage: Basic and clinical pharmaceutical research including Pharmaceutical and therapeutical chemistry, Pharmacology, Pharmacy, Pharmacokinetics, Industrial pharmacy, Pharmaceutical manufacturing, Pharmaceutical technology, Drug delivery, Toxicology, and Traditional herb medicine.

Language: English

Issues/Year: 6

Published by: IACMHR and SDU-DDSC

ISSN: 1881-7831 (Online ISSN 1881-784X)

CODEN: DDTRBX

Editorial and Head Office

Wei TANG, MD PhD
Executive Editor
Drug Discoveries & Therapeutics
Pearl City Koishikawa 603,
2-4-5 Kasuga, Bunkyo-ku,
Tokyo 112-0003, Japan
Tel: 03-5840-9697
Fax: 03-5840-9698
E-mail: office@ddtjournal.com
URL: www.ddtjournal.com



Drug Discoveries & Therapeutics

Editorial Board

Editor-in-Chief:

Kazuhisa SEKIMIZU (*The University of Tokyo, Tokyo, Japan*)

Associate Editor:

Norihiro KOKUDO (*The University of Tokyo, Tokyo, Japan*)

Executive Editor:

Wei TANG (*The University of Tokyo, Tokyo, Japan*)

Managing Editor:

Munehiro NAKATA (*Tokai University, Kanagawa, Japan*)

Web Editor:

Yu CHEN (*The University of Tokyo, Tokyo, Japan*)

English Editors:

Curtis BENTLEY (*Roswell, GA, USA*)

Thomas R. LEBON (*Los Angeles Trade Technical College, Los Angeles, CA, USA*)

China Office:

Wenfang XU (*Shandong University, Shandong, China*)

Editorial Board Members:

Yoshihiro ARAKAWA (<i>Tokyo, Japan</i>)	Yuxiu LIU (<i>Nanjing, China</i>)
Santad CHANPRAPAPH (<i>Bangkok, Thailand</i>)	Hongxiang LOU (<i>Jinan, China</i>)
Fen-Er CHEN (<i>Shanghai, China</i>)	Ken-ichi MAFUNE (<i>Tokyo, Japan</i>)
Zhe-Sheng CHEN (<i>Queens, NY, USA</i>)	Norio MATSUKI (<i>Tokyo, Japan</i>)
Zilin CHEN (<i>Wuhan, China</i>)	Tohru MIZUSHIMA (<i>Kumamoto, Japan</i>)
Guanhua DU (<i>Beijing, China</i>)	Abdulla M. MOLOKHIA (<i>Alexandria, Egypt</i>)
Chandradhar DWIVEDI (<i>Brookings, SD, USA</i>)	Masahiro MURAKAMI (<i>Osaka, Japan</i>)
Mohamed F. EL-MILIGI (<i>Cairo, Egypt</i>)	Yoshinobu NAKANISHI (<i>Ishikawa, Japan</i>)
Harald HAMACHER (<i>Tuebingen, Germany</i>)	Yutaka ORIHARA (<i>Tokyo, Japan</i>)
Hiroshi HAMAMOTO (<i>Tokyo, Japan</i>)	Xiao-Ming OU (<i>Jackson, MS, USA</i>)
Xiaojiang HAO (<i>Kunming, China</i>)	Weisan PAN (<i>Shenyang, China</i>)
Waseem HASSAN (<i>Santa Maria, RS, Brazil</i>)	Rakesh P. PATEL (<i>Gujarat, India</i>)
Langchong HE (<i>Xi'an, China</i>)	Shafiqur RAHMAN (<i>Brookings, SD, USA</i>)
David A. HORNE (<i>Duarte, CA, USA</i>)	Shivanand P. PUTHLI (<i>Mumbai, India</i>)
Yongzhou HU (<i>Hangzhou, China</i>)	Adel SAKR (<i>Cincinnati, OH, USA</i>)
Wei HUANG (<i>Shanghai, China</i>)	Abdel Aziz M. SALEH (<i>Cairo, Egypt</i>)
Yu HUANG (<i>Hong Kong, China</i>)	Tomofumi SANTA (<i>Tokyo, Japan</i>)
Hans E. JUNGINGER (<i>Phitsanulok, Thailand</i>)	Yasufumi SAWADA (<i>Tokyo, Japan</i>)
Amrit B. KARMARKAR (<i>Mumbai, India</i>)	Brahma N. SINGH (<i>Commack, NY, USA</i>)
Toshiaki KATADA (<i>Tokyo, Japan</i>)	Hongbin SUN (<i>Nanjing, China</i>)
Gagan KAUSHAL (<i>Charleston, WV, USA</i>)	Benny K. H. TAN (<i>Singapore, Singapore</i>)
Ibrahim S. KHATTAB (<i>Safat, Kuwait</i>)	Renxiang TAN (<i>Nanjing, China</i>)
Hiromichi KIMURA (<i>Tokyo, Japan</i>)	Chandan M. THOMAS (<i>Bradenton, FL, USA</i>)
Shiroh KISHIOKA (<i>Wakayama, Japan</i>)	Murat TURKOGLU (<i>Istanbul, Turkey</i>)
Kam Ming KO (<i>Hong Kong, China</i>)	Zhengtao WANG (<i>Shanghai, China</i>)
Nobuyuki KOBAYASHI (<i>Nagasaki, Japan</i>)	Stephen G. WARD (<i>Bath, UK</i>)
Toshiro KONISHI (<i>Tokyo, Japan</i>)	Takako YOKOZAWA (<i>Toyama, Japan</i>)
Masahiro KUROYANAGI (<i>Hiroshima, Japan</i>)	Liangren ZHANG (<i>Beijing, China</i>)
Chun Guang LI (<i>Victoria, Australia</i>)	Jianping ZUO (<i>Shanghai, China</i>)
Hongmin LIU (<i>Zhengzhou, China</i>)	
Jikai LIU (<i>Kunming, China</i>)	

(as of June 20, 2010)

Review

- 144 - 167 **Free radicals in the regulation of damage and cell death – basic mechanisms and prevention.**
João P. Silva, Olga P. Coutinho

Brief Reports

- 168 - 174 **3D QSAR investigations on locomotor activity of 5-cyano-N1,6-disubstituted 2-thiouracil derivatives.**
Bhanudas S. Kuchekar, Yogesh V. Pore
- 175 - 178 **Serum fructose concentration in rats after single dose oral administration of Si-Wu-Tang.**
Qiande Liang, Chengrong Xiao, Zengchun Ma, Yuguang Wang, Beibei Lu, Hongling Tan, Baiping Ma, Boli Zhang, Yue Gao

Original Articles

- 179 - 183 ***Rehmanniae Radix* provides most of the free fructose and glucose in Si-Wu-Tang decoction.**
Jing Ma, Qiande Liang, Zengchun Ma, Yuguang Wang, Ming Liu, Beibei Lu, Hongling Tan, Chengrong Xiao, Boli Zhang, Yue Gao
- 184 - 189 **Effects of components present in flaxseed on human colon adenocarcinoma Caco-2 cells: Possible mechanisms of flaxseed on colon cancer development in animals.**
Ajay Bommareddy, Xiaoying Zhang, Radhey S. Kaushik, Chandradhar Dwivedi
- 190 - 201 **Characterization, thermodynamic parameters and *in vivo* antimalarial activity of inclusion complexes of artemether.**
Renu Chadha, Sushma Gupta, Geeta Shukla, Dharamvir S. Jain, Surjit Singh
- 202 - 207 **Isolation and structure elucidation of antioxidant compounds from leaves of *Laurus nobilis* and *Emex spinosus*.**
Ahmed M. Emam, Mamdouh A. Mohamed, Yasser M. Diab, Nadia Y. Megally

CONTENTS

(Continued)

- 208 - 216 **Optimization and characterization of diclofenac sodium microspheres prepared by a modified coacervation method.**
Eman S. El-Leithy, Dalia S. Shaker, Mohamed K. Ghorab, Rania S. Abdel-Rashid
- 217 - 222 **Membrane electrodes for determination of two antihypertensive drugs in pharmaceutical formulations of either single or binary mixtures and in biological fluids.**
Mohamed R. El-Ghobashy, Hala E. Zaazaa

Guide for Authors

Copyright

Review

Free radicals in the regulation of damage and cell death – basic mechanisms and prevention

João P. Silva*, Olga P. Coutinho

GCBMA – Molecular and Environmental Biology Centre, Department of Biology, University of Minho, Braga, Portugal.

ABSTRACT: Reactive oxygen (ROS) and nitrogen (RNS) species are known to accumulate intracellularly due to both exogenous and/or endogenous factors. In normal physiological conditions, these reactive species are maintained in an equilibrium state by the cells' antioxidant defence systems. In addition, they are recognised to play important roles in several physiological functions. However, when an imbalance in the equilibrium between oxidants and antioxidants occurs in favour of the former, we come to a situation defined as oxidative stress. ROS/RNS can cause damage to all biomolecules (namely proteins, lipids, and DNA) and ultimately participate in the regulation of mechanisms leading to cell death, being implicated in the etiology of several pathologies (like neurodegenerative and cardiovascular diseases). To cope with oxidative stress, cells possess effective enzymatic (e.g. superoxide dismutase, catalase, glutathione peroxidase) and non-enzymatic (e.g. glutathione, thioredoxin, coenzyme Q) antioxidant systems. In addition, several compounds present in plants and vegetables (e.g. vitamins C and E, polyphenols) have been described to react with free radicals. However, some drawbacks associated to these natural compounds are in part responsible for the undergoing development of novel synthetic compounds capable of acting as antioxidants and protect cells against oxidative stress-induced cell death. Here, we review the basic mechanisms of ROS/RNS formation, as well as their interaction with biomolecules and regulation of cell death, in order to identify possible drug targets. We also report the importance of natural antioxidant systems and the ongoing research leading to the development of more powerful and effective antioxidant drugs.

Keywords: Oxidative stress, ROS/RNS, antioxidants, cell death

*Address correspondence to:

Dr. João P. Silva, Biology Department, University of Minho, Campus de Gualtar, 4710-057 Braga, Portugal.
e-mail: jpsilva@bio.uminho.pt

1. Oxidative stress

There is a general agreement among the scientific community that significant amounts of oxygen (O₂) first appeared in the Earth's atmosphere about 2.5 billion years ago. However, the toxicity of oxygen led the existing anaerobic organisms to adapt to the new environment by developing defence mechanisms, in order to protect themselves and survive (1). Though some of them chose to live in an oxygen-free micro-environment, others became capable of performing both respiration and fermentation (facultative anaerobes). Only later on there was the development of new species that used respiration in an exclusive way, the aerobic organisms (2,3).

Initially, O₂ toxicity was thought to be due to the inactivation of enzymes, mainly the thiol group of cysteine residues. Later, toxicity was also attributed to the effects of hydrogen peroxide (H₂O₂). Ultimately, molecular biology techniques established that the toxic effects of O₂ are directly linked to its partially reduced forms, the reactive oxygen species (ROS), acting on cellular components (4). More than 50 years ago, Denham Harman, in his "Free Radical Theory of Aging", described these reactive species as being responsible for the most part of cellular damage and as playing a key role in the aging process [*in* (5)]. The discovery of the enzyme superoxide dismutase (SOD) in 1969 by McCord and Fridovich (6) definitively convinced the rest of the scientific community of the importance of free radicals in living systems. This led to further investigation in this field, which resulted in the finding that these free radicals also intervene in the regulation of intracellular signalling. So, as living systems evolved, they have not only adapted to a coexistence with free radicals but have developed various defence mechanisms to protect themselves against the toxicity of oxygen (5,7).

In normal physiological conditions, the production of free radicals and other reactive species is maintained in an equilibrium state by this antioxidant defence system (2). However, when an imbalance occurs between oxidants and antioxidants in favour of the oxidants, we come to a situation defined as oxidative

stress (8). This can result from two different factors: a decrease in antioxidants, due to mutations affecting antioxidant enzymes or depletion of antioxidants along with other essential diet constituents; or an excessive production of oxygen and nitrogen reactive species, for example, by exposure to high levels of O_2 , by the presence of toxins that are metabolised to produce ROS, among others (2).

Oxidative stress can cause damage to all biomolecules and ultimately lead to cell death, being implicated in the etiology of several pathologies, such as atherosclerosis (9), neurodegenerative diseases (10,11), and ischemia-reperfusion injury (12,13).

1.1. Formation of reactive species

Intracellular accumulation of reactive oxygen (ROS) and nitrogen (RNS) species can be triggered by both exogenous and/or endogenous factors (14), as summarised in Figure 1. Mitochondria reduce to water over 95% of all the oxygen used by the cell, mostly due to the presence of an electron transport chain (ETC). However, a small percentage of the total oxygen escapes, resulting in the formation of superoxide radicals, and subsequently other reactive species, like hydrogen peroxide and hydroxyl radicals (15,16). In fact, these organelles are packed with several redox carriers that can potentially leak single electrons to oxygen and convert it into superoxide anion, which, by its turn, leads to the subsequential formation of other ROS. Given the moderate redox potential of the superoxide/dioxygen ($O_2^{\cdot-}/O_2$) couple ($E_{1/2} = -0.16$ V), the reaction of one-electron

reduction of oxygen is thermodynamically favourable for numerous mitochondrial oxidoreductases [*in* (17)].

Considering that superoxide is effectively removed from the reaction by some detoxifying enzymes, like superoxide dismutase, and the possibility of highly reduced state of many redox carriers, the reaction becomes virtually irreversible. So, which of the electron carriers do become the sites of ROS production is kinetically controlled (17,18). Some examples of these carriers include the cytochrome *b5* reductase and the monoamine oxidases (located in the outer mitochondrial membrane), α -glycerophosphate dehydrogenase (outer surface of the inner mitochondrial membrane), succinate dehydrogenase (complex II, situated at the inner surface of the inner membrane), aconitase (in the mitochondrial matrix), and the α -ketoglutarate dehydrogenase complex (associated with the matrix side of the inner membrane). Nevertheless, the majority of ROS are produced in complexes I and III of the mitochondrial respiratory chain (19). Best understood is the Complex III (ubiquinol-cytochrome *c* reductase) contribution to superoxide generation. Within this complex, the transfer of electrons from ubiquinol (UQH_2) to cytochrome *c* proceeds through a set of reactions known as the Q-cycle. However, during this process, the one-electron reduction of oxygen by the ubisemiquinone anion radical ($UQ^{\cdot-}$), an unstable intermediary of the Q-cycle, may lead to the formation of superoxide, in both the inner and outer sides of the inner mitochondrial membrane (17,19).

Complex I (NADH dehydrogenase, also named NADH-ubiquinone oxidoreductase), appears to be the primary source of superoxide formation in the brain,

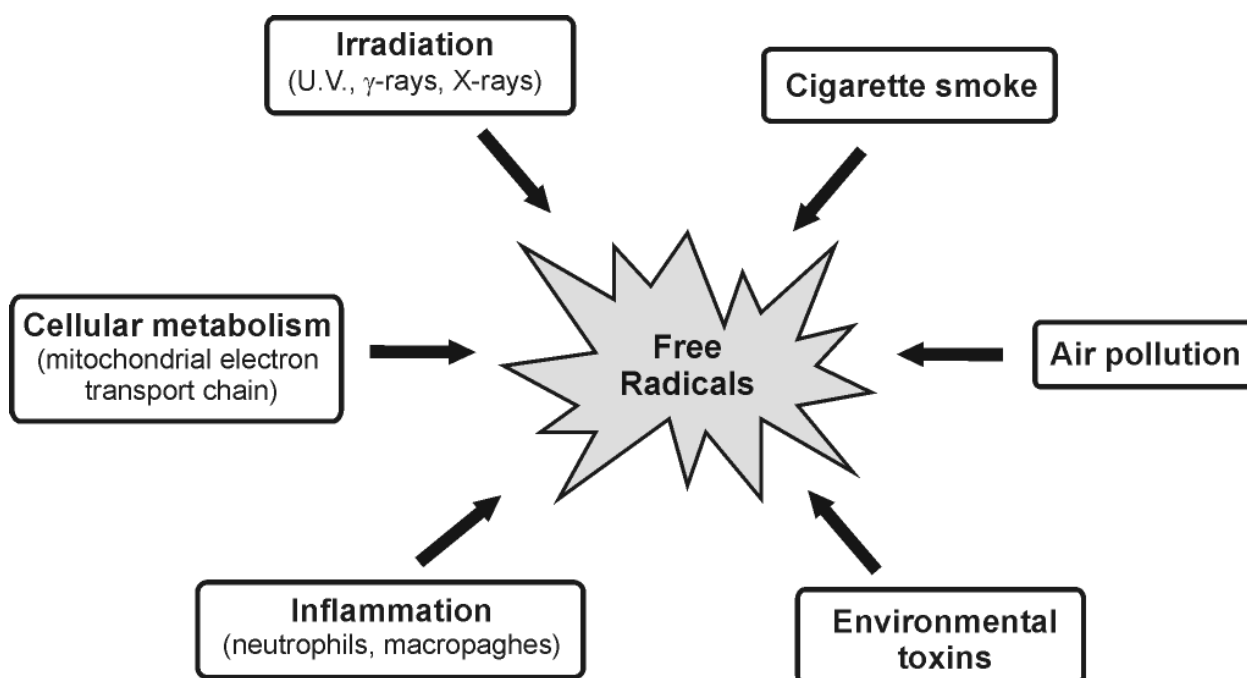


Figure 1. Summary of exogenous and endogenous sources of free radicals.

under normal conditions (18,20). It oxidises NADH using ubiquinone as an electron acceptor in a reversible reaction coupled with a proton pump generating transmembrane potential. To date, the increase in ROS production in this complex has been observed in three different situations: during normally functioning respiratory chain, in the presence of rotenone (an inhibitor that blocks the transfer of electrons from complex I to ubiquinone) and during reverse electron transfer (a set of reactions in the respiratory chain that allow electrons to be transferred against the gradient of redox potentials of electron carriers, from reduced ubiquinone to NAD^+ , instead of oxygen).

Besides mitochondria, there are other endogenous sources of ROS. For example xanthine oxidase, a widely distributed enzyme in the tissues of mammals, during the catalisation of the reaction of hypoxanthine to xanthine and xanthine to uric acid, leads to the reduction of molecular oxygen, forming the superoxide anion in the first step and hydrogen peroxide in the second one (21). Additional sources of cellular ROS are inflammatory cell activation (neutrophils, eosinophils and in particular macrophages) (22), cytochrome P450 metabolism (namely following the breakdown or uncoupling of the P450 catalytic cycle) (23), and peroxisomes, which mainly lead to the production of H_2O_2 (24).

1.2. Chemistry and biochemistry of ROS/RNS

The most common intracellular forms of reactive oxygen and nitrogen species include radical ($\text{O}_2^{\cdot-}$, $\cdot\text{OH}$, $\cdot\text{NO}$, among others), as well as non-radical (O_2 , ONOO^- , H_2O_2 , HOCl , O_3) moieties, that can be deleterious to cells (25).

Free radicals can be defined as molecules or molecular fragments, capable of independent existence, which contain one or more unpaired electrons. The presence of these unpaired electrons confers them a considerable degree of reactivity, since they need another electron to fill the orbital and become stable (1,26). Free radicals are often reactive species, although the opposite is not always true. Hydrogen peroxide (H_2O_2), for example, although considered a reactive species, is not regarded as a free radical since it has no unpaired electrons in its structure (27). On the other hand, molecular oxygen (dioxygen, O_2) has a unique electronic configuration and is considered a reactive species.

The addition of one electron to molecular oxygen forms the superoxide anion radical ($\text{O}_2^{\cdot-}$), which, despite being a free radical, is not highly reactive, since it lacks the ability to cross lipid membranes. In this way, it stays enclosed in the compartment where it is generated (27). It is considered the "primary" ROS, from which "secondary" ROS can be generated (26), and arises mainly through metabolic processes (electron transport chain in the mitochondria, flavoenzymes like

xanthine oxidase, lipoxygenases and cyclooxygenases, and NADPH oxidase). In the presence of superoxide dismutase, two molecules of this radical can easily be transformed to hydrogen peroxide and molecular oxygen (28).

Singlet oxygen is also a very reactive ROS that induces various genotoxic, carcinogenic, and mutagenic effects through its action on polyunsaturated fatty acids (PUFAs) and DNA (29).

Hydrogen peroxide (H_2O_2) is not a free radical. Nonetheless, it is highly important, much because of its ability to penetrate biological membranes. It plays a radical forming role as an intermediate in the production of more reactive ROS molecules including HOCl (hypochlorous acid) by the action of myeloperoxidase (an enzyme present in the phagosomes of neutrophils) and, most importantly, in the formation of the hydroxyl radical *via* oxidation of transition metals (1,27). Once produced, H_2O_2 is removed by at least three antioxidant enzyme systems, namely catalases, glutathione peroxidases, and peroxiredoxins (27).

The hydroxyl radical ($\cdot\text{OH}$) is highly reactive, being able to attack and damage all biomolecules: carbohydrates, lipids, proteins, and DNA (10). Since it has a half-life in aqueous solution of less than 1 nanosecond, when produced *in vivo*, this radical reacts close to its site of formation. Production of $\cdot\text{OH}$ close to DNA could lead to this radical reacting with DNA bases or the deoxyribose backbone of DNA to produce damaged bases or strand breaks (26). It can be generated through several mechanisms, including ionising radiation and photolytic decomposition of alkylhydroperoxides, but the majority of the hydroxyl radicals produced *in vivo* comes from metal catalysed (mainly involving iron and copper) breakdown of hydrogen peroxide, according to the Fenton reaction (21,27). Superoxide also plays an important role in this reaction, by recycling the metal ions.

Transition metals thus play an important function in the formation of various free radicals, as is the case of hydroxyl radicals. The redox state of the cell is largely linked to an iron (and sometimes copper) redox couple and is maintained within strict physiological limits. In fact, iron, for example, is required by the human body for the synthesis of several enzymes and its adequate supply during early life is essential for normal brain development (10,30). However, its ability to transfer single electrons as it oscillates between the ferrous and ferric states makes it a powerful catalyst of free radical reactions (2). These transition metals can be released from proteins like ferritin and the [4Fe-4S] center of different enzymes of the dehydratase-lyase family, by reactions with the superoxide anion (27,31).

Nitric oxide ($\cdot\text{NO}$) is synthesised from L-arginine by three isoforms of nitric oxide synthase (NOS): neuronal nitric oxide synthase (nNOS), endothelial nitric oxide synthase (eNOS), and inducible nitric

oxide synthase (iNOS) (32).

Like superoxide anion, $\cdot\text{NO}$ does not readily react with most biomolecules, despite its unpaired electron. On the other hand, it easily reacts with other free radicals (*e.g.* peroxy and alkyl radicals), generating mainly less reactive molecules (33), thus in fact functioning as a free radical scavenger (27). In addition, nitric oxide seems to be also involved in neurotransmission, regulation of vascular relaxation and in inflammatory processes (32,34). However, it can react with the superoxide anion, yielding peroxynitrite (ONOO^-). This compound has the capacity to act in a hydroxyl radical-like manner to induce lipid and protein oxidation, readily reacts with CO_2 to form nitroso peroxycarboxylate (ONOOCO_2^-), can become protonated as peroxonitrous acid (ONOOH) and undergo homolysis to form either $\cdot\text{OH}$ and $\cdot\text{NO}_2$, or be rearranged to nitrate (NO_3) (35). In addition, peroxynitrite is known to play a key role in neuronal damage associated with excitotoxicity (36).

Other reactive species derived from oxygen that can be formed in living systems include peroxy radicals ($\text{ROO}\cdot$). The simplest peroxy radical is $\text{HOO}\cdot$, which is the protonated form of superoxide and is usually termed either hydroperoxy radical or perhydroxyl radical. Its involvement in the initiation of lipid peroxidation has already been demonstrated (5).

1.3. Physiological functions of reactive species

Reactive species are known to play a dual role in biological systems, since they can be either harmful or beneficial to living systems (26). These species are maintained at low, but measurable, concentrations in the cells, through a balance between their rates of production and their rates of removal by antioxidants. Thus, each cell is characterised by a particular concentration of electrons (redox state) stored in many cellular constituents, and the redox state of a cell and its oscillation determines cellular functioning. A temporary shift of the intracellular redox state towards more oxidising conditions results in a temporary imbalance that represents the physiological basis for redox regulation (37).

A great number of physiological functions are controlled by redox-responsive signalling pathways (7). Several evidences suggest that ROS participate in the defence against intrusion of foreign bodies (38). Activated neutrophils and macrophages produce large quantities of ROS *via* the phagocytic isoform of NAD(P)H oxidase, in order to kill the pathogens. This massive production of ROS during an inflammatory event is called "oxidative burst" and plays an important role as the first line of defence against environmental pathogens (5,27). At a smaller scale, some types of non-phagocytic cells, like fibroblasts, vascular smooth muscle cells, cardiac myocytes and endothelial cells,

are also known to produce ROS by NAD(P)H oxidase to regulate intracellular signalling cascades. Thus, ROS play an important role in the regulation of cardiac and vascular cell functioning (39).

Nitric oxide plays several regulatory functions. In fact, its own production by iNOS, the only isoform of NOS that is not constitutively expressed, is regulated at the transcriptional and post-transcriptional levels by signalling pathways involving redox-dependent transcription factor NF- κ B or mitogen-activated protein kinases (MAPKs). In addition, $\cdot\text{NO}$, in combination with H_2O_2 , leads to the activation of the enzyme soluble guanylate cyclase (sGC), which catalyses the formation of cyclic guanosine monophosphate (cGMP) that, by its turn, is used as an intracellular amplifier and second messenger in a variety of physiological responses, such as modulation of protein kinases, ion channels, smooth muscle tone and inhibition of platelet adhesion (7,40).

In higher organisms, oxygen homeostasis is maintained by a tight regulation of the red blood cell mass and respiratory ventilation. It has been proposed that changes in oxygen concentration are sensed independently by several different ROS-producing proteins, including a *b*-type cytochrome. Other studies also suggested that a change in the rate of mitochondrial ROS may play a role in this oxygen sensing by the carotid bodies, which are sensory organs that detect alterations in arterial blood oxygen. Other responses to changes in oxygen pressure include the regulated production of certain hormones (*e.g.* erythropoietin) controlled by the transcription hypoxia inducible factor-1 (HIF-1) (41,42).

ROS also seem to be involved in cell adhesion, a mechanism that plays an important role in embryogenesis, cell growth, differentiation, wound repair, among other processes. The expression of cell adhesion molecules is stimulated by bacterial lipopolysaccharides and by various cytokines such as TNF, interleukin-1a, and interleukin-1b. The adherence of leukocytes to endothelial cells is also induced by ROS. Moreover, the oxidant-induced adherence of neutrophils is inhibited by hydroxyl radical scavengers or iron chelators, suggesting that the induction of adherence may be mediated by hydroxyl radicals generated from hydrogen peroxide within the cell (7,43).

Reactive oxygen and nitrogen species can directly affect the conformation and/or activities of all sulfhydryl-containing molecules, such as proteins or glutathione (GSH), by oxidation of their thiol moiety. This type of redox regulation affects many proteins important for signal transduction and carcinogenesis, such as protein kinase C, Ca^{2+} -ATPase, collagenase and tyrosine kinases, among many other enzymes and membrane receptors (44). In addition, ROS/RNS are known to trigger apoptotic cell death, by causing Bcl-2 (a protein located in the outer membranes of mitochondria) to activate a related protein, Bax, which

by its turn leads to the release of cytochrome *c* from mitochondria (14,45-47). This release then results in the activation of several other proteins, in a process that will be discussed further ahead (section 3.1.).

2. Oxidative damage to biomolecules

Due to their high reactivity, ROS are prone to cause damage and are thereby potentially toxic, mutagenic, and carcinogenic. Their targets include all biomolecules, namely proteins, lipids, and nucleic acids (48).

2.1. Proteins

Proteins can function as important targets for attack by ROS (48). Direct oxidation of the side chains of all amino acid residues of proteins (especially proline, arginine, lysine, and threonine) by ROS yields reactive carbonyl derivatives, particularly *via* metal-catalysed oxidation (49,50). Protein carbonyl derivatives can also be generated from the cleavage of peptide bonds by the α -amidation pathway or by oxidation of glutamyl residues. In addition, carbonyl groups may be introduced into proteins by secondary reaction of the primary amino group of lysine residues with reactive carbonyl derivatives (ketoamines, ketoaldehydes, deoxyosones), produced by the reaction of reducing sugars or their oxidation products with lysine residues of proteins (glycation/glycooxidation reactions), eventually leading to the formation of advanced glycation end-products (AGEs). Finally, carbonyl groups may be formed by adduction of byproducts of lipid peroxidation. These include malondialdehyde, which reacts with lysine residues and α,β -unsaturated aldehydes (4-hydroxy-2-nonenal and acrolein), which can undergo Michael-addition reactions at their C=C double bond with the sulfhydryl group of cysteine, the ϵ -amino group of lysine or the imidazole group of histidine residues, forming advanced lipoxidation end-products (ALEs) (32,50).

The introduction of carbonyl derivatives may alter the conformation, and/or even cause fragmentation, of the polypeptide chain, thus determining the partial or total inactivation of proteins. In addition, it can result in the loss of enzymatic activity, increased proteolytic degradation, altered cellular functions such as energy production, interference with the creation of membrane potentials and changes in the type and level of cellular proteins (48,50,51).

Protein carbonyl content is the most widely used marker for the measurement of protein oxidation. Highly sensitive assays for the detection of protein carbonyls involve derivatisation of the carbonyl group with 2,4-dinitrophenylhydrazine (DNPH), which results in the formation of a stable 2,4-dinitrophenyl (DNP) hydrazone product. Stable DNP adduct can then be detected spectrophotometrically, a technique that can be

coupled to protein fractionation by high-performance liquid chromatography (HPLC). Alternatively, in recent years, identification of carbonylated proteins has been performed by immunoblotting analysis, with the use of specific antibodies anti-DNP (52).

Protein damage is likely to be repairable and is a known non-lethal event for a cell. However, oxidation of proteins is associated with a number of age-related diseases including (but not limited to) Alzheimer's disease, Parkinson's disease, rheumatoid arthritis, amyotrophic lateral sclerosis, and ageing (49). Additionally, two examples of human pathologies in which pathophysiological aspects of protein carbonylation have been extensively investigated are adult (or acute) respiratory distress syndrome (ARDS) and inflammatory bowel diseases (IBDs) (52).

2.2. Lipids

Polyunsaturated fatty acids (PUFAs), because of their multiple double bonds, are also extremely sensitive to oxidation by free radical attack. In addition, PUFAs can be formed enzymatically by the action of lipoxygenases (53). Arachidonic and linoleic acids are the main PUFAs in the mammalian membranes and are able to undergo both enzymatic and non-enzymatic lipid peroxidation. However, since linoleic acid is much more abundant than arachidonic acid, most of lipid peroxidation products derive from the former (28).

Briefly, the overall process of lipid peroxidation consists of three main stages: initiation, propagation and termination. Lipid peroxidation may be induced when a radical species (*e.g.* hydroxyl radicals generated *via* Fenton reaction) is sufficiently reactive to remove a hydrogen atom from the polyunsaturated lipid (LH), leading to the formation of a lipid radical (L \cdot), which results in the formation of lipid hydroperoxide (LOOH) species (Figure 2). Thus, many molecules of lipids may be oxidised to lipid hydroperoxides for every initiation event. Termination reactions occur when two radical species combine to form non-radical final products or when substrate is depleted (54,55).

Once formed, lipid hydroperoxides can degrade rapidly into a variety of breakdown products, such as malondialdehyde (MDA), C₃-C₁₀ straight chain aldehydes, and α,β -unsaturated aldehydes, including 4-hydroxy-2-nonenal (4-HNE) and acrolein (56,57). In addition, lipid peroxidation also leads to production of isoprostanes and neuroprostanes. Although these molecules do not show toxicity, they serve as excellent markers of arachidonic and docosahexaenoic acid peroxidation in brain and cerebrospinal fluid (57).

Estimates of lipid peroxidation can be obtained by measuring the formation of lipid hydroperoxides and their breakdown products, as well as by quantifying the disappearance of PUFAs. The most widely used method to assess oxidative damage to lipids is the thiobarbituric

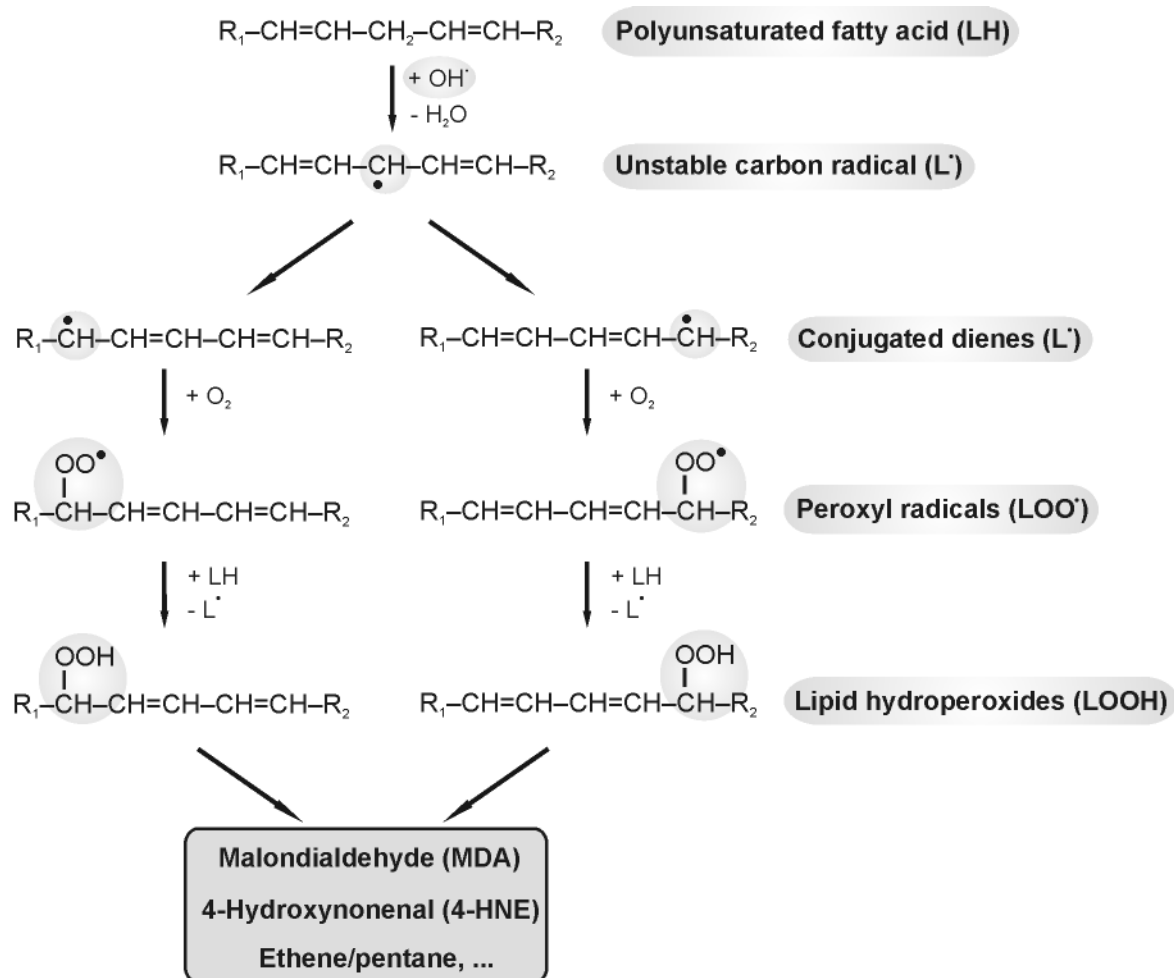


Figure 2. Basic reactions occurring during lipid peroxidation. Reactive species (e.g. hydroxyl radicals) abstract an hydrogen atom from a polyunsaturated fatty acid, yielding a lipid radical (L') that may undergo some molecular rearrangements. Oxygen uptake by these radicals propagates the reaction *via* peroxy radicals (LOO'), which leads to the formation of lipid hydroperoxides (LOOH). These can then combine and generate the final products of lipid peroxidation (e.g. MDA 4-HNE, acrolein, ethane/pentane, among others). Modified from Spiteller, 2001 (28).

acid reactive substances (TBARS) assay, which is thought to reflect the production of MDA (56,58).

Some byproducts of lipid hydroperoxidation have been reported to possess cytotoxic, mutagenic, and genotoxic properties (58). For example, MDA, 4-HNE, and acrolein can damage DNA either by reacting directly with DNA bases or by generating more reactive bifunctional intermediates, which form exocyclic DNA adducts with a five-membered ring (etheno adducts) or a six-membered ring (propane adducts) attached to DNA bases. These adducts can then induce base pair substitution mutations (59). Hydroxynonenal and acrolein are neurotoxic and can, among other things, inhibit enzymes critical for neuron survival (57). Moreover, lipid peroxidation seems to be also involved in atherosclerotic processes. The oxidation of low density lipoproteins (LDL) results in their uptake by phagocytes in the subendothelial space *via* their scavenger receptor. These phagocytic cells then accumulate in the subendothelial space, where they stimulate formation

of atherosclerotic plaques (60).

2.3. DNA

Damage to nuclear DNA has been proposed to occur through two different mechanisms: oxidative modification and DNA fragmentation mediated by endonucleases (an irreversible feature of programmed cell death). While the latter is supposed to take place during the late stage of cell death, oxidative DNA damage is believed to stand for an early event (61,62). Mitochondrial DNA has, by its turn, been reported to be even more susceptible to oxidation than nuclear DNA. The greater accumulation of damage may be related to: mitochondria being the main producers of ROS in the cells; repair capacity of mitochondrial DNA being limited (proteins responsible for DNA repair are expressed in lower levels in mitochondria); and mitochondrial DNA not being protected by histones (63,64).

The attack of ROS and RNS is responsible for

introducing several modifications to DNA, which include: oxidised bases, the most studied being 8-oxo-7,8-dihydroguanine (8-oxo-Gua), a product derived from the oxidation of a guanine by ROS; modifications to the sugar moiety of DNA, which may result in base loss – abasic (apurinic/apyrimidinic) sites – and/or strand breakage (single- and double-strand breaks); DNA-DNA intra-strand adducts and DNA-protein cross-links (65,66). The formation of some of these lesions is summarised in Figure 3. In addition, exposure of cells to UV radiation can result in dimerisation reactions between adjacent pyrimidine bases, yielding cyclobutane pyrimidine dimers (CPDs) and pyrimidine(6-4)pyrimidone photoproducts (67,68).

DNA lesions, if left either un- or mis-repaired, may interfere with DNA-dependent processes (such as transcription, replication, recombination, and chromosome segregation), leading to mutations, chromosomal instability, and even cell death (69). Therefore, cells are equipped with specific and efficient repair mechanisms, which are able to repair the modifications introduced in DNA (70). During these repair processes, cell cycle may be arrested at any checkpoint, which allows a time window to repair damaged DNA (69,71). In addition, it should also be noted that oxidative stress leads to an upregulation of the expression of many repair enzymes, which may result in an enhancement of enzymatic repair mechanisms (26,72).

DNA double-strand breaks are repaired *via* two different mechanisms: homologous recombination (HR), in which the sister chromatid is used as a template to copy the missing information into the

broken locus (73), and non-homologous end joining (NHEJ), which consists in the fusion of the two broken ends with little or no regard for sequence homology, a process that may result in mutations (74). The mismatch repair (MMR) pathway plays an important role in the post-replicative process, by repairing replicative and recombinatorial errors that may result in mismatched bases (mismatches) (75,76). The nucleotide excision repair (NER) pathway recognises bulky adducts, as well as covalent linkages between adjacent pyrimidines resulting from exposure to UV radiation, and removes short DNA oligonucleotides containing a damaged base; it can be classified into global genome repair (GG-NER), which removes DNA damage from the entire genome, and transcription-coupled repair (TC-NER), which specifically removes damage from the transcribed strand of active genes, thereby releasing transcription arrest that occurs at the lesions sites (71,77). However, oxidatively damaged DNA is mainly removed by the base excision repair (BER) pathway, in which oxidised bases are eliminated by different DNA glycosylases, leaving abasic sites (78,79).

Base excision repair consists of four main steps (base removal, apurinic/apyrimidinic site incision, synthesis, and ligation), and can be divided in two sub-pathways, the short patch or single nucleotide replacing pathway and the long patch pathway (Figure 4), which involves the incorporation of up to 13 nucleotides (64,80).

BER follows mainly through the short patch pathway. In the first step of this pathway, a damaged base is recognised and removed from the deoxyribose phosphate moiety (80). Two classes of DNA glycosylases are involved in this step: Class I (bifunctional or complex), which includes, for example, 8-oxoguanine DNA glycosylase 1 (OGG1), an enzyme that removes 8-oxoguanine and nicks the DNA backbone; and Class II (monofunctional or simple), including N-methylpurine DNA glycosylase (MPG) and uracil DNA glycosylase (UDG), which remove alkylated DNA bases or uracil, respectively, but without nicking the DNA backbone (72,81). Due to the catalytic inefficiency of OGG1's lyase activity, this enzyme remains stuck to the site of incision, limiting the overall rate of repair (78,82). So, following the glycosylase reaction, APE1 (apurinic/apyrimidinic endonuclease, also called APEX, HAP1 and Ref-1), easily displaces the glycosylase and cleaves the 5' terminus of the apurinic/apyrimidinic (AP) site, resulting in the loss of a base and a single-strand break with 5'-phosphate and 3'-OH termini (step 2) (64,81). Additionally to its role in BER, APE1 has also been implicated in the redox activation of transcription factors, such as p53 (83). In the third step of BER, the AP site that is generated by the APE1 repair activity is removed by deoxyribosephosphate hydrolase (dRPase) activity provided predominantly by DNA β -polymerase (β -pol). This is then followed by the insertion of a new base by

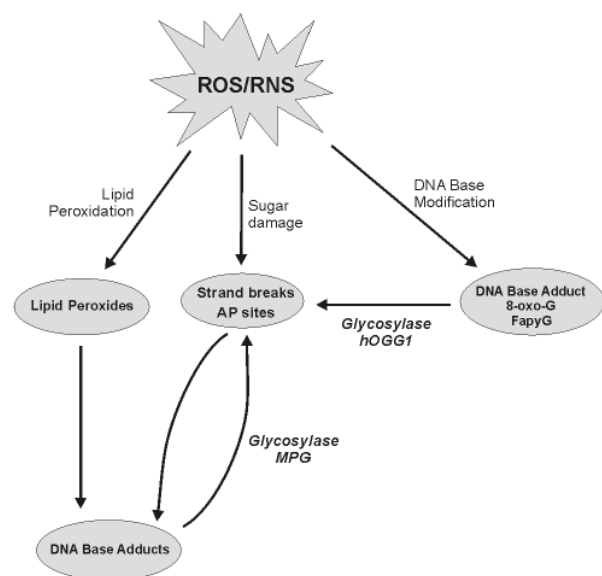


Figure 3. Types of DNA damage induced by reactive oxygen species. Abbreviations: 8-oxo-G, 8-oxo-7,8-dihydroguanine; FapyG, 2,6-diamino-4-hydroxy-5-formamidopyrimidine; hOGG1, human 8-oxoguanine DNA glycosylase 1; MPG, N-methylpurine DNA glycosylase. Modified from Powell *et al.*, 2005 (66).

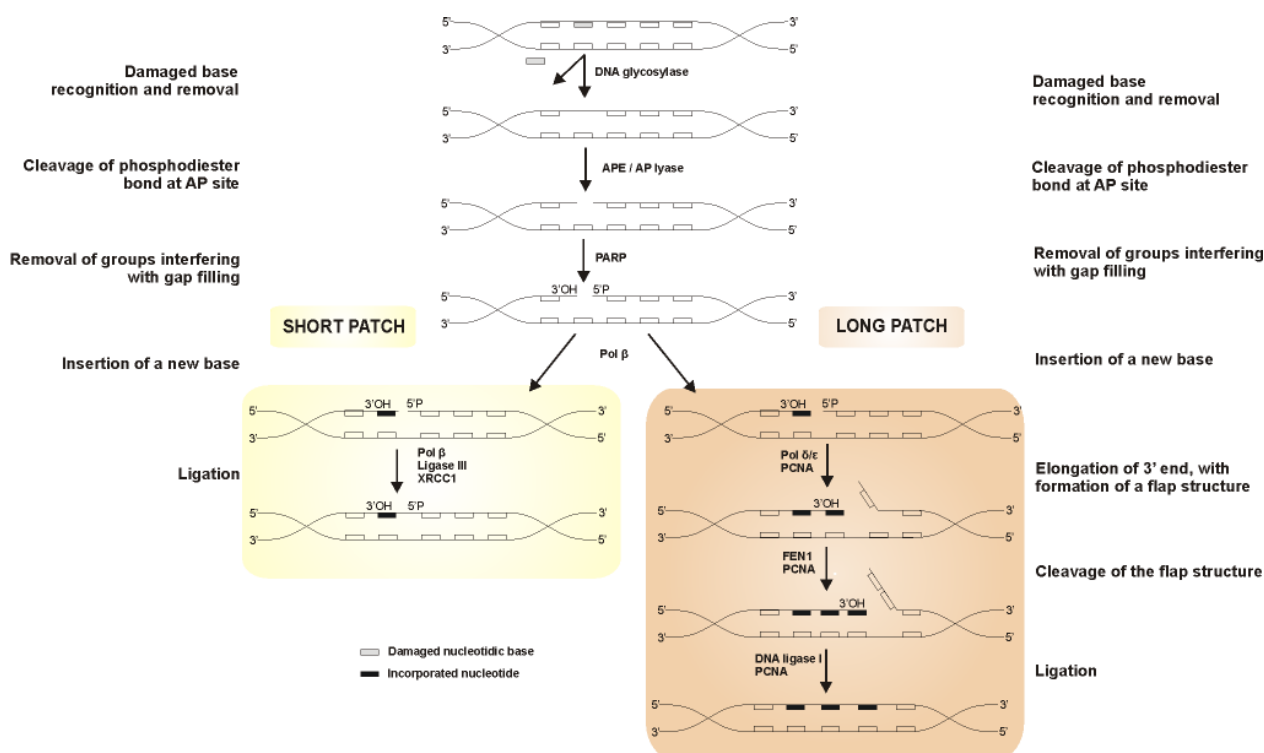


Figure 4. Base excision repair pathways. First, a damaged base is recognised and removed by DNA glycosylases, yielding an apurinic/aprimidinic (AP) site, which is then cleaved by an endonuclease (APE), forming a strand break. Then, after some chemical groups that may interfere with gap filling and ligation are removed, different polymerases (depending whether the short patch or the long patch pathway is active) fill the gap in the DNA strand. Finally, DNA ligase inserts one (SHORT PATCH) or more (LONG PATCH) new bases. Other proteins, like poly (ADP-ribose) polymerase (PARP), XRCC1, proliferating cell nuclear antigen (PCNA), and FEN1 aid in the regulation of these pathways. The bacterial enzymes FPG and Endo III, used in the Comet assay, act on the first step of this pathways (damaged bases recognition and removal). Modified from Tudek *et al.*, 2006 (84).

β -pol and ligation by DNA ligase I (step 4) (72).

The long patch pathway is catalysed by β -pol or other polymerases like δ/ϵ -pol, which have a proof-reading activity associated to them. Repair follows this pathway when the terminal sugar phosphate formed after the APE1 incision (step 2) develops a complex structure that cannot be acted upon by the dRPase activity of β -pol (*e.g.* oxidised abasic site). In this case, the repair synthesis still continues, but in a strand displacement manner (80,84).

It should be noted that despite the presence of all these DNA repair systems, DNA damage still occurs. In fact, DNA is continuously attacked by reactive species, an event that can be attenuated by antioxidant defences. Whereas some of the damage induced by ROS attack to DNA can induce the signalling pathways leading to apoptotic cell death, the majority results in the oxidation of DNA. However, DNA repair enzymes help to maintain an equilibrium state between damage formation and repair, by repairing most of the oxidised DNA (81). This implies that, in normal physiological conditions, oxidative damage is maintained at a tolerable level in terms of genetic stability (81,85). Nevertheless, the oxidised DNA that does not get repaired can become mutated, which may then result in further damage to cells.

There are several methods that allow the

measurement of oxidative DNA damage. However, determining the background levels of the most common product of DNA damage, 8-oxo-Gua, has brought some difficulties, since damage can arise from the preparation of samples. With the purpose of normalizing the procedures to measure this kind of damage, the European Standards Committee on Oxidative DNA Damage (ESCODD) was formed (86,87). Although some chromatographic methods, like gas chromatography (GC) and high performance liquid chromatography (HPLC), usually coupled to mass spectrometry (MS) techniques, have been employed, they have shown inflated values, probably due to erroneous oxidation during DNA isolation. So, a set of enzymatic methods has been described as the most suitable. These methods make use of the bacterial DNA repair enzyme formamidopyrimidine DNA glycosylase (FPG) to convert 8-oxo-Gua to apurinic sites, which can then be measured by the Comet assay, alkaline unwinding or alkaline elution (66,86).

The Comet assay is a simple, fast, and sensitive method that detects DNA strand breaks and abasic sites, although it can detect oxidised bases *via* the use of repair enzymes, such as FPG or endonuclease III (Endo III), which nick DNA at oxidised purines and pyrimidines, respectively, at the initial step of the BER pathway (Figure 4). Moreover, this assay reduced the risk of occurring

oxidation during sample preparation (88).

Oxidative DNA damage can result in the arrest or induction of transcription, induction of signal transduction pathways, replication errors, and genomic instability, all of which have been implicated in cancer and neurodegenerative diseases, besides being associated to the normal process of aging (89,90).

3. Cell death

The exposure to oxidative stress may ultimately result in cell death, as a consequence of severe damage caused to biomolecules by reactive oxygen and nitrogen species (27). Cell death can occur by two main mechanisms: necrosis and programmed cell death (PCD) (91).

Necrosis is usually referred as an "accidental", or uncontrolled, form of cell death (92). During this process, there is a rapid swelling of the cell, leading to the loss of membrane integrity and consequent release of the cells' contents, which is known to evoke an inflammatory response. In this way, cell death becomes a passive consequence of irreparable damage, hence the term "accidental" (92,93).

Apoptosis was initially considered as the only form of programmed cell death. However, more recently, a variety of cell behaviours that may lead to active forms of cell death have been observed. These include the typical apoptotic cell death, autophagic death, mitotic catastrophe, oncosis, anoikis, excitotoxicity, Wallerian degeneration, cornification, and paraptosis. In this way, and using nuclear morphology as a distinction criterion, programmed cell death has been divided into three possible classifications: classical apoptosis, autophagic cell death, and necrosis-like PCD (91,94,95).

Type I PCD or classical apoptosis has been described as an active process by which dying cells are removed in a safe, non-inflammatory manner (96). It is a tightly regulated process, involved in many vital functions, including tissue development, carcinogenesis, immune response, and control of the balance between proliferation and differentiation (45,97,98). At the morphological and biochemical levels, it is characterised by shrinkage of the cell, membrane surface blebbing, oligonucleosomal DNA fragmentation, and the breakdown of the cell into various membrane-bound fragments, called apoptotic bodies. Along with these events, occurs the activation of specific cysteine proteases, named caspases, as well as the loss of membrane phospholipid asymmetry, which results in the externalisation of phosphatidylserine (99). Type II PCD or autophagic cell death is mainly characterised by the presence of double- or multiple-membrane vacuoles, mitochondrial dilation, as well as enlargement of the endoplasmic reticulum (ER) and Golgi apparatus (94). The vacuoles formed during this process, which are also called autophagosomes,

engulf portions of cytoplasm and organelles (like mitochondria and ER), then fuse with lysosomes, where the intravacuolar content is disintegrated by lysosomal enzymes (100). Nevertheless, it should be noted that "autophagic cell death" is a process that differs from autophagy. Indeed, autophagy is a dynamic process of protein degradation, used mainly to provide an alternative source of nutrients, which is usually associated to cell death, with either necrotic or apoptotic phenotype (91,93). The mammalian protein kinase TOR (which stands for "target of rapamycin") plays a major role in the regulation of the autophagic process, by inhibiting this pathway. Downstream of this protein, several other proteins encoded by *Atg* genes intervene in the execution of the autophagic process (92,100). The identification of these genes and the observation that their inactivation protects from this type of death, supports the evidence of this PCD as a specific type of death.

Recently, an active form of necrosis (type III PCD) was found to occur, not only under pathological conditions, but also under normal physiological conditions (91). It lacks caspase and lysosomal involvement and is mainly characterised by an early swelling of intracellular organelles, followed by loss of plasma membrane integrity (although nuclear disintegration is retarded). This type of PCD can also be subdivided into two sub-types: IIIA or "non-lysosomal disintegration", characterised by nuclear disintegration, and IIIB or "cytoplasmic degeneration", which displays karyolysis (complete dissolution of the chromatin of a dying cell). Moreover, programmed necrosis can occur by the induction of the tumour necrosis factor (TNF) or Fas ligand, *via* their respective death receptors, and gives an idea that necrosis is in fact a process that cells can control (91,92,94).

3.1. Programmed cell death pathways

Apoptosis, the most common form of programmed cell death, is a complex process involving both pro- and anti-apoptotic proteins, which can be initiated by two different signalling pathways: the death receptor (extrinsic) pathway and the stress- or mitochondria-mediated (intrinsic) pathway (93,101). A set of highly conserved cysteine-dependent aspartate-specific proteases, named caspases, are regarded as the central executioners of apoptosis. These caspases use a cysteine residue as the catalytic nucleophile and share specificity for cleaving their substrates after aspartic acid residues in target proteins (102,103).

The main intracellular signalling pathways leading to apoptotic cell death are summarised in Figure 5.

The death receptor or extrinsic pathway is activated by the binding of an extracellular ligand, such as Fas (also known as CD95 or APO-1) ligand, tumour necrosis factor (TNF) or TNF-related apoptosis induced

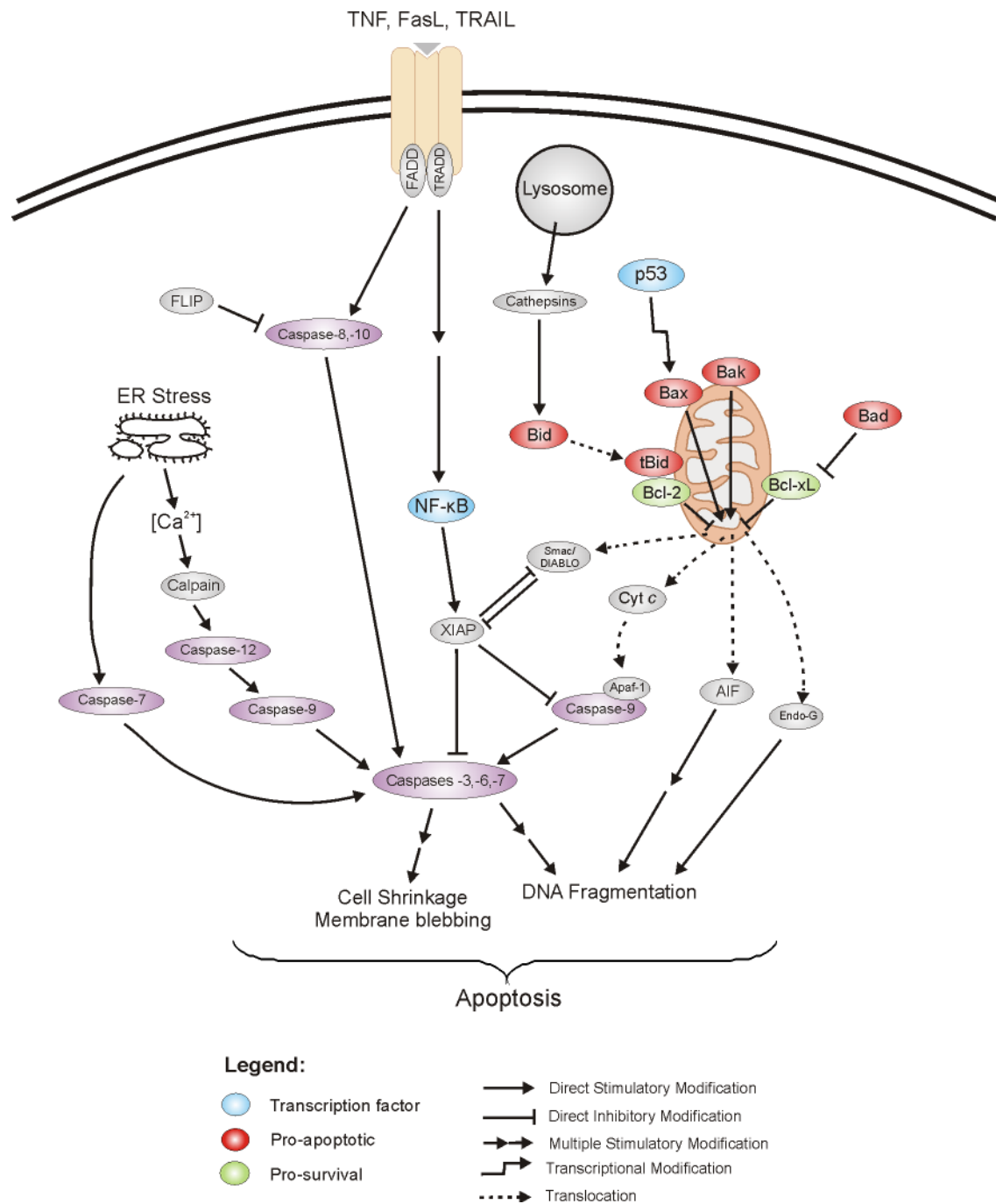


Figure 5. Main intracellular pathways leading to apoptosis and some ways by which they can be regulated. The extrinsic pathway is activated by the binding of an extracellular ligand to specific death receptors, which activate caspase-8. The mitochondrial pathway is activated by Bax or Bak, which bind the mitochondrial outer membrane, inducing the release of several pro-apoptotic factors, such as cytochrome *c*, which then forms the apoptosome upon binding to Apaf-1 and caspase-9. These two pathways can be connected by the cleavage of Bid and both of them result in the induction of effector caspases, like caspase-3, which then activate substrate responsible for the common features of apoptosis. The caspase-independent pathway, mediated by AIF, as well as the lysosomal involvement in cell death and the ER stress-mediated events are also shown in this scheme.

ligand (TRAIL), to their specific death receptors present in the cell membrane (104,105). This results in the recruitment of procaspase-8 and subsequent activation of caspase-8, which then leads to the activation, either directly or indirectly, of downstream caspases, like procaspase-3 (104,106) (Figure 5).

As shown in the same figure (Figure 5), the mitochondrial or intrinsic pathway can be initiated by the translocation of several proapoptotic proteins

from the Bcl-2 family (*e.g.* Bax, Bid or Bad) to the mitochondria (107). These proteins induce the permeabilisation of the mitochondrial outer membrane (MOMP), which has been considered as a point of no return in cell death (101,108). As a consequence of an increase in its permeability, mitochondria release several proapoptotic factors normally present in the intermembrane space, which include cytochrome *c*, the serine protease HtrA2/Omi, the Apoptosis Inducing

Factor (AIF), Smac/DIABLO (which stands for second mitochondria-derived activator of caspases/Direct IAP Binding Protein With Low pI) and endonuclease G (98,102,107).

The released cytochrome *c* can bind to procaspase-9 and Apaf-1 (from apoptotic protease-activating factor 1) in the presence of deoxyadenosine triphosphate (dATP)/adenosine triphosphate (ATP). This complex, termed the apoptosome, results in the activation of caspase-9, which is mainly activated through this mitochondrial pathway (97,109).

The intrinsic and extrinsic pathways can be interconnected by the action of Bid, a protein from the Bcl-2 family (see Figure 5). This protein is normally found in the cytosol, where it can be cleaved by caspase-8. After cleavage, the carboxylic terminus of Bid is translocated to mitochondria, leading, directly or indirectly (by interaction with Bax) to the release of cytochrome *c* (104,110).

Both activated caspase-8 (as well as caspase-2 and -10, also mediators of the death-receptor pathway) and the activated caspase-9 (from the mitochondrial pathway) converge to the downstream activation of effector caspases, such as procaspase-3, -6, and -7 (98). These caspases activate a DNase, which is responsible for the fragmentation of oligonucleosomal DNA (98,111). In addition, other enzymes and/or substrates, like poly-(ADP-ribose) polymerase (PARP), fodrin, p75, actin, among others, are activated in the process, culminating in the display of several of the phenotypic characteristics of apoptotic cell death, including loss of mitochondrial membrane potential, cell blebbing, and redistribution of lipids in the outer plasma membrane (105).

Alternatively to the caspase-dependent pathways, the characteristic features of apoptosis can be induced by a caspase-independent way, mediated by the apoptosis inducing factor (AIF). This is a mitochondrial flavoprotein oxidoreductase that translocates first to the cytosol and then to the nucleus (111,112). Once in the nucleus, AIF interacts with nucleic acids, causing caspase-independent chromatin condensation and DNA fragmentation (94).

The endoplasmic reticulum (ER) can also act in the induction and regulation of apoptosis. ER is known to play a central role in protein biosynthesis and is the major intracellular organelle involved in calcium storage (113). Calcium homeostasis is maintained by some members of the Bcl-2 family, like Bax and Bak, which can also be associated to the ER membrane. Upon an apoptotic stimulus, these proteins induce calcium release through ER calcium channels, such as the inositol 1,4,5-triphosphate (IP₃) receptors, whose opening is mediated by the binding of IP₃. Calcium from the ER is then taken up by mitochondria, causing a calcium overload that subsequently results in the induction of mitochondrial membrane permeabilisation

by mitochondria-located Bax and Bak (114,115). Moreover, calcium release from the ER can induce the activation of calpains and caspase-12, which by their turn lead to the activation of other caspases, resulting in the propagation of the apoptotic signal (113). It should be noted that many factors are able to regulate these pathways, by activating or inhibiting them at specific sites (Figure 5).

Recently, a regulated lysosomal involvement in cell death has also been observed. In fact, partial lysosomal membrane permeabilisation has been described to trigger apoptosis and apoptosis-like cell death, in response to several apoptotic stimuli, such as activation of death receptors of the tumour necrosis factor (TNF) family, p53 activation, oxidative stress, among others (116). These stimuli can then lead to lysosomal membrane permeabilisation through either caspase-dependent or -independent mechanisms, which normally results in the release of a group of proteases named cathepsins (including cathepsins B, D, and L) from the lysosome to the cytosol (117). In addition, lysosomal enzymes have been found to act on mitochondria and induce the formation of mitochondrial ROS, which can then lead to further lysosomal permeabilisation (118). Moreover, it has been reported that mild stress triggers only a limited release of the lysosomal contents to the cytosol followed by apoptosis or apoptosis-like cell death, while elevated stress levels cause a generalised lysosomal rupture and rapid cellular necrosis (119). This lysosomal apoptotic signalling pathway has recently been considered as an attracting drug target, namely in cancer therapeutics (120).

Occasionally, deficiencies in the cell cycle checkpoints, which by its turn lead to aberrant mitosis, may result in another type of programmed cell death, termed mitotic catastrophe. This process is mainly characterised by enlarged and multinucleated cells, incomplete nuclear condensation, chromosome alignment defects, and unequal DNA separation (93,121,122).

3.2. The role of ROS/RNS in the induction of cell death

The intracellular accumulation of reactive oxygen and nitrogen species also plays an important role in the initiation of cell death processes (123). In fact, the amount of reactive species accumulated in the cell, and the way the cell responds to that redox imbalance, can determine that same cell's fate. For example, mild oxidative stress may activate biological responses that can either lead to survival and proliferation, or can induce apoptosis, while the accumulation of high levels of ROS may promote necrosis instead (124,125). Moreover, a sudden burst of ROS, resulting from the response to oxidative stress of cells already committed to apoptosis, can direct those cells towards a necrotic-like death (14,123).

The accumulation of reactive species has been described to precede changes in the mitochondrial membrane, nuclear condensation, and other typical apoptotic events (14,126). Indeed, some studies have reported that an increase in ROS induces cytochrome *c* release from mitochondria (in a voltage-dependent anion channel (VDAC)-dependent way), and caspases activation (13,127,128).

Many studies have shown other evidences for the induction of apoptotic pathways by reactive species. Some mediators of apoptosis (*e.g.* JNK, ERK, PTEN) have been reported to lead to increased levels of ROS (129,130). Similarly, it has been shown that inhibition of the mitochondrial respiratory chain at complex I (131), or an impairment of the electron transfer chain by mutations in mitochondrial DNA, prevent the accumulation of ROS, and consequently protect cells against apoptosis (29,132). In addition, lipid peroxidation has also been reported to occur following an apoptotic signal (133,134). Moreover, and perhaps most important, inhibition of apoptosis by the addition of antioxidants has already been described (11,97,135,136). For example, the antioxidant enzyme MnSOD has been reported to inhibit apoptosis during ischemia/reperfusion injury (137), and "classical" antioxidants such as α -tocopherol and GSH have shown to prevent apoptosis induced by ascorbate-iron (134). Thus, these studies point towards a wide range of actions for ROS/RNS and add further importance to the use of antioxidants to prevent apoptosis and treat several disorders.

3.3. Intracellular regulation of cell death pathways

The intracellular pathways leading to apoptotic cell death can be regulated at several levels, including their blockade at the death-inducing signalling complex (DISC), which is responsible for the recruitment of procaspase-8, or the inhibition of their enzymatic activity. These regulators comprise inhibitors-of-apoptosis proteins (IAPs), the FLICE-like inhibitor protein (FLIP), and calpains (103). IAPs are a family of cellular proteins, including eight mammalian family members with highly conserved and differential expression patterns in various tissues, which bind to the surface of caspases, blocking the catalyzing grooves of caspases. These proteins do not inhibit caspase-8, but they inhibit its substrate, procaspase-3, instead, thus arresting the death-receptor pathway. In the mitochondrial pathway, XIAP, c-IAP1, and c-IAP2 bind directly to procaspase-9, preventing its activation (103,106). FLIP proteins have been described mainly as inhibitors of the death receptor pathway, since they are able, when overexpressed, to inhibit the activation of procaspase-8 at the DISC (138,139).

Calpains represent a family of calcium-dependent, nonlysosomal, cysteine proteases that share many

substrates with caspase-3, including fodrin, calcium-dependent protein kinase, and PARP. In addition, due to the presence of a calmodulin-like calcium-binding site in their structure, these proteases are involved in various calcium-regulated processes, like signal transduction, cell proliferation, platelet activation, and apoptosis (94,103). Moreover, calpains can also cleave Bcl-xL, an antiapoptotic protein, converting it into a pro-apoptotic molecule (113).

Ceramides, which represent the structural backbone of sphingolipids/sphingomyelin, are important second messengers in several cell processes, including apoptosis. Some of their targets in apoptotic signalling pathways include mitochondria, jun kinases (JNK), lysosomal cathepsin D, p38 mitogen-activated protein kinase (MAPK), Bcl-2 family members, among others (140,141). Although the exact mechanism is not yet fully understood, ceramides seem to induce apoptosis by inducing the release of cytochrome *c* from mitochondria to the cytoplasm (142), which might be related to their ability to form protein permeable channels in the mitochondrial membranes (141,143).

The release of cathepsins (a group of proteases that stand for "lysosomal proteolytic enzymes") from lysosomes to cytosol has also been found to be implicated in the regulation of apoptosis (144). This lysosomal permeabilisation seems to be an early event, occurring prior to the loss of mitochondrial transmembrane potential. Bcl-2 family members, particularly Bid, seem to be the main targets of cathepsins. Bid cleavage then leads to the activation of Bax, resulting in the consequent release of apoptogenic factors from mitochondria (94,145).

The activation of the tumour suppressor protein p53 can induce DNA damage. Once activated, p53 may induce the expression of genes that prevent cell division and cause apoptosis (146). This may lead to the activation of pro-apoptotic Bcl-2 family members, like Bax, resulting in the permeabilisation of the outer mitochondrial membrane and subsequent activation of the above mentioned mitochondrial pathway (146-148).

A small peptide derived from the carboxyl terminus of p21, a protein identified as a cyclin-dependent kinase inhibitor and that was known to play an important role in the regulation of cell growth and differentiation, has recently been found to also activate apoptosis by a process involving mitochondria, although the exact pathways are still unclear (101).

4. Oxidative stress and disease

In normal conditions, cells can deal with mild levels of oxidative stress. They do so by upregulating the expression of genes responsible for the synthesis of antioxidant defence mechanisms. However, the intracellular accumulation of high levels of ROS/RNS can result in damage to all types of biomolecules, and

ultimately lead to cell death, which has been associated with many pathological conditions (2,5). However, it should be noted that whereas some diseases may indeed be caused by oxidative damage to biomolecules, in others oxidative stress is a consequence (and not a cause) of the disease. However, even as a secondary event, oxidative stress is of major importance, since it can induce the aggravation of tissue damage in several disorders (1).

A redox imbalance in the cell can lead to oxidative DNA damage, causing mutations that may result in cancer (149,150). The oxidative burst induced by neutrophils and macrophages to kill pathogens may result in chronic inflammation, seen in immune disorders, such as rheumatoid arthritis and inflammatory bowel diseases (151,152). Glycation of proteins leading to accumulation of advanced glycation end-products (AGEs), reduced antioxidant levels, and oxidative DNA damage seem to be present in diabetic complications (153,154). The decline in CD4⁺ lymphocytes (whose functioning is regulated by redox potential) counts has been described to contribute to the progress of HIV infection to AIDS (155,156). Moreover, oxidative stress is involved in ophthalmologic disorders, such as advanced macular degeneration (AMD) and glaucoma (157).

Reactive species also participates in the normal process of aging. Oxidative damage accumulates with age, which leads to an increased impairment of cellular function. This results in a markedly decreased ability for the organism to neutralise free radicals and cope with oxidative stress, as it grows older (158). In addition, it has been reported that the cellular response to oxidants seems to be associated with the mechanisms that regulate longevity. Three gene products, including Forkhead transcription factors, the adaptor protein p66Shc, and the histone deacetylase Sir2, are described as being involved either in the regulation of intracellular ROS concentrations or in the increase in resistance to oxidative stress (159).

Oxidative stress also seems to be important in the etiology of several cardiovascular diseases, like atherosclerosis, ischemic heart disease, cardiomyopathies, and congestive heart failure, among others (5,160). In fact, the heart is one of the most energy demanding tissues in the body and is totally dependent upon oxidative phosphorylation to supply the large amount of ATP required for beat-by-beat contraction and relaxation, which makes it quite susceptible to oxidative stress (161). The enzymes xanthine oxidoreductase, NAD(P)H oxidase, and nitric oxide synthase, as well as the mitochondrial cytochromes and haemoglobin may act as the main sources of oxidative stress in these diseases (162,163). Furthermore, high levels of cholesterol and uptake of oxidised low-density lipoproteins (oxLDL), the main carriers of cholesterol in plasma, is a primary risk for

development of atherosclerosis (164,165). One of the most clinically relevant cardiac problems is ischemia-reperfusion injury. This type of injury involves an impairment of the blood flow to the heart as a result of damage to the myocardium (ischemia), in which the source of oxygen is removed, causing the cessation of oxidative phosphorylation. After a short period of ischemia, blood flow restoration occurs (reperfusion), which can, paradoxically, result in the aggravation of damage occurring during the ischemic period, and can lead to both apoptotic and necrotic cell death. An intracellular calcium overload and oxidative stress are two mechanisms that have been proposed to explain the pathogenesis of ischemia/reperfusion injury. Although the origin of ROS present during these events is yet to be well understood, it has been suggested that xanthine oxidase and NADPH oxidase, as well as mitochondria (*via* the electron transport chain) are mainly responsible for the massive ROS burst occurring during ischemia/reperfusion (161,166). In addition, increased oxidative stress causes abnormalities in the myocyte function, including inhibition of ATPases present in the sarcolemma that, together with calcium release from the sarcoplasmic reticulum, can also contribute to the intracellular calcium overload (5).

To date, many studies have demonstrated the involvement of oxidative stress in neurodegenerative diseases, such as Alzheimer's and Parkinson's (29). For example, in the brains of patients with Alzheimer's disease, a significant amount of ROS/RNS has been detected, in association with a marked accumulation of amyloid- β peptide (the main constituent of senile plaques) and deposition of neurofibrillary tangles and neurophil threads (abnormal neurites) (167). Several observations support the notion that the brain is particularly susceptible to oxidative stress: 1) this organ is known to consume about a fifth of the total oxygen used by the living organism, which increases the probability of ROS formation at the mitochondrial electron transport chain level; 2) neurons are post-mitotic (non-replicating) cells and any damage to brain tissues by ROS tends to be cumulative over time; 3) the high abundance in polyunsaturated fatty acids, which are particularly vulnerable to ROS damage; 4) the presence of high levels of transition metal ions (*e.g.* iron) that catalyse ROS formation through the Fenton reaction and the reduced levels of antioxidants able to segregate these transition metal ions, like transferrin and ceruloplasmin; 5) the release of excitatory neurotransmitters, such as glutamate, that induce a sequence of events in the post-synaptic neuron, which results in the formation of ROS; 6) the release of ROS during the oxidation of dopamine by monoamine oxidase in the nerve terminals of dopaminergic neurons may produce increased oxidative stress in brain regions, such as substantia nigra, which has been suggested to be a causative role in Parkinson's disease; 7) ascorbic acid,

which is present at elevated levels in both white and grey matters, additionally to its antioxidant properties, can act as a pro-oxidant, when the free iron in brain regions increases due to intra-cerebral hemorrhage, for example; 8) in comparison with other tissues, there are low levels of antioxidant defences, such as catalase and glutathione peroxidase, in the brain (1,29,57).

5. Antioxidants as protectors of oxidative stress

The excess of ROS is generally inactivated by endogenous and/or exogenous antioxidant molecules (29).

Antioxidant is a term widely used, but difficult to define clearly. According to some authors, a generic definition should be associated with the notion of the ROS/RNS that have to be neutralised, as well as the target of damage that is measured (2,168). In fact, it is quite natural that an antioxidant gives protection in one system, but fails to protect, and sometimes even causes damage, in others (169). Taken this into account, an antioxidant could be defined as "any substance that, when present at low concentrations compared with those of an oxidisable substrate, significantly delays or prevents oxidation of that substrate" (2,8). However, some authors have stated that the concept of an antioxidant *in vitro* should not be extended to cells, organs, animals or populations until the evidence has been obtained, since a molecule demonstrated to have antioxidant properties *in vitro* might have additional properties in a more complex system (168).

A compound might exert antioxidant actions *in vivo* by inhibiting the generation of ROS, by directly scavenging free radicals or by removing or lowering the local concentrations of metal ions, which catalyse oxidation. Additionally, it might also act by enhancing the endogenous antioxidant defences (*e.g.* by upregulating the expression of the genes encoding for the cells' natural antioxidant enzymes) (29,169). Some examples of antioxidants are discussed below.

5.1. Cellular antioxidant defences

The balance between the physiological production of ROS and their detoxification is maintained in cells by effective enzymatic and non-enzymatic antioxidant systems (170), as summarised in Figure 6.

As a first line of defence, preventive antioxidants act by binding to and sequestering promoters of oxidation and transition metal ions, like iron and copper, which contain unpaired electrons and strongly accelerate the formation of free radicals. Some examples of preventive antioxidants are transferrin, lactoferrin, ceruloplasmin, haptoglobins, hemopexin, and albumin (29,171). This class of preventive antioxidants also comprises the enzymatic antioxidant defences, like superoxide dismutase (SOD), catalase (CAT), and glutathione

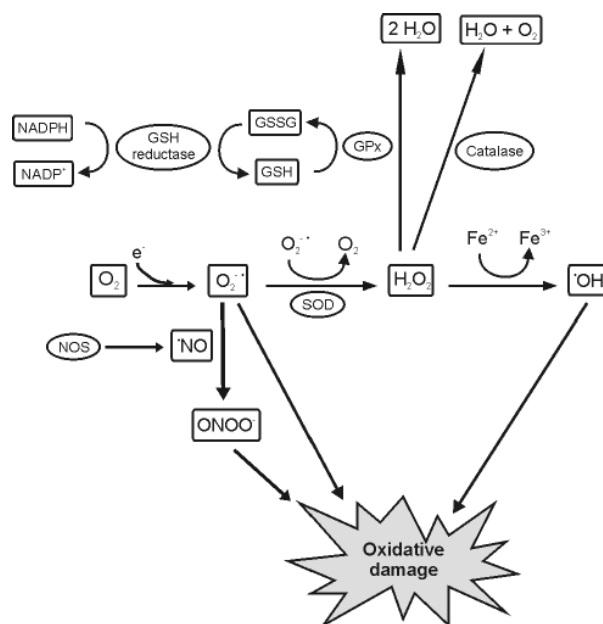


Figure 6. Formation of reactive oxygen and nitrogen species and some of the endogenous antioxidant defence mechanisms. Abbreviations: SOD, superoxide dismutase; GSH, reduced glutathione; GSSG, oxidised glutathione; GPx, glutathione peroxidase.

peroxidase (GPx). These enzymes act on specific ROS following their formation and degrade them to less harmful products (1,29).

One of the most effective intracellular enzymatic antioxidants is superoxide dismutase. This enzyme, whose activity was firstly proven in 1969 (6), catalyses the dismutation of the superoxide anion to molecular oxygen and hydrogen peroxide. The H_2O_2 formed in this reaction is then destroyed by the action of catalases and glutathione peroxidases. In humans, there are three forms of SOD: the cytosolic Cu/Zn-SOD, which contains copper and zinc in its active centre, the mitochondrial Mn-SOD (that contains manganese in the active site), and the extracellular SOD (EC-SOD) (172).

Catalase is a heme-containing enzyme, mainly localised in the peroxisomes of mammalian cells, which decomposes hydrogen peroxide to water and molecular oxygen. Thus, it lowers the risk of $\cdot OH$ formation from H_2O_2 via the Fenton reaction. In addition, catalase is involved in the detoxification of other substrates that work as H^+ donors, such as phenols and alcohols (123).

The selenium-containing peroxidases, of which glutathione peroxidase may be considered the most important example, catalyse the reduction of a variety of hydroperoxides (H_2O_2 or ROOH) in the presence of the reduced form of glutathione (GSH) (123). This enzyme (for which at least four different mammalian forms are known), oxidises two molecules of GSH to GSSG (the oxidised form of glutathione), which can subsequently be reduced to GSH again by glutathione reductase (27).

In addition to these enzymatic defences, cells possess low molecular mass agents that also exert an

antioxidant protection, by removing or degrading ROS to less harmful products, acting as a second line of defence. These include, among others, molecules like glutathione, thioredoxin, and coenzyme Q (2,29).

The tripeptide glutathione exists either in the reduced (GSH) or oxidised (GSSG) form and is ubiquitously present in all cells (distributed between the nucleus, endoplasmic reticulum, and mitochondria). Its main functions include: restoration of oxidised protein sulphhydryls; detoxification of hydrogen peroxide, lipid hydroperoxides, and electrophilic compounds either directly (*via* GPx-catalysed reactions) or indirectly (through glutathione S-transferases-catalysed conjugation reactions); transport of amino acids through the plasma membrane; direct scavenging of hydroxyl radical and singlet oxygen; regeneration of some important antioxidants, like vitamins C and E, to their active forms; and protection of brain tissue from oxidative stress (26,27,173,174).

Along with GSH, thioredoxin, a small and multifunctional disulphide-containing polypeptide, is also important for the maintenance of cellular thiol homeostasis, contributing to the total antioxidant protection (175,176). It mainly functions as a general protein disulfide reductant, but is also able to provide control over several transcription factors that affect cell proliferation and death (27,177).

Coenzyme Q (CoQ), or ubiquinone, is a ubiquitous electron and proton carrier, playing an important role in the mitochondrial electron-transport chain. Its reduced form, ubiquinol, can function as an antioxidant, preventing lipid peroxidation by reduction of peroxy radicals and is also able to interact with α -tocopheroxy radical, thus regenerating endogenous vitamin E within the lipid membrane (178).

Other cellular low molecular mass agents, including bilirubin (36), lipoic acid (179), melatonin (180), and uric acid (181), have been reported to help cells in the removal of free radicals.

Since the processes of prevention and removal of reactive species are not completely effective, damage still accumulates in biomolecules (8). So, adding to the several types of antioxidants mentioned above, cells protect their critical structures by other mechanisms, such as repair and *de novo* enzymes. These act as the last line of defence, by repairing or eliminating damaged molecules, reconstituting them, and even by clearing the toxic and waste products (29,182). This type of antioxidants includes heat shock proteins, DNA repair enzymes, proteases, lipases, and transferases (1).

5.2. Antioxidant protection by compounds derived from the diet

Several compounds present in plants and vegetables have been suggested to have the ability of reacting with free radicals, without generating further radicals. Other

compounds become oxidised after scavenging ROS, and thus need to be regenerated for further use (174).

Vitamins are considered to be antioxidants of major biological importance. Ascorbic acid (vitamin C) is a water-soluble antioxidant, commonly found in relatively high amounts in fruits and vegetables (183). It effectively scavenges several types of ROS/RNS *in vitro*, resulting in the formation of an ascorbyl radical, which can be further oxidised to dehydroascorbate. This molecule can then be regenerated, through the cellular reducing molecules of the cell, to ascorbate. In addition, ascorbic acid can regenerate other small antioxidant molecules from their respective radical species (such as α -tocopherol or GSH). Moreover, it can function as a cofactor for many enzymes, by maintaining the metal ions (such as iron and copper) present in the active centre of those enzymes, in a reduced state. However, the reduction of iron and copper by ascorbate can also result in a pro-oxidant effect, since these ions in the reduced form can be used to fuel the Fenton reaction (178,184).

Vitamin E is a lipophilic vitamin, synthesised only by plants, that exists in eight different forms, of which α -tocopherol is the most active. It is the major membrane-bound antioxidant employed by the cell, whose main function resides in protecting cells against lipid peroxidation (178,185). As mentioned above, during the antioxidant reaction, α -tocopherol is converted to an α -tocopheryl radical, which is then reduced to the original α -tocopherol form by ascorbic acid (164).

Vitamin A and its equivalent in animals, retinol, are also considered important antioxidants. It is present in many foods and can be formed from β -carotene transformation (186,187). Vitamin B comprises a family of chemically distinct water-soluble vitamins that play important roles in cell metabolism, although only some of them show antioxidant properties. Vitamin B₁ (thiamine), for example, has been shown to offer protection in different situations where high levels of oxidative stress were involved (188). In the same way, high levels of vitamins B₂ (riboflavin) and B₁₂ (cobalamin) have also been reported to protect against oxidative injury (189).

Carotenoids, of which β -carotene is probably the most studied, are pigments responsible for the colour of many fruits and vegetables. These substances have been recognised as the most potent quenchers of singlet oxygen (190) and have been described to help in the prevention of cancer, heart disease, and stroke (21,151,191). Other examples of carotenoids with protective effects on oxidative conditions are lycopene (a bright red carotenoid found in red fruits) and xanthophylls (*e.g.* lutein and zeaxanthin) (192,193).

(Poly) phenolic compounds are secondary plant metabolites possessing one or more aromatic rings with one or more hydroxyl groups within their structure

(194). These comprise a wide variety of molecules, divided into several classes (like flavonoids, phenolic acids, stilbenes, and others), commonly found in fruits, vegetables, wine, tea, coffee, and some cocoa products like dark chocolate (157,195). Many studies have reported a wide range of biological activities for these compounds, including anti-inflammatory (196), anti-carcinogenic (23), anti-allergic (197), and anti-hepatotoxic (198), which have been described to be mostly due to their antioxidant activity and also their ability to activate endogenous defence systems (174,199,200).

The interaction of polyphenols with biological systems is sometimes difficult to understand. For example, the metabolism of phenolic compounds *in vivo* may give rise to compounds that lose the original antioxidant activity (174). Moreover, it should be taken into account that, *in vivo*, polyphenols and their metabolites are found at lower concentrations in plasma or tissues than those of other antioxidants (ascorbic acid and α -tocopherol, for example), since polyphenols may need to undergo structure modifications (*e.g.* hydrolysis) in order to be absorbed (195,201).

Despite the numerous beneficial effects mentioned above for these natural compounds, it should be noted that pro-oxidant effects have been described for many of them, resulting in the induction of apoptosis, cell death, and the blocking of cell proliferation (202,203). For example, a high intake of vitamin C has been associated to an increased risk of disease (204,205). In the same way, α -tocopherol has been reported to be involved in the progression of low-density lipoprotein (LDL) oxidation and atherosclerosis, due to its pro-oxidant effects (206). Despite being considered an antioxidant, clinical trials regarding the use of β -carotene for cancer prevention, have demonstrated harmful effects for this compound, as reported by the Alpha-Tocopherol Beta Carotene Cancer Prevention Study Group, in 1994 (207), and also by Omenn *et al.* (208). Some other compounds (polyphenols) have also presented these opposite effects (202,209,210).

5.3. New synthetic molecules with pharmacological potential

The above mentioned drawbacks associated to the use of some natural compounds are in part responsible for the undergoing development of novel synthetic compounds, conceived to protect cells against oxidative injury. In fact, the number of reports identifying new synthetic antioxidants has been growing rapidly (189).

Many studies have described the synthesis of analogues of existing natural molecules known to possess antioxidant properties, which were modified in order to improve features like their stability and cellular uptake, but maintaining the functionality of the original structure (10). In this way, synthetic molecules

that can mimic antioxidant enzymes such as superoxide dismutase, catalase, and glutathione peroxidase have been reported as potential new drugs able to reduce damage caused by oxidative stress (211). For example, salens, which comprise a class of compounds containing manganese (III) complexes, and metalloporphyrins, a class consisting of a porphyrin combined to a metal ion (usually iron or manganese), have been indicated as mimetics of superoxide dismutase activity (212-214). Moreover, compounds like ebselen (a selenium-based compound), as well as diselenide and ditelluride compounds (which contain selenium, sulphur or tellurium in their structures) have been reported to possess glutathione peroxidase-like activity (214). In the same perspective, Ehrlich and colleagues (215) have recently reported the design and synthesis of a group of GSH analogues, which were named UPF peptides, that showed a higher hydroxyl radical scavenging ability and enhanced antiradical efficiency against the α, α -diphenyl- β -picrylhydrazyl (DPPH) radical, when compared to GSH, without influencing cell viability. Structures of molecules produced by plants, with known antioxidant activity, like polyphenols (171,216) or chalcones (217) have also been modified in order to increase their biological activity and stability (218,219).

Butylated hydroxyanisole (BHA), butylated hydroxytoluene (BHT), and *tert*-butyl hydroquinone (*t*-BHQ) are synthetic antioxidants, commonly used as food additives to prevent food spoilage, which are able to block lipid peroxidation. However, probably due to their phenolic nature (presence of OH groups), these compounds have shown contradictory effects (190,220). In addition, other synthetic compounds, like dimethyl sulfoxide (DMSO), lazaroids (21-aminosteroids drugs structurally related to glucocorticoids), salicylates (anti-inflammatory), pyrrolidine dithiocarbamate (PDTC), and dimethylurea have been found to scavenge free radicals and have also been used in therapeutic approaches (29,221).

In the past few years, novel nitrogenated structures, named FMAs, have been studied in our lab (222-224). These compounds, which are composed of an amidine unit linked to a phenol ring and that differ mainly on the number hydroxyl groups within that ring, were synthesised based on different aspects: 1) in living organisms exist several compounds containing nitrogen atoms in their structure (*e.g.* serotonin, purinic and pyrimidinic DNA bases, catecholamines, among others), which are known to easily interact with active centres responsible for different functions in those same organisms (225); 2) the presence of hydroxyl groups within a phenol ring has been reported to be responsible for the antioxidant properties of a compound, since those groups are able to donate an hydrogen (218,226,227); and 3) it has also been acknowledged that molecules incorporating conjugated systems with

nitrogen atoms can stabilise free radicals (228). The combination of these factors was expected to enhance the ability of these new structures to scavenge free radicals. Experiments in cell-free systems, namely by the use of DPPH discolouration and 2-deoxy-D-ribose degradation assays, gave the first indication of the compounds' good antiradical activity. The free radical scavenging properties of the nitrogen compounds were translated into *in vitro* cell models, namely PC12 and H9c2 cells, in which they showed a strong ability to scavenge ROS/RNS and therefore show their ability to act on oxidative stress-mediated injury associated to several pathologies, including neurodegenerative and cardiovascular diseases. In fact, they were able to prevent a series of events related to oxidative stress, like intracellular ROS formation, lipid peroxidation, and oxidative DNA damage, evaluated in adequate cell models. To some extent, they also seemed to act on intracellular signaling mechanisms resulting, for example, in an increase of the capacity to repair oxidative DNA damage and in a regulation of the apoptotic cascade, specifically at the mitochondrial level. In this way, these nitrogen compounds showed superior protection profiles when compared to the traditional antioxidant trolox (a water-soluble analogue of vitamin E) (222,223).

Moreover, a comparative study with polyphenolic compounds, which have somehow related structures (they also possess more than one hydroxyl group), showed some advantages, of these synthetic structures, over the polyphenols, namely their lack of genotoxicity and their ability to increase the activity of DNA repair enzymes (224).

Additionally, novel synthetic diarylamines containing a benzo[*b*]thiophene nucleus, which are also currently being studied in our lab, have shown quite promising results, namely by protecting cells, in particular at the mitochondrial level, from oxidative-induced damage at concentrations in the nanomolar range (229).

6. Conclusions

Reactive oxygen (ROS) and nitrogen (RNS) species are produced as a consequence of both exogenous and/or endogenous stimuli. Depending on the amounts present inside the cells, their effects can be either harmful or beneficial. In low amounts, they act as secondary messengers and regulate intracellular signalling, being their potentially adverse effects counteracted by the cells' antioxidant defence systems. However, their prevalence in higher amounts, resulting from their overproduction, when not balanced by the antioxidant systems, leads to oxidative stress. This condition is known to cause damage to all biomolecules, including proteins, lipids, and nucleic acids. Although cells possess mechanisms to repair some of this oxidative

damage (as is the case of DNA repair pathways), if not duly repaired, modifications to biomolecules can be toxic, mutagenic, and carcinogenic.

Intracellular accumulation of reactive oxygen and nitrogen species can ultimately result in the initiation of cell death processes. In this regard, it should be noted that the amount of reactive species present in the cell and the way as the cell responds to it can determine that same cell's fate: mild oxidative stress may be responsible for the activation of biological responses that can either lead to survival and proliferation, or can induce apoptosis, whereas a great accumulation of ROS/RNS can result in necrosis. Moreover, the association of oxidative stress-induced cell death with several pathological conditions (including cardiovascular and neurodegenerative diseases, among others), either as the cause or the consequence of the disease, has been widely recognized by the scientific community.

Excessive ROS/RNS can be inactivated by endogenous and/or exogenous antioxidant molecules. These may exert their antioxidant actions by inhibiting the generation of free radicals or by scavenging them, by lowering the concentrations of metal ions involved in the formation of ROS/RNS, or even by enhancing the endogenous antioxidant defences *via* upregulation of gene expression.

Usually, cells are able to maintain a balance between the intracellular formation of reactive species and their removal due to the presence of endogenous enzymatic (*e.g.* superoxide dismutase, catalase, and glutathione peroxidase) and non-enzymatic (*e.g.* glutathione, thioredoxin, coenzyme Q) defences. Nevertheless, additional antioxidant protection can also be attributed to some compounds derived from the diet, which may be found in plants and vegetables. These include vitamins (namely A, C, and E), carotenoids, and polyphenolic compounds.

However, there are some drawbacks associated to the use of natural compounds, namely the pro-oxidant effects that have already been described for some of them. Moreover, metabolism *in vivo* of some of these compounds, namely polyphenols, may originate compounds that lose their initial antioxidant activity (and sometimes even yielding toxic derivatives). In addition, the structural modifications those polyphenols need to undergo to be absorbed *in vivo* may result in lower concentrations in plasma and tissues, when compared to other antioxidants (like vitamin C or E, for example).

Therefore, research on the development of new synthetic structures capable of acting beyond and/or potentiate the cells' natural defence mechanisms has dramatically increased in the last few years. These novel structures, some of which are described in this review, are often analogues of naturally occurring molecules or structurally related to them, and clearly have shown increased antioxidant activity, associated to

decreased toxicity in many cases. They look promising and so complementary research regarding their use, as active principles of pharmacological compounds, must go on.

The development of novel synthetic molecules with powerful antioxidant properties, as well as the discovery of new beneficial effects for existing ones, associated to the identification of potential new drug targets has been one of the scientists' concerns over the past years. Success in this field of research can contribute to the reduction of oxidative stress-induced damage in several pathological conditions, namely in cardiovascular and neurodegenerative diseases.

Acknowledgements

Partly supported by the FCT research project PTDC/QUI/68382/2006.

References

1. Wilcox JK, Ash SL, Catignani GL. Antioxidants and prevention of chronic disease. *Crit Rev Food Sci Nutr*. 2004; 44:275-295.
2. Halliwell B, Gutteridge JMC. *Free Radicals in Biology and Medicine* (3rd ed.). Oxford University Press, NY, USA, 1999.
3. Limón-Pacheco J, Gonsebatt ME. The role of antioxidants and antioxidant-related enzymes in protective responses to environmentally induced oxidative stress. *Mutat Res*. 2009; 674:137-147.
4. Gershman R, Nye SW, Dwyer P, Fenn WO. Oxygen poisoning and X-irradiation: a mechanism in Common. *Science*. 1954; 119:623-626.
5. Valko M, Leibfritz D, Moncol J, Cronin MT, Mazur M, Telser J. Free radicals and antioxidants in normal physiological functions and human disease. *Int J Biochem Cell Biol*. 2007; 39:44-84.
6. McCord JM, Fridovich I. Superoxide Dismutase an enzymic function for erythrocyte (hemocuprein). *J Biol Chem*. 1969; 244:6049-6055.
7. Droge W. Free radicals in the physiological control of cell function. *Physiol Rev*. 2002; 82:47-95.
8. Sies H. Oxidative stress: oxidants and antioxidants. *Expe Physiol*. 1997; 82:291-295.
9. Uemura M, Manabe H, Yoshida N, Fujita N, Ochiai J, Matsumoto N, Takagi T, Naito Y, Yoshikawa T. Alpha-tocopherol prevents apoptosis of vascular endothelial cells *via* a mechanism exceeding that of mere antioxidation. *Eur J Pharmacol*. 2002; 456:29-37.
10. Halliwell B. Role of free radicals in the neurodegenerative diseases: therapeutic implications for antioxidant treatment. *Drugs Aging*. 2001; 18:685-716.
11. Jang JH, Aruoma OI, Jen LS, Chung HY, Surh YJ. Ergothioneine rescues PC12 cells from β -amyloid-induced apoptotic death. *Free Radic Biol Med*. 2004; 36:288-299.
12. Aikawa R, Komuro I, Yamazaki T, Zou YZ, Kudoh S, Tanaka M, Shiojima I, Hiroi Y, Yazaki Y. Oxidative stress activates extracellular signal-regulated kinases through Src and ras in cultured cardiac myocytes of neonatal rats. *J Clin Invest*. 1997; 100:1813-1821.
13. He A, Wangi JA, Guil C, Jiang Y, Sun Y, Chen T. Changes of mitochondrial pathway in hypoxia/reoxygenation induced cardiomyocytes apoptosis. *Folia Histochem Cytobiol*. 2007; 45:397-400.
14. Fleury C, Mignotte B, Vayssiere JL. Mitochondrial reactive oxygen species in cell death signaling. *Biochimie*. 2002; 84:131-141.
15. Cadenas E, Davies KJ. Mitochondrial free radical generation, oxidative stress and aging. *Free Radic Biol Med*. 2000; 29:222-230.
16. Somayajulu M, McCarthy S, Hung M, Sikorska M, Borowy-Borowski H, Pandey S. Role of mitochondria in neuronal cell death induced by oxidative stress; neuroprotection by Coenzyme Q10. *Neurobiol Dis*. 2005; 18:618-627.
17. Andreyev AY, Kushnareva YE, Starkov AA. Mitochondrial metabolism of reactive oxygen species. *Biochemistry Mosc*. 2005; 70:200-214.
18. Turrens JF. Mitochondrial formation of reactive oxygen species. *J Physiol (Lond.)*. 2003; 552:335-344.
19. Jezek P, Hlavata L. Mitochondria in homeostasis of reactive oxygen species in cell, tissues, and organism. *Int J Biochem Cell Biol*. 2005; 37:2478-2503.
20. Barja G. Mitochondrial oxygen radical generation and leak: Sites of production in states 4 and 3, organ specificity, and relation to aging and longevity. *J Bioenerg Biomembr*. 1999; 31:347-366.
21. Valko M, Izakovic M, Mazur M, Rhodes CJ, Telser J. Role of oxygen radicals in DNA damage and cancer incidence. *Mol Cell Biochem*. 2004; 266:37-56.
22. Conner EM, Grisham MB. Inflammation, free radicals and antioxidants. *Nutrition*. 1996; 12:274-277.
23. Moon YJ, Wang X, Morris ME. Dietary flavonoids: Effects on xenobiotic and carcinogen metabolism. *Toxicol in Vitro*. 2006; 20:187-210.
24. Gupta M, Dobashi K, Greene EL, Orak JK, Singh I. Studies on hepatic injury and antioxidant enzyme activities in rat subcellular organelles following *in vivo* ischemia and reperfusion. *Mol Cell Biochem*. 1997; 176:337-347.
25. Butterfield DA, Howard B, Yatin S, Koppal T, Drake J, Hensley K, Aksenov M, Aksenova M, Subramaniam R, Varadarajan S, Harris-White ME, Pedigo NW Jr, Carney JM. Elevated oxidative stress in models of normal brain aging and Alzheimer's disease. *Life Sci*. 1999; 65:1883-1892.
26. Valko M, Rhodes CJ, Moncol J, Izakovic M, Mazur M. Free radicals, metals and antioxidants in oxidative stress-induced cancer. *Chem Biol Interact*. 2006; 160:1-40.
27. Nordberg J, Arner ES. Reactive oxygen species, antioxidants and the mammalian thioredoxin system. *Free Radic Biol Med*. 2001; 31:1287-1312.
28. Spiteller G. Lipid peroxidation in aging and age-dependent diseases. *Exp Gerontol*. 2001; 36:1425-1457.
29. Cui K, Luo X, Xu K, Ven Murthy MR. Role of oxidative stress in neurodegeneration: recent developments in assay methods for oxidative stress and nutraceutical antioxidants. *Prog Neuropsychopharmacol Biol Psychiatry*. 2004; 28:771-799.
30. Mwanjewe J, Hui BK, Coughlin MD, Grover AK. Treatment of PC12 cells with nerve growth factor increases iron uptake. *Biochem J*. 2001; 357:881-886.
31. Levi S, Santambrogio P, Corsi B, Cozzi A, Arosio P. Evidence that residues exposed on the three-fold channels have active roles in the mechanism of ferritin

- iron incorporation. *Biochem J.* 1996; 317 (Pt 2):467-473.
32. Beal MF. Oxidatively modified proteins in aging and disease. *Free Radic Biol Med.* 2002; 32:797-803.
 33. Rubbo H, Radi R, Anselmi D, Kirk M, Barnes S, Butler J, Eiserich JP, Freeman BA. Nitric oxide reaction with lipid peroxyl radicals spares alpha-tocopherol during lipid peroxidation. *J Biol Chem.* 2000; 275:10812-10818.
 34. Antunes F, Nunes C, Laranjinha J, Cadenas E. Redox interactions of nitric oxide with dopamine and its derivatives. *Toxicology.* 2005; 208:207-212.
 35. Radi R, Peluffo G, Alvarez MN, Naviliat M, Cayota A. Unraveling peroxy-nitrite formation in biological systems. *Free Radic Biol Med.* 2001; 30:463-488.
 36. Barañano DE, Snyder SH. Neural roles for heme oxygenase: Contrasts to nitric oxide synthase. *Proc Natl Acad Sci U S A.* 2001; 98:10996-11002.
 37. Schafer FQ, Buettner G. Redox environment of the cell as viewed through the redox state of the glutathione disulfide/glutathione couple. *Free Radic Biol Med.* 2001; 30:1191-1212.
 38. Babior BM, Takeuchi C, Ruedi J, Gutierrez A, Wentworth P. Investigating antibody-catalyzed ozone generation by human neutrophils. *Proc Natl Acad Sci U S A.* 2003; 100:3031-3034.
 39. Griendling KK, Sorescu D, Lassegue B, Ushio-Fukai M. Modulation of protein kinase activity and gene expression by reactive oxygen species and their role in vascular physiology and pathophysiology. *Arterioscler Thromb Vasc Biol.* 2000; 20:2175-2183.
 40. Martinez-Ruiz A, Lamas S. S-nitrosylation: a potential new paradigm in signal transduction. *Cardiovasc Res.* 2004; 62:43-52.
 41. Zhu H, Bunn HF. Oxygen sensing and signaling: impact on the regulation of physiologically important genes. *Respir Physiol.* 1999; 115:239-247.
 42. Semenza GL. HIF-1: mediator of physiological and pathophysiological responses to hypoxia. *J Appl Physiol.* 2000; 88:1474-1480.
 43. Sellak H, Franzini E, Hakim J, Pasquier C. Reactive oxygen species rapidly increase endothelial ICAM-1 ability to bind neutrophils without detectable upregulation. *Blood.* 1994; 83:2669-2677.
 44. Dalton TP, Shertzer HG, Puga A. Regulation of gene expression by reactive oxygen. *Annu Rev Pharmacol Toxicol.* 1999; 39:67-101.
 45. Cai J, Jones D. Mitochondrial redox signaling during apoptosis. *J Bioenerg Biomembr.* 1999; 31:327-334.
 46. Montiel-Duarte C, Ansorena E, Lopez-Zabalza MJ, Cenarruzabeitia E, Iraburu MJ. Role of reactive oxygen species, glutathione and NF- κ B in apoptosis induced by 3,4-methylenedioxymethamphetamine ("Ecstasy") on hepatic stellate cells. *Biochem Pharmacol.* 2004; 67:1025-1033.
 47. Nunes C, Almeida L, Laranjinha J. 3,4-Dihydroxy phenylacetic acid (DOPAC) modulates the toxicity induced by nitric oxide in PC12 cells *via* mitochondrial dysfunctioning. *Neurotoxicol.* 2008; 29:998-1007.
 48. Kohen R, Nyska A. Oxidation of biological systems: oxidative stress phenomena, antioxidants, redox reactions, and methods for their quantification. *Toxicol Pathol.* 2002; 30:620-650.
 49. Stadtman ER. Role of oxidant species in aging. *Curr Med Chem.* 2004; 11:1105-1112.
 50. Dalle-Donne I, Aldini G, Carini M, Colombo R, Rossi R, Milzani A. Protein carbonylation, cellular dysfunction, and disease progression. *J Cell Mol Med.* 2006; 10:389-406.
 51. Fagan J, Slecicka BG, Sohar I. Quantitation of oxidative damage to tissue proteins. *Int J Biochem Cell Biol.* 1999; 31:751-757.
 52. Dalle-Donne I, Rossi R, Giustarini D, Milzani A, Colombo R. Protein carbonyl groups as biomarkers of oxidative stress. *Clin Chim Acta.* 2003; 329:23-38.
 53. Niki E, Yoshida Y, Saito Y, Noguchi N. Lipid peroxidation: Mechanisms, inhibition, and biological effects. *Biochem Biophys Res Commun.* 2005; 338:668-676.
 54. Girotti AW. Lipid hydroperoxide generation, turnover, and effector action in biological systems. *J Lipid Res.* 1998; 39:1529-1542.
 55. Lehuédé J, Fauconneau B, Barrier L, Ourakow M, Piriou A, Vierfond JM. Synthesis and antioxidant activity of new tetraarylpyrroles. *Eur J Med Chem.* 1999; 34:991-996.
 56. Meagher EA, FitzGerald GA. Indices of lipid peroxidation *in vivo*: strengths and limitations. *Free Radic Biol Med.* 2000; 28:1745-1750.
 57. Lovell MA, Markesbery WR. Oxidative damage in mild cognitive impairment and early Alzheimer's disease. *J Neurosci Res.* 2007; 85:3036-3040.
 58. McCall MR, Frei B. Can antioxidant vitamins materially reduce oxidative damage in humans? *Free Radic Biol Med.* 1999; 26:1034-1053.
 59. Nair U, Bartsch H, Nair J. Lipid peroxidation-induced DNA damage in cancer-prone inflammatory diseases: A review of published adduct types and levels in humans. *Free Radic Biol Med.* 2007; 43:1109-1120.
 60. Young IS, McEneny J. Lipoprotein oxidation and atherosclerosis. *Biochem Soc Trans.* 2001; 29:358-362.
 61. Cui J, Holmes EH, Greene TG, Liu PK. Oxidative DNA damage precedes DNA fragmentation after experimental stroke in rat brain. *FASEB J.* 2000; 14:955-967.
 62. Nagayama T, Lan J, Henshall DC, Chen DX, O'Horo C, Simon RP, Chen J. Induction of oxidative DNA damage in the peri-infarct region after permanent focal cerebral ischemia. *J Neurochem.* 2000; 75:1716-1728.
 63. Inoue M, Sato EF, Nishikawa M, Park AM, Kira Y, Imada I, Utsumi K. Mitochondrial generation of reactive oxygen species and its role in aerobic life. *Curr Med Chem.* 2003; 10:2495-2505.
 64. Martin LJ. DNA damage and repair: Relevance to mechanisms of neurodegeneration. *J Neuropathol Exp Neurol.* 2008; 67:377-387.
 65. Cadet J, Delatour T, Douki T, Gasparutto D, Pouget JP, Ravanat JL, Sauvaigo S. Hydroxyl radicals and DNA base damage. *Mutat Res.* 1999; 424:9-21.
 66. Powell CL, Swenberg JA, Rusyn I. Expression of base excision DNA repair genes as a biomarker of oxidative DNA damage. *Cancer Lett.* 2005; 229:1-11.
 67. Clingen PH, Arlett CF, Roza L, Mori T, Nikaido O, Green MH. Induction of cyclobutane pyrimidine dimers, pyrimidine(6-4)pyrimidone photoproducts, and Dewar valence isomers by natural sunlight in normal human mononuclear cells. *Cancer Res.* 1995; 55:2245-2248.
 68. Douki T, Reynaud-Angelin A, Cadet J, Sage E. Bipyrimidine photoproducts rather than oxidative lesions are the main type of DNA damage involved in the genotoxic effect of solar UVA radiation. *Biochemistry.* 2003; 42:9221-9226.
 69. Kruman II. Why do neurons enter the cell cycle? *Cell*

- Cycle. 2004; 3:769-773.
70. Evans MD, Dizdaroglu M, Cooke MS. Oxidative DNA damage and disease: induction, repair and significance. *Mutat Res.* 2004; 567:1-61.
 71. de Waard H, Sonneveld E, de Wit J, Esveldt-van Lange R, Hoeijmakers JH, Vrieling H, van der Horst GT. Cell-type-specific consequences of nucleotide excision repair deficiencies: Embryonic stem cells versus fibroblasts. *DNA Repair.* 2008; 7:1659-1669.
 72. Fishel ML, Vasko MR, Kelley MR. DNA repair in neurons: so if they don't divide what's to repair? *Mutat Res.* 2007; 614:24-36.
 73. Helleday T. Pathways for mitotic homologous recombination in mammalian cells. *Mutat Res.* 2003; 532:103-115.
 74. Seluanov A, Mittelman D, Pereira-Smith OM, Wilson JH, Gorbunova V. DNA end joining becomes less efficient and more error-prone during cellular senescence. *Proc Natl Acad Sci U S A.* 2004; 101:7624-7629.
 75. Neri S, Gardini A, Facchini A, Olivieri F, Franceschi C, Ravaglia G, Mariani E. Mismatch repair system and aging: Microsatellite instability in peripheral blood cells from differently aged participants. *J Gerontol A Biol Sci Med Sci.* 2005; 60:285-292.
 76. Gorbunova V, Seluanov A, Mao Z, Hine C. Changes in DNA repair during aging. *Nucleic Acids Res.* 2007; 35:7466-7474.
 77. Hanawalt PC. Subpathways of nucleotide excision repair and their regulation. *Oncogene.* 2002; 21:8949-8956.
 78. Frosina G. Prophylaxis of oxidative DNA damage by formamidopyrimidine-DNA glycosylase. *Int J Cancer.* 2006; 119:1-7.
 79. Coppedé F, Mancuso M, Lo Gerfo A, Manca ML, Petrozzi L, Migliore L, Siciliano G, Murri L. A Ser326Cys polymorphism in the DNA repair gene hOGG1 is not associated with sporadic Alzheimer's disease. *Neurosci Lett.* 2007; 414:282-285.
 80. Rao KS. DNA repair in aging rat neurons. *Neurosci.* 2007; 145:1330-1340.
 81. Collins AR, Gaivão I. DNA base excision repair as a biomarker in molecular epidemiology studies. *Mol Asp Med.* 2007; 28:307-322.
 82. Dodson ML, Lloyd RS. Mechanistic comparisons among base excision repair glycosylases. *Free Radic Biol Med.* 2002; 32:678-682.
 83. Fantini D, Vascotto C, Deganuto M, Bivi N, Gustincich S, Marcon G, Quadrioglio F, Damante G, Bhakat KK, Mitra S, Tell G. APE1/Ref-1 regulates PTEN expression mediated by Egr-1. *Free Radic Res.* 2008; 42:20-29.
 84. Tudek B, Swoboda M, Kowalczyk P, Olinski R. Modulation of oxidative DNA damage repair by the diet, inflammation and neoplastic transformation. *J Physiol Pharm.* 2006; 57:33-49.
 85. Tomasetti M, Alleva R, Collins AR. *In vivo* supplementation with coenzyme Q10 enhances the recovery of human lymphocytes from oxidative DNA damage. *FASEB J.* 2001; 15:1425-1451.
 86. European Standard Committee on Oxidative DNA Damage (ESCODD). Measurement of DNA oxidation in human cells by chromatographic and enzymic methods. *Free Radic Biol Med.* 2003; 34:1089-1099.
 87. Gedik CM, Collins A. Establishing the background level of base oxidation in human lymphocyte DNA: results of an interlaboratory validation study. *FASEB J.* 2004; 18:82-104.
 88. Loft S, Moller P. Oxidative DNA damage and human cancer: need for cohort studies. *Antioxid Redox Signal.* 2006; 8:1021-1031.
 89. Bjelland S, Seeberg E. Mutagenicity, toxicity and repair of DNA base damage induced by oxidation. *Mutat Res.* 2003; 531:37-80.
 90. Cooke MS, Evans MD, Dizdaroglu M, Lunec J. Oxidative DNA damage: mechanisms, mutation, and disease. *FASEB J.* 2003; 17:1195-1214.
 91. Boujrad H, Gubkina O, Robert N, Krantic S, Susin SA. AIF-mediated programmed necrosis: a highly regulated way to die. *Cell Cycle.* 2007; 6:2612-2619.
 92. Henriquez M, Armisen R, Stutzin A, Quest AF. Cell death by necrosis, a regulated way to go. *Curr Mol Med.* 2008; 8:187-206.
 93. de Bruin EC, Medema JP. Apoptosis and non-apoptotic deaths in cancer development and treatment response. *Cancer Treat Rev.* 2008; 34:737-749.
 94. Lorenzo HK, Susin SA. Therapeutic potential of AIF-mediated caspase-independent programmed cell death. *Drug Resist Updat.* 2007; 10:235-255.
 95. Kroemer G, Galluzzi L, Vandenabeele P, *et al.* Classification of cell death: recommendations of the Nomenclature Committee on Cell Death 2009. *Cell Death Differ.* 2008; 16:3-11.
 96. Leist M, Jaattela M. Four deaths and a funeral: from caspases to alternative mechanisms. *Nat Rev Mol Cell Biol.* 2001; 2:589-598.
 97. Gil J, Almeida S, Oliveira CR, Rego AC. Cytosolic and mitochondrial ROS in staurosporine-induced retinal cell apoptosis. *Free Radic Biol Med.* 2003; 35:1500-1514.
 98. Krantic S, Mechawar N, Reix S, Quirion R. Apoptosis-inducing factor: a matter of neuron life and death. *Progr Neurobiol.* 2007; 81:179-196.
 99. Matés JM, Pérez-Gómez C, Núñez de Castro I. Antioxidant enzymes and human diseases. *Clin Biochem.* 1999; 32:595-603.
 100. Kourtis N, Tavernarakis N. Autophagy and cell death in model organisms. *Cell Death Differ.* 2008; 16:21-30.
 101. Dong C, Li Q, Lyu SC, Krensky AM, Clayberger C. A novel apoptosis pathway activated by the carboxyl terminus of p21. *Blood.* 2005; 105:1187-1194.
 102. Hengartner MO. The biochemistry of apoptosis. *Nature.* 2000; 407:770-776.
 103. Chowdhury I, Tharakan B, Bhat GK. Caspases – An update. *Comp Biochem Physiol Biochem Mol Biol.* 2008; 151:10-27.
 104. Beere HM. Death versus survival: functional interaction between the apoptotic and stress-inducible heat shock protein pathways. *J Clin Invest.* 2005; 115:2633-2639.
 105. Reeve JL, Szegezdi E, Logue SE, Chonghaile TN, O'Brien T, Ritter T, Samali A. Distinct mechanisms of cardiomyocyte apoptosis induced by doxorubicin and hypoxia converge on mitochondria and are inhibited by Bcl-xL. *J Cell Mol Med.* 2007; 11:509-520.
 106. Cain K, Bratton SB, Cohen GM. The Apaf-1 apoptosome: a large caspase-activating complex. *Biochimie.* 2002; 84:203-214.
 107. Zimmermann KC, Bonzon C, Green DR. The machinery of programmed cell death. *Pharmacol Ther.* 2001; 92:57-70.
 108. Bouchier-Hayes L, Lartigue L, Newmeyer DD. Mitochondria: pharmacological manipulation of cell death. *J Clin Invest.* 2005; 115:2640-2647.
 109. Schafer ZT, Kornbluth S. The Apoptosome:

- physiological, developmental, and pathological modes of regulation. *Dev Cell*. 2006; 10:549-561.
110. Tang XQ, Zhi JL, Cui Y, Feng JQ, Chen PX. Hydrogen peroxide preconditioning protects PC12 cells against apoptosis induced by dopamine. *Life Sci*. 2005; 78:61-66.
 111. Ferri KF, Jacotot E, Blanco J, Este JA, Zamzami N, Susin SA, Xie ZH, Brothers G, Reed JC, Penninger JM, Kroemer G. Apoptosis control in syncytia induced by the HIV type 1-envelope glycoprotein complex: Role of mitochondria and caspases. *J Exp Med*. 2000; 192:1081-1092.
 112. Bahi N, Zhang JS, Llovera M, Ballester M, Comella JX, Sanchis D. Switch from caspase-dependent to caspase-independent death during heart development: essential role of endonuclease G in ischemia-induced DNA processing of differentiated cardiomyocytes. *J Biol Chem*. 2006; 281:22943-22952.
 113. Nakagawa T, Yuan J. Cross-talk between two cysteine protease families: activation of caspase-12 by calpain in apoptosis. *J Cell Biol*. 2000; 150:887-894.
 114. Lindholm D, Wootz H, Korhonen L. ER stress and neurodegenerative diseases. *Cell Death Differ*. 2006; 13:385-392.
 115. Schwarze SR, Lin EW, Christian PA, Gayheart DT, Kentucky L. Intracellular death platform steps-in: targeting prostate tumors *via* endoplasmic reticulum (ER) apoptosis. *Prostate*. 2008; 68:1615-1623.
 116. Kirkegaard T, Jaattela M. Lysosomal involvement in cell death and cancer. *Biochim Biophys Acta*. 2009; 1793:746-754.
 117. Jaattela M, Cande C, Kroemer G. Lysosomes and mitochondria in the commitment to apoptosis: a potential role for cathepsin D and AIF. *Cell Death Differ*. 2004; 11:135-136.
 118. Zhao M, Antunes F, Eaton JW, Brunt UT. Lysosomal enzymes promote mitochondrial oxidant production, cytochrome *c* release and apoptosis. *Eur J Biochem*. 2003; 270:3778-3786.
 119. Kagedal K, Zhao M, Svensson I, Brunt UT. Sphingosine-induced apoptosis is dependent on lysosomal proteases. *Biochem J*. 2001; 359:335-343.
 120. Berndtsson M, Beaujoin M, Rickardson L, Havelka AM, Larsson R, Liaudet-Coopman E, Linder S. Induction of the lysosomal apoptosis pathway by inhibitors of the ubiquitin-proteasome system. *Int J Cancer*. 2008; 124:1463-1469.
 121. Roninson IB, Broude EV, Chang BD. If not apoptosis, then what? Treatment-induced senescence and mitotic catastrophe in tumor cells. *Drug Resist Updat*. 2001; 4:303-313.
 122. Strauss SJ, Higginbottom K, Juliger S, Maharaj L, Allen P, Schenkein D, Lister T, Joel SP. The proteasome inhibitor Bortezomib acts independently of p53 and induces cell death *via* apoptosis and mitotic catastrophe in B-cell lymphoma cell lines. *Cancer Res*. 2007; 67:2783-2790.
 123. Matés JM. Effects of antioxidant enzymes in the molecular control of reactive oxygen species toxicology. *Toxicology*. 2000; 153:83-104.
 124. Lin Y, Choksi S, Shen HM, Yang QF, Hur GM, Kim YS, Tran JH, Nedospasov SA, Liu ZG. Tumor necrosis factor-induced nonapoptotic cell death requires receptor-interacting protein-mediated cellular reactive oxygen species accumulation. *J Biol Chem*. 2004; 279:10822-10828.
 125. Lopez-Sanchez N, Rodriguez JR, Frade JM. Mitochondrial c-Jun NH2-terminal kinase prevents the accumulation of reactive oxygen species and reduces necrotic damage in neural tumor cells that lack trophic support. *Mol Cancer Res*. 2007; 5:47-60.
 126. Aquilano K, Filomeni G, Di Renzo L, Vito M, Stefano C, Salimei PS, Ciriolo MR, Marfe G. Reactive oxygen and nitrogen species are involved in sorbitol-induced apoptosis of human erithroleukaemia cells K562. *Free Radic Res*. 2007; 41:452-460.
 127. Pias EK, Aw TY. Early redox imbalance mediates hydroperoxide-induced apoptosis in mitotic competent undifferentiated PC12 cells. *Cell Death Differ*. 2002; 9:1007-1016.
 128. Petrosillo G, Ruggiero FM, Paradies G. Role of reactive oxygen species and cardiolipin in the release of cytochrome *c* from mitochondria. *FASEB J*. 2003; 17:2202-2208.
 129. Kim DS, Kim HR, Woo ER, Hong ST, Chae HJ, Chae SW. Inhibitory effects of rosmarinic acid on adriamycin-induced apoptosis in H9c2 cardiac muscle cells by inhibiting reactive oxygen species and the activations of c-Jun N-terminal kinase and extracellular signal-regulated kinase. *Biochem Pharmacol*. 2005; 70:1066-1078.
 130. Zhu Y, Hoell P, Ahlemeyer B, Krieglstein J. PTEN: A crucial mediator of mitochondria-dependent apoptosis. *Apoptosis*. 2006; 11:197-207.
 131. Deshpande SS, Angkeow P, Kuang JP, Ozaki M, Irani K. Rac1 inhibits TNF-alpha-induced endothelial cell apoptosis: dual regulation by reactive oxygen species. *FASEB J*. 2000; 14:1705-1714.
 132. Hiona A, Leeuwenburgh C. The role of mitochondrial DNA mutations in aging and sarcopenia: implications for the mitochondrial vicious cycle theory of aging. *Exp Gerontol*. 2008; 43:24-33.
 133. Matés JM, Sanchez-Jimenez FM. Role of reactive oxygen species in apoptosis: implications for cancer therapy. *Int J Biochem Cell Biol*. 2000; 32:157-170.
 134. Hiroi M, Ogihara T, Hirano K, Hasegawa M, Morinobu T, Tamai H, Niki E. Regulation of apoptosis by glutathione redox state in PC12 cells exposed simultaneously to iron and ascorbic acid. *Free Radic Biol Med*. 2005; 38:1057-1072.
 135. Jung JY, Han CR, Jeong YJ, Kim HJ, Lim HS, Lee KH, Park HO, Oh WM, Kim SH, Kim WJ. Epigallocatechin gallate inhibits nitric oxide-induced apoptosis in rat PC12 cells. *Neurosci Lett*. 2007; 411:222-227.
 136. Choi MM, Kim EA, Hahn HG, Dal Nam K, Yang SJ, Choi SY, Kim TU, Cho SW, Huh JW. Protective effect of benzothiazole derivative KHG21834 on amyloid beta-induced neurotoxicity in PC12 cells and cortical and mesencephalic neurons. *Toxicology*. 2007; 239:156-166.
 137. Marczin N, El-Habashi N, Hoare GS, Bundy RE, Yacoub M. Antioxidants in myocardial ischemia-reperfusion injury: therapeutic potential and basic mechanisms. *Arch Biochem Biophys*. 2003; 420:222-236.
 138. Krueger A, Schmitz I, Baumann S, Krammer PH, Kirchhoff S. Cellular FLICE-inhibitory protein splice variants inhibit different steps of caspase-8 activation at the CD95 death-inducing signaling complex. *J Biol Chem*. 2001; 276:20633-20640.
 139. Golks A, Brenner D, Fritsch C, Krammer PH, Lavrik IN. c-FLIPR, a new regulator of death receptor-induced apoptosis. *J Biol Chem*. 2005; 280:14507-14513.

140. Futerman AH, Hannun YA. The complex life of simple sphingolipids. *EMBO Rep.* 2004; 5:777-782.
141. Lee WK, Thévenod F. Novel roles for ceramides, calpains and caspases in kidney proximal tubule cell apoptosis: lessons from *in vitro* cadmium toxicity studies. *Biochem Pharmacol.* 2008; 76:1323-1332.
142. Grether-Beck S, Felsner I, Brenden H, Krutmann J. Mitochondrial cytochrome *c* release mediates ceramide-induced activator protein 2 activation and gene expression in keratinocytes. *J Biol Chem.* 2003; 278:47498-47507.
143. Kim DH, Jang YY, Han ES, Lee CS. Protective effect of harmaline and harmalol against dopamine- and 6-hydroxydopamine-induced oxidative damage of brain mitochondria and synaptosomes, and viability loss of PC12 cells. *Eur J Neurosci.* 2001; 13:1861-1872.
144. Chwieralski CE, Welte T, Buhling F. Cathepsin-regulated apoptosis. *Apoptosis.* 2006; 11:143-149.
145. Conus S, Simon HU. Cathepsins: key modulators of cell death and inflammatory responses. *Biochem Pharmacol.* 2008; 76:1374-1382.
146. L'Ecuyer T, Sanjeev S, Thomas R, Novak R, Das L, Campbell W, Vander Heide R. DNA damage is an early event in doxorubicin-induced cardiac myocyte death. *Am J Physiol.* 2006; 291:H1273-H1280.
147. Cui H, Schroering A, Ding HF. p53 mediates DNA damaging drug-induced apoptosis through a caspase-9-dependent pathway in SH-SY5Y neuroblastoma cells. *Mol Cancer Ther.* 2002; 1:679-686.
148. Gartel AL. Transcriptional inhibitors, p53 and apoptosis. *Biochim Biophys Acta.* 2008; 1786:83-86.
149. Collins AR, Harrington V, Drew J, Melvin R. Nutritional modulation of DNA repair in a human intervention study. *Carcinogenesis.* 2003; 24:511-515.
150. Bartsch H, Nair J. Chronic inflammation and oxidative stress in the genesis and perpetuation of cancer: role of lipid peroxidation, DNA damage and repair. *Langenbecks Arch Surg.* 2006; 391:499-510.
151. Riso P, Visioli F, Grande S, Guarnieri S, Gardana C, Simonetti P, Porrini M. Effect of a tomato-based drink on markers of inflammation, immunomodulation, and oxidative stress. *J Agric Food Chem.* 2006; 54:2563-2566.
152. Filippin LI, Vercelino R, Marroni NP, Xavier RM. Redox signalling and the inflammatory response in rheumatoid arthritis. *Clin Exp Immunol.* 2008; 152:415-422.
153. Collins AR, Ralová K, Somorovská M, Petrovská H, Ondruvová A, Vohnout B, Fábry R, Dusinská M. DNA damage in diabetes: correlation with a clinical marker. *Free Radic Biol Med.* 1998; 25:373-377.
154. Rolo A, Palmeira CM. Diabetes and mitochondrial function: role of hyperglycemia and oxidative stress. *Toxicol Appl Pharmacol.* 2006; 212:167-178.
155. Gil L, Martinez G, González I, Tarinas A, Álvarez A, Giuliani A, Molina R, Tápanes R, Pérez J, León OS. Contribution to characterization of oxidative stress in HIV/AIDS patients. *Pharmacol Res.* 2003; 47:217-224.
156. Deshmane SL, Mukerjee R, Fan S, Del Valle L, Michiels C, Sweet T, Rom I, Khalili K, Rappaport J, Amini S, Sawaya BE. Activation of the oxidative stress pathway by HIV-1 Vpr leads to induction of hypoxia inducible factor 1 alpha expression. *J Biol Chem.* 2009; 284:11364-11373.
157. Mozaffarieh M, Grieshaber MC, Orgul S, Flammer J. The potential value of natural antioxidative treatment in glaucoma. *Surv Ophthalmol.* 2008; 53:479-505.
158. Bertram C, Hass R. Cellular responses to reactive oxygen species-induced DNA damage and aging. *Biol Chem.* 2008; 389:211-220.
159. Finkel T. Oxidant signals and oxidative stress. *Curr Opin Cell Biol.* 2003; 15:247-254.
160. Berthiaume JM, Wallace KB. Adriamycin-induced oxidative mitochondrial cardiotoxicity. *Cell Biol Toxicol.* 2007; 23:15-25.
161. Halestrap AP, Clarke SJ, Khaliulin I. The role of mitochondria in protection of the heart by preconditioning. *Biochim Biophys Acta.* 2007; 1767:1007-1031.
162. Berry CE, Hare JM. Xanthine oxidoreductase and cardiovascular disease: molecular mechanisms and pathophysiological implications. *J Physiol.* 2004; 555:589-606.
163. Hare JM, Stamler JS. NO/redox disequilibrium in the failing heart and cardiovascular system. *J Clin Invest.* 2005; 115:509-517.
164. Pryor WA. Vitamin E and heart disease: basic science to clinical intervention trials. *Free Radic Biol Med.* 2000; 28:141-164.
165. Podrez EA, Abu-Soud HM, Hazen SL. Myeloperoxidase-generated oxidants and atherosclerosis. *Free Radic Biol Med.* 2000; 28:1717-1725.
166. Dhalla NS, Elmoselhi AB, Hata T, Makino N. Status of myocardial antioxidants in ischemia-reperfusion injury. *Cardiovasc Res.* 2000; 47:446-456.
167. Butterfield DA, Castegna A, Lauderback CM, Drake J. Evidence that amyloid beta-peptide-induced lipid peroxidation and its sequelae in Alzheimer's disease brain contribute to neuronal death. *Neurobiol Aging.* 2002; 23:655-664.
168. Azzi A, Davies KJ, Kelly F. Free radical biology – terminology and critical thinking. *FEBS Lett.* 2004; 558:3-6.
169. Halliwell B, Aeschbach R, Loliger J, Aruoma OI. The characterization of antioxidants. *Food Chem Toxicol.* 1995; 33:601-617.
170. Behl C, Moosmann B. Antioxidant neuroprotection in Alzheimer's disease as preventive and therapeutic approach. *Free Radic Biol Med.* 2002; 33:182-191.
171. Bitto A, Minutoli L, Squadrito F, Polito F, Altavilla D. Raxofelast, (+/-)-5-(acetyloxy)-2,3-dihydro-4,6,7-trimethyl-2-benzofuranacetic acid: a new antioxidant to modulate the inflammatory response during ischemia-reperfusion injury and impaired wound healing. *Mini Rev Med Chem.* 2007; 7:339-343.
172. Buettner GR, Ng CF, Wang M, Rodgers VG, Schafer FQ. A new paradigm: manganese superoxide dismutase influences the production of H₂O₂ in cells and thereby their biological state. *Free Radic Biol Med.* 2006; 41:1338-1350.
173. Drake J, Sultana R, Aksenova M, Calabrese V, Butterfield DA. Elevation of mitochondrial glutathione by gamma-glutamylcysteine ethyl ester protects mitochondria against peroxynitrite-induced oxidative stress. *J Neurosci Res.* 2003; 74:917-927.
174. Masella R, Di Benedetto R, Vari R, Filesi C, Giovannini C. Novel mechanisms of natural antioxidant compounds in biological systems: involvement of glutathione and glutathione-related enzymes. *J Nutr Biochem.* 2005; 16:577-586.
175. Lillig CH, Lonn ME, Enoksson M, Fernandes AP,

- Holmgren A. Short interfering RNA-mediated silencing of glutaredoxin 2 increases the sensitivity of HeLa cells toward doxorubicin and phenylarsine oxide. *Proc Natl Acad Sci U S A*. 2004; 101:13227-13232.
176. Baty JW, Hampton MB, Winterbourn CC. Proteomic detection of hydrogen peroxide-sensitive thiol proteins in Jurkat cells. *Biochem J*. 2005; 389:785-795.
177. Dobra K, Hjerpe A. Targeted therapy – possible new therapeutic option for malignant mesothelioma? *Connect Tissue Res*. 2008; 49:270-272.
178. Shapiro SS, Saliou C. Role of vitamins in skin care. *Nutrition*. 2001; 17:839-844.
179. Vanasco V, Cimolai MC, Evelson P, Alvarez S. The oxidative stress and the mitochondrial dysfunction caused by endotoxemia are prevented by alpha-lipoic acid. *Free Radic Res*. 2008; 42:815-823.
180. Korkmaz A, Reiter RJ, Topal T, Manchester LC, Oter S, Tan DX. Melatonin: an established antioxidant worthy of use in clinical trials. *Mol Med*. 2009; 15:43-50.
181. Cherubini A, Ruggiero C, Polidori MC, Mecocci P. Potential markers of oxidative stress in stroke. *Free Radic Biol Med*. 2005; 39:841-852.
182. Niki E. Oxidative stress and aging. *Intern Med*. 2000; 39:324-326.
183. Arrigoni O, De Tullio MC. Ascorbic acid: much more than just an antioxidant. *Biochim Biophys Acta*. 2002; 1569:1-9.
184. Carr A, Frei B. Does vitamin C act as a pro-oxidant under physiological conditions? *FASEB J*. 1999; 13:1007-1024.
185. Munteanu A, Zingg JM, Ogru E, Libinaki R, Gianello R, West S, Azzi A. Modulation of cell proliferation and gene expression by alpha-tocopheryl phosphates: relevance to atherosclerosis and inflammation. *Biochem Biophys Res Commun*. 2004; 1031:405-411.
186. Robichova S, Slamena D, Chalupa I, Sebova L. DNA lesions and cytogenetic changes induced by *N*-nitrosomorpholine in HepG₂, V79 and VH10 cells: the protective effects of Vitamins A, C and E. *Mutat Res*. 2004; 560:91-99.
187. Romieu I. Nutrition and lung health. *Int J Tuberc Lung Dis*. 2005; 9:362-374.
188. Mehta R, Shangari N, O'Brien PJ. Preventing cell death induced by carbonyl stress, oxidative stress or mitochondrial toxins with vitamin B anti-AGE agents. *Mol Nutr Food Res*. 2008; 52:379-385.
189. Depeint F, Bruce WR, Shangari N, Mehta R, O'Brien PJ. Mitochondrial function and toxicity: role of the B vitamin family on mitochondrial energy metabolism. *Chem Biol Interact*. 2006; 163:94-112.
190. Cemeli E, Baumgartner A, Anderson D. Antioxidants and the Comet assay. *Mutat Res*. 2009; 681:51-67.
191. Tamimi RM, Hankinson SE, Campos H, Spiegelman D, Zhang S, Colditz GA, Willett WC, Hunter DJ. Plasma carotenoids, retinol, and tocopherols and risk of breast cancer. *Am J Epidemiol*. 2005; 161:153-160.
192. Santocono M, Zurria M, Berrettini M, Fedeli D, Falcioni G. Lutein, zeaxanthin and astaxanthin protect against DNA damage in SK-N-SH human neuroblastoma cells induced by reactive nitrogen species. *J Photochem Photobiol B*. 2007; 88:1-10.
193. Rao AV, Rao LG. Carotenoids and human health. *Pharmacol Res*. 2007; 55:207-216.
194. Ferguson LR. Role of plant polyphenols in genomic stability. *Mutat Res*. 2001; 475:89-111.
195. Manach C, Scalbert A, Morand C, Remesy C, Jimenez L. Polyphenols: food sources and bioavailability. *Am J Clin Nutr*. 2004; 79:727-747.
196. Ruiz PA, Haller D. Functional diversity of flavonoids in the inhibition of the proinflammatory NF-kappa B, IRF, and Akt signaling pathways in murine intestinal epithelial cells. *J Nutr*. 2006; 136:664-671.
197. Hendriks JJ, Alblas J, van der Pol SM, van Tol EA, Dijkstra CD, de Vries HE. Flavonoids influence monocytic GTPase activity and are protective in experimental allergic encephalitis. *J Exp Med*. 2004; 200:1667-1672.
198. Lima CF, Fernandes-Ferreira M, Pereira-Wilson C. Phenolic compounds protect HepG₂ cells from oxidative damage: Relevance of glutathione levels. *Life Sci*. 2006; 79:2056-2068.
199. Di Carlo G, Mascolo N, Izzo AA, Capasso F. Flavonoids: old and new aspects of a class of natural therapeutic drugs. *Life Sci*. 1999; 65:337-353.
200. Serafini M, Laranjinha J, Almeida LM, Maiani G. Inhibition of human LDL lipid peroxidation by phenol-rich beverages and their impact on plasma total antioxidant capacity in humans. *J Nutr Biochem*. 2000; 11:585-590.
201. Williamson G, Manach C. Bioavailability and bioefficacy of polyphenols in humans. II. Review of 93 intervention studies. *Am J Clin Nutr*. 2005; 81:243S-255S.
202. Elbling L, Weiss RM, Teufelhofer O, Uhl M, Knasmueller S, Schulte-Hermann R, Berger W, Micksche M. Green tea extract and (-)-epigallocatechin-3-gallate, the major tea catechin, exert oxidant but lack antioxidant activities. *FASEB J*. 2005; 19:807-809.
203. Lambert JD, Hong J, Yang GY, Liao J, Yang CS. Inhibition of carcinogenesis by polyphenols: evidence from laboratory investigations. *Am J Clin Nutr*. 2005; 81:284S-291S.
204. Ahkang S, Jang YJ, Park H. *In vivo* dual effects of vitamin C on paraquat-induced lung damage: dependence on released metals from the damaged tissue. *Free Radic Res*. 1998; 28:93-107.
205. Lee DH, Folsom AR, Harnack L, Halliwell B, Jacobs DR Jr. Does supplemental vitamin C increase cardiovascular disease risk in women with diabetes? *Am J Clin Nutr*. 2004; 80:1194-1200.
206. Schneider C. Chemistry and biology of vitamin E. *Mol Nutr Food Res*. 2005; 49:7-30.
207. The Alpha-Tocopherol Beta Carotene Cancer Prevention Study G. The effect of vitamin E and Beta carotene on the incidence of lung cancer and other cancers in male smokers. *N Engl J Med*. 1994; 330:1029-1035.
208. Omenn GS, Goodman GE, Thornquist MD, Balmes J, Cullen MR, Glass A, Keogh JP, Meyskens FL Jr, Valanis B, Williams J Jr, Barnhart S, Cherniack MG, Brodtkin CA, Hammar S. Risk factors for lung cancer and for intervention effects in CARET, the Beta-Carotene and Retinol Efficacy Trial. *J Natl Cancer Inst*. 1996; 88:1550-1559.
209. Leung HW, Wu CH, Lin CH, Lee HZ. Luteolin induced DNA damage leading to human lung squamous carcinoma CH27 cell apoptosis. *Eur J Pharmacol*. 2005; 508:77-83.
210. Boots AW, Li H, Schins RP, Duffin R, Heemskerk JW, Bast A, Haenen GR. The quercetin paradox. *Toxicol Appl Pharmacol*. 2007; 222:89-96.
211. Lanza V, Vecchio G. New conjugates of superoxide

- dismutase/catalase mimetics with cyclodextrins. *J Inorg Biochem.* 2009; 103:381-388.
212. Trova MP, Gauuan PJ, Pechulis AD, Bubb SM, Bocckino SB, Crapo JD, Day BJ. Superoxide dismutase mimetics. Part 2: synthesis and structure-activity relationship of glyoxylate- and glyoxamide-derived metalloporphyrins. *Bioorg Med Chem.* 2003; 11:2695-2707.
213. Batinic-Haberle I, Spasojevic I, Stevens RD, Bondurant B, Okado-Matsumoto A, Fridovich I, Vujaskovic Z, Dewhirst MW. New PEG-ylated Mn(III) porphyrins approaching catalytic activity of SOD enzyme. *Dalton Trans.* 2006; 4:617-624.
214. Day BJ. Catalase and glutathione peroxidase mimics. *Biochem Pharmacol.* 2009; 77:285-296.
215. Ehrlich K, Viirlaid S, Mahlapuu R, Saar K, Kullisaar T, Zilmer M, Langel U, Soomets U. Design, synthesis and properties of novel powerful antioxidants, glutathione analogues. *Free Radic Res.* 2007; 41:779-787.
216. Siddaiah V, Maheswara M, Rao CV, Venkateswarlu S, Subbaraju GV. Synthesis, structural revision and antioxidant activities of antimutagenic homoisoflavonoids from *Hoffmanosseggia intricata*. *Bioorg Med Chem Lett.* 2007; 17:1288-1290.
217. Vogel S, Ohmayer S, Brunner G, Heilmann J. Natural and non-natural prenylated chalcones: synthesis, cytotoxicity and anti-oxidative activity. *Bioorg Med Chem.* 2008; 16:4286-4293.
218. Cotelle N, Bernier JL, Catteau JP, Pommery J, Wallet JC, Gaydou EM. Antioxidant properties of hydroxy-flavones. *Free Radic Biol Med.* 1996; 20:35-43.
219. Lebeau J, Furman C, Bernier JL, Duriez P, Teissier E, Cotelle N. Antioxidant properties of di-*tert*-butylhydroxylated flavonoids. *Free Radic Biol Med.* 2000; 29:900-912.
220. Suh HJ, Chung MS, Cho YH, Kim JW, Kim DH, Han KW, Kim CJ. Estimated daily intakes of butylated hydroxyanisole (BHA), butylated hydroxytoluene (BHT) and *tert*-butyl hydroquinone (TBHQ) antioxidants in Korea. *Food Addit Contam.* 2005; 22:1176-1188.
221. Macdonald J, Galley HF, Webster NR. Oxidative stress and gene expression in sepsis. *Br J Anaesth.* 2003; 90:221-232.
222. Silva JP, Areias FM, Proença MF, Coutinho OP. Oxidative stress protection by newly synthesized nitrogen compounds with pharmacological potential. *Life Sci.* 2006; 78:1256-1267.
223. Silva JP, Proença MF, Coutinho OP. Protective role of new nitrogen compounds on ROS/RNS-mediated damage to PC12 cells. *Free Radic Res.* 2008; 42:57-69.
224. Silva JP, Gomes AC, Proença F, Coutinho OP. Novel nitrogen compounds enhance protection and repair of oxidative DNA damage in a neuronal cell model: Comparison with quercetin. *Chem Biol Interact.* 2009; 181:328-337.
225. Areias FM. Novos compostos heterocíclicos de azoto com unidades fenólicas: síntese e actividade biológica. Ph.D. Thesis. University of Minho, Braga, Portugal. 2009; p. 259. (Available online at: <http://hdl.handle.net/1822/5941>.)
226. Rice-Evans C, Miller NJ, Paganga G. Structure-antioxidant activity relationships of flavonoids and phenolic acids. *Free Radic Biol Med.* 1996; 20:933-956
227. Lien EJ, Ren S, Bui HH, Wang R. Quantitative structure-activity relationship analysis of phenolic antioxidants. *Free Radic Biol Med.* 1999; 26:285-294.
228. Wentrup C. Reactive molecules: the neutral reactive intermediates in organic chemistry. Wiley, NY, USA, 1984; pp. 23-161.
229. Pinto-Basto D, Silva JP, Queiroz MJ, Moreno AJ, Coutinho OP. Antioxidant activity of synthetic diarylamines: a mitochondrial and cellular approach. *Mitochondrion.* 2009; 9:17-26.

(Received January 22, 2010; Revised March 16, 2010; Accepted March 22, 2010)

Brief Report

3D QSAR investigations on locomotor activity of 5-cyano-N1,6-disubstituted 2-thiouracil derivatives

Bhanudas S. Kuchekar¹, Yogesh V. Pore^{2,*}

¹Department of Pharmaceutical Chemistry, MAEER's Maharashtra Institute of Pharmacy, MIT Campus, Pune, Maharashtra, India;

²Department of Pharmaceutical Chemistry, Government College of Pharmacy, Karad, Maharashtra, India.

ABSTRACT: Three dimensional quantitative structure activity relationship (3D QSAR) investigations were carried out on a series of 5-cyano-N1,6-disubstituted 2-thiouracil derivatives for their locomotor activity. The structures of all compounds were built on a workspace of VLifeMDS3.5 molecular modeling software and 3D QSAR models were generated by applying a partial least square (PLS) linear regression analysis coupled with a stepwise variable selection method. Both derived models were found to be statistically significant in terms of regression and internal and external predictive ability ($r^2 = 0.9414$ and 0.8511 , $q^2 = 0.8582$ and 0.6222 , $\text{pred}_r^2 = 0.5142$ and 0.7917). The QSAR models indicated that both electrostatic and steric interaction energies were contributing significantly to locomotor activity of thiouracil derivatives.

Keywords: 3D QSAR, thiouracil derivatives, locomotor activity, predictive ability, PLS

1. Introduction

It is well known that pyrimidine compounds are associated with a large number of biological activities like antimicrobial (1,2), anticancer (3), antiviral (4), antioxidant (5) and CNS activities (6). There has always been growing interest in design and development of pyrimidine derivatives. In recent years computational chemistry, especially quantitative structure activity relationship studies (QSAR) have become an integral part of drug discovery processes. Significant attention has been focused on QSAR investigations of a variety of heterocyclic compounds and pyrimidines are not exceptional cases (7-11).

Thus, recognizing the biological significance of

pyrimidines, some novel 5-cyano-N1,6-disubstituted 2-thiouracil derivatives were synthesized and evaluated for locomotor activity using actophotometer. QSAR relationships of these compounds were also further established with locomotor activity.

The objective of the present work was to perform three dimensional quantitative structure activity relationship (3D QSAR) studies on 5-cyano-N1,6-disubstituted 2-thiouracil derivatives. Partial least square (PLS) linear regression analysis was used to derive various QSAR models. The models were further validated for their regression coefficient, internal and external predictive ability and statistical significance. The models were interpreted to investigate the contribution of various 3D descriptors in locomotor activity.

2. Materials and Methods

2.1. Molecular modeling software

VLifeMDS (Version 3.5 VLife Sciences Technologies Pvt. Ltd., Pune, India) molecular modeling software was used for construction of molecules and generation of 3D QSAR models.

2.2. Synthesis and biological evaluation of thiouracil derivatives (P1-P24)

The thiouracil derivatives were synthesized and evaluated for locomotor activity by actophotometer according to a reported procedure (12).

2.3. Biological data

A data set of pEC_{50} values (locomotor activity) of twenty four compounds was used for 3D QSAR investigations (Table 1). The negative logarithmic values of micromolar concentrations of compounds required to produce a fifty percent response (EC_{50}) in animals were used as dependent variables.

2.4. Energy minimization and alignment of molecules

The molecules were optimized for energy minimization

*Address correspondence to:

Dr. Yogesh Pore, Department of Pharmaceutical Chemistry, Government College of Pharmacy, Karad, Maharashtra 415124, India.
e-mail: dryogeshpore@rediffmail.com

Table 1. Nature of R group and pEC₅₀ values of thiouracil derivatives

Compound code	Nature of R ₁	Nature of R ₂	pEC ₅₀ (–log EC ₅₀ or log 1/EC ₅₀) (μmol)
P1	C ₆ H ₅	C ₆ H ₅	0.5534
P2	C ₆ H ₅	4-OH-C ₆ H ₅	0.7598
P3	C ₆ H ₅	4-OCH ₃ -C ₆ H ₅	0.8260
P4	4-Cl-C ₆ H ₅	C ₆ H ₅	0.5678
P5	4-Cl-C ₆ H ₅	4-OH-C ₆ H ₅	0.6683
P6	4-Cl-C ₆ H ₅	4-OCH ₃ -C ₆ H ₅	0.7735
P7	4-CH ₃ -C ₆ H ₅	C ₆ H ₅	0.7927
P8	4-CH ₃ -C ₆ H ₅	4-OH-C ₆ H ₅	0.7749
P9	4-CH ₃ -C ₆ H ₅	4-OCH ₃ -C ₆ H ₅	0.7761
P10	4-OCH ₃ -C ₆ H ₅	C ₆ H ₅	0.7958
P11	4-OCH ₃ -C ₆ H ₅	4-OH-C ₆ H ₅	0.7657
P12	4-OCH ₃ -C ₆ H ₅	4-OCH ₃ -C ₆ H ₅	0.8535
P13	4-F-C ₆ H ₅	C ₆ H ₅	0.5712
P14	4-F-C ₆ H ₅	4-OH-C ₆ H ₅	0.6928
P15	4-F-C ₆ H ₅	4-OCH ₃ -C ₆ H ₅	0.7814
P16	2, 4-CH ₃ -C ₆ H ₅	C ₆ H ₅	0.7975
P17	2, 4-CH ₃ -C ₆ H ₅	4-OH-C ₆ H ₅	0.7601
P18	2, 4-CH ₃ -C ₆ H ₅	4-OCH ₃ -C ₆ H ₅	0.8045
P19	3-CH ₃ -C ₆ H ₅	C ₆ H ₅	0.7629
P20	3-CH ₃ -C ₆ H ₅	4-OH-C ₆ H ₅	0.7610
P21	3-CH ₃ -C ₆ H ₅	4-OCH ₃ -C ₆ H ₅	0.7667
P22	4-NO ₂ -C ₆ H ₅	C ₆ H ₅	0.5581
P23	4-NO ₂ -C ₆ H ₅	4-OH-C ₆ H ₅	0.6638
P24	4-NO ₂ -C ₆ H ₅	4-OCH ₃ -C ₆ H ₅	0.7899

using MMFF (Merck Molecular Force Field) in the MOPAC module of VLifeMDS software. The threshold value for root mean square (rms) gradient was kept at 0.001 kcal/mol·Å. All molecules were subsequently aligned by a template based alignment technique using a common structure as a template. The most active molecule was selected as a template for alignment of the molecules. The alignment is useful for studying shape variation with respect to the base structure selected for alignment.

2.5. Descriptor calculation

For 3D QSAR analysis, the VLife Molecular Design Suite (VLifeMDS) allows the user to choose probe, grid size, and grid interval for the generation of descriptors. After suitable alignment of a given set of molecules, a common rectangular grid (lattice) was generated around the molecules. The steric, electrostatic and hydrophobic interaction energies were computed at the lattice points of the grid using a methyl probe of charge +1. These interaction energy values were considered for relationship generation and utilized as descriptors.

2.6. Statistical analysis

The descriptors were taken as independent variables and biological activity as dependent variables. The Partial Least Squares Regression (PLSR) method of analysis was used to derive the 3D QSAR equations. Statistical parameters employed were the number of compounds in regression n , the regression coefficient r^2 , the F -test (Fischer's value) for statistical significance F , the cross-validated correlation coefficient q^2 and the standard error of estimation r^2 and q^2 . The regression coefficient r^2 represents the part of variation in the observed data that is explained by the regression. Correlation coefficient values closer to 1.0 represent the better fit of the regression. The F -test is the ratio of the variance explained by the model and the variance due to error in the regression. High values of the F -test indicate that the model is statistically significant. The predictive ability (internal) of the generated models was evaluated by a cross validation method using a 'leave-one-out' scheme. Validation parameters considered were cross validated q^2 . The predictive ability (external) of the selected model was also confirmed by external

validation of test set compounds which is denoted with pred_r^2 .

3. Results

The QSAR investigations of 5-cyano-N1,6-disubstituted 2-thiouracil analogues resulted in several 3D QSAR equations. The two best equations are discussed.

3.1. Validation of QSAR models

Table 2 illustrates validation parameters for 3D QSAR models. Model 1 was obtained by a classical sphere

exclusion type algorithm of training and test data selection (13-16) whereas model 2 was obtained by a random method of training and test set data selection (17). As indicated, both QSAR models were found to be statistically significant and predictive in terms of r^2 , q^2 , F and pred_r^2 values (18-22). Table 3 shows comparative predicted activities along with residuals of the two models. Figures 1 and 2 represent the fitness plots (R^2) of observed vs. predicted biological activity for models 1 and 2, respectively.

Model 1 has shown excellent fit ($r^2 = 0.9414$), good internal predictive ability ($q^2 = 0.8542$) and a good fitness plot ($R^2 = 0.8519$) with an optimal ability

Table 2. Comparative data of validation parameters employed for 3D QSAR equations

Model/Parameters	Model 1	Model 2
Equation	$\text{pEC}_{50} = +0.4431 E_{86} - 187.1126 S_{753} + 0.0044 S_{284} + 0.0104 S_{606} - 7.6961$	$\text{pEC}_{50} = -104.9810 S_{753} + 0.6250 E_{86} + 0.0031 S_{284} + 0.0161 E_{524} + 0.0312 S_{434} - 3.8624$
Training set size (n)	19	18
Test set size	5 (P1, P20, P2, P9, and P15)	6 (P6, P8, P10, P15, P22, and P24)
Degree of freedom	15	14
r^2	0.9414	0.8511
r^2 se	0.0238	0.0385
F test	80.3745	26.6740
q^2	0.8582	0.6222
q^2 se	0.0370	0.0613
pred_r^2	0.5142	0.7917
pred_r^2 se	0.0681	0.0428
R^2 for fitness plot	0.8519	0.8365

Table 3. Comparative observed and predicted activities (LOO) of thiouracil derivatives by 3D QSAR models

Compounds	Observed activity pEC_{50}	Predicted activity pEC_{50} ^a			
		3D Model 1	Residuals	3D Model 2	Residuals
P1	0.5534	0.6158 ^b	-0.0624	0.6196	-0.0662
P2	0.7598	0.6939 ^b	0.0659	0.7285	0.0313
P3	0.8260	0.8256	0.0004	0.8137	0.0123
P4	0.5678	0.5826	-0.0148	0.5758	-0.008
P5	0.6683	0.6617	0.0066	0.6947	-0.0264
P6	0.7735	0.7303	0.0432	0.7153 ^b	0.0582
P7	0.7927	0.7685	0.0242	0.7247	0.068
P8	0.7749	0.8124	-0.0375	0.8114 ^b	-0.0365
P9	0.7761	0.8509 ^b	-0.0748	0.8304	-0.0543
P10	0.7958	0.7754	0.0204	0.8037 ^b	-0.0079
P11	0.7657	0.7775	-0.0118	0.8096	-0.0439
P12	0.8535	0.8585	-0.005	0.8366	0.0169
P13	0.5712	0.5730	-0.0018	0.5521	0.0191
P14	0.6928	0.6531	0.0397	0.6786	0.0142
P15	0.7814	0.7782 ^b	0.0032	0.7415 ^b	0.0399
P16	0.7975	0.7991	-0.0016	0.7994	-0.0019
P17	0.7601	0.7702	-0.0101	0.7680	-0.0079
P18	0.8045	0.7952	0.0093	0.7687	0.0358
P19	0.7629	0.7798	-0.0169	0.7764	-0.0135
P20	0.7610	0.6922 ^b	0.0688	0.7234	0.0376
P21	0.7667	0.7802	-0.0135	0.7552	0.0115
P22	0.5581	0.5895	-0.0314	0.5574 ^b	0.0007
P23	0.6638	0.6730	-0.0092	0.6924	-0.0286
P24	0.7899	0.7844	0.0055	0.7372 ^b	0.0527

^a Indicates predicted activity by leave one out cross validation; ^b Indicates molecules of test set.

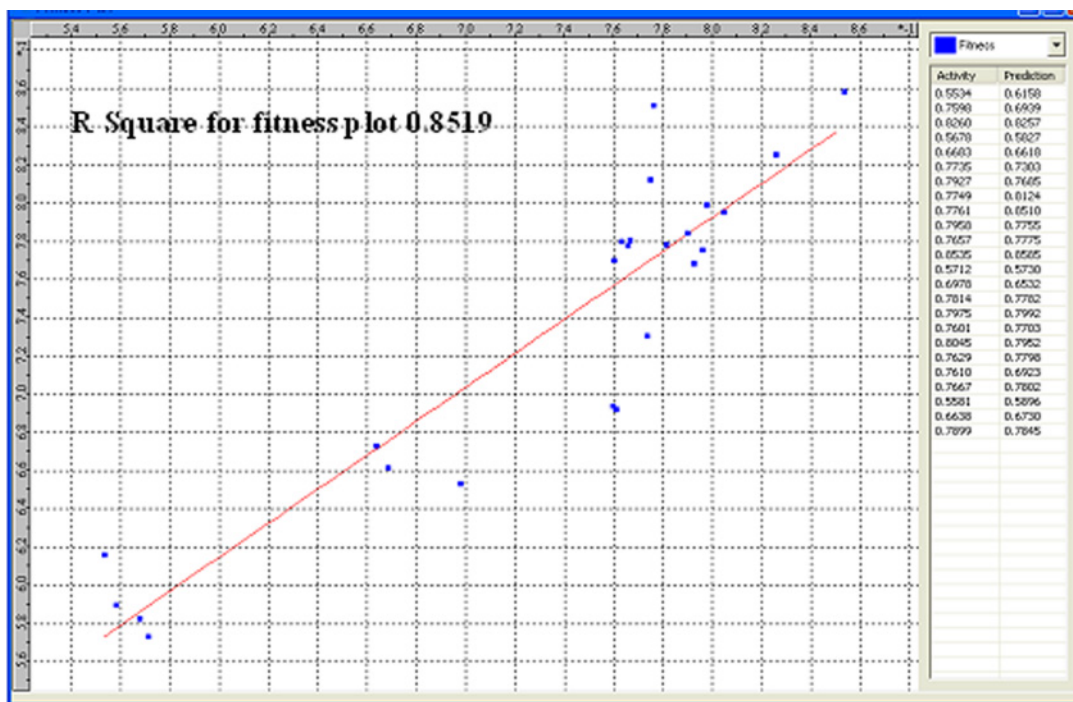


Figure 1. The plot of observed *versus* predicted activity for 3D model 1.

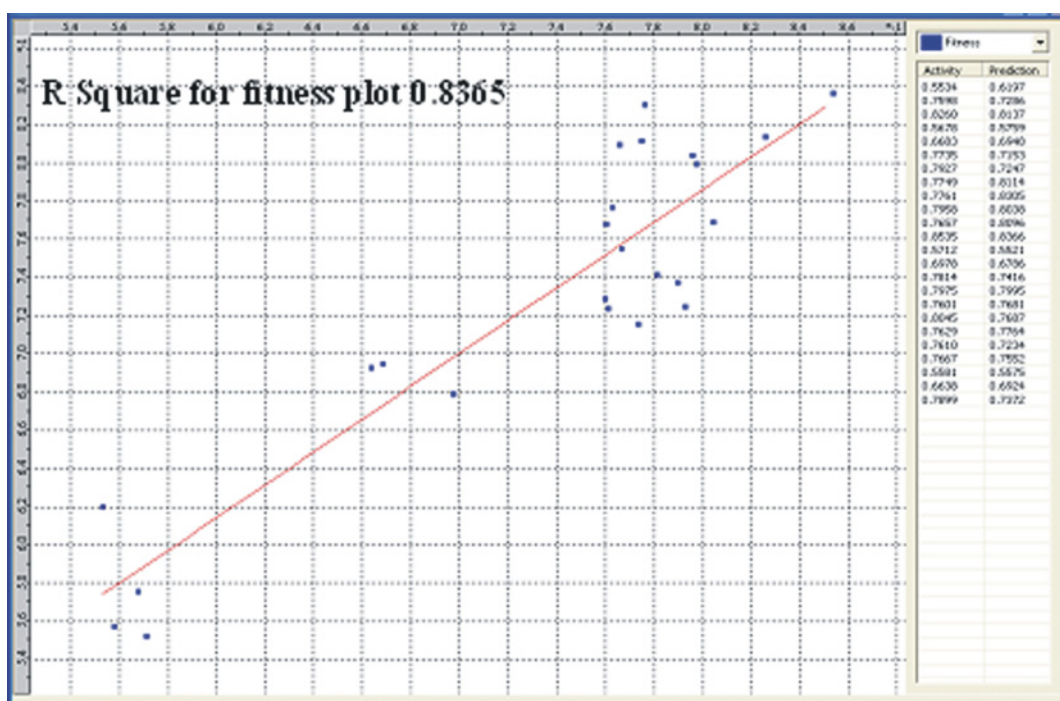


Figure 2. The plot of observed *versus* predicted activity for 3D model 2.

to predict the activities of test set molecules ($\text{pred}_r^2 = 0.5182$) which have not been included to build the QSAR model.

Model 2 has also displayed a good correlation coefficient ($r^2 = 0.8511$), optimal internal predictive ability ($q^2 = 0.6222$) with a fitness plot of ($R^2 = 0.8109$). However, the ability of model 2 to predict the activities of test set molecules is certainly excellent ($\text{pred}_r^2 =$

0.7917) as compared to model 1.

From the equations, it could be concluded that 94.14% ($r^2 = 0.9414$) and 85.11% ($r^2 = 0.8511$) of the variation in the biological activity was accounted for by the parameters used in equations 1 and 2, respectively. This signifies that in both the models, a good correlation exists between their corresponding descriptors and biological activity (23). Further, in

both cases the high values of F tests indicated that the statistical significance of 99.99% of the models meant that probability of failure of the models was 1 in 10,000.

3.2. Interpretation of QSAR models

The local fields around aligned molecules of those

found to be important for activity variation in model 1 and model 2 are shown in Figures 3 and 4, respectively.

As shown in the figures, two electrostatic field descriptors E_{86} and E_{524} (blue points) and four steric field descriptors S_{753} , S_{284} , S_{606} , and S_{434} (green points) are contributing significantly for locomotor activity of the molecules. The electrostatic

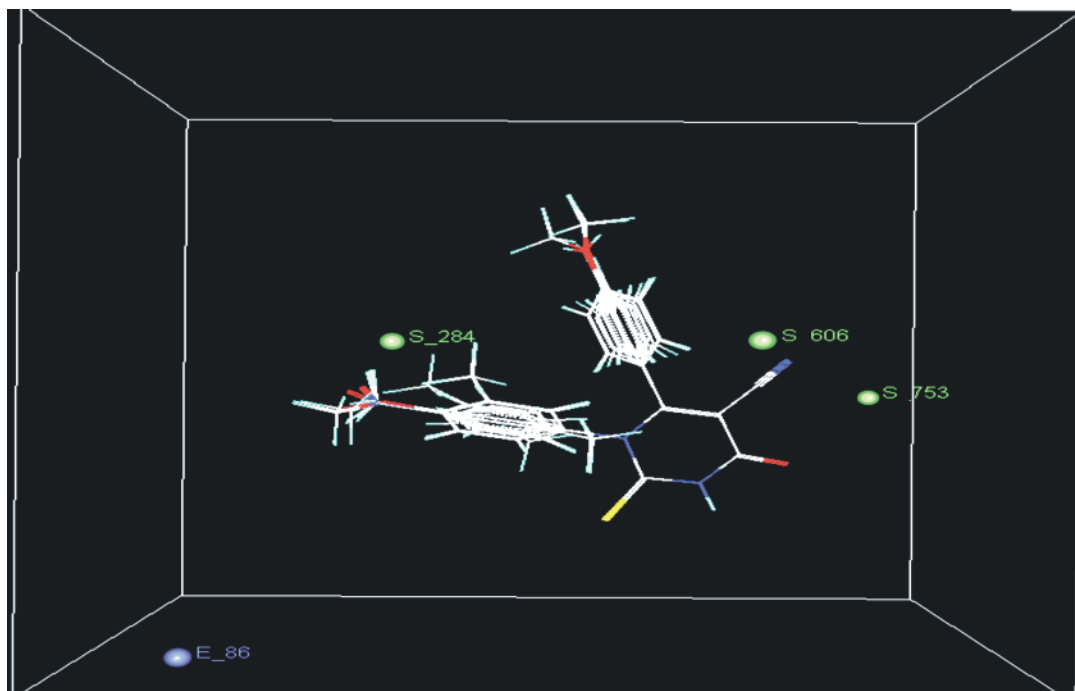


Figure 3. Relative positions of the local fields around aligned molecules for 3D model 1.

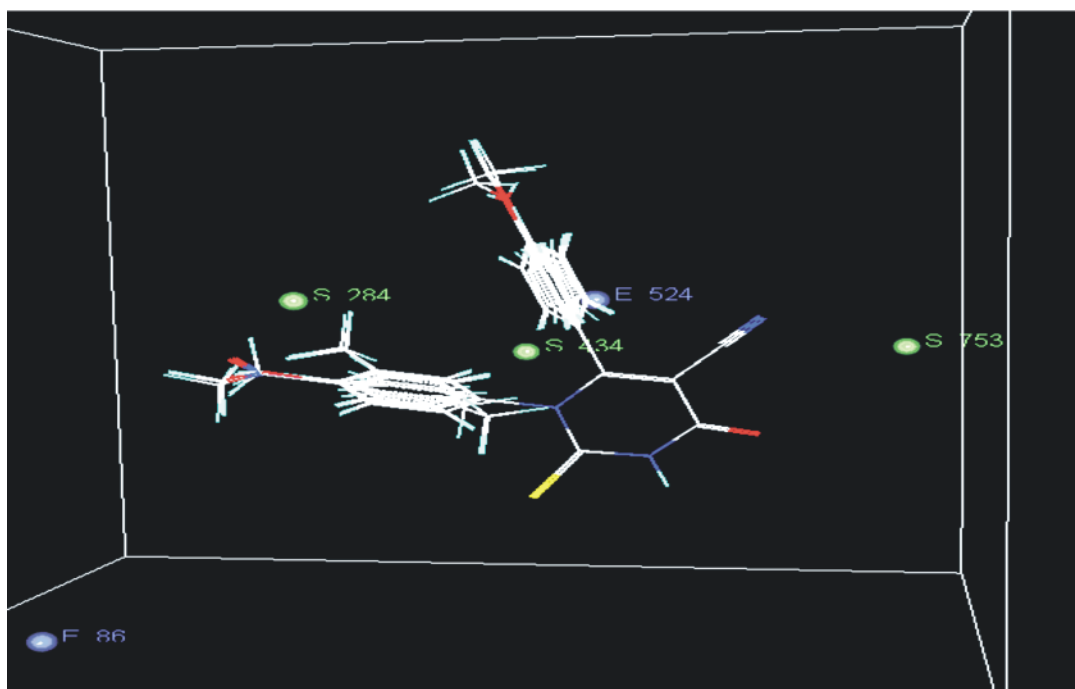


Figure 4. Relative positions of the local fields around aligned molecules for 3D model 2.

field descriptor E_86 and steric field descriptors S_753, and S_284 are common in both models. The positive range for E_86 and E_524 indicate that positive electrostatic potential is favorable for increase in activity and hence a less electronegative substituent should be preferred in these regions.

The steric field descriptors S_284, S_606, and S_434 contribute positively which indicates that positive steric potential is favorable for an increase in activity and hence a more bulky substituent is preferred in these regions. However, a negative contribution of S_753 indicates that the bulky substituent can not be tolerated and steric interactions should be reduced in that region for optimal biological activity.

Thus these relative positions and ranges of the corresponding important electrostatic and steric fields in the above models could be helpful in design of new molecules with improved locomotor activity.

4. Conclusions

The present QSAR investigations demonstrated that the generated 3D QSAR models were statistically significant in terms of their correlation with biological activity and internal and external predictive abilities. It could be concluded that the locomotor activity of thiouracil derivatives was positively contributed by electrostatic interaction fields. In addition the increase in steric interactions (bulky aromatic or cycloaliphatic substituents) at certain lattice points could be beneficial for improved potency of the thiouracil derivatives. Thus the developed 3D QSAR models may raise a scope for the design of new thiouracil derivatives with improved biological profiles (locomotor activity).

Acknowledgements

Authors are thankful to Principal, Bharati Vidyapeeth's College of Pharmacy, Kolhapur, Maharashtra, India, for providing software facilities for QSAR studies. Authors are very much thankful to Principal, Govt. College of Pharmacy, Karad, Maharashtra, India, for providing laboratory facilities and constant encouragement.

References

- Sunduru N, Agarwal A, Katiyar SB, Nishi, Goyal N, Gupta S, Chauhan PM. Synthesis of 2,4,6-trisubstituted pyrimidine and triazine heterocycles as antileishmanial agents. *Bioorg Med Chem.* 2006; 14:7706-7715.
- George S, Parameswaran MK, Chakraborty AR, Ravi TK. Synthesis and evaluation of the biological activities of some 3-{{[5-(6-methyl-4-aryl-2-oxo-1,2,3,4-tetrahydropyrimidin-5-yl)-1,3,4-oxadiazol-2-yl]-imino}-1,3-dihydro-2H-indol-2-one derivatives. *Acta Pharm.* 2008; 58:119-129.
- Gangjee A, Yu J, Kisliuk LR, Halie HW, Sobrero G, McGuire JJ. Design, synthesis and biological activities of classical N-4-[2-(2-amino-4-ethylpyrrolo[2,3-d]pyrimidin-5-yl)ethyl]benzoyl-L-glutamic acid and its 6-methyl derivative as potential dual inhibitors of thymidylate synthase and dihydrofolate reductase and as potential antitumor agents. *J Med Chem.* 2003; 46:591-600.
- Rostom SF, Fahmy HY, Saudi MS. Synthesis and *in vitro* anti-HIV screening of certain 2-(benzoxazol-2-ylamino)-3H-4-oxopyrimidines. *Sci Pharm.* 2003; 71:57-74.
- Gordon LB, Donald EA, Banitt SL, Kenneth LB, Stephen AM, Palmer JR, Tustin JM. Synthesis of novel 2,4-diamino pyrrolo[2,3-d]pyrimidines with antioxidant neuroprotective and antiasthama activity. *J Med Chem.* 1995; 38:4161-4163.
- Matosiuk D, Tkaczynski T, Stefanczyk J. Synthesis and CNS activity of new 1-alkyl-2-aryl-7-hydroxy-5(1H)oxo-imidazo[1,2-a]pyrimidines. *Acta Pol Pharm.* 1996; 53:209-212.
- Jarmuła A, Cieplak P, Krygowski TM, Rode W. The effect of 5-substitution in the pyrimidine ring of dUMP on the interaction with thymidylate synthase: Molecular modeling and QSAR. *Bioorg Med Chem.* 2007; 15:2346-2358.
- Shrikant K, Debnath B, Jha T. QSAR study on adenosine kinase inhibition of pyrrolo[2,3-d]pyrimidine nucleoside analogues using the hansch approach. *Bioorg Med Chem Lett.* 2002; 12:899-902.
- Chakraborti AK, Gopalakrishnan B, Sobhia ME, Malde A. 3D-QSAR studies on thieno[3,2-d]pyrimidines as phosphodiesterase IV inhibitors. *Bioorg Med Chem Lett.* 2003; 13:1403-1408.
- Prabhakar YS, Ram VJ. A QSAR study on the antileishmanial activity of some substituted pyrimidines and pyrazolo [1,5-a] pyrimidines. *Indian J Pharm Sci.* 1997; 59:286-291.
- Jain P, Soni LK, Gupta AK, Kashkedikar SG. QSAR analysis of 2,4-diaminopyrido[2,3-d]pyrimidines and 2,4-diaminopyrrolo[2,3-d]pyrimidines as dihydrofolate reductase inhibitors. *Indian J Biochem Biophys.* 2005; 42:315-320.
- Pore Y, Kuchekar B, Bhatia M, Ingale K. Quantitative structure activity relationship (QSAR) studies on 5-cyano, N1,6-disubstituted, 2-thiouracil derivatives as central nervous system depressants. *Digest Journal of Nanomaterials and Biostructures.* 2009; 4:373-382.
- Coi A, Fiamingo FL, Livi O, Calderone V, Martelli A, Massarelli I, Bianucci AM. QSAR studies on BK channel activators. *Bioorg Med Chem.* 2009; 17:319-325.
- Golbraikh A, Tropsha A. Predictive QSAR modeling based on diversity sampling of experimental data sets for the test and training set selection. *J Comp Aid Molec Des.* 2002; 16:357-369.
- Golbraikh A. Molecular data set diversity indices and their applications to comparison of chemical databases and QSAR analysis. *J Chem Inf Comput Sci.* 2000; 40:414-425.
- Guha R, Serra JR, Jurs PC. Generation of QSAR sets with a self-organizing map. *J Mol Graph Model.* 2004; 23:1-14.
- Chakraborti AK, Gopalakrishnan B, Sobhia ME, Malde A. 3D-QSAR studies of indole derivatives as phosphodiesterase IV inhibitors. *Eur J Med Chem.* 2003; 38:975-982.
- Puratchikody A, Nagalakshmi G, Doble M. Experimental and QSAR studies on antimicrobial activity of

- benzimidazole derivatives. Chem Pharm Bull. 2008; 56:273-281.
19. Tropsha A, Gramatica P, Gombar VK. The importance of being earnest: Validation is the absolute essential for successful application and interpretation of QSPR models. QSAR Comb Sci. 2003; 22:69-77.
 20. Golbraikh A, Tropsha A. Beware of q^2 ! J Mol Graph Model. 2002; 20:269-276.
 21. Afantitis A, Melagraki G, Sarimveis H, Igglessi-Markopoulou O, Kollias G. A novel QSAR model for predicting the inhibition of CXCR3 receptor by 4-*N*-aryl-[1,4] diazepane ureas. Eur J Med Chem. 2009; 44:877-884.
 22. Ravichandran V, Mourya VK, Agrawal RK. QSAR prediction of HIV-1 reverse transcriptase inhibitory activity of benzoxazinone derivatives. Internet Electron J Mol Des. 2007; 6:363-374.
 23. VLifeMDS3.5 Molecular Design Suite, Vlife Sciences Technologies Pvt. Ltd., Pune, India (www.vlifesciences.com) (2008).

(Received February 18, 2010; Accepted March 14, 2010)

Brief Report

Serum fructose concentration in rats after single dose oral administration of Si-Wu-Tang

Qiande Liang^{1,*}, Chengrong Xiao^{1,*}, Zengchun Ma¹, Yuguang Wang¹, Beibei Lu¹, Hongling Tan¹, Baiping Ma¹, Boli Zhang², Yue Gao^{1,**}

¹ Beijing Institute of Radiation Medicine, Beijing, China;

² Tianjin University of Traditional Chinese Medicine, Tianjin, China.

ABSTRACT: Our previous study showed that fructose is an important active constituent that is responsible for Si-Wu-Tang's (SWT) effects promoting hematopoiesis and immunity. In order to provide primary data for analysis of the mechanism of fructose's bioactivity, the concentration of serum fructose in rats after a single oral administration dose of Si-Wu-Tang was determined. The concentration of serum fructose in fasting rats was 0.34 ± 0.24 mg/dL. After oral administration of 7.2 mL per kg body weight of SWT extract (1 mL extract corresponds to 1 g SWT dried herbs), serum fructose levels reached a peak concentration of 1.03 ± 0.25 mg/dL within 60 min, and then declined to the baseline level within 180 min, a pattern which is similar to the one reported for oral administration of pure fructose. The peak concentration was only 2-3 times higher than the baseline serum fructose concentration. These results showed that the increase of blood fructose concentration after oral administration of SWT is small and transient, which is very probably due to the quick metabolism of fructose by the liver. We suggest, for future research, it is necessary to consider the probability that fructose's bioactivity on hematopoiesis and immunity is not exerted by fructose in its original form, but after it is metabolized by the liver.

Keywords: Blood, concentration, fructose, rat, serum, Si-Wu-Tang

1. Introduction

Si-Wu-Tang (SWT), a traditional Chinese formula

consisting of *Rehmanniae Radix*, *Angelica Radix*, *Chuanxiong Rhizoma* and *Paeoniae Radix*, has traditionally been used in China for about one thousand years (1). Dai *et al.* reported that SWT has been used for the treatment of gynecologic diseases (*e.g.* dysmenorrhea, menoxenia, metrorrhagia, abortion), cutaneous diseases (*e.g.* pruritus, urticaria, eczema, dermatitis), and chronic inflammation (*e.g.* chronic nephritis, pelvic inflammation) (2). It has been reported to possess sedative, anti-coagulant and antibacterial activities and to exhibit effects of vasodilatation, hematopoiesis, enhancement of cellular immunity and radio-protection (3,4). Our interest has been focused on SWT's hematopoiesis-related activities. Using 3.5 Gy ⁶⁰Co γ -ray irradiated mice as a model of anemia, we found that SWT increases the number of peripheral leukocytes and four types of progenitor cells in bone marrow, colony-forming unit-granulocyte-macrophages (CFU-GM), colony-forming unit-mature erythroid (CFU-E), colony-forming unit-immature erythroid (BFU-E) and colony-forming unit-multipotential (CFU-mix) cells (5). In our latest report, fructose was shown to be an important active constituent responsible for SWT's effect promoting hematopoiesis and immunity after oral administration (6). Therefore, it has currently become one of the major concerns of our research effort to find out the mechanism of fructose's bioactivity.

To study the mechanism of fructose's bioactivity, changes of blood concentration after SWT administration is primarily required. It will help us to know the characteristics of the absorption, metabolism and elimination process of fructose after oral administration of SWT, which should help us analyze the possible mechanism of fructose's bioactivity. On the other hand, if *in vitro* experiments to study the mechanism of fructose's bioactivity are to be performed in the future, a proper concentration of fructose will be required. In the present study, we investigated the changes of serum fructose concentration in rats after oral administration of SWT for the purpose of providing primary data for the mechanism of analysis of fructose's bioactivity.

*The first two authors contributed equally to this article.

**Address correspondence to:

Dr. Yue Gao, Department of Pharmacology and Toxicology, Beijing Institute of Radiation Medicine, 27 Tai-ping Road, Beijing 100850, China.
e-mail: gaoyue@yahoo.com

2. Materials and Methods

2.1. Animals

Female Sprague-Dawley rats (274 ± 20 g) were purchased from the Experimental Animal Center of the Academy of Military Medical Sciences (Beijing, China). They were housed in an environmentally controlled breeding room with free access to standard animal chow and tap water, and were allowed at least three days acclimatization before an experiment. Each rat was used once and treated in accordance with the National Institutes of Health guidelines for the care and use of laboratory animals and was fasted for 24 h before the test.

2.2. Drugs and reagents

An extract of SWT was prepared by decocting the dried prescription of herbs with boiling water. After the first decoction the duration of which was about 30 min, the suspension was filtered and water was added for the second decoction of about 20 min. The filtered and mixed suspension from two decoctions was condensed to a concentration of 1 g dried herb weight/mL solution and then stored at -20°C before administration. The ingredients of 41 g SWT include 15 g of *Rehmannia Radix*, 10 g of *Angelica Radix*, 6 g of *Chuanxiong Rhizoma* and 10 g of *Paeoniae Radix*. These ingredients correspond to the following plants: *Rehmannia glutinosa* LIBOSCH. (*Scrophulariaceae*), *Angelica sinensis* (OLIV.) (*Umbelliferae*) DIELS, *Ligusticum chuanxiong* HORT. (*Umbelliferae*), and *Paeonia lactiflora* PALL (*Paeoniaceae*), respectively. These plant materials were purchased from Tongrentang, Ltd. (Beijing, China) and identified by Dr. Baiping Ma in our laboratory. Fructose was purchased from Sinopharm Chemical Reagent Co., Ltd. Glucose, sucrose, potassium carbonate and anhydrous magnesium sulfate were purchased from Beijing Chemical Reagent Company. FA-20 fructose assay kit, glucose oxidase and catalase were purchased from Sigma-Aldrich Co., St. Louis (MO, USA). Perchloric acid was purchased from Jinlu Chemical Co., Ltd. (Shanghai, China).

2.3. Content of fructose in SWT

To calculate the administered dose of fructose, the contents of fructose and sucrose in SWT were quantitatively determined using our previously reported high performance liquid chromatography (HPLC) method (7) for simultaneous determination of fructose, glucose, and sucrose, with slight modifications. Briefly, 1 mL of the SWT extract was diluted to 100 mL with water and then added to 400 mL ethanol and filtered to remove precipitation. The filtered solution was evaporated and solubilized with 50 mL of 50% ethanol

solution. Two μL of this solution was injected into an Angilent 1100 HPLC system with a SHISEIDO carbohydrate column ($5 \mu\text{m}$, 150×2.0 mm) and a PL-ELS 2100 evaporative light scattering detector (ELSD) for analysis. The mobile phase was isocratic acetonitrile and water (75:25, v/v). The flow rate was 0.2 mL/min. The evaporation temperature, nebulization temperature and gas flow of ELSD were 25°C , 25°C , and 1.0 mL/min, respectively. The contents of fructose, glucose, and sucrose in the SWT extract were determined to be 41.6, 37.5, and 92.4 mg/mL, respectively, using an external standard method.

2.4. Collection and measurement of blood samples

Each rat was administered a single oral dose of 7.2 mL per kg body weight of SWT extract (1 mL extract corresponds to 1 g dried herbs of SWT). At time zero and at times of 15, 30, 60, 90, 120, 180, 240, 360, 540 min after dosing, a blood sample (3-5 mL) was collected from the aorta of the rat under anesthesia. Within 60 min after blood withdrawal, the samples were centrifuged and the separated serum samples were frozen in polypropylene tubes at -20°C prior to analysis. Following the procedure described by Beuter HO (8), the serum samples (1.5-2.5 mL) were deproteinized with an equal volume of 0.6 M perchloric acid solution. The concentrations of fructose were then measured with the FA-20 fructose assay kit. In this method, hexokinase, phosphoglucose isomerase, and glucose-6-phosphate dehydrogenase are used and the increase in absorbance at 340 nm is directly proportional to fructose concentration. Data were expressed as mean \pm standard deviation (mean \pm S.D.).

3. Results and Discussion

All experimental subjects were female Sprague-Dawley rats (274 ± 20 g). All rats orally received a single dose of 7.2 mL SWT extract per kg body weight. One mL extract corresponds to 1 g dried herbs of SWT and contained 41.6 mg fructose and 92.4 mg sucrose (determined by HPLC). Fructose in both free monosaccharide form and disaccharide form (sucrose) in 1 mL SWT extract was calculated to be 90.2 mg ($41.6 + 92.4 \times 180/342 = 90.2$). As shown in Figure 1, fructose concentration in fasting rat serum was 0.34 ± 0.24 mg/dL. The peak rat serum fructose concentration after the single dose of SWT was 1.03 ± 0.25 mg/dL. This was reached within 60 min and then declined to baseline levels within 180 min.

This is the first report concerning blood fructose concentrations after SWT oral administration. Fructose was shown in our previous research to be an important active constituent responsible for SWT's effect promoting hematopoiesis and immunity. To analyze the possible mechanism of fructose's bioactivity, we

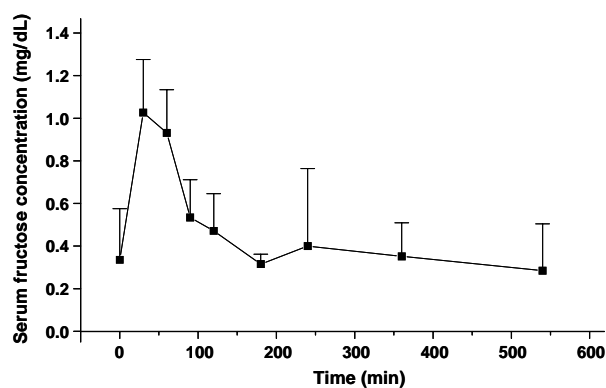


Figure 1. Concentration of serum fructose after SWT administration in rats. Each rat was administered a single oral dose of 7.2 mL per kg body weight of SWT extract (1 mL extract corresponds to 1 g dried herbs of SWT). Data represent means \pm S.D.

need blood fructose concentration data after SWT administration. To be consistent with our previous studies on SWT's bioactivity performed on female mice, an equal dose was used in this study of rats, which was converted from mice (calculated from the human clinical dose) to rats through normalization of the body surface area (BSA), and the gender of rats was also female. SWT contains a large amount of fructose, in both free monosaccharide form (*i.e.*, fructose) and disaccharide form (*i.e.*, sucrose). Sucrose is hydrolyzed by sucrase in the digestive tract after oral consumption and each molecule of sucrose produces one molecule of fructose and one molecule of glucose. In this study, the contents of fructose and sucrose in the SWT extract were determined to be 41.6 and 92.4 mg/mL, respectively. Therefore, the total fructose content (in both forms) in 1 mL SWT extract was about 90.2 mg, and the single dose of 7.2 mL/kg SWT extract received by the rats approximately corresponds to a fructose load of 0.65 g/kg. If extrapolated to the human equivalent dose through normalization to BSA, it approximately corresponds to a fructose load of 0.14 g/kg for human.

The results showed that the increase of blood fructose concentration after a single oral administration dose of SWT was very small. The maximum serum fructose concentration was only 2-3 times higher than the baseline level, which occurred within 60 min. These patterns were similar to reported patterns of blood fructose concentration after a single oral dose of pure fructose. Reportedly the concentration of fructose in fasting blood of healthy humans is typically 1 mg/dL or less, and after oral administration of a fructose load in doses ranging from approximately 18 g (0.25 g/kg of body weight) to 100 g, the mean plasma or serum fructose concentration increased to values ranging from 4.5-13.0 mg/dL. Peak fructose concentrations were seen 30-60 min after fructose ingestion (9). The study on rats showed that after oral pure fructose consumption (6.9 μ mol/g), the plasma fructose concentration of rats reached its peak value at about 60 min (10). Similarly in

our study, the concentration of serum fructose in fasting rats was 0.34 ± 0.24 mg/dL. After oral administration of SWT extract, serum fructose levels reached a peak concentration of 1.03 ± 0.25 mg/dL within 60 min, and then declined to baseline levels within 180 min. Such a small and transient increase of blood fructose concentration after SWT administration may be explained by the quick and efficient metabolism of fructose by the liver. According to Havel's review (11), after consumption of moderate amounts of fructose, the absorbed fructose arrives at the liver *via* the portal vein and is efficiently taken up by the liver such that little escapes hepatic metabolism and enters the systemic circulation. A 1 g/kg oral dose of fructose results in a blood fructose level of only 9 mg/dL. In fact the total dose of fructose received by the rats in our study was even smaller than the "moderate amounts" mentioned in Havel's review, which was only about 0.14 g/kg when extrapolated to the human equivalent dose.

Generally, there are two hypotheses for mechanisms by which the fructose in SWT may help the body's hematopoiesis and immunity. The first one is that the fructose, after entering the blood circulation, acts directly on a certain target (*e.g.* the bone marrow cells) in its intact monosaccharide form. The other one is that the fructose produces its effect after it is metabolized by the body. Given the reported feature of quick metabolism of pure fructose from oral administration as well as the results confirmed in our experiment with SWT oral administration and suppose that fructose helps the body's hematopoiesis and immunity. If the fructose acts directly on a certain target in its intact monosaccharide form, it does not seem very convincing that fructose could produce a remarkable biological effect with such a small and transient increase in blood concentration. Therefore we suggest, for future research, it is necessary to consider the probability that the fructose helps the body's hematopoiesis and immunity, not in its original form, but after it is metabolized by the body.

The liver is the primary metabolic site of fructose disposal. According to Owen's review (12), three factors contribute to this: (i) enzymes essential for the metabolism of fructose, fructokinase, and triokinase are highly expressed in the liver; (ii) the liver is exposed to higher concentrations of orally administered fructose than other tissues; and (iii) the high first pass extraction of fructose by the liver limits the availability of fructose for metabolism by peripheral tissues. Current knowledge of fructose's metabolism has shown that, in the liver, fructose is metabolized by fructokinase to fructose-1-phosphate that is cleaved by aldolase B to form dihydroxyacetone phosphate and glyceraldehyde, both of which can be further metabolized in the glycolytic pathway (13). On the other hand, it was reported that low-dose fructose (infused into the duodenum) could increase hepatic

glucose uptake and glycogen storage, which is possibly due to the activation of glucokinase by a trace amount of fructose acting on the glucokinase regulatory protein (14). Stimulating effects on insulin-stimulated hepatic glycogen synthesis from low-dose fructose were also reported (15). Therefore, it is necessary to consider the possibility that fructose may help the body's hematopoiesis and immunity by participating in and/or regulating glucose metabolism. In our previous studies on SWT and fructose's bioactivities, the model of anemia was induced by γ -ray radiation. Interestingly, according to Fang Y (16), a higher intake of energy is required by irradiated experimental animals because radiation may: (i) inhibit the oxidation phosphorylation process and lead to a low P/O ratio; (ii) affect Krebs cycle and decrease production of NADH and FADH₂ which are materials for the oxidation phosphorylation process; and (iii) increase the basal metabolic rate. The lack of energy or nutrition increases the body's sensitivity to radiation, and experiments showed that an enhanced energy supply prevents dogs from loss of body weight after irradiation. According to Fang, radiation decreases the activity of hexose kinase and thereby interrupts the transformation from glucose to glucose-6-phosphate, which is the first step of the glycolytic pathway. However, the transformation from fructose to fructose-1-phosphate is unaffected because the activity of fructokinase is not changed by radiation. The experiment demonstrated that among four different sugars (sucrose, dextrin, cornstarch, and glucose), glucose showed the most significant therapeutic effect against radiation injury, but when comparing the therapeutic effect of glucose with fructose, fructose was even better. Therefore, a possible explanation for the mechanism of fructose's bioactivity is that fructose may help the body's hematopoiesis and immunity by improving the body's carbohydrate metabolism or energy supply which is relatively insufficient in irradiated animals. Further studies concerning the relationship between fructose metabolism as well as carbohydrate metabolism and radiation injury are required.

Acknowledgements

The authors are grateful for financial support from National Nature Science Foundation of China (Project No. 30730112 and 30672628).

References

- Ohta H, Ni JW, Matsumoto K, Watanabe H, Shimizu M. Peony and its major constituent, paeoniflorin, improve

- radial maze performance impaired by scopolamine in rats. *Pharmacol Biochem Behav.* 1993; 45:719-723.
- Dai Y, But PP, Chan YP, Matsuda H, Kubo M. Antipruritic and antiinflammatory effects of aqueous extract from Si-Wu-Tang. *Biol Pharm Bull.* 2002; 25:1175-1178.
- Hsu HY, Ho YH, Lin CC. Protection of mouse bone marrow by Si-Wu-Tang against whole body irradiation. *J Ethnopharmacol.* 1996; 52:113-117.
- Lee SE, Oh H, Yang JA, Jo SK, Byun MW, Yee ST, Kim SH. Radioprotective effects of two traditional Chinese medicine prescriptions: si-wu-tang and si-jun-zi-tang. *Am J Chin Med.* 1999; 27:387-396.
- Liang QD, Lu XQ, Ma ZC, Tan HL, Ma BP, Gao Y, Wang SQ. Preliminary study on hematopoietic constituents of si-wu-tang. *Zhongguo Zhong Yao Za Zhi.* 2004; 29:546-549. (in Chinese)
- Liang QD, Gao Y, Tan HL, Guo P, Li YF, Zhou Z, Tan W, Ma ZC, Ma BP, Wang SQ. Effects of four Si-Wu-Tang's constituents and their combination on irradiated mice. *Biol Pharm Bull.* 2006; 29:1378-1382.
- Liang QD, Ma BP, Wang SQ. Determination of monosaccharide and disaccharide in condensed Siwu Decoction by HPLC-ELSD. *Zhong Cao Yao.* 2004; 35:395-397. (in Chinese)
- Beuter HO. *Methods of Enzymatic Analysis* (3rd ed.), Vol. 6 (Bergmeyer HU, ed.). Verlag Chemie, Weinheim, Germany, 1985; pp. 321-327.
- Gaby AR. Adverse effects of dietary fructose. *Altern Med Rev.* 2005; 10:294-306.
- Prieto PG, Cancelas J, Villanueva-Peñacarrillo ML, Valverde I, Malaisse WJ. Plasma D-glucose, D-fructose and insulin responses after oral administration of D-glucose, D-fructose and sucrose to normal rats. *J Am Coll Nutr.* 2004; 23:414-419.
- Havel PJ. Dietary fructose: implications for dysregulation of energy homeostasis and lipid/carbohydrate metabolism. *Nutr Rev.* 2005; 63:133-157.
- McGuinness OP, Cherrington AD. Effects of fructose on hepatic glucose metabolism. *Curr Opin Clin Nutr Metab Care.* 2003; 6:441-448.
- Michal G. *Biochemical Pathways: An Atlas of Biochemistry and Molecular Biology* (Michal G, ed.). John Wiley & Sons Inc., New York, USA, 1999; p. 27.
- Watford M. Small amounts of dietary fructose dramatically increase hepatic glucose uptake through a novel mechanism of glucokinase activation. *Nutr Rev.* 2002; 60:253-257.
- Petersen KF, Laurent D, Yu C, Cline GW, Shulman GI. Stimulating effects of low-dose fructose on insulin-stimulated hepatic glycogen synthesis in humans. *Diabetes.* 2001; 50:1263-1268.
- Fang YZ. *Theory and Application of Free Radical Biology* (Fang YZ, Zheng RL, eds.). Science Press, Beijing, China, 2002; pp. 681-682. (in Chinese)

(Received March 23, 2010; Revised April 11, 2010; Accepted April 16, 2010)

Original Article

Rehmanniae Radix provides most of the free fructose and glucose in Si-Wu-Tang decoction

Jing Ma^{1,*}, Qiande Liang^{2,*}, Zengchun Ma², Yuguang Wang², Ming Liu², Beibei Lu², Hongling Tan², Chengrong Xiao², Boli Zhang¹, Yue Gao^{2,**}

¹ Tianjin University of Traditional Chinese Medicine, Tianjin, China;

² Beijing Institute of Radiation Medicine, Beijing, China.

ABSTRACT: Our previous study showed that free fructose is an important active constituent responsible for Si-Wu-Tang's (SWT) effect promoting hematopoiesis and immunity. However, the contribution from SWT's four ingredient drugs to the free fructose content in the SWT decoction was not clear. To answer this question, in this study, the fructose, glucose and sucrose content in the SWT decoction, in the decoctions of each single ingredient drug, and in the decoctions of the four formulae lacking each single ingredient drug were determined by HPLC-ELSD. The results showed that the fructose and glucose content in the decoction of single *Rehmanniae Radix* were almost the same as those in the SWT decoction. In the single *Rehmanniae Radix* decoction concentrations were: 4.25 ± 0.53 mg/mL for fructose, and 3.43 ± 0.60 mg/mL for glucose; in the SWT decoction concentrations were: 4.10 ± 0.43 mg/mL for fructose, and 3.42 ± 0.32 mg/mL for glucose, while the content of fructose and glucose in the decoctions of single *Angelica Radix*, single *Paeoniae Radix*, single *Chuanxiong Rhizoma* and the formula lacking *Rehmanniae Radix* were either very small or undetectable. On the other hand, the fructose and glucose content in the decoctions of the formulae lacking *Angelica Radix*, lacking *Paeoniae Radix* and lacking *Chuanxiong Rhizoma* also were approximately the same as those in the SWT decoction. This indicated that *Rehmanniae Radix* provides most of the free fructose and glucose in the SWT decoction, and therefore plays an important role in SWT's effect promoting hematopoiesis and immunity. As for sucrose in the SWT decoction, *Angelica Radix* was shown to be a major donor.

Keywords: Si-Wu-Tang, fructose, glucose, *Rehmanniae Radix*

1. Introduction

Si-Wu-Tang (SWT), a traditional Chinese formula consisting of *Rehmanniae Radix*, *Angelica Radix*, *Paeoniae Radix*, and *Chuanxiong Rhizoma*, has traditionally been used in China for about one thousand years (1). Dai *et al.* reported that SWT has been used for the treatment of gynecologic diseases (*e.g.* dysmenorrhea, menoxenia, metrorrhagia, abortion), cutaneous diseases (*e.g.* pruritus, urticaria, eczema, dermatitis), and chronic inflammation (*e.g.* chronic nephritis, pelvic inflammation) (2). It has been reported to possess sedative, anti-coagulant and antibacterial activities, and has been reported to exhibit effects on vasodilatation, hematopoiesis, enhancement of cellular immunity and radio-protection (3,4). Our interest has been focused on SWT's hematopoiesis-related activities. Using 3.5 Gy ⁶⁰Co γ -ray irradiated mice as a model of anemia, we found that SWT increases the number of peripheral leukocytes and four types of progenitor cells in bone marrow, colony-forming unit-granulocyte-macrophage (CFU-GM), colony-forming unit-mature erythroid (CFU-E), colony-forming unit-immature erythroid (BFU-E) and colony-forming unit-multipotential (CFU-mix) cells (5). In our latest report, free fructose (*i.e.*, dissociative form of fructose) was shown to be an important active constituent that is responsible for SWT's effect promoting hematopoiesis and immunity after oral administration of the SWT decoction (6). Oral administration of pure fructose, at a dose equal to the natural content of free fructose in the SWT decoction, showed positive effects on peripheral leukocytes, on bone marrow progenitor cells and on thymus index, which were similar to the SWT decoction. Therefore, comprehensive studies on the nature of fructose in the SWT decoction have been required. This may help us to further understand the mechanism of

*The first two authors contributed equally to this article.

**Address correspondence to:

Dr. Yue Gao, Department of Pharmacology and Toxicology, Beijing Institute of Radiation Medicine, 27 Tai-ping Road, Beijing 100850, China.
e-mail: gaoyue@yahoo.com

SWT's bioactivity and the reasons for the composition of the SWT formula. One of the fundamental questions is which ingredient drug is the donor of free fructose in the SWT decoction. However, to our knowledge, there is no research concerning this question. It had been reported that *Rehmanniae Radix* contains a significant amount of free fructose (7,8), but whether or not other ingredient drugs of SWT also contain free fructose, or how much does each ingredient drug contribute to the total amount of free fructose in the SWT decoction is unknown. To answer these questions, in this study, we determined the content of free fructose in the SWT decoction, in the decoctions of each single ingredient drug of SWT, and in the decoctions of the four formulae each lacking an ingredient drug, by high performance liquid chromatography (HPLC) with evaporated light scattering detection (ELSD). Since this method is capable of simultaneous determination of fructose, glucose and sucrose, the glucose and sucrose content in the above-mentioned decoctions were also determined.

2. Materials and Methods

2.1. Drugs and reagents

Rehmanniae Radix, *Angelica Radix*, *Paeoniae Radix*, and *Chuanxiong Rhizoma*, corresponding to *Rehmannia glutinosa* LIBOSCH. (Scrophulariaceae), *Angelica sinensis* (OLIV.) (Umbelliferae) DIELS, *Paeonia lactiflora* PALL (Paeoniaceae), and *Ligusticum chuanxiong* HORT. (Umbelliferae), respectively, were purchased from Tongrentang Ltd. (Beijing, China) and identified by Dr. Baiping Ma in our laboratory. Fructose was purchased from Sinopharm Chemical Reagent Co., Ltd. (Shanghai, China). Glucose and sucrose were purchased from Beijing Chemical Reagent Company (Beijing, China). Acetonitrile was of HPLC grade (Fisher Scientific, Fair Lawn, New Jersey, USA). Deionized water was prepared using a Millipore water purification system.

2.2. Chromatographic apparatus and conditions

A Waters Acquity UPLC system consisting of a binary solvent manager, a sample manager and an

evaporative light scattering detector (ELSD), and an analytical workstation with Waters Masslynx (v4.1) software was used. Separations were carried out with a SHISEIDO carbohydrate column (5 μ m, 150 \times 2.0 mm). The mobile phase was isocratic acetonitrile and water (80:20). The temperature of the column was kept at 24°C and the flow rate was 0.6 mL/min. The drift tube temperature, gas pressure and gain of ELSD were 40°C, 40 psi and 25, respectively. The sample injection volume was 2 μ L. The compounds were identified by comparing their retention time values with standards.

2.3. Calibration curve, Sample preparations and measurement

Each standard compound, fructose, glucose, and sucrose, was accurately weighed and dissolved in 50% acetonitrile to give serial concentrations within the range of 0.8-10 mg/mL. Log/log calibration curves were obtained from the log values of the peak areas over the log values of the concentrations of the standard solutions. Thirty-six samples were divided into nine groups (4 repetitive samples in each group). The formula composition of each group is listed in Table 1. Drugs of each sample were accurately weighed, dropped into 650 mL water for 60 min at room temperature and boiled for 30 min. The suspension was filtered and 410 mL water was added for the second decoction of 20 min duration. The filtered and mixed suspension from the two decoctions was adjusted to a volume of 820 mL. 20 mL of the decoction was precipitated by adding 80 mL alcohol and filtered. The filtrates were evaporated to less than 1 mL at about 50°C *in vacuo*. The evaporated residue was dissolved with 50% acetonitrile into a volumetric flask. The final volume of the sample solution was set to 25 mL. The solutions of standards and samples were filtered through a 0.45 μ m membrane before injection into the UPLC system. The injection volume was 2 μ L.

3. Results

3.1. Typical chromatograms

Typical chromatogram of the standard compounds and

Table 1. Formula composition of each group

Groups	Composition
1	<i>Rehmanniae Radix</i> (30 g), <i>Angelica Radix</i> (20 g), <i>Paeoniae Radix</i> (20 g), <i>Chuanxiong Rhizoma</i> (12 g)
2	<i>Rehmanniae Radix</i> (30 g)
3	<i>Angelica Radix</i> (20 g)
4	<i>Paeoniae Radix</i> (20 g)
5	<i>Chuanxiong Rhizoma</i> (12 g)
6	<i>Angelica Radix</i> (20 g), <i>Paeoniae Radix</i> (20 g), <i>Chuanxiong Rhizoma</i> (12 g)
7	<i>Rehmanniae Radix</i> (30 g), <i>Paeoniae Radix</i> (20 g), <i>Chuanxiong Rhizoma</i> (12 g)
8	<i>Rehmanniae Radix</i> (30 g), <i>Angelica Radix</i> (20 g), <i>Chuanxiong Rhizoma</i> (12 g)
9	<i>Rehmanniae Radix</i> (30 g), <i>Angelica Radix</i> (20 g), <i>Paeoniae Radix</i> (20 g)

typical chromatograms of the nine groups of decoctions are given in Figures 1 and 2, respectively. Fructose, glucose, and sucrose were perfectly separated. Among the four groups of single ingredient drug (group 2 through group 5), obvious peaks of fructose and glucose could be seen only in the *Rehmanniae Radix* group (group 2). On the other hand, among the four groups of the formulae lacking each ingredient drug (group 6 through group 9), only the exclusion of *Rehmanniae Radix* (group 6) showed a significant decrease of fructose and glucose. As for sucrose, both *Angelica Radix* (group 3) and *Chuanxiong Rhizoma* (group 5) showed obvious peaks, and the exclusion of *Angelica Radix* (group 7) showed a significant decrease of peak intensity.

3.2. Calibration curve, contents of fructose, glucose and sucrose in each decoction group

Log/log calibration curves showed a good linear relation between the log values of the peak areas and the log values of the concentrations of the standard solutions (Table 2) for fructose, glucose, and sucrose. The contents of fructose, glucose, and sucrose in each decoction group are summarized in Table 3. The contents of fructose and glucose in the decoction of *Rehmanniae Radix* alone (group 2) were almost the same as those of the SWT decoction (group 1) (in the *Rehmanniae Radix* alone decoction: 4.25 ± 0.53 mg/mL was seen for fructose, and 3.43 ± 0.60 mg/mL for glucose; in the SWT decoction: 4.10 ± 0.43

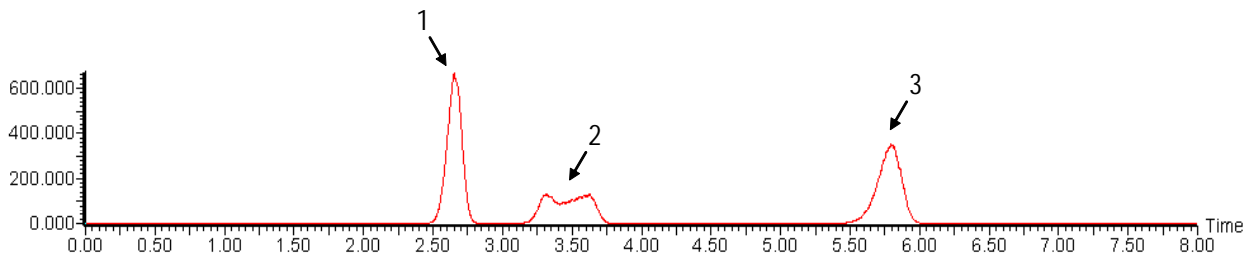


Figure 1. Typical chromatogram of the standard compounds. Peaks 1-3 denote fructose, glucose, and sucrose, respectively.

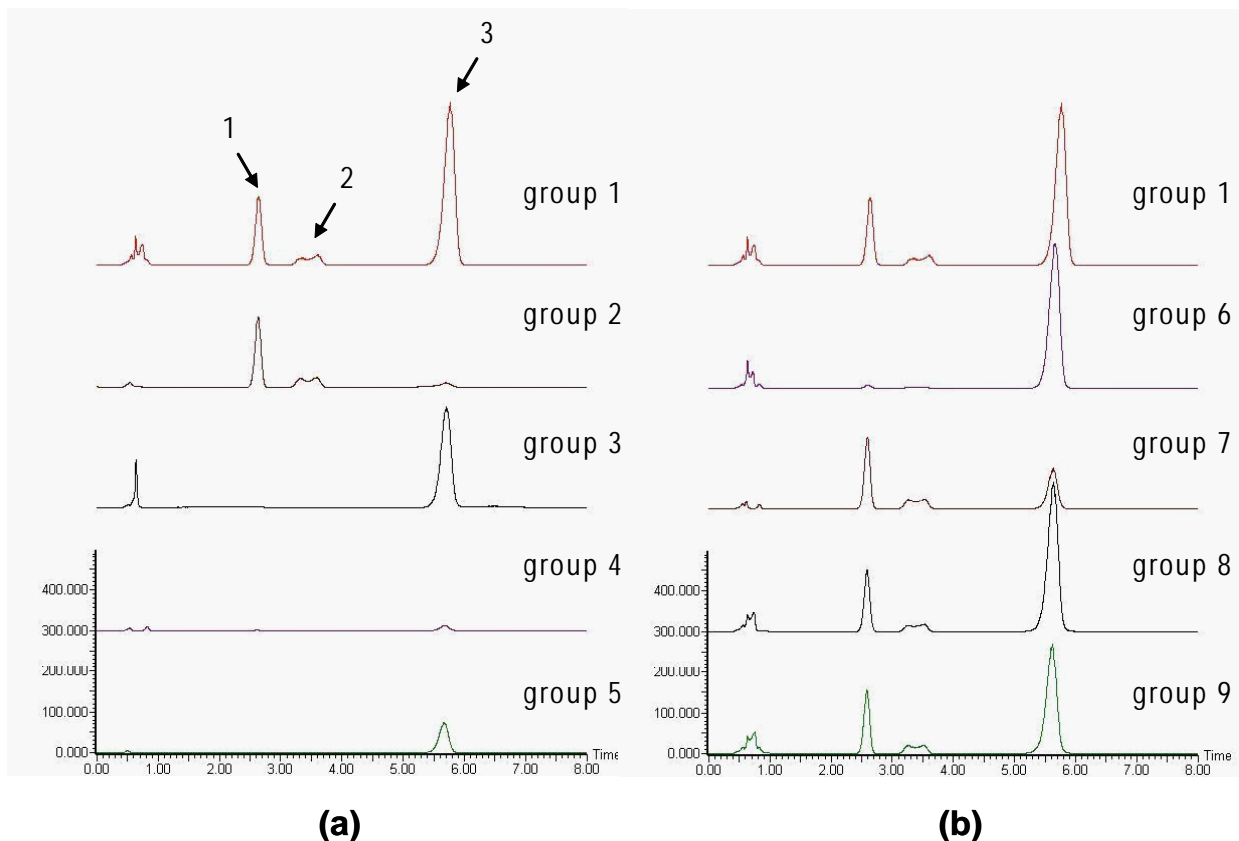


Figure 2. Typical chromatogram of groups 1-5 (a) and groups 1 and 6-9 (b). Peak intensity of all samples was normalized to a uniform value. Peaks 1-3 denote fructose, glucose, and sucrose, respectively.

Table 2. Linear relation between the log values of the peak areas and the log values of the concentrations of the standard solutions

Compounds	Regression equation	r	Linear range (mg/mL)
Fructose	$y = -2.44885 + 0.70281x$	0.99874	0.8-10
Glucose	$y = -2.01709 + 0.64336x$	0.99964	0.8-10
Sucrose	$y = -2.24556 + 0.67214x$	0.99914	0.8-10

x: log value of peak area; y: log value of concentration.

Table 3. Content of fructose, glucose, and sucrose in each group of decoctions

Groups ^a	Concentration ^b (mg/mL)		
	Fructose	Glucose	Sucrose
1	4.10 ± 0.43	3.42 ± 0.32	12.33 ± 1.25
2	4.25 ± 0.53 [§]	3.43 ± 0.60 [§]	0.76 ± 0.50 ^{**}
3	0.47 ± 0.48 ^{**}	n.d.	9.90 ± 0.30 [*]
4	0.18 ± 0.01 ^{**}	n.d.	1.12 ± 0.13 ^{**}
5	n.d.	n.d.	2.85 ± 1.30 ^{**}
6	0.43 ± 0.11 ^{**}	0.52 ± 0.35 ^{**}	11.69 ± 1.93 [§]
7	4.33 ± 0.32 [§]	3.73 ± 0.53 [§]	4.33 ± 0.72 ^{**}
8	3.81 ± 0.35 [§]	3.34 ± 0.33 [§]	11.67 ± 1.40 [§]
9	4.29 ± 0.17 [§]	3.82 ± 0.29 [§]	10.78 ± 0.64 [§]

^a See Table 1; ^b Data expressed mean ± S.D., n = 4; n.d.: not detected. ^{*} p < 0.05, ^{**} p < 0.001, [§] p > 0.1 as compared to group 1.

mg/mL was seen for fructose, and 3.42 ± 0.32 mg/mL for glucose), while the contents of fructose and glucose in decoctions of *Angelica Radix* alone (group 3), *Paeoniae Radix* alone (group 4), *Chuanxiong Rhizoma* alone (group 5) and the formula lacking *Rehmanniae Radix* (group 6) were either very small or undetectable. On the other hand, the contents of fructose and glucose in the decoctions of the formulae lacking *Angelica Radix* (group 7), lacking *Paeoniae Radix* (group 8) and lacking *Chuanxiong Rhizoma* (group 9) were also approximately the same as those in the SWT decoction. The content of sucrose in the decoction of *Angelica Radix* alone (group 3) was 9.90 ± 0.30 mg/mL, about 4/5 of that seen in the SWT decoction (12.33 ± 1.25 mg/mL, group 1). The sucrose content when *Angelica Radix* was excluded (group 7, 4.33 ± 0.72 mg/mL) was about 1/3 of the amount in the SWT decoction.

4. Discussion

This is the first report concerning the contributions among SWT's four ingredient drugs to the content of the SWT decoction's free fructose, which was shown in our previous study as an important active constituent responsible for the effect promoting hematopoiesis and immunity from the use of SWT (6). In this study, in order to assess the ability to provide free fructose from each ingredient drug of SWT when decocted, we determined the free fructose content not only in the decoctions prepared from each single ingredient drug,

but also in decoctions prepared from the four formulae lacking each ingredient drug. They were all compared with the free fructose content in the SWT decoction. The adoption of such experimental design was with the consideration of possible interactions between different ingredient drugs when decocted together, which may affect the release of fructose from each ingredient drug. All groups of samples were prepared with the identical method to ensure their comparability. The determination method was established and reported by ourselves in 2004 (9). This method is capable of simultaneous determination of fructose, glucose and sucrose in the SWT decoction.

The results clearly indicated that *Rehmanniae Radix* provides most of the free fructose and glucose in the SWT decoction, because the contents of fructose and glucose in the decoctions were approximately equal to those in the SWT decoction if only the formula contained *Rehmanniae Radix*. The fructose and glucose content was either very low or undetectable if the formula did not contain *Rehmanniae Radix*. Although it had been reported that *Rehmanniae Radix* contains a significant amount of free fructose (7,8) and we had anticipated that the contribution of *Rehmanniae Radix* to the free fructose content in the SWT decoction should be significant, we had not expected that the contribution was so exclusive. We had not expected that the contribution of *Rehmanniae Radix* to the free glucose content in the SWT decoction was also exclusive. Since free fructose was shown to be an important active constituent responsible for SWT's effect promoting hematopoiesis and immunity after oral administration of SWT (6), and *Rehmanniae Radix* provides most of the free fructose in the SWT decoction, it is inferred that *Rehmanniae Radix* plays an important role in SWT's effect promoting hematopoiesis and immunity. In fact, according to the conventional theory of traditional Chinese medicine (TCM) which uses "Jun" ("emperor", the most important ingredient or plays a central role in a formula), "Chen" ("minister"), "Zuo" ("assistant"), and "Shi" ("emissary") to identify the importance and roles of different ingredient drugs in a formula, *Rehmanniae Radix* is the "Jun" in the SWT formula (10). Our deduction based on modern studies is consistent with judgment based on traditional TCM theory. In addition, it is necessary to point out that the *Rehmanniae Radix* used in SWT is not raw but has been processed by braising, and our recent study, the data of which will be published elsewhere, has revealed that the major amount of fructose and glucose contained in *Rehmanniae Radix* used in SWT is produced during the braising process. Perhaps such an intentional choice of drug variety, i.e., the choice of processed *Rehmanniae Radix*, which contains significantly more free fructose and glucose than the raw drug, indicates again the importance of these monosaccharides for SWT's

therapeutic effects. The results of this study showed that *Angelica Radix* is a major donor of sucrose in the SWT decoction, and next to *Angelica Radix* is *Chuanxiong Rhizoma*. Interestingly they both belong to the Umbelliferae family.

The mechanism of the bioactivity of free fructose in SWT on hematopoiesis and immunity is still to be studied. Current knowledge of fructose's metabolism has shown that the liver is the primary metabolic site of fructose disposal, where fructose is metabolized by fructokinase to fructose-1-phosphate that is cleaved by aldolase B to form dihydroxyacetone phosphate and glyceraldehyde, both of which can be further metabolized in the glycolytic pathway (11). It was reported that low-dose fructose (infused into the duodenum) could increase hepatic glucose uptake and glycogen storage, which is possibly due to the activation of glucokinase by trace amounts of fructose acting on the glucokinase regulatory protein (12). The stimulating effects on insulin-stimulated hepatic glycogen synthesis of low-dose fructose were also reported (13). Therefore it is necessary to consider the possibility that fructose may help the body's hematopoiesis and immunity by participating in and/or regulating glucose metabolism. In our former studies on SWT and fructose's bioactivities (5,6), the model of anemia was induced by γ -ray radiation. Interestingly, according to Fang Yunzhong (14), a higher energy intake is required for irradiated experimental animals because radiation may: (i) inhibit the oxidation phosphorylation process and lead to a low P/O ratio; (ii) affect the Krebs cycle and decrease production of NADH and FADH which are materials for the oxidation phosphorylation process; and (iii) increase the basal metabolic rate. Lack of energy or nutrition increases the body's sensitivity to radiation, and experiments showed that enhanced energy supplies prevents dogs from loss of body weight after irradiation. And among four different sugars (sucrose, dextrin, cornstarch and glucose), glucose showed the most significant therapeutic effect against radiation injury, but when comparing the therapeutic effect of glucose with fructose, fructose was even better. According to Fang, radiation decreases the activity of hexose kinase and thereby interrupts the transformation from glucose to glucose-6-phosphate, which is the first step of the glycolytic pathway. The transformation from fructose to fructose-1-phosphate is unaffected because the activity of fructokinase is not changed by radiation. The current study has affirmed the exclusive role of *Rehmanniae Radix* in providing free fructose and glucose in SWT and to some extent revealed the meaning of *Rehmanniae Radix* in the composition of the SWT formula.

Acknowledgement

The authors are grateful for financial support from National Nature Science Foundation of China (Project No. 30730112 and 30672628).

References

- Ohta H, Ni JW, Matsumoto K, Watanabe H, Shimizu M. Peony and its major constituent, paeoniflorin, improve radial maze performance impaired by scopolamine in rats. *Pharmacol Biochem Behav.* 1993; 45:719-723.
- Dai Y, But PP, Chan YP, Matsuda H, Kubo M. Antipruritic and antiinflammatory effects of aqueous extract from Si-Wu-Tang. *Biol Pharm Bull.* 2002; 25:1175-1178.
- Hsu HY, Ho YH, Lin CC. Protection of mouse bone marrow by Si-Wu-Tang against whole body irradiation. *J Ethnopharmacol.* 1996; 52:113-117.
- Lee SE, Oh H, Yang JA, Jo SK, Byun MW, Yee ST, Kim SH. Radioprotective effects of two traditional Chinese medicine prescriptions: si-wu-tang and si-jun-zi-tang. *Am J Chin Med.* 1999; 27:387-396.
- Liang QD, Lu XQ, Ma ZC, Tan HL, Ma BP, Gao Y, Wang SQ. Preliminary study on hematopoietic constituents of si-wu-tang. *Zhongguo Zhong Yao Za Zhi.* 2004; 29:546-549. (in Chinese)
- Liang QD, Gao Y, Tan HL, Guo P, Li YF, Zhou Z, Tan W, Ma ZC, Ma BP, Wang SQ. Effects of four Si-Wu-Tang's constituents and their combination on irradiated mice. *Biol Pharm Bull.* 2006; 29:1378-1382.
- Wen XS, Yang SL, Ma XJ, Zheng JH. HPLC chromatogram changes with processing for roots of *Radix Rehmanniae*. *Zhong Cao Yao.* 2004; 35:153-156. (in Chinese)
- Tomoda M, Katō S, Ōnuma M. Water-soluble constituents of *rehmanniae radix*. I. Carbohydrates and acids of *Rehmannia glutinosa* f. *hueichingensis*. *Chem Pharm Bull.* 1971; 19:1455-1460.
- Liang QD, Ma BP, Wang SQ. Determination of monosaccharide and disaccharide in condensed Siwu Decoction by HPLC-ELSD. *Zhong Cao Yao.* 2004; 35:395-397. (in Chinese)
- Li F. Fang Ji Xue. People's Medical Publishing House, Beijing, China, 2002.
- Michal G. Biochemical pathways: an atlas of biochemistry and molecular biology. John Wiley & Sons Inc., New York, NY, USA, 1999.
- Watford M. Small amounts of dietary fructose dramatically increase hepatic glucose uptake through a novel mechanism of glucokinase activation. *Nutr Rev.* 2002; 60:253-257.
- Petersen KF, Laurent D, Yu C, Cline GW, Shulman GI. Stimulating effects of low-dose fructose on insulin-stimulated hepatic glycogen synthesis in humans. *Diabetes.* 2001; 50:1263-1268.
- Fang YZ, Zheng RL. Theory and application of free radical biology. Science Press, Beijing, China, 2002.

(Received February 28, 2010; Revised March 15, 2010; Accepted March 22, 2010)

Original Article**Effects of components present in flaxseed on human colon adenocarcinoma Caco-2 cells: Possible mechanisms of flaxseed on colon cancer development in animals**Ajay Bommareddy¹, Xiaoying Zhang², Radhey S. Kaushik^{3,4}, Chandradhar Dwivedi^{2,*}¹ Department of Pharmaceutical Sciences, Nesbitt School of Pharmacy, Wilkes University, Wilkes Barre, PA, USA;² Department of Pharmaceutical Sciences, South Dakota State University, Brookings, SD, USA;³ Department of Veterinary Science, South Dakota State University, Brookings, SD, USA;⁴ Department of Biology/Microbiology, South Dakota State University, Brookings, SD, USA.

ABSTRACT: Previous studies from our laboratory have shown chemopreventive effects of dietary flaxseed on azoxymethane-induced colon tumor development in male Fischer rats and Apc^{Min} mice. Tumorigenesis is associated with uncontrolled cell growth and loss of apoptosis. Accordingly, the objective of this investigation was to study the effects of mammalian lignans (enterodiol and enterolactone) and ω -3 polyunsaturated fatty acid α -linolenic acid, principal active components in flaxseed on cell proliferation and apoptosis in human colon adenocarcinoma Caco-2 cells, thus elucidating possible mechanism of action. BrdU incorporation assay was used for cell proliferation and fluorescence-activated cell sorting (FACS) analysis of annexin V/propidium iodide staining was used for determining apoptotic cells. Results showed that enterodiol, enterolactone and α -linolenic acid at different concentrations caused a significant ($p < 0.05$) increase in apoptotic cells and decrease in cell proliferation. Therefore, dietary flaxseed containing α -linolenic acid and lignans causes a decrease in cell proliferation and an increase in apoptosis resulting in the effective chemoprevention for intestinal and colon tumor development.

Keywords: Flaxseed, enterodiol, enterolactone, α -linoleic acid, colon cancer

1. Introduction

Colorectal cancer is the most common cancer in

**Address correspondence to:*

Dr. Chandradhar Dwivedi, Department of Pharmaceutical Sciences, 116 Intramural Building, College of Pharmacy, Box 2202C, South Dakota State University, Brookings, SD 57007, USA.

e-mail: Chandradhar.Dwivedi@sdstate.edu

Western countries and the third leading cause of cancer related deaths. An estimated 102,900 new colon and 39,670 new rectal cases, and 51,370 colorectal deaths are expected in 2010 (1). The pathogenesis of colon cancer is a complex interplay of environmental factors such as consumption of high-fat diet, red meat, obesity, alcohol and genetic factors (1,2). Among the all risk factors of colon cancer, diet is a major but controllable factor that affects colorectal carcinogenesis; both risk factors and protective factors have been studied extensively (3).

Many studies suggest that fatty acid composition of dietary fat plays a vital role in colon tumor development (4-6). Corn oil, one of the important vegetable fats in the United States diet, contains high levels of ω -6 polyunsaturated fatty acids (PUFAs) such as linoleic acid and has been shown to enhance colon tumorigenesis in rodents (7). In contrast, fish oil, which is rich in ω -3 PUFAs such as α -linolenic acid (ALA), eicosapentanoic acid (EPA) and docosahexanoic acid (DHA) reduces azoxymethane-induced colon tumor development in rats (2,5). In addition to ω -3 PUFAs, mammalian lignans such as enterolactone (EL) and enterodiol (ED) have been suggested to prevent breast and colon tumor development in experimental animals (8-11).

Flax is perennial plant cultivated from ancient times for its fiber which was used in making linen. Flaxseed was used for nutritional and medicinal purpose of anti-tumoral, relieving pain and anti-inflammatory (12). Flaxseed meal contains a high percentage of α -linolenic acid, an ω -3 fatty acid and a high amount of secoisolarciresinol diglucoside, which is metabolized into mammalian lignans ED and EL by the gut microflora (8). Studies from our laboratory have reported that dietary flaxseed oil and meal have chemopreventive effects on azoxymethane-induced colon tumor development in male Fischer rats and also inhibits intestinal tumor development in Apc^{Min} mice by increasing ω -3 fatty acid levels, lignans

and decreasing COX-1 and COX-2 levels (13,14). However, the precise mechanism(s) of flaxseed on colon tumor development remain largely unknown. In term of mechanistic studies, it has been well known that tumorigenesis is associated with uncontrolled cell replication and loss of apoptotic death of cells (15,16). Accordingly, the purpose of the present investigation was to study the role of these active components, EL, ED and ALA, present in flaxseed on cell proliferation and apoptosis in human colon adenocarcinoma Caco-2 cells.

2. Materials and Methods

2.1. Materials and reagents

EL, ED, and ALA were purchased from Sigma-Aldrich Chemicals (St. Louis, MO, USA). The purity for ED, EL is > 95% and for ALA is > 99% by HPLC analysis. Dulbecco's modified Eagle's medium (DMEM), fetal bovine serum (FBS), trypsin EDTA and phosphate buffered saline (PBS) were from Mediatech, Inc. (Herndon, VA, USA). Dimethyl sulfoxide (DMSO) was obtained from Fisher Scientific (Fair Lawn, NJ, USA). Cell proliferation ELISA kit was from Roche Diagnostics GmbH (Mannheim, Germany). Vybrant apoptosis kit 2 was purchased from Molecular Probes (Eugene, OR, USA). Other reagents were obtained in their highest purity grade available commercially.

2.2. Cell culture

Human colon adenocarcinoma Caco-2 cell line were grown in DMEM supplemented with 10% FBS with 100 unit/mL of penicillin and 100 µg/mL of streptomycin in a humidified atmosphere containing 5% CO₂ and 95% air at 37°C.

2.3. Preparation of EL, ED and ALA stock solution

EL, ED, and ALA were dissolved in DMSO respectively as stock solutions. Stock solutions were diluted in DMEM at different concentrations and immediately used. In all the assays, the final concentrations of DMSO in DMEM were less than 0.3%.

2.4. Cell proliferation assay

Cell proliferation assay was carried as previously described by Zhang *et al.* (16) using Cell proliferation ELISA, BrdU (colorimetric) kit commercially available (Roche Applied Science, Indianapolis, IN, USA). Briefly 1×10^4 cells were plated in 96 well plates and allowed to attach. Following attachment, cells were treated with various concentrations of EL, ED or ALA for desired time points. At time points 24, 48, and 72 h; 10 µL/well of BrdU labeling solution

was added to the media and cells were incubated for 3 h in an incubator with 5% CO₂ at 37°C. After incubation, the labeling solution was removed by tapping off the plate; cell plate was then dried using hair-dryer for about 15 min. 200 µL/well of FixDenat solution was added to each well of the plate and incubated at room temperature for 30 min. FixDenat solution was removed by tapping off and anti-BrdU-POD (100 µL/well) was added and incubated for 90 min at room temperature. Antibody conjugate was removed by flicking off the plate, followed by washing with 200 µL of washing buffer three times. After the final wash, the washing buffer was removed and 100 µL of substrate solution was added to each well and incubated for 20 min at room temperature. After incubation, the reaction was stopped by adding 25 µL of 1 M H₂SO₄ per well, the plate was incubated for 1 min on the shaker in the cell plate reader. Absorbance was measured at 450 nm (with a reference wave length of 690 nm). Cell proliferation was expressed as the percentage of the absorbance values of drug treated groups to cells incubated with normal media.

2.5. Apoptosis assay

Vybrant Apoptosis Kit 2 (Molecular Probes) was used to quantitate apoptosis. The percent apoptotic cells were determined by using the manufacturer's protocol. Briefly 2×10^5 cells were grown in 6 well plates and allowed to attach. Following attachment, cells were treated with various concentrations of EL, ED or ALA for 72 h. At the end of the treatment, adherent and non-adherent cells were harvested and washed twice with ice-cold PBS, and then resuspended in $1 \times$ annexin-binding buffer (approximately 300 µL per treatment). Cells were resuspended 5 µL of Alexa Flour 488 annexin V (component A) and 1 µL of the 100 µg/mL of propidium iodide (PI) working solution was added to each 100 µL of cell suspension. The cells were then incubated at room temperature for 15 min. After incubation, 400 µL of $1 \times$ annexin-binding buffer was added to each sample and the samples were kept on ice until analyzed. Samples were analyzed with BD FACScan™ flow cytometry (BD Biosciences, San Jose, CA, USA). The percentage of apoptotic cells in the cell samples was analyzed using CellQuest Software (BD Biosciences, San Jose, CA, USA).

2.6. Statistical analysis

Data were analyzed with INSTAT software (Graph Pad, San Diego, CA, USA). ANOVA followed by Tukey post test was applied to compare the statistical difference of different treatment groups with DMSO groups as controls. Significance in all the experiment was considered at $p < 0.05$. Values were expressed as mean ± the standard deviation (S.D.) of the mean.

3. Results

3.1. Effects of lignans on cell proliferation

Caco-2 cells were plated and allowed to grow until 70-90% confluence was observed. At that point the growth media was removed and the cells were treated with increasing concentrations of EL, ED and combination of EL and ED. Cell proliferation data for human colon cancer Caco-2 cells using various concentrations of EL, ED both alone and in combination are shown in Figure 1. IC₅₀ for EL, ED

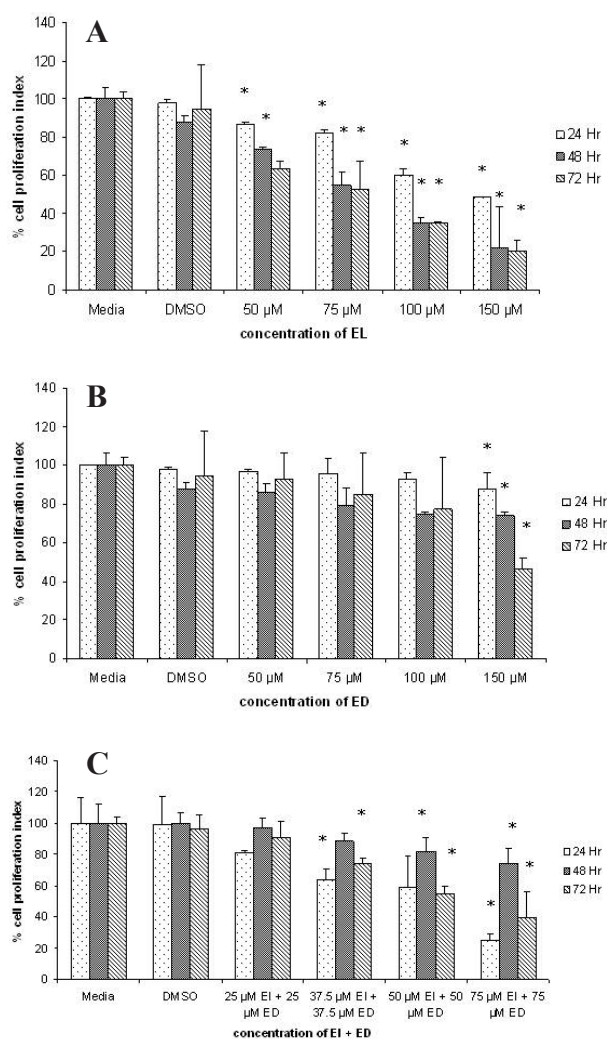


Figure 1. Effects of lignans on cell proliferation in Caco-2 cells. Cells in Media groups were treated with media only, whereas, cells in DMSO groups were treated with media containing same concentration of DMSO of treated groups. Thus, DMSO groups were performed as control group. (A) Cells were treated with different concentrations of EL (0-150 μM) for 24, 48, and 72 h, respectively. (B) Cells were treated with different concentrations of ED (0-150 μM) for 24, 48, and 72 h, respectively. (C) Cells were treated with combinations of EL and ED for 24, 48, and 72 h, respectively. At the end of respective treatment, BrdU incorporation assays were performed as detailed in the "Materials and Methods". Values of BrdU incorporation assay are mean ± S.D. of three samples in each treatment. *, $p < 0.05$ indicates statistical significance in treated groups as compared to DMSO control groups.

was found to be 60 μM and 150 μM, respectively. EL and ED significantly ($p < 0.05$) inhibited cell proliferation of Caco-2 cells starting at 50 μM and 150 μM, respectively, as shown in Figure 1. Thus, EL significantly ($p < 0.05$) decreased cell proliferation at relatively lower concentrations when compared to ED. However, both EL and ED decreased BrdU uptake into the DNA in a concentration-dependent manner.

Various concentrations of a combination of EL and ED were used to study cell proliferation at different time periods as shown in Figure 1C. A combination of 37.5 μM of EL and 37.5 μM of ED showed significant ($p < 0.05$) decrease in cell proliferation.

3.2. Effects of ALA on cell proliferation

Caco-2 cells were plated and allowed to grow until 70-90% confluence was observed. At that point the growth media was removed and the cells were treated with increasing concentrations of ALA and combination of ALA + EL and ALA + ED as shown in Figure 2. The IC₅₀ for ALA was found to be around 750 μM. ALA in concentration of 700 μM significantly ($p < 0.05$)

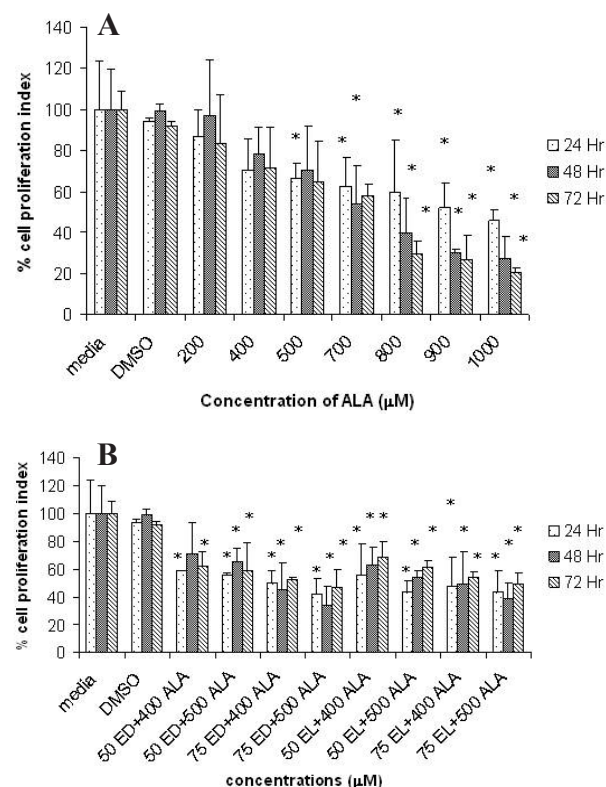


Figure 2. Effects of ALA and combinations of ALA with either EL or ED on cell proliferation in Caco-2 cells. (A) Cells were treated with different concentrations of ALA (0-1,000 μM) for 24, 48, and 72 h, respectively. (B) Cells were treated with combinations of ALA with either EL or ED for 24, 48, and 72 h, respectively. At the end of respective treatment, BrdU incorporation assays were performed. Values of BrdU incorporation assay are mean ± S.D. of three samples in each treatment. *, $p < 0.05$ indicates statistical significance in treated groups as compared to DMSO control groups.

reduced cell proliferation.

As shown in Figure 2B, a combination of 50 μM of ED and 400 μM of ALA showed significant ($p < 0.05$) decrease in cell proliferation. Similarly, a combination of 50 μM of EL and 400 μM of ALA also significantly ($p < 0.05$) inhibited cell proliferation. As compared to ALA alone, combination of ALA with either ED or EL, ALA exhibited significant inhibition of cell proliferation in Caco-2 cells at a relatively lower concentration.

3.3. Effects of lignans on apoptosis

Flow cytometric analysis of Caco-2 cells with various concentrations of EL and ED both alone and in combination is shown in Figure 3. Both EL and ED at the concentration of 100 μM significantly ($p < 0.05$) induced apoptosis in Caco-2 cells as compared to DMSO treated control group. However, EL treated cells showed higher increase of apoptotic cells when compared to ED. The percentage of apoptotic cells was higher at 150 μM of EL when compared to other concentrations of ED alone and combination with 75 μM of ED and 75 μM of EL.

3.4. Effects of ALA on apoptosis

Flow cytometric analysis of Caco-2 cells using various concentrations of ALA alone and in combination with EL and ED is given in Figure 4. ALA alone significantly ($p < 0.05$) induced apoptosis in relatively higher concentrations (800 μM and 1,000 μM). Even ALA combined with either ED or EL significantly ($p < 0.05$) induced apoptosis at 500 μM of ALA with either 75 μM of ED or 75 μM of EL, respectively, which are relatively higher concentrations as compared to the combination of EL and ED.

4. Discussion

Colorectal cancer continues to pose a serious health problem in the United States leading to the third most prevalent cancer in the United States and accounting for 10% of cancer deaths (1). Colorectal cancer evolves from a multistep process and is a disease strongly influenced by diet. Prevention of colorectal cancer at early stages has been improving due to several advances in diagnosis and cellular biology.

Among dietary factors, there is growing epidemiological, clinical and experimental evidence which suggests a protective role of ω -3 PUFAs found in fish oil, flaxseed oil, perilla oil on colon cancer. In contrast, dietary lipids rich in ω -6 PUFAs found in vegetable oils, corn oil enhance the development of colon tumors. This is significant because the typical Western diet contains 10-20 times more ω -6 than ω -3 PUFAs (2,7).

Dietary flaxseed meal which has a high percentage of ω -3 PUFAs and lignans grown in the Dakotas, was

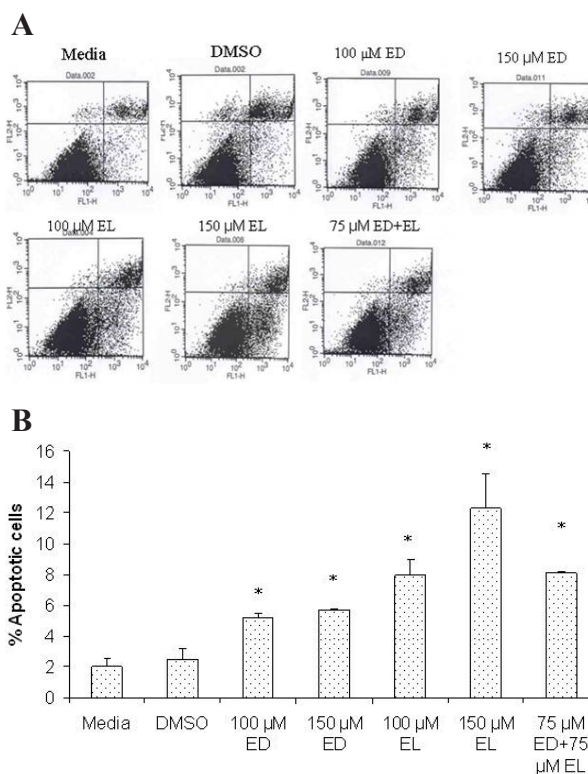


Figure 3. Effects of lignans on apoptosis in Caco-2 cells as measured by annexin V/PI staining. Cells were treated with EL alone, ED alone and combination of EL and ED for 72 h, and then cells were collected by brief trypsinization. (A) Dot plot of annexin V (FL1-H)/PI (FL2-H) staining of Caco-2 cells by flow cytometry. The lower left quadrant includes viable cells, which exclude PI and are negative for annexin V staining. The lower right quadrant is apoptotic cells, which exclude PI but bind to green fluorescence labeled annexin V. The upper quadrants represent necrotic cells or dead cells that do not exclude PI. (B) shows percentages of apoptotic cells after analysis of the FACS data using CellQuest software. In each case data represent mean \pm S.D. of three observations. *, $p < 0.05$ indicates statistical significance in treated groups as compared to DMSO control.

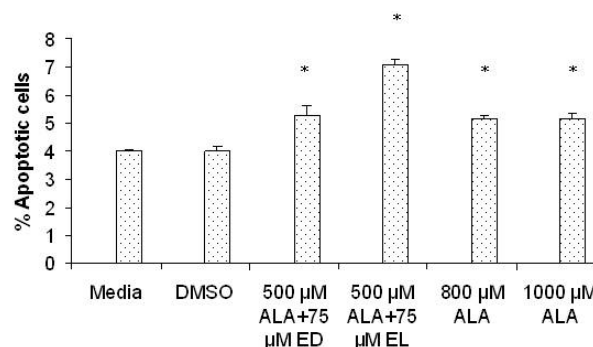


Figure 4. Effects of ALA and combinations of ALA with either EL or ED in Caco-2 cells as judged by annexin V/PI staining. Cells were treated with ALA alone or combination of ALA with either EL or ED for 72 h, and then cells were collected by brief trypsinization. Graph shows percentages of apoptotic cells after analysis of the FACS data using CellQuest software. In each case data represent mean \pm S.D. of three observations. *, $p < 0.05$ indicates statistical significance in treated groups as compared to DMSO control.

tested as a possible chemopreventive agent in colon and intestinal tumor development. Studies from our laboratory have been reported that dietary flaxseed meal showed substantial chemopreventive effects on colon tumor development and intestinal tumor development in male Fischer rats and Apc^{Min} mice model, respectively, by increasing levels of ω -3 fatty acid and lignans (13,14).

The present study was undertaken to elucidate the possible mechanism of action of flaxseed meal on colon tumor development *in vivo* by investigating the effects of components of flaxseed meal on cell proliferation and apoptosis in human colon adenocarcinoma Caco-2 cells. Results showed that major components of dietary flaxseed meal, EL, ED, and ALA can inhibit colon tumor cell proliferation, with EL being more effective than ED and ALA. Mammalian lignans such as EL and ED have been shown to reduce proliferation of estrogen sensitive breast tumor cells such as ZR-75-1 and MCF-7 in culture (11). This effect has been related to a number of mechanisms including the ability of lignans to act as antiestrogen *i.e.*, competing with estrogens for binding with estrogen receptors. In case of colon tumor cells, evidence of estrogen receptors is conflicting. Therefore, the growth inhibitory activity of colon tumor cells may be mediated through other mechanisms (11).

The protective effects of lignans against colon tumor cell proliferation might be through apoptosis mediated cell death and also through their antioxidant property. A recent study showed that EL suppressed Colo 201 human colon cancer cell growth both *in vitro* and *in vivo* and the suppressive mechanisms were attributed to apoptosis and decreased cell proliferation (10).

The current study showed that mammalian lignans along with ALA were effective in inducing apoptosis and inhibiting cell proliferation in human colon adenocarcinoma Caco-2 cells. However, the concentration of ALA which could result in a significant effect was relatively higher than EL and ED. A possible reason may be that ALA is metabolized to EPA and DHA and these metabolites alone or in combination with ED and EL may provide higher effects on inhibiting cell proliferation and inducing apoptosis in Caco-2 cells.

Several *in vitro* studies have already showed that ω -3 fatty acid, EPA has antitumoral effects through inhibition of cell proliferation or induction of apoptosis (17). In another study, it was shown that growth inhibitory and cytotoxic effects of PUFAs with methylene-interrupted double bonds such as arachidonic acid and EPA are due to peroxidation products that are generated during lipid peroxidation and COX activity (18).

In conclusion, this study demonstrated that components of flaxseed meal are effective in decreasing cell proliferation of colon cancer cells and inducing apoptosis of cancerous cells. Consumption

of dietary flaxseed leading to the circulating level of ALA, EPA, DHA, EL, and ED could be effective for the management of colon cancer. Further studies are needed on the effects of ALA, EPA, DHA, EL, and ED on other cell lines on other biomarkers of colon cancer development to completely understand the mechanism of action.

Acknowledgements

Authors thank Dr. Jack Carter for arranging financial support from North Dakota Oilseed Council. This investigation is partly supported by Translational Cancer Research Center funded as a 2010 Research Initiative Center by the State of South Dakota.

References

1. American Cancer Society Publication. Cancer facts and figures 2010. (<http://www.cancer.org>)
2. Reddy BS. Chemoprevention of colon cancer by dietary fatty acids. *Cancer Metastasis Rev.* 1994; 13:285-302.
3. Bruce WR, Giacca A, Medline A. Possible mechanisms relating to diet and risk of colon cancer. *Cancer Epidemiol Biomarkers Prev.* 2000; 9:1271-1279.
4. Torosian MH, Charland SL, Lippin JA. Differential effects of omega-3 and omega-6 fatty acids on tumor growth and metastasis. *Int J Oncol.* 1995; 7:667-672.
5. Dwivedi C, Muller LA, Goetz-Parten DE, Kasperon K, Mistry VV. Chemopreventive effects of dietary mustard oil on colon tumor development. *Cancer Lett.* 2003; 196:29-34.
6. Hong MY, Lupton JR, Morris JS, Wang N, Carroll RJ, Davidson LA, Elder RH, Chapkin RS. Dietary fish oil reduces O⁶-methylguanine DNA adduct levels in rat colon in part by increasing apoptosis during tumor initiation. *Cancer Epidemiol Biomarkers Prev.* 2000; 9:819-826.
7. Reddy BS, Burill C, Rigotty J. Effect of diets high in omega-3 and omega-6 fatty acids on initiation and post initiation stages of colon carcinogenesis. *Cancer Res.* 1991; 51:487-491.
8. Jenab M, Thompson LU. The influence of flaxseed and lignan on colon carcinogenesis and β -glucuronidase activity. *Carcinogenesis.* 1996; 17:1343-1348.
9. Chen J, Hui E, Ip T, Thompson LU. Dietary flaxseed enhances the inhibitory effect of tamoxifen on the growth of estrogen-dependent human breast cancer (MCF-7) in nude mice. *Clin Cancer Res.* 2004; 10:7703-7711.
10. Danbara N, Yuri T, Tsujita-Kyutoku M, Tsukamoto R, Uehara N, Tsubura A. Enterolactone induces apoptosis and inhibits growth of Colo 201 human colon cancer cells both *in vitro* and *in vivo*. *Anticancer Res.* 2005; 25:2269-2276.
11. Sung MK, Lautens M, Thompson LU. Mammalian lignans inhibit growth of estrogen-independent human colon tumor cells. *Anticancer Res.* 1998; 18:1405-1408.
12. Tokachev ON, Zhuchenko AA. Biologically active substances of flax: medicinal and nutritional properties. *Pharmaceut Chem J.* 2000; 34:23-30.
13. Bommareddy A, Arasada BL, Mathees DP, Dwivedi C. Chemopreventive effects of dietary flaxseed on colon

- tumor development. *Nutr Cancer*. 2006; 54:216-222.
14. Bommarreddy A, Zhang X, Schrader D, Kaushik RS, Zeman D, Mathees DP, Dwivedi C. Effects of dietary flaxseed on intestinal tumorigenesis in *Apc^{Min}* mouse. *Nutr Cancer*. 2009; 61:276-283.
 15. Kaur M, Agarwal C, Singh RP, Guan X, Dwivedi C, Agarwal R. Skin cancer chemopreventive agent, α -santalol, induces apoptotic death of human epidermoid carcinoma A431 cells *via* caspase activation together with dissipation of mitochondrial membrane potential and cytochrome *c* release. *Carcinogenesis*. 2005; 26:369-380.
 16. Zhang X, Bommarreddy A, Chen W, Khalifa S, Kaushik RS, Fahmy H, Dwivedi C. Sarcophine-diol, a chemopreventive agent of skin cancer, inhibits cell growth and induces apoptosis through extrinsic pathway in human epidermoid carcinoma A431 cells. *Transl Oncol*. 2009; 2:21-30.
 17. Clarke RG, Lund EK, Lathan O, Pinder AC, Johnson IT. Effect of EPA on the cell proliferation and incidence of apoptosis in colorectal cell line HT 29. *Lipids*. 1999; 34:1287-1295.
 18. Dommels YE, Haring MM, Keestra NG, Alink GM, van Bladeren PJ, van Ommen B. The role of cyclooxygenase in n-6 and n-3 polyunsaturated fatty acid mediated effects on cell proliferation, PGE₂ synthesis and cytotoxicity in human colorectal carcinoma cell lines. *Carcinogenesis*. 2003; 24:385-392.

(Received April 7, 2010; Accepted April 18, 2010)

Original Article

Characterization, thermodynamic parameters and *in vivo* antimalarial activity of inclusion complexes of artemether

Renu Chadha^{1,*}, Sushma Gupta¹, Geeta Shukla², Dharamvir S. Jain³, Surjit Singh⁴

¹ University Institute of Pharmaceutical Sciences, Panjab University, Chandigarh, India;

² Department of Microbiology, Panjab University, Chandigarh, India;

³ Department of Chemistry, Panjab University, Chandigarh, India;

⁴ Guru Nanak Dev University, Amritsar, Punjab, India.

ABSTRACT: The present study aimed to improve solubility, dissolution and ultimate bioavailability of poorly soluble artemether, an antimalarial drug, by encapsulating it in β -cyclodextrin (β -CD) and its methyl and hydroxypropyl derivatives. The effect of these complexes was confirmed by *in vivo* studies. Phase solubility studies indicated 1:1 stoichiometry and were supported by mass spectrometry and proton nuclear magnetic resonance (¹H-NMR) spectroscopy. True inclusion of artemether into the cyclodextrin cavity was observed in lyophilized complexes by differential scanning calorimetry (DSC), powder X-ray diffraction (PXRD) and Fourier transform infrared spectroscopy (FT-IR) studies. The mode of inclusion was supported by two-dimensional (2D) NMR. Solution calorimetry was used to confirm 1:1 stoichiometry by determining the enthalpy of interaction between the drug and cyclodextrins. The stability constant (K) of inclusion and other thermodynamic parameters such as enthalpy (ΔH) as well as entropy (ΔS) of binding accompanying the encapsulation were determined. The calculated value of K indicated that M- β -CD has maximum complexing efficiency. Dissolution studies indicated that the highest release rate was observed for lyophilized complexes. *In vivo* studies of lyophilized complexes of M- β -CD showed a 3-fold increase in antimalarial activity compared to artemether and resulted in 100% eradication of parasite. However, 83% and 50% survival rates were achieved in 40 days using HP- β -CD and β -CD complexes respectively. The study concludes that encapsulation of artemether by cyclodextrins is a good alternative to enhance the bioavailability of the drug.

Keywords: Artemether, β -cyclodextrins, inclusion complex, stoichiometry, *in vivo* studies

1. Introduction

Malaria is the most life threatening disease among parasitic infections. Of the four human malaria parasites, *Plasmodium falciparum* is the overwhelming cause of serious disease and death (1). Artemether, a rapidly acting antimalarial drug is potent, efficient against acute and severe *P. falciparum* malaria. WHO has listed it as an essential drug for the treatment of severe multiple resistant malaria (2). It acts by generating free radicals from the endoperoxy bridge of the drug and interacts with heme molecules located in the food vacuole of the parasite which is essential for its antimalarial activity (3). The therapeutic efficacy of artemether is greatly hampered due to its poor bioavailability and low aqueous solubility (3). One of the approaches to overcome these problems is to use cyclodextrins (CDs) as drug carriers. These oligosaccharides are most interesting because they form drug complexes in both the solution and solid state, wherein either the whole guest, or part of it (commonly the less polar part), is sequestered inside the hydrophobic cavity (4). The present study reports the preparation of inclusion complexes of artemether with β -CD (β -cyclodextrin), M- β -CD (methyl- β -cyclodextrin) and HP- β -CD (hydroxypropyl- β -cyclodextrin) and is aimed at improving its solubility and bioavailability. The data available regarding the formation of complexes of this important antimalarial drug (3,5) lack detailed characterization and thermodynamic parameters as well as *in vivo* studies except for one recent report (6) where the authors have used only HP- β -CD. Thus, the emphasis of the current study is both on formation of complexes and on an *in vivo* model to monitor the suitability of these complexes to enhance the bioavailability and dose of artemether.

*Address correspondence to:

Dr. Renu Chadha, University Institute of Pharmaceutical Sciences, Panjab University, Chandigarh 160014, India.
e-mail: renukachadha@rediffmail.com

2. Materials and Methods

2.1. Preparation of artemether inclusion complexes

The inclusion complexes of artemether with different types of CDs were prepared at a stoichiometric molar ratio of 1:1 using physical mixing, kneading and freeze-drying. Physical mixtures were prepared by simple mixing of drug with different CDs in a mortar. In the kneading method, cyclodextrins were wetted with water in a glass mortar until a paste was obtained, the drug was added and the slurry was kneaded for 90 min. An appropriate amount of water was added in order to maintain a suitable consistency. The product was dried under vacuum at 40°C for 48 h and sieved through 150 µm mesh. In the freeze-drying method, the required stoichiometric amount of drug was added to an aqueous solution of different CDs and solutions in the presence and absence of CDs were agitated on a magnetic stirrer for 24 h. The resulting solutions were frozen at (-80°C) overnight. The products were lyophilized under 17.2 mTorr for 48 h. The sample was transferred into a vacuum desiccator and dried over silica gel under vacuum for at least 24 h.

2.2. Characterization

The complexes were characterized using a differential scanning calorimeter (DSC) (7,8), mass spectrometry, Fourier transform infrared spectrometry (FT-IR) (9,10), powder X-ray diffraction (PXRD) (11,12), proton nuclear magnetic resonance spectroscopy (¹H-NMR) (13-15) methods *vis-à-vis* phase solubility (16,17) and dissolution studies (18). Solution calorimetry was used to directly measure the enthalpy changes associated with encapsulation (19,20).

2.3. Phase solubility studies

Phase solubility studies were carried out according to the method described by Higuchi and Connors (21). These were performed by adding excess amounts of drug to 10 mL of simulated intestinal fluid (pH 6.8) solution in the absence or presence of increasing concentrations (0.001 to 0.015 M) of β-CD and M-β-CD and HP-β-CD. Suspensions were sealed and shaken in a water-bath shaker MSW-275 (Macroscientific Works, Delhi, India) at 37 ± 0.5°C for 24 h to ensure equilibrium. The samples were filtered through 0.45 µm Millipore filter paper and analyzed at 240 nm spectrophotometrically using a UV/VIS spectrophotometer (Perkin Elmer Lambda 15, USA). The presence of CDs did not interfere with the spectrophotometric assay of the drug.

2.4. Differential scanning calorimetry (DSC)

DSC thermograms of artemether, pure CDs and their

inclusion complexes were obtained on DSC, Q20, TA instruments-Waters LLC, USA. The calorimeter was calibrated for temperature and heat flow accuracy using the melting of pure indium (mp 156.6°C and ΔH of 25.45 Jg⁻¹). The temperature range was from 25-350°C with a heating rate of 10°C per minute.

2.5. Powder X-ray diffraction (PXRD) analysis

Powder diffraction patterns of artemether and their inclusion complexes were recorded on an X-ray diffractometer (XPRT-PRO PANanalytical, Netherlands) using Cu as tube anode. The diffractograms were recorded under the following conditions: voltage 40 kV, 35 mA, angular range 5, fixed divergence slit.

2.6. Mass spectrometry

Mass spectrometric studies were performed using a Q-ToF quadrupole time of flight mass spectrometer (Waters) equipped with an electrospray source. After optimization of the MS parameters, the spray voltage was set to 2.5 kV in the positive mode, and the heated metal capillary temperature was set at 80°C.

2.7. Fourier transform infrared (FT-IR) spectroscopic studies

The FT-IR spectra of artemether and inclusion complexes forms were recorded on an FT-IR spectrometer (Mode spectrum RXI, Perkin Elmer, UK) over the range 400-4,000 cm⁻¹. Dry KBr (50 mg) was finely ground in a mortar and samples of drug and their complexes (1-2 mg) were subsequently added and gently mixed. A manual press was used to form the pellets.

2.8. Two-dimensional (2D) and proton nuclear magnetic resonance (¹H-NMR) spectroscopy

¹H-NMR and two-dimensional (2D) COSY spectra in d₆-DMSO of artemether and inclusion complexes were recorded with a Bruker AC 300°C NMR spectrometer apparatus operating at 300 MHz using tetramethylsilane as an internal standard. For 2D COSY experiments, samples were equilibrated for at least 24 h.

2.9. Solution calorimetry

Isoperibol solution calorimeter (ISC) model 4300 (Calorimetry Science Corporation, Lindon, UT, USA) was used for thermal measurements. It is a semi-adiabatic calorimeter with temperature resolution, after noise reduction, close to 1 µK, which corresponds to a heat resolution of 1-4 mJ in a 25 mL buffer (pH 6.8) reaction vessel. The details are given in our previous

papers (22,23). The performance of the system was tested by measuring enthalpy of solution of potassium chloride (17.301 kJ/mol) in triple distilled water, which is in good agreement with known enthalpy of solution of 17.322 kJ/mol. The precision of any individual measurement was better than ± 0.03 kJ/mol for three consecutive experiments.

2.10. Dissolution studies

The dissolution studies were performed on the inclusion complexes of artemether prepared by all three methods using a USP (I2) apparatus equipped with paddle type tribune at 50 rpm in 900 mL of simulated intestinal fluid (pH 6.8) pre-equilibrated at $37 \pm 0.5^\circ\text{C}$. Inclusion complexes equivalent to 100 mg of artemether were filled into hard gelatin capsules. Sample was withdrawn at different intervals for a period of 4 h and analyzed spectrophotometrically at 240 nm. Three replicates were made for each experiment.

2.11. In vivo studies

2.11.1. Parasite strain

Plasmodium berghei (NK 65 strain) was used for evaluation of antimalarial activity *in vivo* studies and was maintained in BALB/c mice by intraperitoneal (*i.p.*) inoculation of infected blood. Percent parasitaemia was quantitated on every alternate day in Giemsa stained tail vein blood films and was calculated by counting at least 500 red blood cells (RBCs).

2.11.2. Animals

Four to five weeks old BALB/c mice (25-30 g) were procured and maintained in the Central Animal House and were provided with standard pellet diet and water *ad libitum*. Experiments were performed according to National Science Academy Guidelines Committee for the purpose of control and supervision of experiments on animals (CPC-SEA). The experimental protocol was approved by Institutional Animal Ethics Committee

(A. I. E. C.).

Animals were divided into 2 major groups. Animals belonging to group I were used for dose standardization and animals of group II were used to monitor the efficacy and potency of prepared lyophilized complexes. Groups I and II were further subdivided as follows. Group I (56 animals) was subdivided into the following 7 groups (Table 1): Group IA, *P. berghei* infected animals (control); Group IB, animals treated with a single dose of artemether (4 mg/kg) on day 3 post inoculation (PI) up to 7 days; Group IC, animals treated twice a day with dose (5 mg/kg) on day 3 PI up to 7 days; Group ID, animals treated twice a day with dose (5 mg/kg) on day 2 PI for 3 consecutive days; Group IE, animals treated twice a day with dose (5 mg/kg) on day 2 PI for 7 consecutive days; Group IF, animals treated with dose (16 mg/kg) on day 1 PI, followed by a single dose (8 mg/kg) after 8 h and then two times a day up to 7 days; Group IG, animals treated with a single dose (10 mg/kg) after 8 h of PI followed by single dose therapy two times a day up to 7 days.

Animals of Group II were subdivided into 5 groups and each group comprised of 6 animals ($n = 6$). Artemether, Am- β -CD, Am-M- β -CD and Am-HP- β -CD were administered to group IIB, group IIC, group IID and group IIE respectively (Table 2). These were treated with single dose therapy (5 mg/kg) two times a day on 1 day of PI for 7 days.

2.11.3. Preparation and administration of doses

Artemether and its complexes were suspended in 0.5% carboxymethyl cellulose (CMC). Each animal was treated with 100 μL artemether and its various lyophilized complexes (Table 1).

2.11.4. Challenge of the experimental animals and follow up of the experimental animals

All the mice belonging to groups I and II were challenged with 10^6 *P. berghei* infected RBCs (*i.p.*). After challenge the mean percent parasitaemia, percent activities of various complexes of artemether along with animal survivability were monitored.

Table 1. Dose standardization of antimalarial drug artemether in *P. berghei* infected mice ($n = 8$)

Groups	Artemether treated (mg/kg)*	Day of treatment	No. of survivals/ total No. of animals	Survival time ($t = 40$ days)
IA	0	NA	0/8	8 days
IB	4	SDT on day 3 PI up to 7 days	0/8	12-16 days
IC	5	TD on day 3 PI up to 7 days	0/8	15-18 days
ID	5	TD on day 2 PI up to 3 days	0/8	14-20 days
IE	5	TD on day 2 PI up to 7 days	2/8	40 days
IF	8	DD on day 1 PI followed by SD after 8 h. BD on day 2 PI up to 6 days.	5/8	40 days
IG	10	SD after 8 h PI followed by BD up to 7 days of infection	8/8	40 days

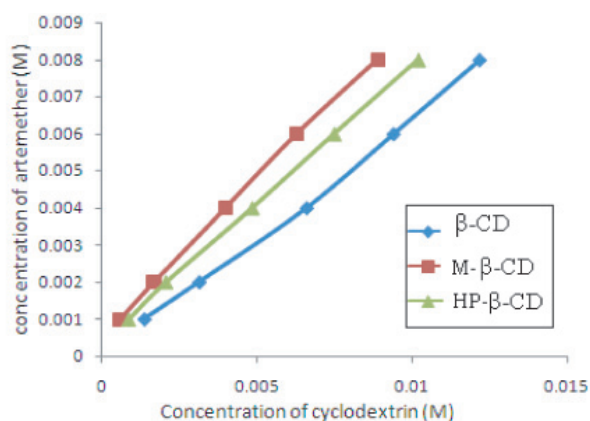
*Animals were treated with indicated amounts of artemether in 0.5% CMC.

Abbreviations: NA, not applicable; SDT, single dose therapy; TD, twice a day; DD, double dose; SD, single dose; PI, post inoculation.

Table 2. Antimalarial activity of complexes of artemether in *P. berghei* infected mice

Groups	Treatments	% Parasitaemia on day 8 PI	% Mortality (n = 6, t = 40 days)
IIA	0.5% CMC solution	35.56	100
IIB	Artemether (5 mg/kg)	4.9	66.7
IIC	Am- β -CD (5 mg/kg of Am)	4.6	50
IID	Am-M- β -CD (5 mg/kg of Am)	0.0002	16.7
IIE	Am-HP- β -CD (5 mg/kg of Am)	1.45	0

Abbreviations: *t*, No. of days; *n*, No. of animals per group; PI, post inoculation; Am- β -CD, artemether- β -cyclodextrins complex; Am-M- β -CD, artemether-methyl- β -cyclodextrins complex; Am-HP- β -CD, artemether-hydroxypropyl- β -cyclodextrins complex.

**Figure 1. Phase solubility curves of artemether with β -CD and its derivatives at 37°C.**

2.11.5. Percent parasitaemia

Percent parasitaemia was monitored on every alternate day for up to 40 days using tail blood smears, fixed in methanol and stained with Giemsa stain. At least 500 cells were counted.

2.11.6. Statistical analysis

Data was expressed as mean \pm S.D. and parasitaemia of the artemether and its inclusion complexes were statistically assessed by one-way ANOVA followed by Turkey test using Jandel Sigma Stat 2.0 version. Differences were considered significant at $p < 0.05$.

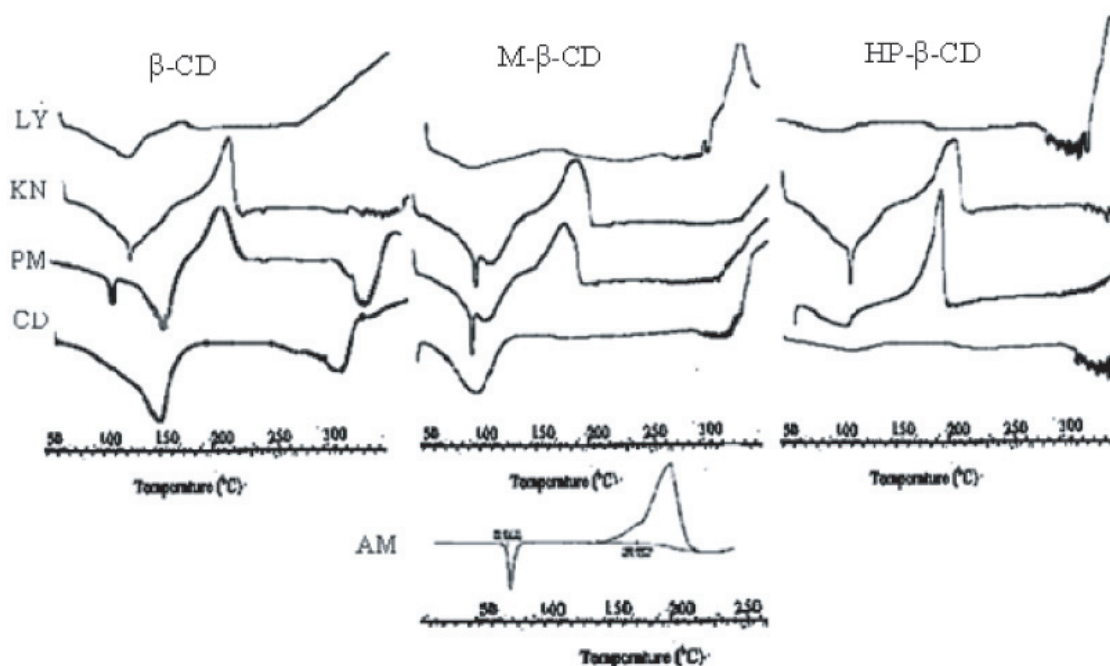
3. Results and Discussion

3.1. Phase solubility analysis

The solubility of artemether increased in a linear fashion as a function of β -CD, M- β -CD and HP- β -CD concentration and followed an A_1 -type system showing that a soluble complex was formed and no precipitation was observed over the entire concentration range studied. This linear host-guest correlation with a slope less than one suggested the formation of first order molar soluble complexes (Figure 1).

3.2. DSC analysis

DSC was used to provide detailed information about the physical state of the inclusion complex (Figure 2). The DSC thermograms of artemether were typical

**Figure 2. DSC thermograms of artemether-CD solid systems. AM, artemether; CDs, β -CD, M- β -CD and HP- β -CD; PM, physical mixtures; KN, kneaded complex; Ly, lyophilized complex.**

of an anhydrous crystalline substance, exhibiting a sharp endothermic peak at 86.61°C, corresponding to the melting point of the drug. The complexes of the physical mixtures as well as the kneaded complexes of β -CD, M- β -CD, and HP- β -CD, and the phase transition thermal profile of artemether remained recognizable with reduction and broadening of the drug fusion peak, with a concomitant shift to lower temperature. The complete disappearance of the endothermic peak was observed for lyophilized systems indicating formation of a true inclusion complex. Decomposition was shifted to a higher temperature and was greatly reduced which further supports that the inclusion of the drug has enhanced its physical stability.

3.3. PXRD analysis

The diffraction pattern of artemether showed sharp diffraction peaks at $2\theta^\circ = 9.5622, 9.6787, 10.2706, 10.35353, \text{ and } 19.3998$ indicating its crystalline state and these were still detectable in the respective physical mixtures and kneaded complexes, though with evident reduction in their intensity. On the other hand, as expected the lyophilized products showed complete disappearance of drug diffraction peaks in M- β -CD, and HP- β -CD (Figure 3).

3.4. Mass spectrometry

The prepared lyophilized complexes of β -CD, M- β -

CD, and HP- β -CD were introduced into the mass spectrometer and peaks were observed at m/z 1136, 1434, 1609, and 1679 corresponding to the charged $[\beta\text{-CD} + \text{H}]^+$, $[\text{Am} + \beta\text{-CD} + \text{H}]^+$, $[\text{Am} + \text{M-}\beta\text{-CD} + \text{H}]^+$, and $[\text{Am} + \text{HP-}\beta\text{-CD} + \text{H}]^+$, respectively, indicating 1:1 stoichiometry as suggested by phase solubility analysis (Figure 4). There is no trace of 1:2 stoichiometric complexes (24,25).

3.5. FT-IR spectroscopic studies

FT-IR could not give much useful information as the spectra of complexes of β -CD, M- β -CD, and HP- β -CD were found quite similar to their corresponding pure CDs because of the coincident absorption of both the host and guest molecules in most of spectral region. Bands of the included part of the guest molecule are masked by the bands of the spectrum of CDs (Figure 5).

3.6. NMR spectroscopic studies

NMR spectroscopy assures the existence of complexes in solution and also predicts its geometry by determining the chemical shift changes of drug protons due to its insertion into the hydrophobic cavity of cyclodextrins. A downfield shift in the cycloheptane protons H-d, H-g, H-h, H-m, and H-n of drug revealed the presence of artemether molecule in the cyclodextrin cavity (Figure 6B). The most plausible mode is that cycloheptane ring with endoperoxide group enters the cavity from

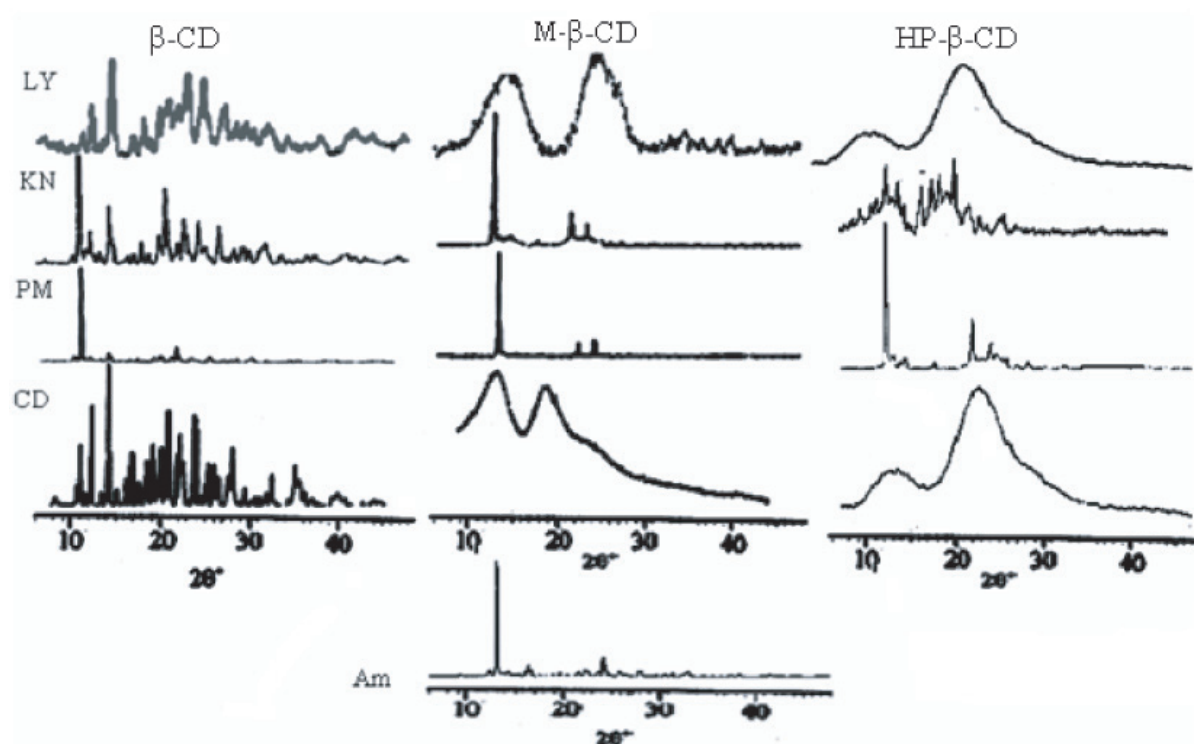


Figure 3. PXRD diffraction pattern of artemether-CD solid systems. AM, artemether; CDs, β -CD, M- β -CD and HP- β -CD; PM, physical mixtures; KN, kneaded complex; Ly, lyophilized complex.

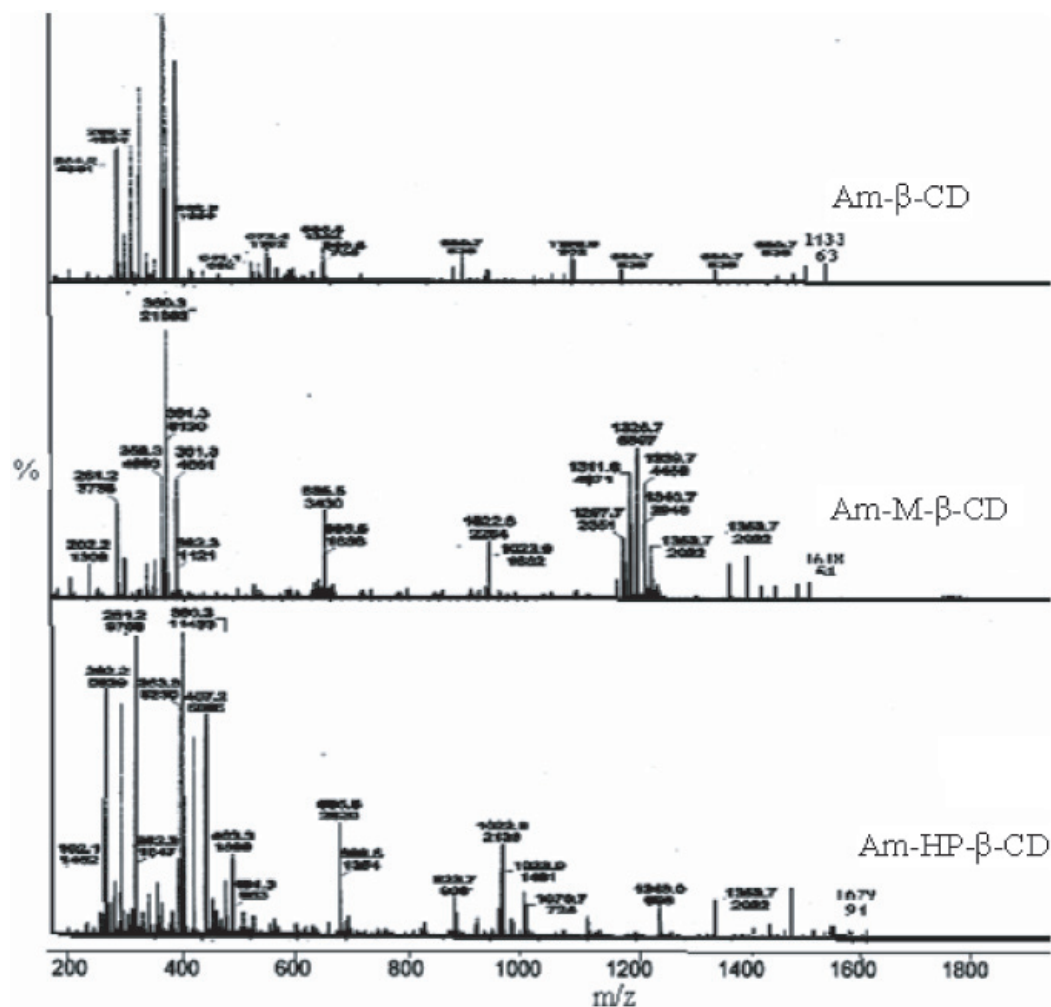


Figure 4. Mass spectra of lyophilized complexes of artemether.

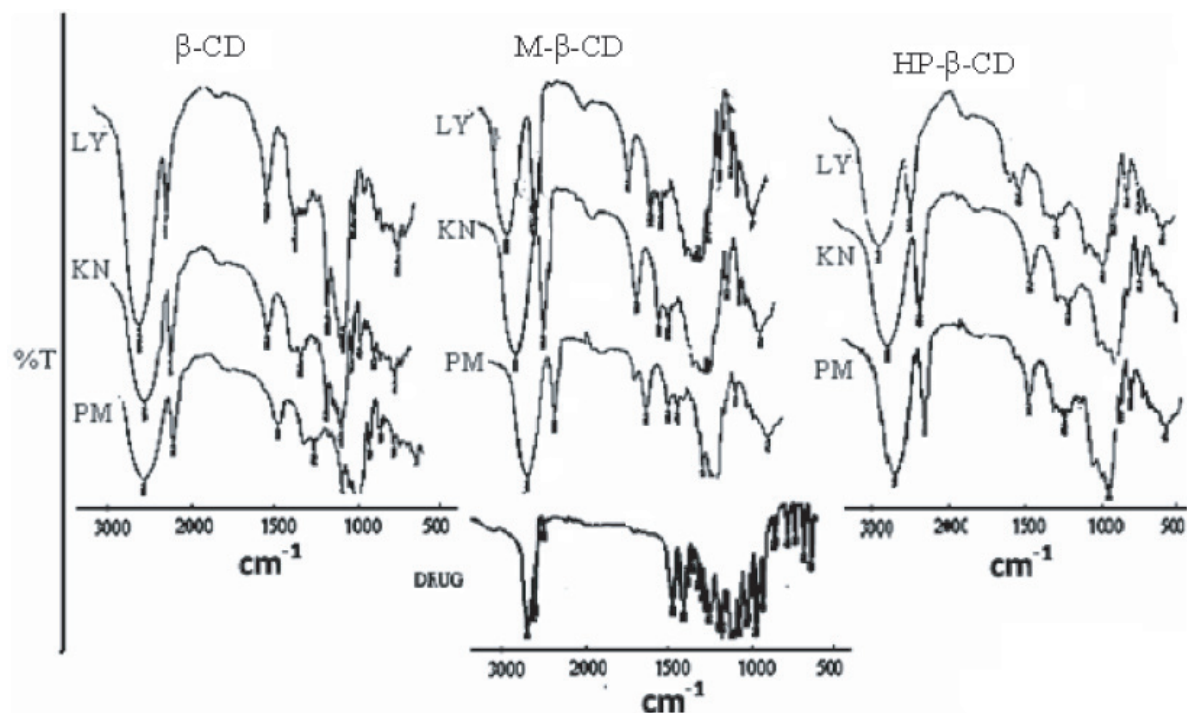


Figure 5. FTIR spectra of artemether-CDs solid systems. PM, physical mixtures; KN, kneaded complex; Ly, lyophilized complex.

the secondary face because of its narrower dimension (2.89 Å), whereas the opposite end of the molecule consisting of two cyclohexane rings with groups having dimensions of 6.9 Å is partially protruding (Figures 6A and 6C). A downfield displacement (Table 3) indicates that these protons are closer to the electronegative atom (oxygen) whereas, an upfield shift in protons H-e,

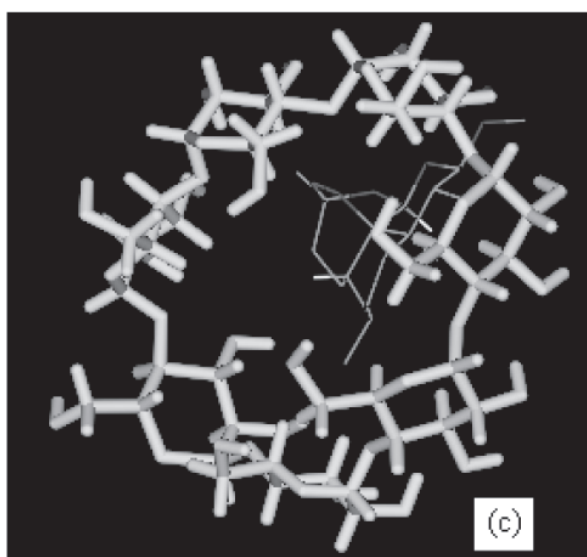
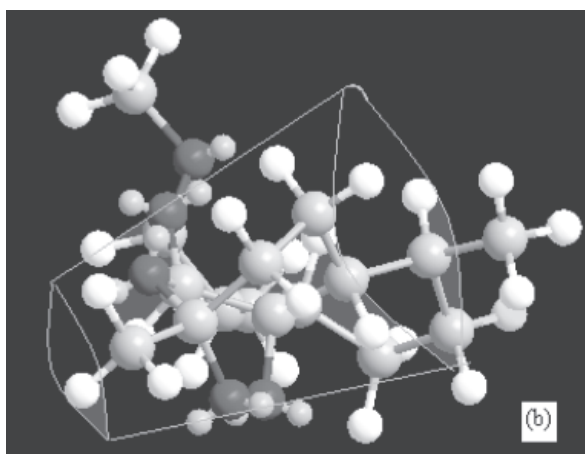
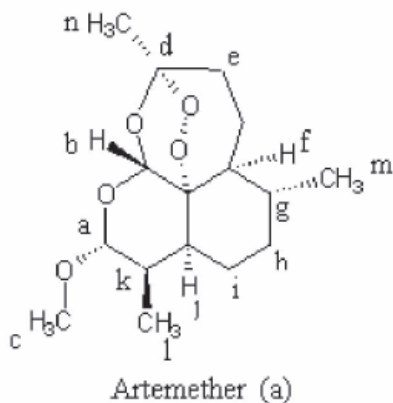


Figure 6. Chemical structure of artemether (a), inclusion mode of artemether with β -CDs (b), and molecular representation of inclusion complex of artemether with β -cyclodextrin cavity (c).

H-b, and H-f of the molecule indicates variation in the local polarity due to weaker interactions with hydrogen atoms (shielding effect due to Van der Waals forces between drug and carbohydrates) (26-29). 2D COSY spectra were further used to get more insight into the geometry of the complex. It provides information about the spatial proximity between host and guest atoms by observing intermolecular cross-relations. The appearance of cross peaks (Figure 7) between H-5 protons of CD and H-b and H-n protons support our proposed inclusion mode involving insertion of the cycloheptane ring with endoperoxide bridge (trioxane ring) deep into the cavity. Cross peaks are also present between H-3 protons of CD and H-a protons of the oxygen containing cyclohexane ring of the drug. These results were in agreement with Yuen *et al.* and Illapakurthy *et al.* (30,31). However, it contrasts with findings obtained by Bo *et al.* (6). The encapsulation prevents decomposition leading to enhancement in physical stability as shown by DSC scans.

3.7. Stoichiometry by solution calorimetry

Solution calorimetry was employed to confirm the stoichiometry as well as to evaluate the stability constants and thermodynamic parameters associated with the binding process and are summarized in Table 4. The molar enthalpy of solution ($\Delta_{\text{sol}}H_{(M)}$) was found to be exothermic (-13.18 kJ/mol) for artemether and was even more exothermic for the solution of artemether in the presence of CDs ($\Delta_{\text{sol}}H_{(M)(CD)}$). This is due to interaction between drug and cyclodextrins. Enthalpy of interaction was calculated by subtracting the enthalpy of solution of drug in cyclodextrins from that in pure buffer. The enthalpy of interaction was calculated from the equation 1:

$$\Delta H_{\text{int}(\text{exp})} = \frac{\Delta H_{(CD)} - \Delta H}{v(l)} \quad (\text{Eq. 1})$$

where $\Delta H_{\text{int}(\text{exp})}$ denotes enthalpy of interaction between drug and cyclodextrin per liter of solution; ΔH and $\Delta H_{(CD)}$ denote enthalpy of solution of drug in buffer and in buffered aqueous solution of cyclodextrins, respectively; and $v(l)$ denotes volume of sample cell in liters (0.025 L).

Enthalpy of interaction per mole of drug and cyclodextrin ($\Delta_{\text{sol}}H_{(M)}$) were calculated from equation 2:

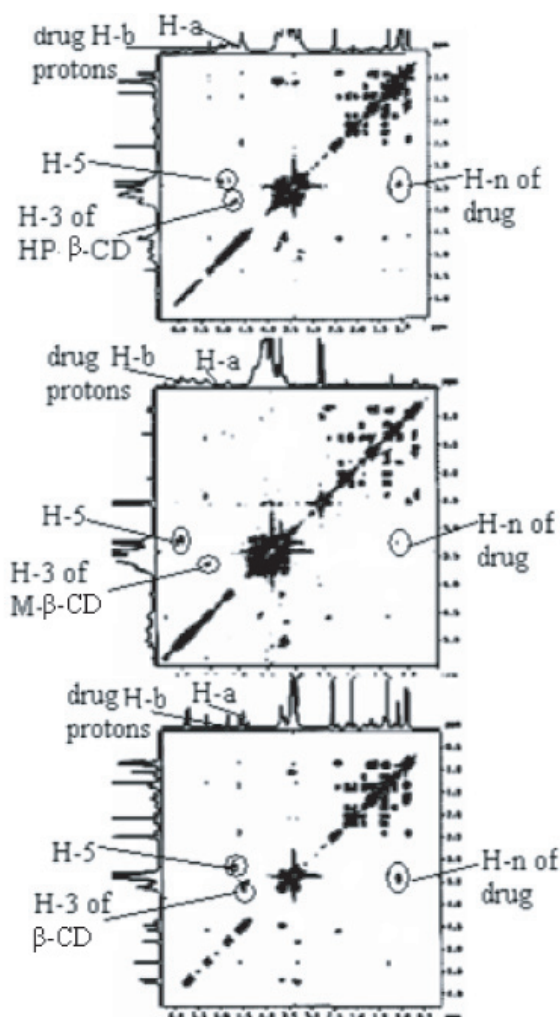
$$\Delta H_{\text{int}(M)} = \frac{\Delta H_{\text{int}(\text{exp})}}{a + b} = \frac{\Delta_{\text{sol}}H_{(M)(CD)} - \Delta_{\text{sol}}H_{(M)}}{1 + X_2/X_1} \quad (\text{Eq. 2})$$

where, a and b denote initial molar concentration of drug and cyclodextrin, respectively, in solution; X_1

Table 3. Values of ¹H chemical shifts before and after inclusion

Artemether	δ_{drug}	$\delta_{\beta\text{-CD complex, M-}\beta\text{-CD complex, HP-}\beta\text{-CD complex, respectively}}$	$\Delta\delta$ (ppm)
H-a	4.6845	4.8279, 4.5685, 4.5783	0.1434, -0.116, -0.016
H-b	5.3163	5.7255, 5.2974, 5.3003	0.4092, -0.0189, -0.1062
H-c	3.4023	3.3756, 3.2918, 3.2835	-0.0267, -0.1105, -0.1188
H-d	2.1766	2.1853, 2.1681, 2.0437	0.0087, 0.02787, 0.01297
H-e	1.144	1.1519, 1.14068, 1.1574	0.0123, -0.003327, -0.00127
H-f, j	1.355	1.347, 1.34832, 1.3538	-0.00802, -0.0068, -0.01336
H-g	2.3928	2.4014, 2.4051, 2.4032	0.00856, 0.0123, 0.0104
H-h	1.7731	1.7949, 1.7976, 1.6597	0.0218, 0.02446, -0.01134
H-i	1.5938	1.5525, 1.6039, 1.5575	-0.04132, 0.0101, -0.03627
H-k	2.5073	2.5066, 2.5072, 2.5072	-0.0007, -0.0001, -0.0001
H-l	0.8958	0.8905, 0.8928, 0.8445	-0.00525, -0.003, -0.00545
H-m	0.8390	0.8400, 0.8423, 0.8949	0.00105, 0.0033, 0.009
H-n	1.2865	1.2933, 1.2944, 1.2946	0.0068, 0.0079, 0.0099

$$\Delta\delta = \delta_{(\text{complex})} - \delta_{(\text{free})}$$

**Figure 7. COSY spectra of inclusion complexes of artemether with β -CD, M- β -CD and HP- β -CD.**

and X_2 denote apparent mole fractions of the drug and cyclodextrin, respectively, ignoring the concentration of buffers.

The detailed calorimetric results for artemether- β -CD complexation are summarized in Table 4. Similar calculations were obtained for M- β -CD and HP- β -CD.

The stoichiometry of the complex was ascertained

utilizing a continuous variation method (Job's plot) (32) by plotting $\Delta_{\text{sol}}H_{(\text{M})}$ versus X_2 (Figure 8). It is clear that the minima occurs at $X_2 = 0.5$ confirming the 1:1 stoichiometry as proposed by phase solubility, mass spectrometry, and proton NMR studies.

The thermodynamic constants were calculated assuming the following equilibria:



The experimentally calculated enthalpy of interaction ($\Delta H_{\text{int}(\text{exp})}$) is proportional to the product of molar concentration of the CD:artemether complex (c) in solution at equilibrium and enthalpy of binding per mole of drug (ΔH°).

$$\Delta H_{\text{int}(\text{exp})} = \Delta H^\circ \times c \quad (\text{Eq. 4})$$

The equilibrium constant for equation 3 can be represented by

$$K = (c)/(a - c)(b - c) \quad (\text{Eq. 5})$$

The concentration of complex corresponds to equation 6.

$$c = [A - \sqrt{\{(A)^2 - 4ab\}}]/2 \quad (\text{Eq. 6})$$

where, $A = a + b + 1/K$. Putting equation 6 in equation 4,

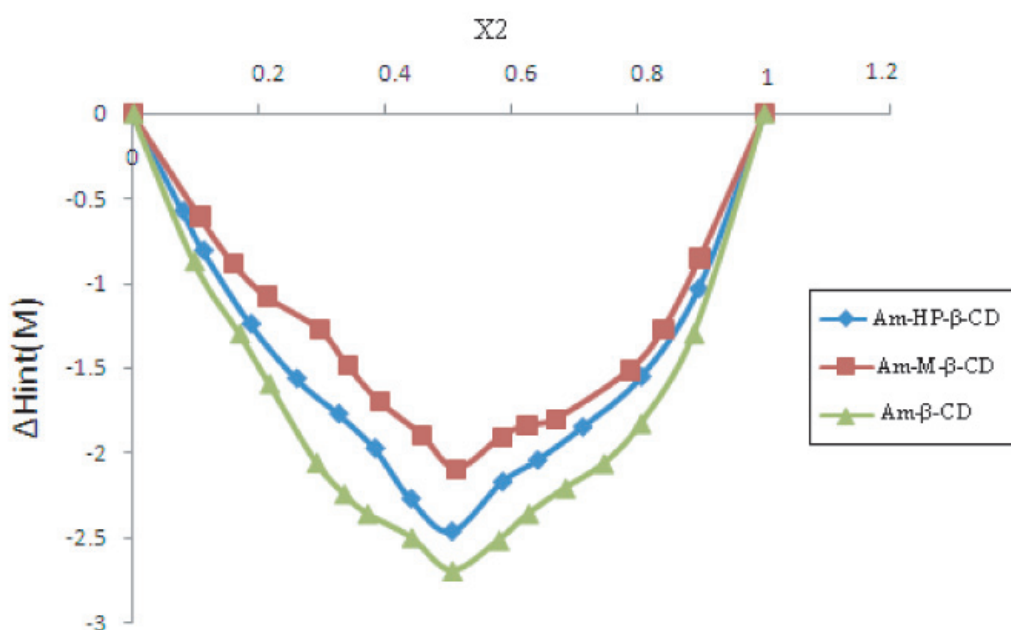
$$\Delta H_{\text{int}(\text{exp})} = \Delta H^\circ \times [(A - \sqrt{\{(A)^2 - 4ab\}})/2] \times v \quad (\text{Eq. 7})$$

The binding constant K and enthalpy of binding (ΔH°) were computed from the experimentally calculated enthalpy of interaction ($\Delta H_{\text{int}(\text{exp})}$). The calculations were done by our computer program utilizing an iterative non-linear least square regression method to minimize the value of $\sum(\Delta H_{\text{int}(\text{exp})} - \Delta H_{\text{int}(\text{calc})})^2$ and are summarized in Table 5.

The values of free energy of inclusion (ΔG°) and entropy of inclusion (ΔS°) were calculated from the

Table 4. Interaction enthalpy of inclusion complexes of artemether with β -CD at pH 6.8

X_2	M_{AM} (mM)	$M_{\beta-CD}$ (mM)	$\Delta_{sol}H_{(CD)}$ (J)	$\Delta_{sol}H_{int(exp)}$ (J/L)	$\Delta_{sol}H_{int(M)}$ (kJ/mol)
0.895595	0.410704	3.5496	-0.23773	-4.09495	-1.034
0.80532	0.8552	3.5376	-0.45245	-6.82378	-1.5534
0.6407	0.712095	1.2698	-0.32635	-3.66651	-1.85
0.71212	0.76508	1.89252	-0.38802	-5.43479	-2.045
0.5849	0.62684	0.88316	-0.28864	-3.28199	-2.1735
0.50453	0.8888	0.90536	-0.40355	-4.42512	-2.4664
0.4398	1.1804	0.9267	-0.50879	-4.79028	-2.2734
0.38254	1.5302	0.948	-0.62668	-4.89445	-1.975
0.3249	0.806972	0.38836	-0.31891	-2.11813	-1.772
0.2592	1.0769	0.3768	-0.41172	-2.27213	-1.563
0.1865	1.6604	0.38062	-0.61052	-2.53189	-1.2405
0.11131	1.488592	0.18644	-0.52439	-1.35142	-0.8068
0.07896	2.2206	0.17534	-0.76625	-1.37599	-0.5743

**Figure 8. Plot of $\Delta H_{int(M)}$ vs. X_2 of β -CD, M- β -CD, and HP- β -CD of artemether (AM) at pH 6.8 in simulated intestinal fluid (SIF).****Table 5. Thermodynamic parameters of artemether with β -CD, M- β -CD, and HP- β -CD at pH 6.8 in SIF, determined using solution calorimetry**

System	K (M^{-1})	ΔH° (kJ/mol)	ΔG° (kJ/mol)	ΔS° (J/mol \cdot K)
Artemether + β -CD	1,175	-10.00	-18.22	26.51
Artemether + M- β -CD	2,500	-8.90	-20.16	36.34
Artemether + HP- β -CD	2,440	-11.8	-20.10	26.78

following equations:

$$\Delta G^\circ = -RT \ln K \quad (\text{Eq. 8})$$

$$\Delta S^\circ = (\Delta H^\circ - \Delta G^\circ)/T \quad (\text{Eq. 9})$$

The values of K are between 1,100 to 2,500 M^{-1} , which is a favorable range for better bioavailability. Both enthalpic and entropic factors drive the inclusion process. The inclusion of drug was found to be an exothermic

process while the entropy of reaction is positive in all these cases leading to values of Gibbs free energy (ΔG°) between -18.2 to 20.2 kJ/mol. The magnitude of the equilibrium constant (K) indicates that both methyl- β -CD and HP- β -CD have nearly the same complex formation ability and which is further confirmed by dissolution and animal studies.

3.8. Dissolution studies

Rapid dissolution is the characteristic behavior of inclusion complexes but the comparative release of active material was strongly affected by the method of formulation. The lyophilized product exhibited the best dissolution properties and was followed by kneaded complex and physical mixtures (Figure 9). Moreover, the highest dissolution rate was found for M- β -CD complex followed by that of HP- β -CD and β -CD in simulated intestinal fluid (pH 6.8). The improvement

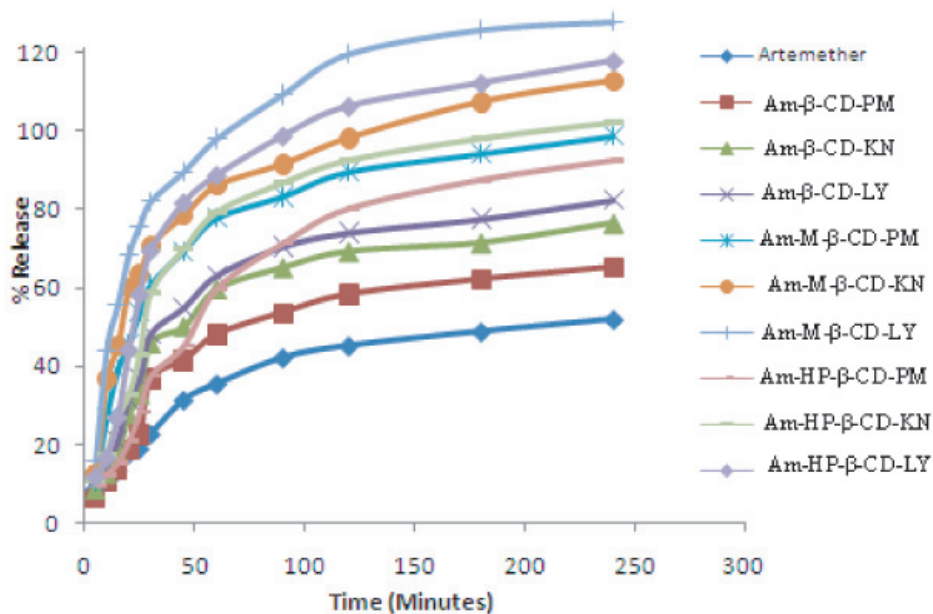


Figure 9. Dissolution profile of artemether and its complexes.

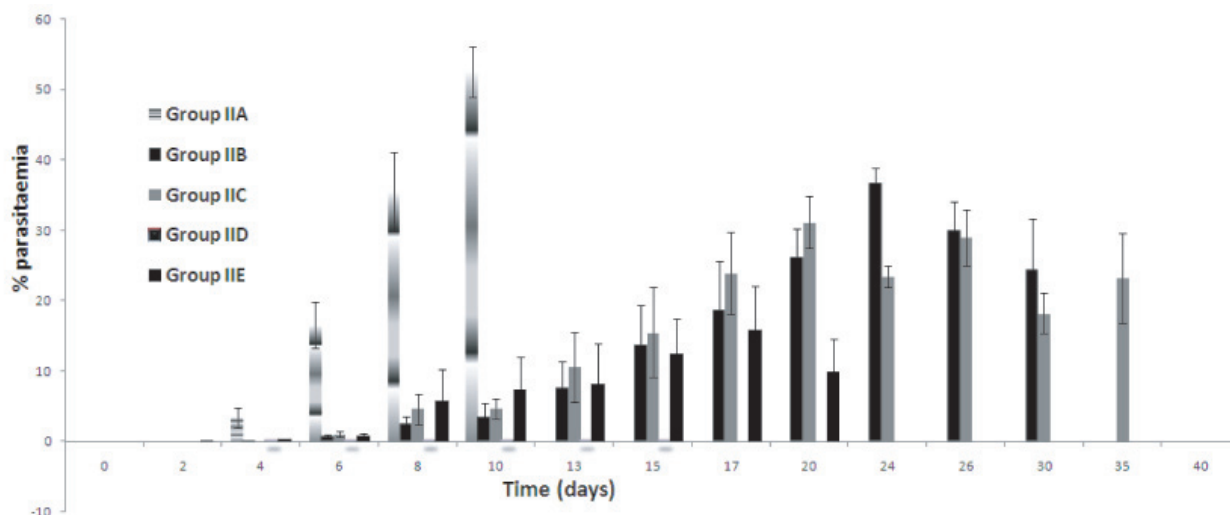


Figure 10. Percent parasitaemia observed in *P. berghei* infected mice ($n = 6$).

in the dissolution rate of lyophilized complexes may be attributed to the amorphous state of the active material, together with the increase in wettability and the solubility of the drug. Thus, the lyophilized complex with the highest dissolution rate is the most suitable product for animal studies.

3.9. In vivo studies

To monitor the protective efficacy of artemether and its inclusion complexes with β -CD complexes against *P. berghei* infection, dose standardization was carried out (Table 1). It was observed that artemether (Group IB) is insufficient to prevent mortality. However, survival time was increased (days 12-16) compared to control (day 8). Animals of Group IC, Group ID, and Group IE

were treated with different dose therapies as given in experiment section and were again unable to eradicate the percent parasitaemia. Therefore, the dose was increased to 8 mg/kg and was started on day 2 PI. It was also found to be ineffective in preventing mortality. Then a dose of 8 mg/kg was given after 8 h of PI and treatment was continued up to 7 days. This treatment schedule was effective to eradicate the parasitaemia completely in 63% of animals. To achieve 100% survivality, the dose was again increased to 10 mg/kg and was continued for 7 days. Out of the entire tested doses the 5 mg/kg dose schedule was selected for the complexes to compare and differentiate them on the basis of their protective efficacy and potency compared to artemether.

The results are given in Table 2. It was observed that percent mortality rate with artemether alone, β -CD

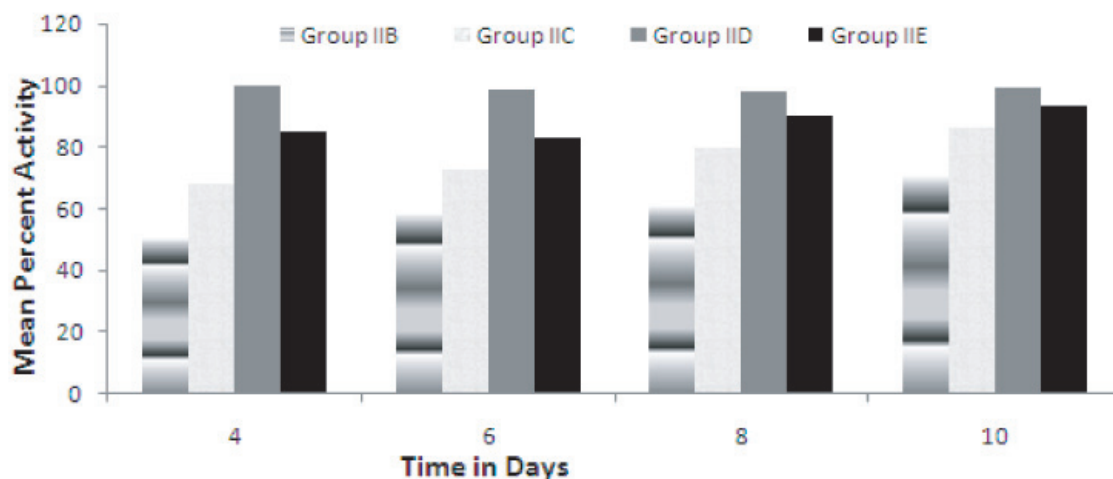


Figure 11. Antimalarial activity of lyophilized complexes of artemether in *P. berghei* infected mice ($n = 6$) as compared to control.

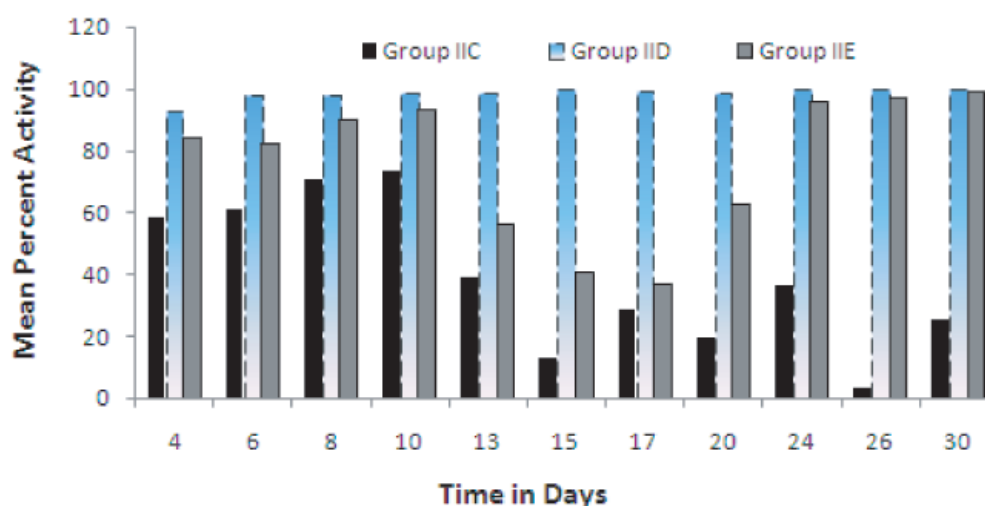


Figure 12. Antimalarial activity of lyophilized complexes of artemether in *P. berghei* infected mice ($n = 6$) as compared to drug.

complex, and HP- β -CD complex activity on day 1 PI were 33%, 50%, and 83.3%, respectively. However, M- β -CD (Group IIB) complexes resulted in complete clearance of the parasite from peripheral blood. Thus, the M- β -CD complex has shown a 3-fold increase in antimalarial activity compared to drug alone and the ANOVA have also shown a significant ($p < 0.05$) antimalarial activity for all the complexes compared to artemether (Figures 10-12).

4. Conclusions

In the present research work the results obtained from NMR, mass spectrometry and solution calorimetry showed a 1:1 complex of artemether with β -CD, M- β -CD, and HP- β -CD. The stability constant obtained from solution calorimetry suggested a stronger complex with M- β -CD. *In vivo* studies have shown a 3-fold increase in antimalarial activity of the lyophilized M- β -CD complex leading to the conclusion of successful

development of encapsulated artemether.

Acknowledgements

The financial assistance provided by Indian Council of Medical research, New Delhi, India and the calorimeter procured under DST, New Delhi, India are gratefully acknowledged.

References

1. Balint GA. Artemisinin and its derivatives an important new class of antimalarial agents. *Pharmacol Ther.* 2001; 90:261-265.
2. Joshi M, Pathak S, Sharma S, Patravale V. Design and *in vivo* pharmacodynamic evaluation of nanostructured lipid carriers for parenteral delivery of artemether: Nanoject. *Int J Pharm.* 2008; 364:119-126.
3. Hartell MG, Hicks R, Bhattacharjee AK, Koser BW, Carvalho K, Van Hamont JE. Nuclear magnetic resonance and molecular modeling analysis of the

- interaction of the antimalarial drugs artemisinic acid and artesunic acid with β -cyclodextrin. *J Pharm Sci.* 2004; 93:2076-2088.
- de Araújo MV, Vieira EK, Lázaro GS, de Souza Conegero L, Ferreira OP, Almeida LS, Barreto LS, da Costa NB Jr, Gimenez IF. Inclusion complexes of pyrimethamine in 2-hydroxypropyl- β -cyclodextrin: characterization, phase solubility and molecular modeling. *Bioorg Med Chem.* 2007; 15:5752-5759.
 - Jacqueline PV, Margriet G. Inclusion complexes of artemisinin or derivatives with cyclodextrins. Patent No. WO/2004075921. April, 2004.
 - Yang B, Lin J, Chen Y, Liu Y. Artemether/hydroxypropyl- β -cyclodextrin host-guest system: characterisation, phase solubility and inclusion mode. *Bioorg Med Chem.* 2009; 17:6311-6317.
 - Figueiras A, Ribeiro L, Torres-Labandeira JJ, Veiga Francisco JB. Evaluation of host-guest complex formation between a benzimidazolic derivative and cyclodextrins by UV-VIS spectrophotometry and differential scanning calorimetry. *J Incl Phenom Macrocycl Chem.* 2007; 57:531-535.
 - Ventura CA, Giannone I, Musumeci T, Pignatello R, Ragni L, Landolfi C, Milanese C, Paolino D, Puglisi G. Physico-chemical characterization of disoxaril-imethyl- β -cyclodextrin inclusion complex and *in vitro* permeation studies. *Eur J Med Chem.* 2006; 41:233-240.
 - Crupi V, Ficarra R, Guardo M, Majolino D, Stancanelli R, Venuti V. UV-VIS and FTIR-ATR spectroscopic techniques to study the inclusion complexes of genistein with beta-cyclodextrins. *J Pharm Biomed Anal.* 2007; 44:110-117.
 - Figueiras A, Carvalho RA, Ribeiro L, Torres-Labandeira JJ, Veiga Francisco JB. Solid-state characterization and dissolution characteristics on the inclusion complex of omeprazole with native and chemically modified β -cyclodextrin. *Eur J Pharm Biopharm.* 2007; 67:531-539.
 - Figueiras A, Ribeiro L, Vieira MT, Veiga Francisco JB. Preparation and physicochemical characterization of omeprazole: methyl-beta-cyclodextrin inclusion complex in solid state. *J Incl Phenom Macrocycl Chem.* 2007; 57:173-177.
 - Sinha VR, Anitha R, Ghosh S, Nanda A, Kumria R. Complexation of celecoxib with β -cyclodextrin: characterization of the interaction in solution and in solid state. *J Pharm Sci.* 2005; 94:676-687.
 - Chao JB, Tong HB, Liu DS, Huang SP. Preparation and characterization of inclusion complexes of pefloxacin mesylate with three kinds of cyclodextrins. *Spectrochim Acta A Mol Biomol Spectrosc.* 2006; 64:166-170.
 - Perry CS, Charman SA, Pranker RJ, Chiu FC, Scanlon MJ, Chalmers D, Charman WN. The binding interaction of synthetic ozonide antimalarials with natural and modified β -cyclodextrins. *J Pharm Sci.* 2006; 95:146-158.
 - Torri G, Bertini S, Giavana T, Guerrini N, Puppini T, Zoppetti G. Inclusion complex characterization between progesterone and hydroxypropyl- β -cyclodextrin in aqueous solution by NMR study. *J Incl Phenom Macrocycl Chem.* 2007; 57:317-321.
 - Brun H, Paul M, Razzouq N, Binhas M, Gibaud S, Astier A. Cyclodextrin inclusion complexes of the central analgesic drug nefopam. *Drug Dev Ind Pharm.* 2006; 32:1123-1134.
 - Buchanan CM, Buchanan NL, Edgar KJ, Lambert JL, Posey-Dowty JD, Ramsey MG, Wempe MF. Solubilization and dissolution of tamoxifen-hydroxybutenyl cyclodextrin complexes. *J Pharm Sci.* 2006; 95:2246-2255.
 - Lahiani-Skiba M, Coquard A, Bounoure F, Verite P, Arnaud P, Skiba M. Mebendazole complexes with various cyclodextrins: preparation and physicochemical characterization. *J Incl Phenom Macrocycl Chem.* 2007; 57:197-201.
 - Rekharsky MV, Inoue Y. Complexation thermodynamics of cyclodextrins. *Chem Rev.* 1998; 98:1875-1917.
 - Royall PG, Gaisford S. Application of solution calorimetry in pharmaceutical and biopharmaceutical research. *Curr Pharm Biotech.* 2005; 6:215-222.
 - Higuchi T, Connors KA. Phase solubility techniques. *Adv Anal Chem Instr.* 1965; 4:117-212.
 - Chadha R, Kashid N, Jain DV. Characterization and quantification of amorphous content in some selected parenteral cephalosporins by calorimetric method. *J Therm Anal Calorim.* 2005; 81:277-284.
 - Chadha R, Kashid N, Jain DV. Microcalorimetric evaluation of the *in vitro* compatibility of amoxicillin/clavulanic acid and ampicillin/sulbatam with ciprofloxacin. *J Pharm Biomed Anal.* 2004; 36:295-307.
 - Kobetic R, Jursic BS, Bonnette S, Tsai SC, Salvatore SJ. Study of the lorazepam: cyclodextrin inclusion complexes using electrospray ionization mass spectrometry. *Tetrahedron Lett.* 2001; 42:6077-6082.
 - Cai Y, Tarr MA, Xu GX, Yalcin T, Cole RB. Studies of cyclodextrin inclusion complexes by electronic (UV-VIS absorption and emission) spectroscopy. *J Am Soc Mass Spectrom.* 2003; 14:449-459.
 - Djedaine F, Lin S, Perly B, Wouessidjewe D. Highfield nuclear magnetic resonance techniques for the investigation of a beta-cyclodextrin:indomethacin inclusion complex. *J Pharma Sci.* 1990; 79:643-646.
 - Loukas Y, Vraka V, Gregoriadis G. Use of a nonlinear least-squares model for the kinetic determination of the stability constant of cyclodextrin inclusion complexes. *Int J Pharm.* 1996; 144:225-231.
 - Ganza-Gonzalez A, Vila-Jato JL, Anguiano-Igea S, Otero-Espinar FJ, Blanco-Mendez J. A proton nuclear magnetic resonance of the inclusion complex of naproxen with beta-cyclodextrin. *Int J Pharm.* 1994; 106:179-185.
 - Zornoza A, Martin C, Sanchez M, Velaz I, Piquer A. Inclusion complexation of glisentide with α -, β - and γ -cyclodextrins. *Int J Pharm.* 1998; 169:239-244.
 - Yuen KH, Chan KL, Gan EK, Wong JW, Tuck TW, San Ho DS. Formulation of artemisinin. Patent No. US 2002/0147177 A1. Oct, 2002.
 - Illapakurthy AC, Sabins YA, Avery BA, Avery MA, Wyandt CM. Interaction of Artemisinin and its related compounds with hydroxypropyl- β -cyclodextrin in solution state: experimental and molecular-modeling studies. *J Pharm Sci.* 2003; 92:649-655.
 - Job P. Recherches sur la formation de complexes minéraux en solution et sur leur stabilité. *Ann Chem.* 1928; 9:113-203.

(Received January 4, 2010; Revised March 3, 2010; Accepted March 12, 2010)

Original Article

Isolation and structure elucidation of antioxidant compounds from leaves of *Laurus nobilis* and *Emex spinosus*

Ahmed M. Emam¹, Mamdouh A. Mohamed¹, Yasser M. Diab^{1,*}, Nadia Y. Megally²

¹ Biochemistry Department, Faculty of Agriculture, Fayoum University, Egypt;

² Chemistry and Physics Department, Faculty of Education, Alexandria University, Egypt.

ABSTRACT: In recent years, there has been increasing interest in finding naturally occurring antioxidants from plants for use in food and medicinal materials to replace synthetic antioxidants since such antioxidants are being restricted due to their side effects like carcinogenicity. The aim of this work was to examine the *in vitro* antioxidant activity of *Laurus nobilis* and *Emex spinosus* leaves and to isolate and structurally elucidate the active compounds in those leaves. The aqueous ethanolic extracts (70%) of *Laurus nobilis* and *Emex spinosus* leaves exhibited free radical scavenging action against 1,1-diphenyl-2-picrylhydrazyl (DPPH). Their concentrations of 50% inhibition (IC₅₀) were 25.3 and 20.73 µg/mL, respectively. Activity-guided separation of these extracts using a combination of different chromatographic methods (TLC and column chromatography) resulted in the isolation of five chromatographically pure compounds (three from *Laurus nobilis* and two from *Emex spinosus* leaves). Spectroscopic methods (¹H, ¹³C-NMR, UV and MS) and chemical methods (detection tests and acidic hydrolysis) revealed the isolated antioxidant compounds to be flavonoid substances that were identified as kaempferol, kaempferol-3-rhamnopyranoside, and kaempferol-3,7-dirhamnopyranoside from *Laurus nobilis* extract and luteolin and rutin from *Emex spinosus* extract. The five flavonoids had varying ability to inhibit DPPH radicals (IC₅₀ from 4 to 35.8 µg/mL). Luteolin and rutin had strong scavenging action with an IC₅₀ of 4 and 4.6 µg/mL, respectively, and this action was stronger than that of synthetic antioxidant BHA, *i.e.*, butylated hydroxyanisole (IC₅₀ = 5.6 µg/mL).

Keywords: Plant antioxidants, flavonoids, *Laurus nobilis*, *Emex spinosus*, DPPH

*Address correspondence to:

Dr. Yasser Mohamed Diab, Biochemistry Department, Faculty of Agriculture, Fayoum University, Fayoum 63514, Egypt.
e-mail: ydiab@hotmail.com

1. Introduction

Free radical reactions occur in the human body and food systems. Reactive oxygen/nitrogen species (ROS and RNS) are produced as a part of normal metabolic processes. The imbalance between production of these species and the capacity of normal detoxification systems in favor of the oxidant leads to oxidative stress, which causes cell damage as a result of the interaction of reactive species with cellular constituents. This then leads to the development of various acute and chronic human diseases such as cancer, cataracts, and heart disease (1). Since antioxidants block the oxidation process that produces free radicals, they may be used as a way to prevent chronic diseases and health problems.

In addition to the adverse health effects of reactive species, the oxidative deterioration of components in foods is responsible for rancid odors and flavors. These odors and flavors decrease the organoleptic and nutritional quality of processed foods. The addition of synthetic antioxidants such as butylated hydroxyanisole (BHA) occurs widely in the food industry. However, the use of these synthetic antioxidants has been questioned due to their potential risks and toxicity (2).

Many antioxidant compounds that naturally occur from plant sources have been identified as free radical or active oxygen scavengers (3).

Recently, interest has increased considerably in finding natural antioxidants from plant material for use in food or medicinal materials to replace synthetic antioxidants. In addition, natural antioxidants have the capacity to improve food quality and stability and can also act as nutraceuticals to terminate free radical chain reactions in biological systems and thus may provide additional health benefits to consumers (4).

Laurus nobilis is an evergreen tree. It grows spontaneously in scrubland and woods in Europe and around the Mediterranean. It is also popular as an ornamental tree in gardens. It has long been used to flavor food. It has medicinal uses as a stimulant of gastric secretion, a diaphoretic, and is used to treat rheumatic complaints (5).

Emex spinosus is a common wild herbaceous plant known as dirs el-agooz in Egypt, where its leaves

are used in traditional medicine to relieve stomach disorders and to stimulate appetite (6).

The aim of this work was to examine the antioxidant activity of *Laurus nobilis* and *Emex spinosus* leaves and to also isolate and structurally identify the active constituent(s) responsible for this activity.

2. Materials and Methods

2.1. Plant materials

Leaves of *Emex spinosus* (Polygonaceae) and *Laurus nobilis* (Lauraceae) were collected at the flowering stage in April 2008 from the Experimental Farm of the Faculty of Agriculture, Fayoum University and El Shorouk Farm, located on the Cairo-Alexandria Desert Road 72 km north of Cairo, respectively. Species were authenticated by the Botany Department, Faculty of Science, Cairo University. Vouchered specimens of both plants (ES₁₀, LN₁₂, respectively) were deposited in the herbarium of the Biochemistry Department, Faculty of Agriculture, Fayoum University.

2.2. Extraction of bioactive constituent(s)

Ground, air-dried leaves of *Laurus nobilis* and *Emex spinosus* (350 g each) were extracted three times with 700 mL each of EtOH/H₂O (7:3, v/v) at room temperature (28 ± 2°C). After filtration, the combined extracts were evaporated under reduced pressure to yield 37.5 g and 42.3 g, respectively. The residue of aqueous ethanolic extract of each plant (35 g and 40 g, respectively) was suspended in water (150 mL) and extracted with CHCl₃ (3 × 100 mL) to yield CHCl₃ soluble components (Fraction A). The aqueous layer was freeze-dried and then extracted with EtOAc (3 × 150 mL) to yield EtOAc soluble components (Fraction B) and aqueous soluble components (Fraction C). The three fractions of chloroform, ethyl acetate, and water were concentrated to yield 8.8 g (Fraction A), 7.2 g (Fraction B), and 18.4 g (Fraction C) from *Laurus nobilis* extract and 10.2 g (Fraction A), 8.1 g (Fraction B), and 21.1 g (Fraction C) from *Emex spinosus* extract. These fractions were tested for their free radical scavenging activity.

2.3. Antioxidant activity

The antioxidant activity of the aqueous ethanolic extracts, fractions, BHA, and isolated compounds was assessed by measuring free-radical scavenging activity via the decoloration of a methanol solution of the free radical 1,1-diphenyl-2-picrylhydrazyl (DPPH) as described elsewhere (7) as follows: two mL of methanol solution of each test material at various concentrations (2-50 µg/mL) were added to a 2 mL solution of DPPH (25 mg/L) in methanol, and the reaction mixture was

shaken vigorously.

After incubation at room temperature for 30 min, the absorbance (A) of DPPH was determined with a spectrophotometer at 517 nm, and the radical scavenging activity of each sample was expressed as percentage inhibition:

$$\% \text{ inhibition} = [(A_{\text{control}} - A_{\text{sample}}) / A_{\text{control}}] \times 100$$

IC₅₀ (sample concentration required for 50% inhibition) was obtained by linear regression analysis of the dose response curve, plotted as the % inhibition and concentration (µg/mL). Butylated hydroxyanisole (BHA), which is a well-known antioxidant, was used as a positive control. The mean values were obtained from triplicate analysis.

2.4. Isolation of antioxidant compound(s)

Isolation of antioxidant compounds was done as follows using the most abundant active fraction B (EtOAc fraction) from each plant.

First, *Laurus nobilis* 7.0 g was subjected to column chromatography (CC) over Sephadex LH-20 (40 g) and eluted with methanol to yield 40 fractions of 10 mL each. Based on the differences in composition indicated by thin-layer chromatography (TLC) (CH₃Cl/CH₃OH/H₂O, 75:25:2, v/v), six fractions designated I, II, III, IV, V, and VI were obtained and then tested for free radical scavenging activity. The active fraction VI (928 mg) was chromatographed over a silica gel column (20 g; 230-400 mesh, Merck) and eluted with 100 mL of the following solvent mixtures of CH₃Cl/CH₃OH/H₂O (90:10:0, v/v; 80:20:2, v/v; and 75:25:2, v/v) for each eluent. In accordance with the differences in composition revealed by TLC, five fractions designated VIa, VIb, VIc, VI d, and VIe were obtained. The fractions VIa (180 mg) eluted with CH₃Cl/CH₃OH/H₂O (90:10:0, v/v, between 0-50 mL), VI d (245 mg) eluted with CH₃Cl/CH₃OH/H₂O (80:20:2, v/v, between 60-100 mL), and VIe (228 mg) eluted with CH₃Cl/CH₃OH/H₂O (75:25:2, v/v, between 0-100 mL) that contained the major compounds were further purified by preparative TLC using CH₃Cl/CH₃OH/H₂O (90:10:0, v/v; 80:20:2, v/v; and 75:25:2, v/v, respectively) to yield the pure compounds A (126 mg), B (190 mg), and C (132 mg), respectively.

Second, *Emex spinosus* 8.0 g was chromatographed over a silica gel column (200 g; 230-400 mesh, Merck) and eluted with the solvent mixtures of CH₃Cl/CH₃OH/H₂O (70:30:1, v/v, and 50:50:2, v/v; 650 mL each eluent). Thirty-two fractions of each eluent were collected. The eluates were combined on the basis of similarity of TLC profiles to yield 8 fractions designated 1 to 8 and then tested for free radical scavenging activity. The active fractions 2 (1.38 g; eluted with 70:30:1, v/v, between 80-340 mL) and 5 (1.57 g; eluted with 50:50:2,

v/v, between 70-160 mL) were further purified several times over Sephadex LH-20 and silica gel columns as shown in Figure 1 to yield two active compounds, D (283 mg) and E (312 mg).

2.5. Analytical and preparative TLC

Analytical and preparative TLC were carried out on Merck precoated silica gel plates (F₂₅₄ thickness: 0.25 mm and 2.0 mm, respectively) using the following solvent systems: 1) *n*-butanol-acetic acid-water (4:1:5, v/v, upper layer), 2) ethyl acetate-acetic acid-formic acid-water (100:11:11:27, v/v), 3) dichloromethane-methanol-water (50:25:5, v/v), 4) chloroform-acetone (50:6, v/v), 5) chloroform-methanol (90:10, v/v, and 80:20, v/v), and 6) chloroform-methanol-water (80:20:2, v/v; 75:25:2, v/v; 70:30:1, v/v; 50:50:2, v/v; and 70:30:5, v/v).

Spots on TLC were detected under UV light (254 and 365 nm) and by spraying with concentrated H₂SO₄ followed by heating at 105°C for 5 min and or by 5% AlCl₃. Sugars were detected by spraying with naphthoresorcinol-phosphoric acid followed by heating at 105°C for 10 min.

2.6. Structure identification of antioxidant compounds

Antioxidant compounds were characterized by chemical investigation (detection tests and acid hydrolysis) and spectroscopic methods.

2.6.1. Detection tests

Isolated compounds were detected according to methods described elsewhere (8).

2.6.2. Acid hydrolysis

Acid hydrolysis was performed in a sealed tube at 100°C for 4 h with 2 mg of the isolated compound in 2 mL of 10% HCl. The aglycon moiety was extracted with Et₂O and analyzed by TLC with system 4. The aqueous layer was neutralized with *N,N*-dioctylamine (10% in CHCl₃). After evaporation to dryness, the sugars were identified by TLC with system 3 by comparison with authentic samples.

2.6.3. Spectroscopic methods

Nuclear magnetic resonance (MMR) spectroscopy – ¹H and ¹³C-NMR spectra of the isolated compounds were recorded in CD₃OD on a Varian Mercury VXR-300 spectrometer at the Central Laboratory, Faculty of Science, Cairo University, Egypt. Chemical shifts (ppm) were related to that of the solvent.

Mass spectrometry (MS) – Mass spectra were recorded on a GC-MS QP1000 EX Shimadzu mass spectrometer at the Micro Analytical Laboratory, Faculty of Science, Cairo University, Egypt.

Ultra violet spectrometry (UV) – UV spectra were recorded on a Cecil Series 3000 spectrophotometer in accordance with the method of Mabry *et al.* (13).

3. Results and Discussion

The antioxidant activity of the aqueous ethanolic extracts (70%) and isolated compounds of *Laurus nobilis* and *Emex spinosus* leaves is shown in Table 1. The aqueous ethanolic extract of both types of leaves exhibited free radical scavenging action against

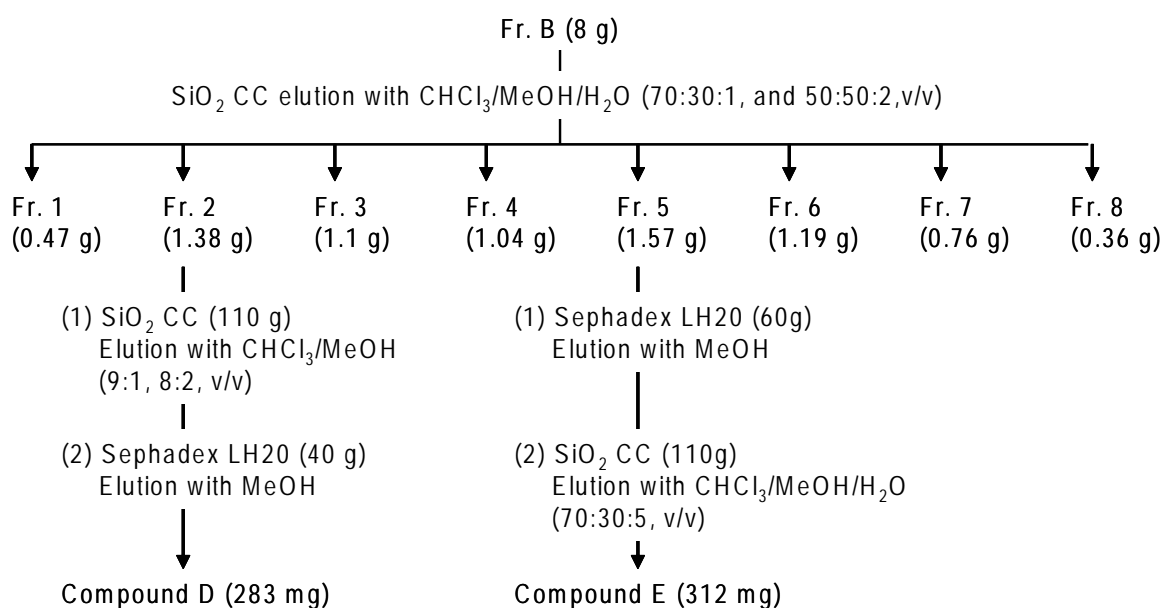


Figure 1. Flow diagram for the isolation of antioxidant compounds D and E from *Emex spinosus*.

1,1-diphenyl-2-picrylhydrazyl (DPPH). As is evident, EtOH extract of *Emex spinosus* was more potent as an antioxidant than EtOH extract of *Laurus nobilis* since its IC₅₀ value was lower than those of the *Laurus* extract (IC₅₀ = 20.73 and 25.30 µg/mL, respectively). IC₅₀ was defined as the concentration of the antioxidant needed to scavenge 50% of DPPH present in the test solution. A lower IC₅₀ value reflects better DPPH radical scavenging activity (9). The variation in the antioxidant effect of the two active extracts may be due to the differences in their secondary constituents (10-12).

Activity-guided separation of these extracts as described previously resulted in the isolation of five chromatographically pure compounds designated A, B, and C from *Laurus nobilis* and D and E from *Emex spinosus* extracts. The results in Table 1 indicate that the five compounds A, B, C, D, and E had varying IC₅₀ values ranging from 4 (compound D) to 35.8 µg/mL (compound C). Among the three isolated free radical scavengers from *Laurus nobilis* extract, i.e., A, B, and C, compound A was the most potent (IC₅₀ = 7.7 µg/mL). However, the lowest effective compound was C (IC₅₀ = 35.8 µg/mL). This variation in potency is probably due to structural differences.

In contrast, compounds D and E isolated from *Emex*

spinosus extract had the highest level of scavenging action with an IC₅₀ of 4 and 4.6 µg/mL, respectively. Thus, the isolated compounds from each plant were in part responsible for the antioxidant activity of the aqueous ethanolic extracts of *Laurus nobilis* and *Emex spinosus*. The results in Table 1 also show that compounds D and E had stronger scavenging action than did the positive control BHA (butylated hydroxyanisole), which is known to be a very efficient synthetic antioxidant agent (IC₅₀ = 5.6 µg/mL).

The structures of the five active isolated compounds (A to E, Figure 2) were identified as kaempferol (A), kaempferol-3-*O*-α-L-rhamnoside (B), kaempferol-3,7-di-*O*-α-L-rhamnoside (C), luteolin (D), and rutin (E) from the results obtained from chemical and spectroscopic methods as well as by comparing the spectroscopic data (Table 2) with data in the literature (13-17).

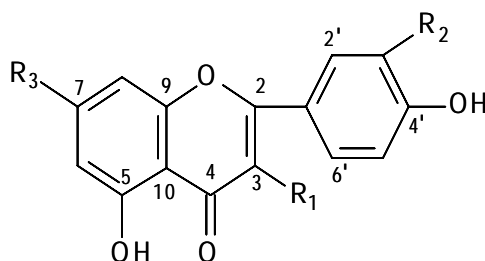
The differences in structure for the five isolated compounds explain the variation in the antioxidant effect of these compounds. The structure-activity relationship revealed that a free OH group at C-3 (like kaempferol) and 2 hydroxyl groups *ortho* to each other on ring B (like luteolin and rutin) enhanced antioxidant activity whereas *O*-glycosylation at C-3 and C-7 (like kaempferol glycosides B and C) decreased such activity. This relationship has previously been reported (18,19).

The present results revealed that the five isolated antioxidant compounds are flavonoids or rather are the most common and abundant classes of flavonoids, i.e., flavones (luteolin, D), flavonols (kaempferol, A), and flavonol glycosides (kaempferol-3-rhamnopyranoside, kaempferol-3,7-dirhamnopyranoside and rutin B, C, and E, respectively). These classes of flavonoids seem to be the most potent at protecting the human body against reactive oxygen species (20). Body cells and tissues are continuously threatened by the damage caused by free radical and reactive oxygen

Table 1. Antioxidant activity of aqueous ethanolic extracts (70%) and isolated compounds (A to E) from the leaves of *Laurus nobilis* and *Emex spinosus* on DPPH free radical

Test materials	IC ₅₀ (µg/mL) ^a
Aqueous EtOH extract of <i>Laurus nobilis</i>	25.30
Aqueous EtOH extract of <i>Emex spinosa</i>	20.73
Compound A	7.70
Compound B	20.87
Compound C	35.80
Compound D	4.00
Compound E	4.60
Butylated hydroxyanisole (BHA)	5.60

^a: Amount required for 50% reduction of DPPH free radicals after 30 min.



Compounds	R ₁	R ₂	R ₃	[M] ⁺	MF	UVλ(nm)/MeOH
A	OH	H	OH	286	C ₁₅ H ₁₀ O ₆	265, 365
B	<i>O</i> -rhamnosyl	H	OH	432	C ₂₁ H ₂₀ O ₁₀	265, 350
C	<i>O</i> -rhamnosyl	H	<i>O</i> -rhamnosyl	578	C ₂₇ H ₃₀ O ₁₄	265, 350
D	H	OH	OH	286	C ₁₅ H ₁₀ O ₆	250, 350
E	<i>O</i> -rutinosyl	OH	OH	610	C ₂₇ H ₃₀ O ₁₆	265, 360

Figure 2. Structural formula of the isolated compounds.

Table 2. ^1H , ^{13}C -NMR chemical shifts (ppm) of the five isolated compounds in CD_3OD

Atom	A		B		C		D		E	
	δC	δH								
Aglycon										
2	156.2	–	161.3	–	161.6	–	166.1	–	158.4	–
3	130.9	–	133.8	–	134.1	–	103.2	6.5 s	135.6	–
4	178.8	–	179.1	–	178.9	–	183.8	–	179.3	–
5	162.1	–	162.9	–	162.6	–	163.2	–	162.8	–
6	100.1	6.14 d $J=2.1$	100.7	6.19 d $J=2.1$	101.8	6.31 d $J=2.1$	100.5	6.20 d $J=2.2$	99.9	6.19 d $J=2.1$
7	168.2	–	168.7	–	167.2	–	166.3	–	165.9	–
8	94.9	6.36 d $J=2.4$	95.4	6.35 d $J=2.1$	96.8	6.49 d $J=2.1$	95.00	6.41 d $J=1.9$	94.9	6.39 d $J=2.1$
9	158.4	–	158.7	–	158.5	–	160.1	–	159.3	–
10	105.6	–	105.4	–	105.7	–	105.1	–	105.6	–
1'	122.1	–	122.6	–	122.8	–	123.7	–	123.6	–
2'	130.9	7.7 d $J=8.7$	131.2	7.8 d $J=8.4$	131.6	7.6 d $J=8.4$	114.2	7.4 d $J=6.0$	116.2	7.9 d $J=2.1$
3'	115.4	6.7 d $J=8.4$	115.9	6.8 d $J=8.1$	116.0	6.8 d $J=8.2$	147.2	–	145.7	–
4'	161.6	–	161.7	–	161.5	–	151.2	–	149.7	–
5'	116.5	6.7 d $J=8.4$	116.8	6.8 d $J=8.1$	116.8	6.8 d $J=8.2$	120.32	6.9 d $J=8.1$	123.1	6.9 d $J=8.7$
6'	131.6	7.7 d $J=8.7$	131.9	7.8 d $J=8.4$	131.6	7.6 d $J=8.4$	117.2	7.4 d $J=6.0$	117.7	7.63 dd $J=2.1, 8.7$
Rha										
1	–	–	101.6	5.7 d $J=1.8$	101.4	5.3 d $J=1.5$	–	–	104.7	4.5 d $J=1.5$
2	–	–	69.8	3.3-3.6 m	70.1	3.2-3.7 m	–	–	72.0	3.3-3.7 m
3	–	–	71.9	3.3-3.6 m	71.4	3.2-3.7 m	–	–	72.2	3.3-3.7 m
4	–	–	72.8	3.3-3.6 m	72.7	3.2-3.7 m	–	–	73.9	3.3-3.7 m
5	–	–	68.5	3.3-3.6 m	68.9	3.2-3.7 m	–	–	69.6	3.3-3.7 m
6	–	–	17.5	0.9 d $J=6$	17.4	0.81 d $J=6.4$	–	–	17.8	1.1 d $J=6.2$
Glc or Rha										
1	–	–	–	–	102.1	5.2 d $J=1.4$	–	–	102.3	5.1 d $J=7.2$
2	–	–	–	–	70.3	3.2-3.7 m	–	–	75.6	3.3-3.7 m
3	–	–	–	–	71.8	3.2-3.7 m	–	–	78.1	3.3-3.7 m
4	–	–	–	–	72.6	3.2-3.7 m	–	–	71.3	3.3-3.7 m
5	–	–	–	–	69.1	3.2-3.7 m	–	–	77.1	3.3-3.7 m
6	–	–	–	–	17.7	0.87 d $J=6.1$	–	–	68.6	3.48, 3.83 d

Abbreviations: Glc, glucose; Rha, Rhamnose.

species (ROS) that are produced during normal oxygen metabolism or are induced by exogenous damage (21). Flavonoids cannot be produced by the human body and have thus to be taken in mainly through one's daily diet. They have been found in dietary components, included fruits, vegetables, olive oil, tea, and red wine (22). Several beneficial properties have been attributed to these dietary compounds, including anticarcinogenic, anti-inflammatory, and antiviral action (18). In addition, they inhibit lipid peroxidation, platelet aggregation, and the activity of enzyme systems like the lipoxigenase enzyme system. The flavonoids display these types of action as antioxidants, chelators of divalent cations, and free radical scavengers and thus may be involved in preventing free radical mediated cytotoxicity and lipid peroxidation, both of which are associated with cell aging and chronic diseases such as atherosclerosis (23,24). Their remarkable antioxidant properties are

due to three aspects. First is the hydrogen donating-substituents (hydroxyl groups) attached to the aromatic ring structures of flavonoids, allowing flavonoids to undergo a redox reaction that helps them to scavenge free radicals more easily. Second is a stable delocalization system consisting of aromatic and hetero cyclic rings as well as multiple unsaturated bonds that helps to delocalize the resulting free radicals. Third is the presence of certain structural groups that are capable of forming transition metal-chelating complexes that can regulate the production of ROS such as OH^\bullet and O_2^{-2} (25). Because flavonoids are widely distributed in edible plants and beverages and have previously been used in traditional medicine, they are likely to have minimal toxicity (26). Moreover, the leaves of *Laurus nobilis* have long been used to flavor food (5) while the leaves of *Emex spinosus* are used in traditional medicine to relieve stomach disorders and to stimulate appetite (6).

4. Conclusion

In this study, it was found that *Laurus nobilis* and *Emex spinosus* leaves were potential sources of antioxidant components that would help to increase the overall antioxidant capacity of an organism and protect it against lipid peroxidation induced by oxidative stress or used as food additive to delay the oxidative deterioration of foods.

The aqueous ethanolic of *Emex spinosus* showed higher activity than *Laurus nobilis* leaves and its strong antioxidant activity could be related to the activity of flavonoids compounds found in this extract. Further studies are needed to investigate the *in vivo* pharmacological and toxicological properties of *Emex spinosus* extract, since the high activity could be considered as a new antioxidant ingredient for the nutraceutical or functional food market.

References

- Halliwell B, Gutteridge JM, Cross CE. Free radical, antioxidants and human disease: where are we now? *J Lab Clin Med.* 1992; 119:598-619.
- Ito N, Fukushima S, Hagiwara A, Shibata M, Ogiso T. Carcinogenicity of butylated hydroxyanisole in F344 rats. *J Natl Cancer Inst.* 1983; 70:340-352.
- Zheng W, Wang SY. Antioxidant activity and phenolic compounds in selected herbs. *J Agric Food Chem.* 2001; 49:5165-5170.
- Kumaran A, Karuna J, Karan R. *In-vitro* antioxidant activities of methanol extracts of five *Phyllanthus* species from India. *Lebenson Wiss Technol.* 2007; 40:344-352.
- Bianchini F, Corbetta F, Laurel B. In: *Heath Plants of the World-Atlas of Medicinal Plant* (3rd ed.). John Wiley and Sons, New York, USA, 1979; p. 26.
- Abdel-Fattah H, Zaghoul AM, Mansour ES, Halim AF, Weght ES. Anthraquinones, sterols and steryl glycoside of *Emex spinosus*. *Egypt J Pharm Sci.* 1990; 31:93-98.
- Brand-Williams W, Cuvelier ME, Berset C. Use of free radical method to evaluate antioxidant activity. *Lebenson Wiss Technol.* 1995; 28:25-30.
- Farnsworth NR. Biological and phytochemical screening of plants. *J Pharm Sci.* 1966; 55:225-276.
- Molyneux P. The use of the stable free radical diphenylpicrylhydrazyl (DPPH) for estimating antioxidant activity. *Songklanakarin J Sci Technol.* 2004; 26:211-219.
- Osawa T, Katsuzaki H, Hagiwara Y, Hagiwara H, Shibamoto T. A novel antioxidant isolated from young green barley leaves. *J Agric Food Chem.* 1992; 40:1135-1138.
- Pizzale L, Bortomeazzi R, Vichi S, Uberegger E, Conte LS. Antioxidant of sage (*Salvia officinalis* and *Salvia fruticose*) and oregano (*Origanum onites* and *Origanum onites*) extracts related to their phenolic compound content. *J Sci Food Agric.* 2002; 82:1645-1651.
- Sudjaroen Y, Haubner R, Wartele G, Hull WE, Erben G, Spiegelhalder B, Changbumrung S, Bartsch H, Owen RW. Isolation and structure elucidation of phenolic antioxidants from Tamarind (*Tamarindus indica* L.) seeds and pericarp. *Food Chem Toxicol.* 2005; 43:1673-1682.
- Mabry TJ, Markham KR, Thomas MB. *The Systematic Identification of Flavonoids.* Springer Verlag, Berlin, Germany, 1970.
- Markham KR, Ternai B, Stanley R, Gelger H, Mabry TJ. Carbon-13 NMR studies of flavonoids-III naturally occurring flavonoid glycosides and their acylated derivatives. *Tetrahedron.* 1978; 34:1389-1397.
- Markham KR. Flavones, Flavonols and their glycosides. In: *Methods in Plant Biochemistry* (Harborne JB, ed.). Academic Press, New York, USA, 1989; pp. 197-232.
- Lin JH, Lin YT. Flavonoids from the leaves of *Loranthus kanoi*. *J Food & Drug Anal.* 1999; 7:185-190.
- Wawer I, Zielinska A. ¹³C CP/MAS NMR studies of flavonoids. *Magn Reson Chem.* 2001; 39:374-380.
- Pathak D, Pathak K, Singla AK. Flavonoids as medicinal agents – recent advances. *Fitotrapia.* 1991; 5:371-389.
- Rice-Evans C, Miller N, Paganga G. Structure-antioxidant activity relationships of flavonoids and phenolic acid. *Free Rad Biol Med.* 1996; 20:933-956.
- Nijveldt RJ, van Nood E, van Hoorn DE, Boelens PG, van Norren K, van Leeuwen PA. Flavonoids: a review of probable mechanisms of action and potential applications. *Am J Clin Nutr.* 2001; 74: 418-425.
- de Groot H. Reactive oxygen species in tissue injury. *Hepatology.* 1994; 41:328-332.
- Harborn JB. *The Flavonoids Advance in Research since 1986.* Chapman and Hall, London, UK, 1999.
- Mora A, Paya M, Rios JL, Alcaraz MJ. Structure activity relationships of polymethoxyflavones and other flavonoids as inhibitors of non-enzymic lipid peroxidation. *Biochem Pharmacol.* 1990; 40:793-797.
- Dastmalchi K, Damien Dorman HJ, Kosar M, Hiltunen R. Chemical composition and *in-vitro* antioxidant evaluation of water-soluble Moldavian balm (*Dracocephalum moldavica* L.) extract. *Lebenson Wiss Technol.* 2007; 40:239-248.
- Pietta PG. Flavonoids as antioxidants. *J Nat Prod.* 2000; 63:1035-1042.
- Cushnie TP, Lamb AJ. Antimicrobial activity of flavonoids. *Int J Antimicrob Agents.* 2005; 26:343-356.

(Received March 13, 2010; Revised April 14, 2010; Accepted April 18, 2010)

Original Article

Optimization and characterization of diclofenac sodium microspheres prepared by a modified coacervation method

Eman S. El-Leithy*, Dalia S. Shaker, Mohamed K. Ghorab, Rania S. Abdel-Rashid

Pharmaceutics Department, College of Pharmacy, Helwan University, Cairo, Egypt.

ABSTRACT: A modified coacervation method for preparing diclofenac sodium loaded chitosan (DFS-C) microspheres, using sodium citrate as cross-linking agent was optimized. A full 2^3 factorial design was used to evaluate the effect of chitosan (CS) concentration, cross-linking agent concentration, and cross-linking time on the properties of the prepared microspheres. The modified coacervation method resulted in higher yield of spherical microspheres even with a lower concentration of CS (0.3%, w/v). The morphology of the microspheres was found to be dependent on the formulation and process parameters. The cross-linking agent concentration had the largest impact on swelling, mucoadhesion, and drug release. Kinetic analysis of the release data revealed a quasi-Fickian diffusion mechanism.

Keywords: Diclofenac sodium, chitosan microspheres, modified coacervation, factorial design

1. Introduction

Diclofenac sodium (DFS) is an inhibitor to prostaglandin synthetase. It is used to relieve pain and inflammation in conditions such as rheumatoid arthritis, osteoarthritis, ankylosing spondylitis, and acute gout. Diclofenac sodium is rapidly absorbed from the gastrointestinal tract with the plasma peak level reached in 1-2 h (1). It has a very short plasma half-life and circulates in a bound-to-free equilibrium with plasma proteins. It is hydroxylated in the liver and undergoes enterohepatic recirculation (2). The most common side effects in long term therapy involve gastrointestinal side effects including gastritis, peptic ulcers, and bleeding (3). Although several approaches, such as enteric-coating and sustained release have been studied, none of them

have yet solved the drug problems completely (4-7).

Carrier technology has offered an intelligent approach to modulate the release and absorption characteristics of drugs by coupling them to polymeric carriers (such as microspheres, nanoparticles, and liposomes). In general, microspheres have the potential to be used to target and control release of drugs. However, coupling a bioadhesive polymer like chitosan (CS) to microspheres provides an additional advantage of efficient drug absorption and bioavailability due to a high surface to volume ratio and a much more intimate contact with mucus (8-10).

Chitosan microspheres were used to improve the bioavailability of degradable substances such as protein, as well as to enhance the uptake of hydrophilic substances across epithelial membranes (11). Various methods of microsphere preparations were reported including ionotropic gelation (12), complex-coacervation (13), modified emulsification (14), spray drying (15), and precipitation by either salting out (16) or chemical cross-linking (17).

The present study aimed to optimize a modified coacervation method for the preparation of diclofenac sodium loaded chitosan (DFS-C) microspheres, using sodium citrate as cross-linking agent with no need for a complex apparatus and/or special precautions. A 2^3 full factorial design was used to predict an optimum formula for the microspheres that would prolong drug release and minimize its side effects.

2. Materials and Methods

2.1. Chemicals

Diclofenac sodium was kindly donated from Novartis Pharmaceutical Co., Cairo, Egypt. Chitosan with 85% degree of deacetylation was obtained from Sigma Chemical Co., St. Louis, MO, USA. Analytical grades of acetic acid (96%) and sodium citrate were obtained from El-Nasr Pharmaceutical Chemical Co., Cairo, Egypt.

2.2. Preparation of chitosan microspheres

Diclofenac sodium loaded CS microspheres were

*Address correspondence to:

Dr. Eman Saddar El Leithy, Helwan University, Pharmaceutics Department, College of Pharmacy, Pharmacy Building, Ain Helwan, Cairo, Egypt.
e-mail: eman_sad@hotmail.com

prepared by a modified method of the coacervation process previously described by Berthold *et al.* (16). A new spraying technique was adopted based on spraying a solution of the drug and cross-linking agent over the polymeric solution. This method was found to overcome the difficulties encountered in preparation of microspheres by the capillary extrusion method. The technique developed allowed the use of DFS in its soluble form instead of its dispersion in an acidic solution of CS. It also permitted the use of high concentrations of the polymer solution without the possibility of plugging the spray nozzle with the viscous polymer solution.

Diclofenac sodium (1%, w/v) was added to 20 mL of aqueous solutions of 5, 7.5, or 10% (w/v) sodium citrate. After the drug was thoroughly dissolved, the solution was sprayed into a magnetically stirred CS solution (0.3, 0.4, or 0.5%, w/v) in 20 mL acetic acid (2%, v/v) using an atomizer with 0.7 mm inner diameter. The microspheres were collected by filtration and washed thoroughly with distilled water, then allowed to dry at 40°C.

2.3. Factorial design and statistical analysis

An experimental design (2³ full factorial design with one central point) was used to evaluate the effect of formulation variables on the physicochemical properties of the DFS-C microspheres (Table 1). Statistical analysis of the experimental data was performed by an ANOVA test using JMP software version 4.0.4 (SAS Institute, Cary, NC, USA).

2.4. Particle size and morphological characterization

The mean particle size (MPS) of microspheres was determined using a particle size analyzer (Microvision image analysis system APSI stage micrometer scale, London). The analysis was performed using samples of microspheres uniformly dispersed in purified water. The surface morphology was examined using scanning electron microscopy (SEM). The microspheres were vacuum dried, coated with gold palladium and examined microscopically (JEOL, JXA 840A electron probe microanalyzer, Japan).

2.5. Percent yield, drug loading and encapsulation efficiency

The percentage yield of the microspheres was determined with respect to the drug and polymer weight. Total drug content was determined according to the method described by Acikgoz *et al.* (18). Ten milligrams of DFS-C microspheres were dispersed in 10 mL hydrochloric acid solution (1%, v/v) and magnetically stirred for 2 h. This mixture was allowed to stand at 50°C to allow for polymer dissolution

Table 1. The independent formulation variables of a 2³ full factorial design with one central point*

Independent variables	Levels	
Sodium citrate concentration (% w/v)	5	10
Cross-linking time (h)	1	3
Chitosan concentration (% w/v)	0.3	0.5

* Central points of the variables were 7.5% (w/v), 2 h, and 0.4% (w/v) for the sodium citrate, cross-linking time and chitosan concentration, respectively.

and complete drug dispersion. The mixture was then centrifuged and the supernatant was decanted. The residue was dried, dissolved in methanol and the absorbance was measured after appropriate dilution using a UV spectrophotometer (Lambda EZ 201, PerkinElmer, USA) at 276 nm. The drug encapsulation efficiency (%EE) of the microspheres was calculated as a percentage according to the following equation:

$$\%EE = \frac{\text{practical drug loading}}{\text{theoretical drug loading}} \times 100 \quad \text{---- Eq. 1}$$

Theoretical drug loading was based on the assumption that the entire drug present in the chitosan solution was entrapped in the microspheres and no loss occurred at any stage of preparation.

2.6. Swelling behavior

Water-absorbing capacity of the microspheres was determined by a gravimetric method (19). On a previously weighed stainless steel support one hundred milligrams of microspheres were accurately weighed (W_0) before soaking the support together with the microspheres in water at room temperature. At predetermined time intervals, the stainless steel support and the swelled microspheres were removed from the medium, blotted carefully with cleansing tissues and immediately weighed to determine the weight of swelled microspheres (W). Measurements were made in triplicate and the percent degree of swelling (%DS) was calculated as follows:

$$\%DS = \frac{(W_t - W_0)}{W_0} \times 100 \quad \text{---- Eq. 2}$$

where W_t and W_0 were the weights of the microspheres after soaking for time t and in the dry state, respectively.

2.7. In vitro mucoadhesive studies

The bioadhesive properties of the microspheres were determined according to the everted sac method (20). Non-fasting male rats 300-400 g were sacrificed and their intestinal tissue was excised and flushed with 10 mL of ice-cold phosphate buffered saline (pH 7.4) containing 200 mg/dL glucose (PBSG). Segments of the jejunum (6 cm) were everted using a stainless steel

rod and washed with PBSG to remove the contents. The segment sacs were filled with 1-1.5 mL of PBSG and ligatures were placed at both ends. 60 mg of microspheres were suspended in test tubes, each containing 5 mL saline and one intestinal segment. The sets were shaken at 37°C in a water bath shaker. After 30 min, the sacs were removed and the remaining microsphere dispersion was centrifuged for 20 min at 3,000 rpm. The supernatant fluid was discarded and the residual microspheres were allowed to dry in an incubator (FTC 90-E, Refrigerated incubator, made in Europe) at 40°C. The weight of bound microspheres was determined by subtraction of the weight of the dried residual microspheres from their initial weight and was recorded as percent mucoadhesion.

2.8. *In vitro* drug release studies

The release of DFS from microspheres was carried out using a USP type II dissolution apparatus (Hanson Research Dissolution tester, Chatsworth, LA, USA). A total volume of 100 mL phosphate buffer (pH 7.4) was kept at 37°C and rotated at 100 rpm. Twenty five mg of the microspheres containing a known amount of DFS were placed in an open-end glass tube with one side wrapped with a cellophane membrane (Spectrapor membrane tubing No. 2, Spectrum Medical Industries, Houston, TX, USA) and the other was attached to the shaft of the apparatus. At predetermined intervals, 1 mL of the dissolution medium was taken and replaced with an equal volume of fresh dissolution medium. The sample was diluted to 5 mL with phosphate buffer and analyzed for drug concentration using a UV spectrophotometer at 276 nm.

2.9. Kinetic analysis of the drug release data

To examine the kinetics and mechanism of drug release, the release data were fitted to models representing zero-order, first-order and Higuchi's square root of time. The correlation coefficients were determined from regression plots of m vs. t , $\log(m_0 - m)$ vs. t and m vs. $t^{1/2}$, for zero-order, first-order and Higuchi's model, respectively. In these plots, m presented the percent

of drug released at time t , and $m_0 - m$ was the percent of drug remaining after time t . To understand the mechanism of DFS diffusion from CS microspheres, the results were further analyzed according to the Korsmeyer-Peppas equation (Eq. 3):

$$m_t/m_\infty = k \cdot t^n \quad \text{---- Eq. 3}$$

where m_t/m_∞ was the fraction of the drug released after time t and n was a characteristic exponent for the release mechanism. Based on the Korsmeyer-Peppas equation, values of the n exponent equal to or less than 0.5 were characteristic of Fickian or quasi-Fickian diffusion, whereas values in the range of 0.5 to 1 were an indication of an anomalous mechanism for drug release. On the other hand, a unity value for n would be expected for zero-order release.

3. Results

3.1. Particle size and morphology

The MPS of all the microspheres batches ranged between 13-25 μm depending on the composition of each formula (Table 2). The results revealed that sodium citrate concentration was the major factor affecting the MPS of the microspheres whereas, increasing its concentration from 5 to 10% (w/v) resulted in a decrease in the MPS from about 24 μm to 14 μm . Changing the cross-linking time and/or the CS concentration had no effect on the microsphere MPS (22-25 μm).

Figures 1a and 1b represent the SEM photographs of the microspheres containing 1% (w/v) DFS, and 0.3% (w/v) chitosan that were cross-linked for 1 h with 5% and 10% (w/v) sodium citrate, respectively. The photographs revealed the formation of solid dense microspheres with CS solutions less than 1% (w/v). This result was contrary to the results of Shu and Zhu (21), who reported that 1% (w/v) CS solution was the minimum requirement to obtain microspheres.

Generally, the microspheres were not completely spherical in shape and had a rough surface. The microspheres prepared with 5% sodium citrate (Figure 1a)

Table 2. Properties of the DFS-C microspheres prepared according to 2³ full factorial design

Formula code	Sodium citrate concentration (% w/v)	Cross-linking time (h)	Chitosan concentration (% w/v)	Mean particle size (μm)	%Yield	%Encapsulation efficiency	%Degree of swelling	%Mucoadhesion
F1	5	1	0.3	23	93	90	133	51
F2	10	1	0.3	16	46	24	193	40
F3	5	3	0.3	25	96	100	110	50
F4	10	3	0.3	18	69	32	183	37
F5	5	1	0.5	24	100	91	119	50
F6	10	1	0.5	13	60	61	188	39
F7	10	3	0.5	14	76	66	183	50
F8	5	3	0.5	22	93	100	106	54
F9	7.5	2	0.4	23	94	90	165	44

were relatively denser, more spherical and smoother than those prepared with 10% sodium citrate which seemed to be more porous in structure (Figure 1b).

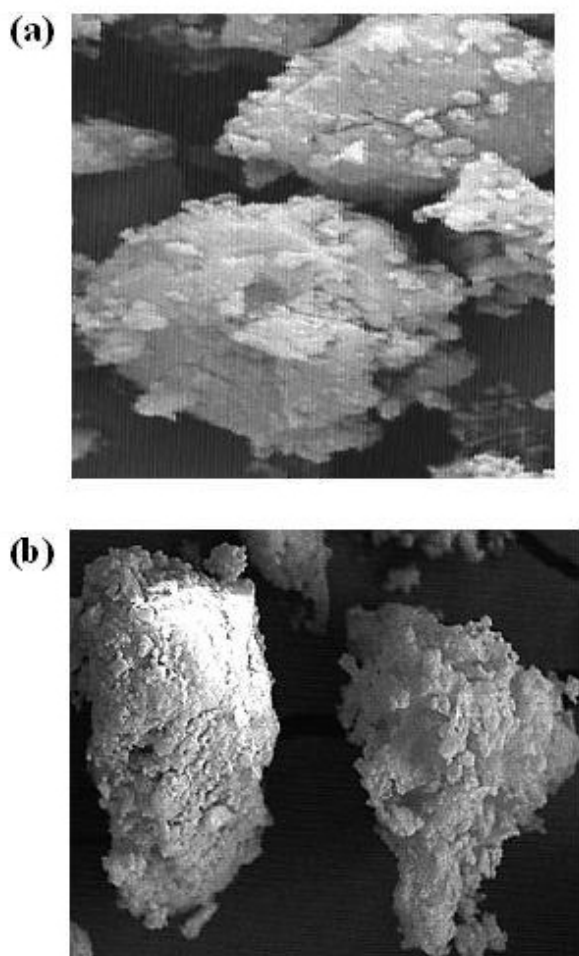


Figure 1. SEM photographs of DFS-C microspheres prepared with 0.3% (w/v) chitosan and cross-linked for 1 h with 5% (w/v) (a) and 10% (b) sodium citrate.

3.2. Percentage yield and encapsulation efficiency

The %yield and encapsulation efficiency of the microspheres were taken as an indication of the reproducibility and efficiency of the processing technique. The greater %yield and %EE of the prepared formulas (Table 2) were statistically significant with the low level of sodium citrate (5%, w/v) compared to the high level (10%, w/v) (Table 3). The estimated negative coefficient for sodium citrate concentration verified the decrease in the %yield and %EE with the increase in sodium citrate concentration. The ANOVA results showed that the cross-linking time had a significant influence on the %yield and %EE ($F < 0.0001$) (Table 3). On the contrary, the chitosan concentration had only a significant effect on the %EE which had a positive coefficient.

Three-dimensional response surface plots were drawn to show the effects of the interaction of the sodium citrate concentration and cross-linking time on the %yield as well as the interaction of the sodium citrate concentration and CS concentration on the %EE (Figures 2 and 3, respectively). The two figures showed no obvious effect from increasing the cross-linking time or CS concentration on %yield and %EE, respectively, at the low level of the cross-linking agent (5%, w/v sodium citrate). However, a pronounced effect was observed at the high level of the cross-linking concentration significantly increased the %yield and %EE, respectively, at the high level of sodium citrate (positive coefficients).

3.3. Swelling behavior

All the formulas prepared at the low level of cross-linking agent (5%, w/v sodium citrate) had %DS in the range of 106-133 (Table 2). On the other hand,

Table 3. Statistical analysis for the effect of independent variables and their interactions on the microspheres characteristics

			%Yield	%Encapsulation	%Swelling	%Mucoadhesion	%Release after 6 h
Variables	Sodium citrate concentration	<i>F</i> -value	< 0.0001*	< 0.0001*	< 0.0001*	< 0.0001*	< 0.0001*
		Estimate coefficient	-16.54	-24.50	35.29	-6.26	13.75
	Cross-linking time	<i>F</i> -value	0.0021*	< 0.0001*	< 0.0001*	0.19	< 0.0001*
		Estimate coefficient	4.54	9.13	-7.16	-1.16	-2.9
	Chitosan concentration	<i>F</i> -value	0.033	< 0.0001*	0.0352	0.75	0.016
		Estimate coefficient	2.95	4.34	-2.92	-0.27	1.37
Variables interaction	Sodium citrate concentration vs. Cross-linking time	<i>F</i> -value	0.0004*	0.0154	0.0015*	0.303	0.004*
		Estimate coefficient	5.54	-0.81	4.1	0.91	1.68
	Sodium citrate concentration vs. Chitosan concentration	<i>F</i> -value	0.1446	< 0.0001*	0.236	0.89	< 0.0001*
		Estimate coefficient	1.96	8.59	1.5	0.115	-5.98
	Chitosan concentration vs. Cross-linking time	<i>F</i> -value	0.1446	0.084	0.362	0.67	0.98
		Estimate coefficient	1.96	-0.56	1.23	0.36	0.0104

* Significant at $p < 0.01$.

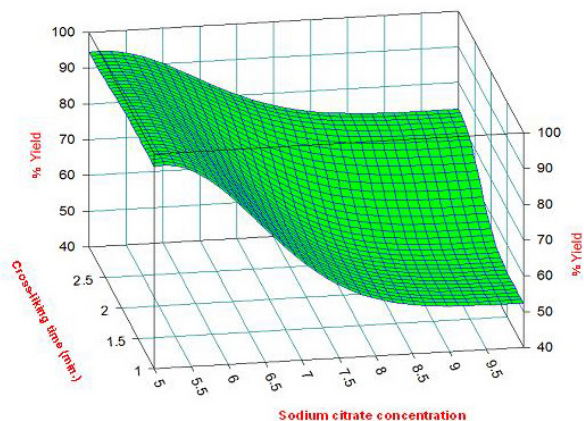


Figure 2. Effect of the interaction between sodium citrate concentration and cross-linking time on %yield of DFS-C microspheres.

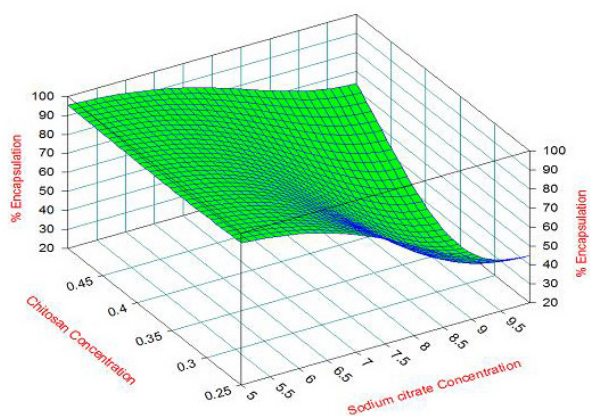


Figure 3. Effect of the interaction between sodium citrate concentration and chitosan concentration on %encapsulation efficiency of DFS-C microspheres.

the microspheres prepared at the high level of sodium citrate (10%, w/v) showed an increase in %DS values to the 183-193 range. The results also showed that cross-linking time and CS concentration had a lesser effect on %DS. The ANOVA results (Table 3) revealed linking time and CS concentration had a lesser effect on %DS. The ANOVA results (Table 3) revealed a significant effect of both the cross-linking agent concentration and time on the %DS but showed no significant effect for the CS concentration. The interaction between sodium citrate concentration and cross-linking time had the only significant effect on the swelling behavior (F value = 0.0015). This interaction presented in Figure 4, revealed that increased sodium citrate concentration increased the %DS at the second level of cross-linking time.

3.4. Mucoadhesive studies

The percentage mucoadhesion for all the microspheres formulas ranged between 39 and 54% (w/w) (Table 2).

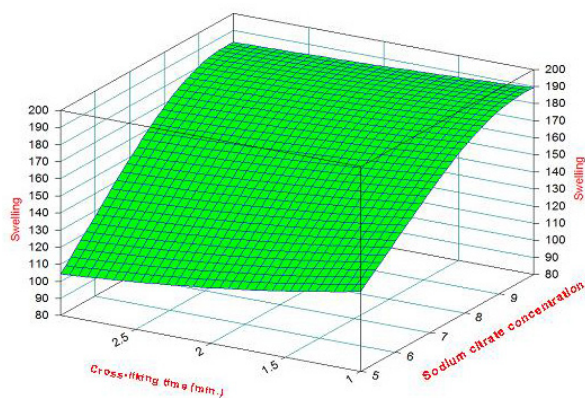


Figure 4. Effect of the interaction between sodium citrate concentration and cross-linking time on %degree of swelling of DFS-C microspheres.

The ANOVA results (Table 3) demonstrated a significant correlation between microsphere mucoadhesiveness and the sodium citrate concentration ($F < 0.0001$). The negative estimated coefficient observed for the effect of sodium citrate on the %mucoadhesion indicated that the higher the sodium citrate concentration the lower the mucoadhesive property of the microspheres. However, CS concentration and cross-linking time had no effect on the mucoadhesive properties of the microspheres.

3.5. *In vitro* release studies

The *in vitro* release profiles of DFS from different batches of DFS-C microspheres are shown in Figure 5. The profiles of all prepared microspheres exhibited a biphasic pattern of drug release. An initial burst effect was shown during the first hour that may be related to immediate release of the surface associated drug, followed by a slow release phase of the entrapped drug.

As expected, the sodium citrate concentration had a strong influence on the drug release behavior (Figure 5a). Increasing sodium citrate concentration from 5% (F5) to 10% (w/v) (F6) resulted in an increase in the percentage of drug released after 6 h from 69% to 97%. Figures 5b and 5c showed a decrease in the initial burst release within the first hour by increasing either the cross-linking time from 1 h (F1) to 3 h (F3) or the CS concentration from 0.3% (w/v) (F1) to 0.4% and 0.5% (w/v) (F9 and F7, respectively). After the first hour, all the profiles showed a continuous slow release of the drug entrapped within the microsphere matrix.

ANOVA results (Table 3) showed a significant effect of all variables on the percentage drug released. The significance of these factors was in order; concentration of sodium citrate > the cross-linking time > the CS concentration ($p < 0.01$). A significant interaction was also recorded for the cross-linking

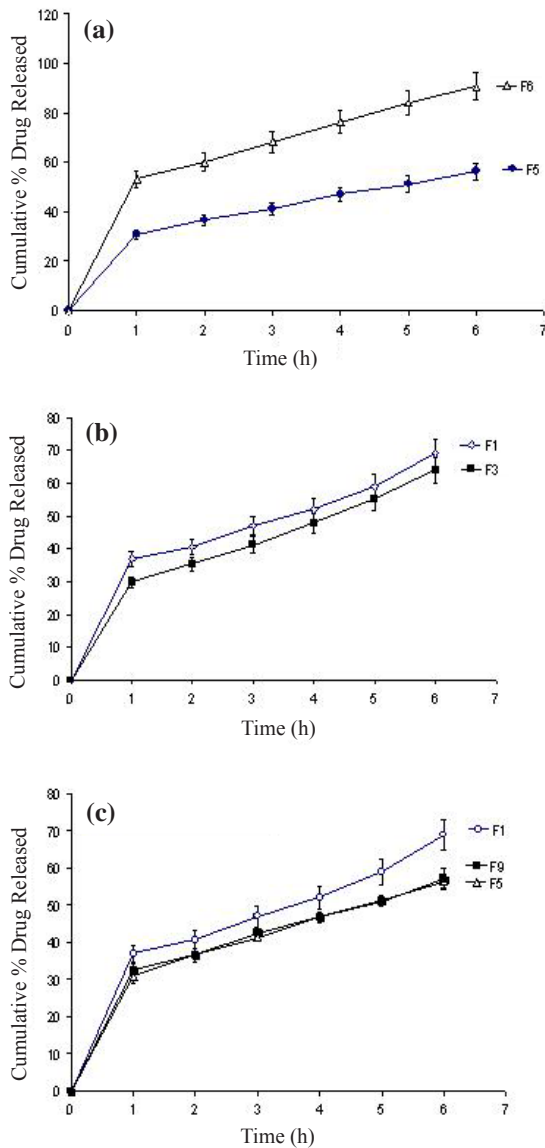


Figure 5. *In vitro* release profiles of diclofenac sodium from DFS-C microspheres under various conditions. A, sodium citrate concentration; B, cross-linking time; C, chitosan concentration.

agent concentration with either the cross-linking time or the CS concentration ($F = 0.004$ and < 0.0001 , respectively). The three dimensional profiles showed that increasing sodium citrate concentration greatly increased the percentage of drug released which was more obvious at the lower level of the CS concentration and cross-linking time (Figure 6).

3.6. Kinetic analysis of release data

The coefficients of the drug release kinetics (r^2) and the exponent "n" for equation 3 are presented in Table 4. It could be seen that the r^2 values for zero-order and Higuchi kinetics were much closer to 1 than the first-order. The release data were also fitted to the Korsmeyer-model where the exponent "n" values for all formulas were found to be in the range of 0.26-0.48.

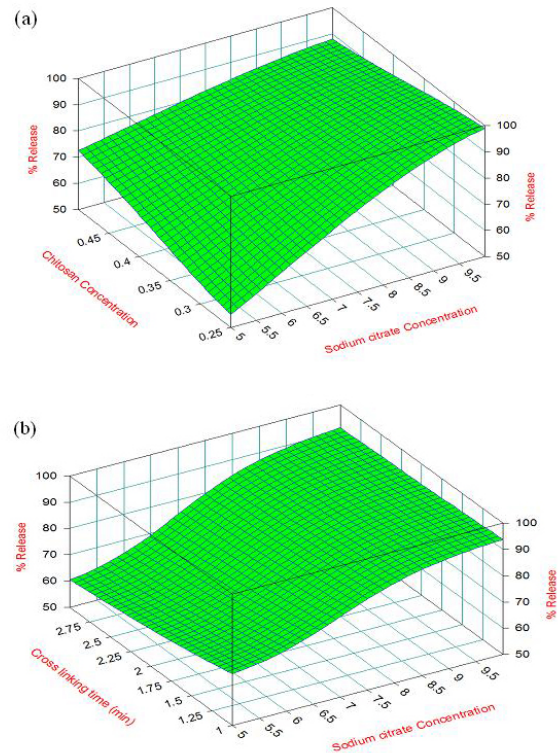


Figure 6. Effect of the interaction of sodium citrate concentration with (a) chitosan concentration and (b) cross-linking time on the percent of drug released after 6 h.

4. Discussion

The use of factorial design allows for testing a number of factors simultaneously and precludes the use of a huge number of independent runs when the traditional step by step approach is used. The effect of three independent variables namely, the cross-linking agent concentration, the cross-linking time and CS concentration were studied at two levels. The irregularity of the microsphere shape and the roughness of their surface might be due to the deposition of drug microparticles on the microsphere outer surface. On the other hand, the observed porous structure of microspheres prepared with 10% (w/v) sodium citrate was related to the effect of increasing sodium citrate concentration on the matrix cross-linking. The difference in the physical characteristics of the microspheres was related to the effect of pH on the degree of CS ionization and its cross-linking properties. Doubling the concentration of sodium citrate from 5% to 10% (w/v) increased the pH of the cross-linking solutions from pH 5 to 6.5, respectively. At pH 5, the amino groups of CS had a higher degree of ionization that would provide a better condition for electrostatic interaction between the protonated amine groups of CS and the negatively charged carboxylate groups of the citrate anions. Thus, more cross-linked polyelectrolyte complexes were formed at 5% sodium

Table 4. Kinetic analysis for the percentage drug released from DFS-C microspheres*

Formulas	r^2				'n' **
	Zero-order ($m_0 - m = k \cdot t$)	First-order ($\ln [m] = \ln [m_0 - k \cdot t]$)	Higuchi-model ($m_t/m_\infty = k \cdot t^{1/2}$)	Korsmeyer-model ($m_t/m_\infty = k \cdot t^n$)	
F1	0.999	0.995	0.996	0.995	0.41
F2	0.985	0.959	0.996	0.996	0.34
F3	0.994	0.996	0.999	0.997	0.37
F4	0.994	0.902	0.994	0.990	0.26
F5	0.999	0.990	0.995	0.993	0.41
F6	0.999	0.970	0.997	0.995	0.37
F7	0.996	0.984	0.994	0.998	0.39
F8	0.999	0.995	0.998	0.994	0.48
F9	0.981	0.974	0.996	0.950	0.38

* Analyzed by the regression coefficient method; r^2 : Coefficient of determination; ** Diffusional exponent Korsmeyer-model indicative of the mechanism of drug release.

citrate leading to a relatively spherical, smoother surface microsphere.

The relationship between the morphological characteristics of ionically cross-linked microspheres and the pH of the medium was explained by Shu *et al.* (22) and Lee *et al.* (23). They reported that as pH of the CS (weak polybasic) solution decreased the ionization of amine groups increased. Ko *et al.* (24) also showed that microparticles prepared with tri-polyphosphate solution at a low pH value (pH 2.5) had a more spherical shape and smoother surface than those prepared at a high pH of 8.6. They related such results to the tendency of the former solution to form a high density cross-linked matrix. Accordingly, at pH 6.5 (10%, w/v sodium citrate) the CS polymer had a lower degree of ionization, cross-linking sites and cross-linking density to constrain the polymer matrix (*i.e.*, low density structure). This led to a decrease in the %yield and %EE along with an increase in the %DS.

The significant effect of sodium citrate concentration and cross-linking time on the swelling behavior of the microspheres (Figure 4) clearly revealed that the concentration of sodium citrate (cross-linking agent) was the most prominent effective variable on the %DS of the microspheres. The results also confirmed that the effect of increasing the curing time was not remarkable as the pH of the medium shifted from pH 5 to 6.5.

Moreover, the effect of the sodium citrate concentration on the pH of the medium and %DS was found to influence the mucoadhesive behavior of the chitosan microspheres. Thus, the lower the cross-linking agent concentration used the higher was the degree of CS ionization and the mucoadhesion properties of the microspheres. A similar result was reported by Dhawan *et al.* (25) who found that the amount of chitosan adsorbed on the tissue increased with a decrease in the cross-linking level. Mortazavi and Smart (26) also reported that a certain degree of swelling was essential for microsphere adhesion to

mucin, whereas, over swelling led to slipping of the microspheres over the tissue surface.

The biphasic release pattern was related to the release of the drug particles adsorbed on the microsphere surfaces during the first hour, followed by slow release of the drug from the matrix. The increase in the percentage drug released with increasing the sodium citrate concentration was attributed to the increase in pH of the medium and the consequent decrease in the polymer cross-linking. Shu *et al.* (22) showed that chitosan films cross-linked with sodium citrate possessed pH-sensitive swelling and drug release properties. They also reported that preparation of CS microparticles in an acidic pH led to a dense matrix with complete ionic cross-linking that enabled a controlled drug release. Ozbas-Turan *et al.* (27) recorded a fast release pattern for interleukin-2 from chitosan microspheres when a larger volume of sodium sulfate (ionic cross-linking agent) was used during preparation.

The noticeable decrease in the percent drug released with an increase of cross-linking time might be attributed to an increase in the time allowed for polymer matrix to constrain. Ko *et al.* (24) reported the impact of curing time on the formation of a tripolyphosphate-chitosan matrix and the release of the drug. The results were also in accordance with Acikgoz *et al.* (18) who reported the formation of a denser matrix by increasing the curing time. This was thought to be associated with a decrease in the release of drug.

Moreover, the decrease in the percent drug released by increasing the CS concentration was attributed to the increase in the viscosity of the swollen microspheres accompanied by an increase in the diffusion path length traversed by the drug molecules. Ko *et al.* (24) illustrated the relationship between the drug release behavior and the viscosity of the chitosan solution. The increase in the viscosity of the solution led to the formation of relatively strong-walled microparticles. Lim *et al.* (28) reported the

formation of weak microspheres with the use of a low concentration of chitosan solution.

For the kinetics analysis data, although the correlation coefficients (r^2) of the release data closely fitted zero-order and Higuchi kinetics models, the low values of n (< 0.5) indicated that the mechanism of drug release from all the formulas could be described as a quasi-Fickian diffusion mechanism.

5. Conclusion

The addition of diclofenac sodium and cross-linking agent onto the chitosan solution in the form of spray droplets was shown to be a simple efficient technique for preparing microspheres. The microspheres were characterized by good percent yield, encapsulation efficiency, swelling and mucoadhesion properties along with controlled drug release. The concentration of the cross-linking agent and the pH of its solution must be taken into consideration as the most effective variables influencing the properties of the microspheres.

From the results it can be concluded that formula F8 with the composition of 1% DFS, 0.5% CS, 5% sodium citrate and cross-linked for 3 h, fulfilled the requisites for an optimum formulation.

Acknowledgements

The authors are thankful to Novartis Pharma Co., Cairo, Egypt for providing a gift sample of diclofenac sodium and University of Helwan, Ain Helwan for providing the facilities to complete this work.

References

1. Chuasuwana B, Binjesoh V, Polli JE, Zhang H, Amidon GL, Junginger HE, Midha KK, Shah VP, Stavchansky S, Dressman JB, Barends DM. Biowaiver monographs for immediate release solid oral dosage forms: diclofenac sodium and diclofenac potassium. *J Pharm Sci.* 2009; 98:1206-1219.
2. Huntjens DR, Strougo A, Chain A, Metcalf A, Summerfield S, Spalding DJ, Danhof M, Della Pasqua O. Population pharmacokinetic modelling of the enterohepatic recirculation of diclofenac and rofecoxib in rats. *Br J Pharmacol.* 2008; 153:1072-1084.
3. Bassotti G, Bucaneve G, Furno P, Morelli A, Del Favero A. Double-blind, placebo-controlled study on effects of diclofenac sodium and indomethacin on postprandial gastric motility in man. *Dig Dis Sci.* 1998; 43:1172-1176.
4. Nande VS, Barabde UU, Morkhade DM, Patil AT, Joshi SB. Sustained release microspheres of diclofenac sodium using PEGylated rosin derivatives. *Drug Dev Ind Pharm.* 2007; 33:1090-1100.
5. Al-Taani B, Khanfar MS, Salem MS, Sallam A. Release behaviour of diclofenac sodium dispersed in Gelucire(R) and encapsulated with alginate beads. *J Microencapsul.* 2008; 3:1-4.
6. Kibria G, Roni MA, Absar MS, Jalil RU. Effect of plasticizer on release kinetics of diclofenac sodium pellets coated with Eudragit RS 30 D. *AAPS PharmSciTech.* 2008; 9:1240-1246.
7. Mutalik S, Manoj K, Reddy MS, Kushtagi P, Usha AN, Anju P, Ranjith AK, Udupa N. Chitosan and enteric polymer based once daily sustained release tablets of aceclofenac: *in vitro* and *in vivo* studies. *AAPS PharmSciTech.* 2008; 9:651-659.
8. Pan Y, Li YJ, Zhao HY, Zheng JM, Xu H, Wei G, Hao JS, Cui FD. Bioadhesive polysaccharide in protein delivery system: chitosan nanoparticles improve the intestinal absorption of insulin *in vivo*. *Int J Pharm.* 2002; 249:139-147.
9. Pan Y, Zheng JM, Zhao HY, Li YJ, Xu H, Wei G. Relationship between drug effects and particle size of insulin-loaded bioadhesive microspheres. *Acta Pharmacol Sin.* 2002; 23:1051-1056.
10. Martinac A, Filipovic-Grcic J, Voinovich D, Perissutti B, Franceschinis E. Development and bioadhesive properties of chitosan-ethylcellulose microspheres for nasal delivery. *Int J Pharm.* 2005; 291:69-77.
11. Gu YH, Wang LY, Tan TW, Ma GH. Preparation of uniform-sized chitosan microspheres and application as carriers for protein drugs. *Sheng Wu Gong Cheng Xue Bao.* 2006; 22:150-155. (in Chinese)
12. Bodmeier R, Paeratakul O. Spherical agglomerates of water-insoluble drugs. *J Pharm Sci.* 1989; 78:964-967.
13. Hussain MR, Maji TK. Preparation of genipin cross-linked chitosan-gelatin microcapsules for encapsulation of Zanthoxylum limonella oil (ZLO) using salting-out method. *J Microencapsul.* 2008; 25:414-420.
14. Maculotti K, Tira EM, Sonaggere M, Perugini P, Conti B, Modena T, Pavanetto F. *In vitro* evaluation of chondroitin sulphate-chitosan microspheres as carrier for the delivery of proteins. *J Microencapsul.* 2009; 26:535-543.
15. Lorenzo-Lamosa ML, Remuñán-López C, Vila-Jato JL, Alonso MJ. Design of microencapsulated chitosan microspheres for colonic drug delivery. *J Control Release.* 1998; 52:109-118.
16. Berthold A, Cremer K, Kreuter J. Influence of cross-linking on the acid stability and physicochemical properties of chitosan microspheres. *STP Pharm Sci.* 1996; 6:358-364.
17. Thanoo BC, Sunny MC, Jayakrishnan A. Cross-linked chitosan microspheres: preparation and evaluation as a matrix for the controlled release of pharmaceuticals. *J Pharm Pharmacol.* 1992; 44:283-286.
18. Acikgoz M, Kas HS, Orman M, Hincal AA. Chitosan microspheres of diclofenac sodium: I. application of factorial design and evaluation of release kinetics. *J Microencapsul.* 1996; 13:141-159.
19. Remuñán-López C, Portero A, Vila-Jato JL, Alonso MJ. Design and evaluation of chitosan/ethylcellulose mucoadhesive bilayered devices for buccal drug delivery. *J Control Release.* 1998; 55:143-152.
20. Santos CA, Jacob JS, Hertzog BA, Freedman BD, Press DL, Harnpicharnchai P, Mathiowitz E. Correlation of two bioadhesion assays: the everted sac technique and the CAHN microbalance. *J Control Release.* 1999; 61:113-122.
21. Shu XZ, Zhu KJ. Chitosan/gelatin microspheres prepared by modified emulsification and ionotropic gelation. *J Microencapsul.* 2001; 18:237-245.

22. Shu XZ, Zhu KJ, Song W. Novel pH-sensitive citrate cross-linked chitosan film for drug controlled release. *Int J Pharm.* 2001; 212:19-28.
23. Lee ST, Mi FL, Shen YJ, Shyu SS. Equilibrium and kinetic studies of copper (II) ion uptake by chitosan-tripolyphosphate chelating resin. *Polymer.* 2001; 42:1879-1892.
24. Ko JA, Park HJ, Hwang SJ, Park JB, Lee JS. Preparation and characterization of chitosan microparticles intended for controlled drug delivery. *Int J Pharm.* 2002; 249:165-174.
25. Dhawan S, Singla AK, Sinha VR. Evaluation of mucoadhesive properties of chitosan microspheres prepared by different methods. *AAPS PharmSciTech.* 2004; 5:e67.
26. Mortazavi SA, Smart J. An investigation into the role of water movement and mucus gel hydration in mucoadhesion. *J Control Release.* 1993; 25:197-203.
27. Ozbas-Turan S, Akbuga J, Aral C. Controlled release of interleukin-2 from chitosan microspheres. *J Pharm Sci.* 2002; 91:1245-1251.
28. Lim LY, Wan LSC, Thai PY. Chitosan microspheres prepared by emulsification and ionotropic gelation. *Drug Dev Ind Pharm.* 1997; 23:981-985.

(Received January 29, 2010; Revised March 3, 2010; Accepted March 10, 2010)

Original Article

Membrane electrodes for determination of two antihypertensive drugs in pharmaceutical formulations of either single or binary mixtures and in biological fluids

Mohamed R. El-Ghobashy, Hala E. Zaazaa*

Analytical Chemistry Department, Faculty of Pharmacy, Cairo University, Cairo, Egypt.

ABSTRACT: Membrane-selective electrodes were used to determine benazepril hydrochloride (BZ) and trandolapril (TR) in their binary mixtures with hydrochlorothiazide (HZ) and verapamil (VR), respectively. This method involves construction of four water insoluble ion-association complexes: benazepril-tetraphenyl borate (BZ-TPB), benazepril-reineckate (BZ-R), trandolapril-tetraphenyl borate (TR-TPB), and trandolapril-reineckate (TR-R). These complexes were used as electroactive materials in polyvinyl chloride (PVC) matrix membrane sensors in order to determine the two aforementioned drugs in their pharmaceutical formulations and in plasma. The performance characteristics of these sensors, evaluated according to IUPAC recommendations, revealed a fast, stable, and linear response for BZ and TR. The suggested procedures were checked using laboratory-prepared mixtures and were successfully used to analyze their pharmaceutical preparations. The results obtained using the proposed method were statistically analyzed and compared with those obtained using previously reported methods.

Keywords: Benazepril hydrochloride, trandolapril, ion selective electrodes, PVC membranes, ammonium reineckate, sodium tetraphenyl borate

1. Introduction

Benazepril hydrochloride (BZ) is 3(S)-3-[[[(1S)-1-ethoxy-carbonyl]-3-phenylpropyl] amino]-2,3,4,5-tetrahydro-2-oxo-1H-1-benzazepine-1-acetic acid, while trandolapril (TR) is 1-[2-[1-(ethoxycarbonyl)-3-phenylpropyl]amino]-1-oxypropyl[octahydro-1H-indol-2-carboxylic acid (1). They belong to the class

of angiotensin-converting enzyme inhibitors used as antihypertensive drugs either alone or in combination with hydrochlorothiazide (HZ) or verapamil (VR), respectively (2).

Several analytical methods, including spectrophotometry, have been described for simultaneous determination of BZ/HZ in their binary mixture; these methods include the derivative technique (3,4), the chemometric method (4,5), Vierordt's technique (6,7), the absorbance ratio method (4,6), and isosbestic point measurement (8). Other methods involve HPLC (7,9,10) and TLC techniques (10). BZ has been determined alone using potentiometric coated wire electrodes (11).

A review of the literature revealed that there are few methods of determining TR, including HPLC (12-14) and enantioselective biosensors (15,16). TR and verapamil have been simultaneously determined using HPLC (17) and HPTLC densitometric methods (18).

The current work describes simple potentiometric sensors based on the use of the ion association complexes of both BZ and TR cations with tetraphenyl borate and reineckate anions as ion exchangers in a plasticized PVC matrix. These sensors were found to be suitable for the selective determination of BZ in a binary mixture with hydrochlorothiazide and for the determination of TR in a binary mixture with verapamil; neither determination required preliminary separation or extraction. These sensors also allow the potentiometric determination of both drugs BZ and TR in plasma without preliminary extraction and separation steps. The advantages of the suggested potentiometric sensors are their simplicity, low cost, fast response, wide working pH range, wide response range, and use with turbid and colored solutions.

2. Materials and Methods

2.1. Apparatus

Potentiometric measurements were made at $25 \pm 1^\circ\text{C}$ with a Hanna (Model 211) pH/mV meter. A single-junction calomel reference electrode (Model HI 5412) was used in conjunction with the drug sensor. A WPA pH

*Address correspondence to:

Dr. Hala E. Zaazaa, Analytical Chemistry Department, Faculty of Pharmacy, Cairo University, El-Kasr El-Aini St., ET-11562 Cairo, Egypt.
e-mail: hazaza@hotmail.com

combined glass electrode (Model CD 740) was used for pH measurements.

2.2. Reagents

All chemicals were of analytical reagent grade unless otherwise stated and doubly distilled deionized water was used.

The working standard for BZ was graciously supplied by Novartis Pharma Co., Cairo, Egypt. Its purity was certified to be $99.79 \pm 0.80\%$ according to a previously reported method (8). The working standard for TR was graciously supplied by Abbott Laboratory, USA. The purity of the sample was found to be $99.94 \pm 1.69\%$ according to a previously reported method (17).

Aqueous 1.00×10^{-3} – 1.00×10^{-6} M BZ and TR solutions were prepared by serial dilution of 1.00×10^{-2} M stock solutions. All pharmaceutical samples of BZ and TR were obtained from local drug stores.

Tetrahydrofuran (THF) 99% (Lab Scan), high molecular weight (10,000) polyvinyl chloride (PVC) powder, dibutyl sebacate (DBS) plasticizer, sodium tetraphenyl borate (TPB), and ammonium reineckate (AR) were obtained from Sigma-Aldrich. A phosphate buffer, pH 4, was prepared.

Laboratory-prepared mixtures of BZ/HZ were prepared as follows: aliquoted portions of 2.5, 5, 2.5, 1.25, and 2.5 mL of BZ from a stock solution of 1.00×10^{-2} M were accurately transferred to a series of 25-mL measuring flasks. Aliquoted portions from a 1.00×10^{-2} M HZ solution were added to prepare mixtures containing 1:1, 2:1, 1:2, 0.5:1, and 1:0.5 of BZ and HZ, respectively.

Laboratory-prepared mixtures of TR/VR were prepared as follows. Aliquot portions 2.5, 10, 2.5, 2.5 and 2.5 mL of TR from its stock solution 1.00×10^{-2} M was transferred accurately to a series of 25-mL measuring flasks. Aliquot portions from 1.00×10^{-2} M VR solution were added to prepare mixtures containing 1:1, 4:1, 1:2, 1:4 and 1:6 of TR and VR, respectively.

2.3. Preparation of BZ and TR ion exchangers

Benazepril-tetraphenyl borate (BZ-TPB), benazepril-reineckate (BZ-R), trandolapril-tetraphenyl borate (TR-TPB), and trandolapril-reineckate (TR-R) ion pair complexes were prepared by slow addition of 20.00 mL of 1.00×10^{-2} M BZ and TR aqueous solutions to 10.00 mL aliquots of TPB and AR, separately. The mixtures were stirred for 10 min; the precipitates were filtered off, washed with doubly distilled water, dried at room temperature, and ground to a fine powder. Elemental analyses confirmed the formation of 1:2 complexes.

2.4. BZ and TR-PVC membrane sensors

In a glass Petri dish (5.00 cm diameter), 10.00 mg of BZ ion exchanger or TR ion exchanger were thoroughly

mixed with 350.00 mg of DBS and 190.00 mg of PVC powder. The mixture was dissolved in 5.00 mL of THF. The Petri dish was covered with filter paper and allowed to stand overnight to allow solvent evaporation at room temperature. A master membrane with a thickness of 0.10 mm was obtained.

2.5. Sensor assembly

A disk of an appropriate diameter (about 8.00 mm) was cut from the previously prepared master membranes and glued onto the flat end of PVC tubing with THF. A mixed solution consisting of equal volumes of 1.00×10^{-2} M BZ or TR and 1.00×10^{-2} M sodium chloride was used as an internal reference solution. Ag/AgCl coated wire (3.00 mm diameter) served as an internal reference electrode. The sensors were conditioned by soaking overnight in a solution of 1.00×10^{-2} M of either of the two drugs and storage in the same solution when not in use.

2.6. Sensor calibration

Along with the single-junction calomel reference electrode, the prepared electrodes were immersed in aqueous solutions of BZ and TR in a range of 1.00×10^{-6} – 1.00×10^{-2} M. The membrane sensors were washed with water between measurements.

A calibration graph was constructed by plotting the potential change with respect to the logarithm of the BZ and TR concentrations. The regression equations for the linear portion of the curves were computed and used to subsequently determine unknown concentrations of BZ and TR.

2.7. Selectivity measurements

Potentiometry selectivity coefficients ($K_{BZ \text{ or } TR, I}^{\text{pot}}$) were evaluated according to IUPAC guidelines using the separate solutions method (19,20).

2.8. Application to laboratory-prepared mixtures

Along with the single-junction calomel reference electrode, the membrane sensors were immersed in corresponding laboratory-prepared mixtures. The sensors were washed with water between measurements. The electromotive force (EMF) produced for each mixture was measured with the proposed electrodes and then the concentration of BZ and TR was determined from the corresponding regression equation.

2.9. Application to pharmaceutical formulations

2.9.1. BZ in Cibadrex tablets

Ten tablets were weighed and powdered. A quantity

of the powdered tablets was transferred to a 50-mL volumetric flask, and then the flask was completed to the mark with phosphate buffer (pH 4) and sonicated for 15 min to prepare 1.00×10^{-3} M of BZ. The EMF produced by immersing the prepared electrodes, along with single junction calomel reference electrode, in the prepared solutions was determined and then the concentration of BZ was calculated from the regression equation of the corresponding electrode.

2.9.2. TR in Tarka tablets

Ten tablets were weighed and powdered. A quantity of the powdered tablets was transferred to 50-mL volumetric flask, and then the flask was completed to the mark with phosphate buffer (pH 4) and sonicated for 15 min to prepare 1.00×10^{-3} M of TR. The assay was completed as described above.

2.10. Application to plasma samples

Four-point five mL of plasma were placed into 4 stoppered shaking tubes, and then 0.5 mL of 1.00×10^{-2} and 1.00×10^{-3} M BZ and TR were each added separately and shaken. The membrane sensor was immersed in these solutions along with the single junction calomel reference electrode. The sensor was washed with water between measurements. The EMF produced by each solution was measured using the four proposed electrodes and then the concentration of BZ and TR was determined from the corresponding regression equations.

3. Results and Discussion

The development and use of ion-selective electrodes continue to be of interest in pharmaceutical analysis because these sensors offer the advantages of simple design, reasonable selectivity, and fast response.

The method proposed here has the advantages of being sensitive, allowing determination of BZ in the presence of HZ. The proposed electrodes have a longer life span than potentiometric coated wire electrodes for determination of BZ alone as were previously reported (11).

In addition, TR was formulated with VR in a medicinally recommended ratio of 1:100. Analysis of such a mixture is challenging because the amount of the major component, VR, is much greater than the amount of the minor component, TR. Therefore, the aim of this work was to develop simpler and less complicated methods for the determination of a minor component like TR in a binary mixture.

The present investigation is based on the fact that both BZ and TR behave as cations in acidic medium due to the presence of amino groups. This property suggests the use of anionic ion exchangers in the formation of ion

association complexes. These are physically compatible with the matrix and serve as rapid ion exchangers for the two drugs at the membrane-sample interface.

BZ and TR reacted with sodium TPB and AR to form stable 1:2 water insoluble ion association complexes. This ratio was confirmed by elemental analysis data and by the Nernstian response of the suggested sensors. That response was about 30 mV (for both BZ and TR), the typical value for divalent drugs (21).

PVC acts as a standard support matrix and as a trap for the sensed ions, but its use requires the use of a plasticizer (22). In the present investigation, DBS was chosen from among dicarboxylic acid esters as a plasticizer. With PVC, dicarboxylic acid esters were found to be the optimum plasticizers; they dissolve the ion association complex and adjust both the membrane permittivity and ion exchange site mobility to yield the highest possible selectivity and sensitivity (23,24).

Electrochemical performance characteristics of the proposed sensors were evaluated according to IUPAC recommendations (21) (Table 1). The electrodes were found to display constant and stable potential readings within 2 mV day-to-day, and the calibration slopes for the four electrodes changed by less than 2 mV per concentration decade over a period of 1 month.

The response time of the electrodes was tested for concentrations of the two drugs from 1.00×10^{-5} – 1.00×10^{-2} M. The measurements were characterized by a fast stable response within 20-30 sec for concentrations less than 1.00×10^{-4} M and 10-20 sec for concentrations over 1.00×10^{-4} M.

The pH effect was optimized from the point of view of both sensor function and chemical form of the test substance. As shown in Figures 1 and 2, the potential-pH profiles indicated that the sensor responses were fairly steady over pH 3-5 (phosphate buffer). Within this range, drug cations are completely ionized and dissociated and therefore can be sensed. Above and below this pH range, the potentials displayed by the electrodes were noisy.

The potentiometric response of the four studied electrodes at the optimum pH was linear with constant

Table 1. Response characteristics of the four investigated electrodes

Parameter	BZ-TPB	BZ-R	TR-TPB	TR-R
Slope (mv/decad)	-31.58	-30.57	-36.64	-31.44
Intercept (mV)	83.28	91.02	22.39	3.24
Correlation coefficient	0.9997	0.9992	0.9997	0.9991
Detection limit (M)	2.8×10^{-6}	4.6×10^{-6}	5.2×10^{-6}	6.6×10^{-6}
Response time (sec)	20-30	20-30	20-30	20-30
Working pH range	3-5	3-5	3-5	3-5
Concentration range (M)	10^{-5} - 10^{-2}	10^{-5} - 10^{-2}	10^{-5} - 10^{-2}	10^{-5} - 10^{-2}
Life span (weeks)	4-6	4-6	4-6	4-6
Average recovery (%)	99.07	99.13	100.09	99.98
R.S.D. % ^a	0.75	0.91	1.26	1.43

^aResults of four determinations.

slopes over a drug concentration range of 1.00×10^{-5} – 1.00×10^{-2} M for BZ and TR, respectively (Figures 3 and 4).

The accuracy of the proposed membrane sensors at quantifying blind samples of BZ and TR was assessed using the four sensors. Results indicated average recovery of 99.07 ± 0.75 , 99.13 ± 0.91 , 100.09 ± 1.26 , and 99.98 ± 1.43 for the BZ-TPB, BZ-R, TR-TPB, and TR-R sensor, respectively.

As shown in Tables 2 and 3, the proposed method was valid and suitable for determining BZ in different laboratory-prepared mixtures with HZ or

for determining TR in different laboratory-prepared mixtures with VR. Mean percentage recovery was 100.21 ± 0.86 and 99.78 ± 1.24 , for BZ by BZ-TPB and BZ-R, respectively, and 100.71 ± 1.22 and 100.73 ± 0.78 for TR by TR-TPB and TR-R, respectively.

The performance of the four sensors in the presence of some nitrogenous compounds such as amines, amino acids, and some inorganic cations was assessed by measuring and comparing potentiometric selectivity coefficients ($K^{\text{pot}}_{\text{Drug, i}}$). The separate solutions method with a fixed concentration of the interferent (1.00×10^{-3} M) was used to evaluate selectivity. Results obtained

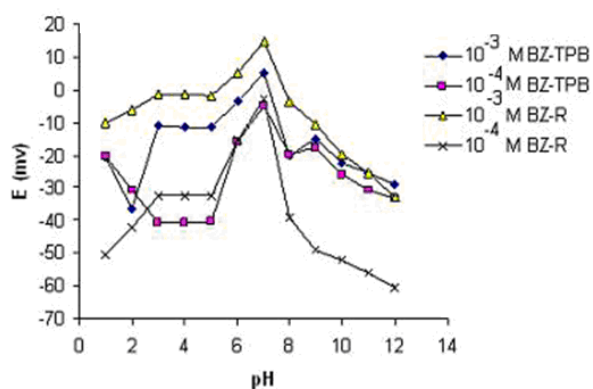


Figure 1. Effects of pH on the response of a benazepril hydrochloride-tetraphenyl borate electrode (BZ-TPB) and a benazepril hydrochloride-reineckate electrode (BZ-R).

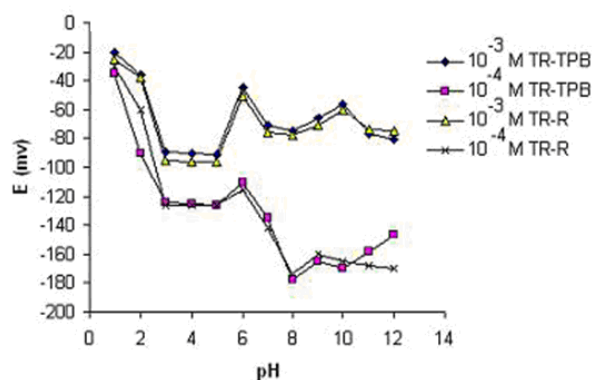


Figure 2. Effects of pH on the response of a trandolapril-tetraphenyl borate electrode (TR-TPB) and a trandolapril-reineckate electrode (TR-R).

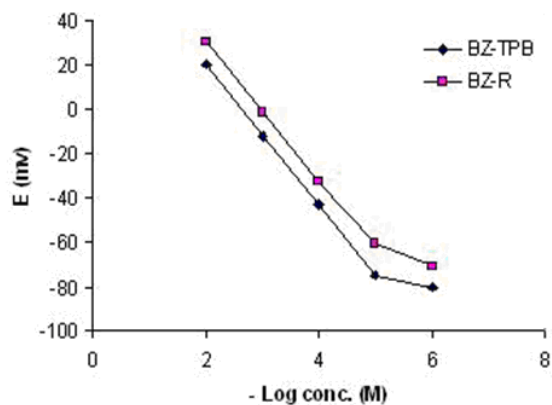


Figure 3. Profile of the potential in mV with respect to the – log concentration of benazepril hydrochloride with TPB and R.

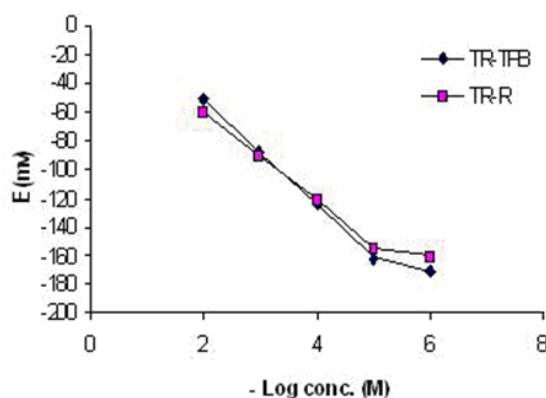


Figure 4. Profile of the potential in mV with respect to the – log concentration of trandolapril with TPB and R.

Table 2. Results of using the two electrodes to analyze benazepril hydrochloride in different laboratory-prepared mixtures with hydrochlorothiazide

Ratio of BZ:HZ	Recovery of benazepril hydrochloride (%) ^a	
	BZ-TPB	BZ-R
1:1	100.58	98.41
2:1	101.24	98.92
1:2	99.51	99.47
0.5:1	100.58	100.71
1:0.5	99.15	101.37
Mean ± S.D. (%)	100.21 ± 0.86	99.78 ± 1.24

^a Average of three determinations.

Table 3. Results of using the two electrodes to analyze trandolapril in different laboratory-prepared mixtures with verapamil

Ratio of TR:VR	Recovery of trandolapril (%) ^a	
	TR-TPB	TR-R
1:1	100.98	100.35
4:1	101.23	100.86
1:2	98.64	99.87
1:4	100.88	100.59
1:6	101.83	101.96
Mean ± S.D. (%)	100.71 ± 1.22	100.73 ± 0.78

^a Average of three determinations.

with the developed sensors indicated that they had a reasonable level of selectivity (Table 4).

Pharmaceutical additives, diluents, and ingredients commonly used in drug formulations such as lactose, sucrose, magnesium sulphate, talc, and methyl cellulose did not produce interference. Thus, analysis was carried out without prior treatment or extraction. BZ-TPB and BZ-R sensors were successfully used to determine BZ in Cibadrex tablets (Table 5), and TR-TPB and TR-R sensors were used to determine TR in Tarka tablets

(Table 5).

When used in biological fluids, the four electrodes were found to produce stable results as revealed by the high precision and accuracy of recovery of the spiked plasma samples. This indicated the lack of interference from plasma electrolytes (Table 6).

A statistical comparison of the results obtained using the proposed method and the previously reported procedure for BZ (8) or that for TR (17) is shown in Table 7. The values of the calculated t and F were

Table 4. Potentiometric selectivity coefficients of the four proposed electrodes according to the separate solutions method

Interferent	Selectivity coefficient			
	BZ-TPB	BZ-R	TR-TPB	TR-R
Verapamil	–	–	3.56×10^{-4}	3.48×10^{-4}
Hydrochlorothiazide	3.51×10^{-4}	3.23×10^{-4}	–	–
Na ⁺	3.53×10^{-3}	2.27×10^{-3}	2.08×10^{-3}	2.78×10^{-3}
K ⁺	3.07×10^{-3}	2.38×10^{-3}	2.51×10^{-3}	3.35×10^{-3}
NH ₄ ⁺	2.47×10^{-3}	1.46×10^{-3}	3.70×10^{-3}	4.31×10^{-3}
Ca ²⁺	3.22×10^{-3}	2.36×10^{-3}	3.08×10^{-3}	2.84×10^{-3}
Mg ²⁺	3.43×10^{-3}	2.74×10^{-3}	2.87×10^{-3}	2.85×10^{-3}
Glucose	2.14×10^{-3}	1.89×10^{-3}	2.85×10^{-3}	2.38×10^{-3}
Lactose	3.26×10^{-3}	3.72×10^{-3}	2.86×10^{-3}	2.23×10^{-3}
Sucrose	2.66×10^{-3}	3.22×10^{-3}	2.52×10^{-3}	1.68×10^{-3}
Urea	2.56×10^{-3}	3.05×10^{-3}	2.97×10^{-3}	2.16×10^{-3}
L-Phenylalanin	2.92×10^{-3}	3.23×10^{-3}	2.70×10^{-3}	2.29×10^{-3}
Methyl cellulose	3.47×10^{-3}	2.52×10^{-3}	5.55×10^{-3}	5.71×10^{-3}
Talc	3.21×10^{-3}	1.96×10^{-3}	5.84×10^{-3}	6.31×10^{-3}

Table 5. Quantitative determination of benazepril hydrochloride in Cibadrex tablets and trandolapril in Tarka tablets using the proposed electrodes

Pharmaceutical dosage forms	Recovery ± S.D. (%) [*]
Benazepril hydrochloride in Cibadrex tablets (batch No. Y0002)	
BZ-TPB	99.15 ± 0.81
BZ-R	99.29 ± 1.06
Trandolapril in Tarka tablets (batch No. 551918D)	
TR-TPB	100.37 ± 0.92
TR-R	99.87 ± 1.27

^{*} Average of three determinations.

Table 6. Determination of benazepril hydrochloride and trandolapril in spiked human plasma using the four electrodes proposed

Concentration (M)	Recovery ± S.D. of benazepril hydrochloride (%) [*]		Recovery ± S.D. of trandolapril (%) [*]	
	BZ-TPB	BZ-R	TR-TPB	TR-R
1×10^{-3}	99.41 ± 1.46	98.73 ± 1.67	100.35 ± 0.97	99.75 ± 1.26
1×10^{-4}	99.57 ± 1.32	99.03 ± 1.84	100.12 ± 1.11	99.84 ± 1.44

^{*} Average of three determinations.

Table 7. Statistical analysis of the results obtained using the proposed method and previously reported methods to analyze benazepril hydrochloride (8) and trandolapril (17)

Values	BZ-TPB	BZ-R	Reported method (ref. 8)	TR-TPB	TR-R	Reported method (ref. 17)
Mean ± S.D.	99.07 ± 0.75	99.13 ± 0.91	99.79 ± 0.80	100.09 ± 1.26	99.98 ± 1.43	99.94 ± 1.69
n	4	4	6	4	4	5
Variance	0.563	0.828	0.640	1.588	2.045	2.856
t	1.427	1.213	–	0.147	0.038	–
	(2.306) [*]	(2.306) [*]	–	(2.365) [*]	(2.365) [*]	–
F	1.14	1.29	–	1.80	1.40	–
	(9.01) [*]	(5.41) [*]	–	(9.12) [*]	(9.12) [*]	–

^{*} The values in parentheses correspond to the theoretical values of t and F at $p = 0.05$.

less than the tabulated ones, which reveals that there was no significant difference with respect to accuracy and precision between the proposed method and the previously reported procedures.

4. Conclusion

The proposed sensors for BZ and TR offer the advantages of high stability, fast response over a wide range of concentrations and pH levels, low cost, ease of fabrication, adequate selectivity in the presence of hydrochlorothiazide (for BZ) or verapamil (for TR) and related species, and direct use with turbid and colored drug solutions without any pretreatment. The proposed method can be used to determine the aforementioned drugs in pure form, in plasma, and in pharmaceutical formulations.

References

- Maryadele J O' Neil. Merck Index, 14th ed., Merck, Darmstadt, 2006.
- Delgado JN, Remers WA. Text Book of Organic Medicinal and Pharmaceutical Chemistry, 10th ed., Willson CP, Gisvold O, eds., Lippincott Co., Philadelphia and New York, USA, 1998.
- Panderi IE. Simultaneous determination of benazepril hydrochloride and hydrochlorothiazide in tablets by second-order derivative spectrophotometry. *J Pharm Biomed Anal.* 1999; 21:257-265.
- El-Gindy A, Ashour A, Abdel-Fattah L, Shabana L. Spectrophotometric determination of benazepril hydrochloride and hydrochlorothiazide in binary mixture using second derivative, second derivative of the ratio spectra and chemometric methods. *J Pharm Biomed Anal.* 2001; 25:299-307.
- Dinc E, Baleanu D. Application of the wavelet method for the simultaneous quantitative determination of benazepril and hydrochlorothiazide in their mixtures. *J AOAC Int.* 2004; 87:834-841.
- Erk N. Determination of active ingredients in the pharmaceutical formulations containing hydrochlorothiazide and its binary mixtures with benazepril hydrochloride, triamterene and cilazapril by ratio spectra derivative spectrophotometry and vierordt's method. *J Pharm Biomed Anal.* 1999; 20:155-167.
- Banoglu E, Ozkan Y, Atay O. Dissolution tests of benazepril hydrochloride and hydrochlorothiazide in commercial tablets: comparison of spectroscopic and high-performance liquid chromatography methods. *Farmaco.* 2000; 55:477-483.
- Abdel-Kawy M, Amer SA, Lotfy HM, Zaazaa HE. Simple spectrophotometric analysis of benazepril hydrochloride or valsartan in combined pharmaceutical dosages with hydrochlorothiazide. *Bull Fac Pharm Cairo Univ.* 2006; 44:25-32.
- Hassib S, El-Sherif Z, El-Bagary R, Youssef N. Reversed-phase high performance liquid chromatographic and thin layer chromatographic methods for the simultaneous determination of benazepril hydrochloride and hydrochlorothiazide in Cibadrex tablets. *Anal Lett.* 2000; 33:3225-3237.
- El-Gindy A, Ashour A, Abdel-Fattah L, Shabana L. Application of LC and HPTLC-densitometry for the simultaneous determination of benazepril hydrochloride and hydrochlorothiazide. *J Pharm Biomed Anal.* 2001; 25:171-179.
- Khalil S, Abd El-Aliem S. Potentiometric and thermal studies of a coated-wire benazepril-selective electrode. *J Pharm Biomed Anal.* 2002; 27:25-29.
- Gumieniczek A, Hopkala H. High-performance liquid chromatographic assay of trandolapril in capsules. *Acta Pol Pharm.* 2000; 57:253-255.
- Cendrowska I, Bańkowski K, Iskra-Jopa J. A study on the stereochemical purity of trandolapril and octahydro-1H-indole-2-carboxylic acid by HPLC method. *Acta Pol Pharm.* 2003; 60:141-144.
- Nirogi RV, Kandikere VN, Shrivastava W, Mudigonda K. Quantification of trandolapril and its metabolite trandolaprilat in human plasma by liquid chromatography/tandem mass spectrometry using solid-phase extraction. *Rapid Commun Mass Spectrom.* 2006; 20:3709-3716.
- Stefan RI, Van-Staden JF, Aboul-Enein HY. Detection of S-enantiomer of cilazapril, pentopril and trandolapril using potentiometric, enantioselective membrane electrode. *Electroanalysis.* 1999; 11:192-194.
- Stefan RI, Van-Staden JF, Aboul-Enein HY. Analysis of chiral drugs with enantioselective biosensors. An overview. *Electroanalysis.* 1999; 11:1233-1235.
- Gumieniczek A, Hopkala H. Development and validation of a liquid chromatographic method for the determination of trandolapril and verapamil in capsules. *J Liq Chrom Relat Tech.* 2001; 24:393-400.
- Kowalczyk D. Simultaneous high-performance thin-layer chromatography densitometric assay of trandolapril and verapamil in the combination preparation. *J AOAC Int.* 2005; 88:1525-1529.
- Hassan SS, Amer MM, Abd El-Fatah SA, El-Kosasy AM. Microcoated wire sensors for the determination of anticancer drugs cyclophosphamide and ifosfamide in the presence of their degradates. *Talanta.* 1998; 46:1395-1403.
- El-Ragehi NA, El-Kosasy AM, Abbas SS, El-khateeb SZ. Polymeric membrane electrodes for selective determination of the central nervous system acting drugs fluphenazine hydrochloride and nortriptyline hydrochloride. *Anal Chim Acta.* 2000; 418:93-100.
- IUPAC Analytical Chemistry Division. Commission on analytical nomenclature. *Pure Appl Chem.* 2000; 72:1852-1856.
- Zyka J. Instrumentation in Analytical Chemistry, Vol. 2, Ellis Horwood, Chichester, UK, 1994.
- Freiser H. Ion Selective Electrodes in Analytical Chemistry, Vol. 2, Plenum Press, New York, USA, 1978.
- Diamond D. Principles of Chemical and Biological Sensors. In: *Chemical Analysis*, Vol. 150, Chapter 2, John Wiley & Sons, Inc., New York, USA, 1998.

(Received January 28, 2010; Revised March 4, 2010; Accepted March 9, 2010)

Drug Discoveries & Therapeutics

Guide for Authors

1. Scope of Articles

Drug Discoveries & Therapeutics mainly publishes articles related to basic and clinical pharmaceutical research such as pharmaceutical and therapeutical chemistry, pharmacology, pharmacy, pharmacokinetics, industrial pharmacy, pharmaceutical manufacturing, pharmaceutical technology, drug delivery, toxicology, and traditional herb medicine. Studies on drug-related fields such as biology, biochemistry, physiology, microbiology, and immunology are also within the scope of this journal.

2. Submission Types

Original Articles should be reports new, significant, innovative, and original findings. An Article should contain the following sections: Title page, Abstract, Introduction, Materials and Methods, Results, Discussion, Acknowledgments, References, Figure legends, and Tables. There are no specific length restrictions for the overall manuscript or individual sections. However, we expect authors to present and discuss their findings concisely.

Brief Reports should be short and clear reports on new original findings and not exceed 4,000 words with no more than two display items. *Drug Discoveries & Therapeutics* encourages younger researchers and doctors to report their research findings. Case reports are included in this category. A Brief Report contains the same sections as an Original Article, but Results and Discussion sections must be combined.

Reviews should include educational overviews for general researchers and doctors, and review articles for more specialized readers.

Policy Forum presents issues in science policy, including public health, the medical care system, and social science. Policy Forum essays should not exceed 2,000 words.

News articles should not exceed 500 words including one display item. These articles should function as an international news source with regard to topics in the life and social sciences and medicine. Submissions are not restricted to journal staff - anyone can submit news articles on subjects that would be of interest to *Drug Discoveries & Therapeutics'* readers.

Letters discuss material published in *Drug Discoveries & Therapeutics* in the last 6 months or issues of general interest. Letters should not exceed 800 words and 6 references.

3. Manuscript Preparation

Preparation of text. Manuscripts should be written in correct American English and submitted as a Microsoft Word (.doc) file in a single-column format. Manuscripts must be paginated and double-spaced throughout. Use Symbol font for all Greek characters. Do not import the figures into the text file but indicate their approximate locations directly on the manuscript. The manuscript file should be smaller than 5 MB in size.

Title page. The title page must include 1) the title of the paper, 2) name(s) and affiliation(s) of the author(s), 3) a statement indicating to whom correspondence and proofs should be sent along with a complete mailing address, telephone/fax numbers, and e-mail address, and 4) up to five key words or phrases.

Abstract. A one-paragraph abstract consisting of no more than 250 words must be included. It should state the purpose of the study, basic procedures used, main findings, and conclusions.

Abbreviations. All nonstandard abbreviations must be listed in alphabetical order, giving each abbreviation followed by its spelled-out version. Spell out the term upon first mention and follow it with the abbreviated form in parentheses. Thereafter, use the abbreviated form.

Introduction. The introduction should be a concise statement of the basis for the study and its scientific context.

Materials and Methods. Subsections under this heading should include sufficient instruction to replicate experiments, but well-established protocols may be simply referenced. *Drug Discoveries & Therapeutics* endorses the principles of the Declaration of Helsinki and expects that all research involving humans will have been conducted in accordance with these principles. All laboratory animal studies must be approved by the authors' Institutional Review Board(s).

Results. The results section should provide details of all of the experiments that are required to support the conclusions of the paper. If necessary, subheadings may be used for an orderly presentation. All figures, tables, and photographs must be referred in the text.

Discussion. The discussion should include conclusions derived from the study and supported by the data. Consideration should be given to the impact that these conclusions have on the body of knowledge in which context the experiments were conducted. In Brief Reports, Results and Discussion sections must be combined.

Acknowledgments. All funding sources should be credited in the Acknowledgments section. In addition, people who contributed to the work but who do not fit the criteria for authors should be listed along with their contributions.

References. References should be numbered in the order in which they appear in the text. Cite references in text using a number in parentheses. Citing of unpublished results and personal communications in the reference list is not recommended but these sources may be mentioned in the text. For all references, list all authors, but if there are more than fifteen authors, list the first three authors and add "*et al.*" Abbreviate journal names as they appear in PubMed. Web references can be included in the reference list.

Example 1:

Hamamoto H, Akimitsu N, Arimitsu N, Sekimizu K. Roles of the Duffy antigen and glycoprotein A in malaria infection and erythrocyte. *Drug Discov Ther.* 2008; 2:58-63.

Example 2:

Zhao X, Jing ZP, Xiong J, Jiang SJ. Suppression of experimental abdominal aortic aneurysm by tetracycline: a preliminary study. *Chin J Gen Surg*. 2002; 17:663-665. (in Chinese)

Example 3:

Mizuochi T. Microscale sequencing of N-linked oligosaccharides of glycoproteins using hydrazinolysis, Bio-Gel P-4, and sequential exoglycosidase digestion. In: *Methods in Molecular Biology: Vol. 14 Glycoprotein analysis in biomedicine* (Hounsell T, ed.). Humana Press, Totowa, NJ, USA, 1993; pp. 55-68.

Example 4:

Drug Discoveries & Therapeutics. Hot topics & news: China-Japan Medical Workshop on Drug Discoveries and Therapeutics 2007. <http://www.ddtjournal.com/hotnews.php> (accessed July 1, 2007).

Figure legends. Include a short title and a short explanation. Methods described in detail in the Materials and methods section should not be repeated in the legend. Symbols used in the figure must be explained. The number of data points represented in a graph must be indicated.

Tables. All tables should have a concise title and be typed double-spaced on pages separate from the text. Do not use vertical rules. Tables should be numbered with Arabic numerals consecutively in accordance with their appearance in the text. Place footnotes to tables below the table body and indicate them with lowercase superscript letters.

Language editing. Manuscripts submitted by authors whose primary language is not English should have their work proofread by a native English speaker before submission. The Editing Support Organization can provide English proofreading, Japanese-English translation, and Chinese-English translation services to authors who want to publish in *Drug Discoveries & Therapeutics* and need assistance before submitting an article. Authors can contact this organization directly at <http://www.iacmhr.com/iac-eso>.

IAC-ESO was established in order to facilitate manuscript preparation by researchers whose native language is not English and to help edit work intended for international academic journals. Quality revision, translation, and editing services are offered by our staff, who are native speakers of particular languages and who are familiar with academic writing and journal editing in English.

4. Figure Preparation

All figures should be clear and cited in numerical order in the text. Figures must fit a one- or two-column format on the journal page: 8.3 cm (3.3 in.) wide for a single column; 17.3 cm (6.8 in.) wide for a double column; maximum height: 24.0 cm (9.5 in.). Only use the following fonts in the figure: Arial and Helvetica. Provide all figures as separate files. Acceptable file formats are JPEG and TIFF. Please note that files saved in JPEG or TIFF format in PowerPoint lack sufficient resolution for publication. Each Figure file should be smaller than 10 MB in size. Do not compress files. A fee is charged for a color illustration or photograph.

5. Online Submission

Manuscripts should be submitted to *Drug Discoveries & Therapeutics* online at <http://www.ddtjournal.com>. The manuscript file should be smaller than 10 MB in size. If for any reason you are unable to submit a file online, please contact the Editorial Office by e-mail: office@ddtjournal.com

Editorial and Head Office

Wei TANG, MD PhD
Executive Editor
Drug Discoveries & Therapeutics
Pearl City Koishikawa 603,
2-4-5 Kasuga, Bunkyo-ku,
Tokyo 112-0003, Japan
Tel: 03-5840-9697
Fax: 03-5840-9698
E-mail: office@ddtjournal.com

Cover letter. A cover letter from the corresponding author including the following information must accompany the submission: name, address, phone and fax numbers, and e-mail address of the corresponding author. This should include a statement affirming that all authors concur with the

submission and that the material submitted for publication has not been previously published and is not under consideration for publication elsewhere and a statement regarding conflicting financial interests.

Authors may recommend up to three qualified reviewers other than members of Editorial board. Authors may also request that certain (but not more than three) reviewers not be chosen.

The cover letter should be submitted as a Microsoft Word (.doc) file (smaller than 1 MB) at the same time the work is submitted online.

6. Accepted Manuscripts

Proofs. Rough galley proofs in PDF format are supplied to the corresponding author *via* e-mail. Corrections must be returned within 4 working days of receipt of the proofs. Subsequent corrections will not be possible, so please ensure all desired corrections are indicated. Note that we may proceed with publication of the article if no response is received.

Transfer of copyrights. Upon acceptance of an article, authors will be asked to agree to a transfer of copyright. This transfer will ensure the widest possible dissemination of information. A letter will be sent to the corresponding author confirming receipt of the manuscript. A form facilitating transfer of copyright will be provided. If excerpts from other copyrighted works are included, the author(s) must obtain written permission from the copyright owners and credit the source(s) in the article.

Cover submissions. Authors whose manuscripts are accepted for publication in *Drug Discoveries & Therapeutics* may submit cover images. Color submission is welcome. A brief cover legend should be submitted with the image.

Revised June 20, 2009



Drug Discoveries & Therapeutics



Editorial Office

Pearl City Koishikawa 603,
2-4-5 Kasuga, Bunkyo-ku,
Tokyo 112-0003, Japan

Tel: 03-5840-9697

Fax: 03-5840-9698

E-mail: office@ddtjournal.com

URL: www.ddtjournal.com

JOURNAL PUBLISHING AGREEMENT

Ms No:

Article entitled:

Corresponding author:

To be published in Drug Discoveries & Therapeutics

Assignment of publishing rights:

I hereby assign to International Advancement Center for Medicine & Health Research Co., Ltd. (IACMHR Co., Ltd.) publishing Drug Discoveries & Therapeutics the copyright in the manuscript identified above and any supplemental tables and illustrations (the articles) in all forms and media, throughout the world, in all languages, for the full term of copyright, effective when and if the article is accepted for publication. This transfer includes the rights to provide the article in electronic and online forms and systems.

I understand that I retain or am hereby granted (without the need to obtain further permission) rights to use certain versions of the article for certain scholarly purpose and that no rights in patent, trademarks or other intellectual property rights are transferred to the journal. Rights to use the articles for personal use, internal institutional use and scholarly posting are retained.

Author warranties:

I affirm the author warranties noted below.

- 1) The article I have submitted to the journal is original and has not been published elsewhere.
- 2) The article is not currently being considered for publication by any other journal. If accepted, it will not be submitted elsewhere.
- 3) The article contains no libelous or other unlawful statements and does not contain any materials that invade individual privacy or proprietary rights or any statutory copyright.
- 4) I have obtained written permission from copyright owners for any excerpts from copyrighted works that are included and have credited the sources in my article.
- 5) I confirm that all commercial affiliations, stock or equity interests, or patent-licensing arrangements that could be considered to pose a financial conflict of interest regarding the article have been disclosed.
- 6) If the article was prepared jointly with other authors, I have informed the co-authors(s) of the terms of this publishing agreement and that I am signing on their behalf as their agents.

Your Status:

I am the sole author of the manuscript.

I am one author signing on behalf of all co-authors of the manuscript.

Please tick one of the above boxes (as appropriate) and then sign and date the document in black ink.

Signature:

Date:

Name printed:

Please return the completed and signed original of this form by express mail or fax, or by e-mailing a scanned copy of the signed original to:

Drug Discoveries & Therapeutics office

Pearl City Koishikawa 603, 2-4-5 Kasuga, Bunkyo-ku, Tokyo 112-0003, Japan

e-mail: proof-editing@ddtjournal.com

Fax: +81-3-5840-9698

